UNCLASSIFIED

AD NUMBER
AD486861
LIMITATION CHANGES
TO: **Approved for public release; distribution is unlimited.**
FROM: **Distribution authorized to DoD only; Critical Technology; AUG 1964. Other requests shall be referred to Electronic Systems Division, ATTN: ESTI, Hanscom AFB, MA.**
AUTHORITY
ESD ltr dtd 1 May 1968

THIS PAGE IS UNCLASSIFIED

ESD-TR-66-480
ESTI File Copy

NOTICE: When government or other drawings, specifications or other data are used for any purpose other than in connection with a definitely related government procurement operation, the U. S. Government thereby incurs no responsibility, nor any obligation whatsoever; and the fact that the Government may have formulated, furnished, or in any way supplied the said drawings, specifications, or other data is not to be regarded by implication or otherwise as in any manner licensing the holder or any other person or corporation, or conveying any rights or permission to manufacture, use or sell any patented invention that may in any way be related thereto.

UNCLASSIFIED

AD 486861L

DEFENSE DOCUMENTATION CENTER

FOR

SCIENTIFIC AND TECHNICAL INFORMATION

CAMERON STATION, ALEXANDRIA, VIRGINIA



UNCLASSIFIED

AD0486861

ESD-TR-66-480

APPLICABILITY OF LASER TECHNIQUES.

AUG 1964

283p.

DEPUTY FOR COMMUNICATION SYSTEMS
ELECTRONIC SYSTEMS DIVISION
AIR FORCE SYSTEMS COMMAND
United States Air Force
L.G. Hanscom Field, Bedford, Massachusetts

A-1

ICS-64-TR-480,
ICS-64-TR-481

This document is subject to special export controls and each transmittal to foreign governments or foreign nationals may be made only with prior approval of Hq ESD(ESTI).

Each transmittal of this document outside the Department of Defense must have prior approval of Hq ESD (ESTI).

DDC
AUG 16 1966

(Prepared by ITT Communication Systems, Inc., Paramus, New Jersey under Contract AF19(628)-3414.)

TABLE OF CONTENTS

Section		Page
1	INTRODUCTION	1-1 and 1-2
	1.0 FAVORABLE CHARACTERISTICS	1-1
	2.0 PROBLEMS	1-1
	3.0 TECHNICAL APPROACH	1-1
2	SUMMARY	2-1 thru 2-3
3	POTENTIAL LASER COMMUNICATION SYSTEM APPLICATIONS	3-1 thru 3-15
	1.0 FIXED, GROUND-BASED POINT-TO-POINT APPLICATIONS	3-2
	2.0 TACTICAL, GROUND-BASED POINT-TO-POINT WIDEBAND COMMUNICATION SYSTEM	3-8
	3.0 TACTICAL AIR-GROUND APPLICATIONS	3-9
	4.0 TACTICAL AIR-AIR APPLICATIONS	3-9
	5.0 AIRBORNE RADIO RELAY	3-11
	6.0 AIRCRAFT OVER-THE-HORIZON COMMUNICATION	3-11
	7.0 SPACE-SPACE LINKS	3-12
	8.0 PIPED LASER COMMUNICATION APPLICATIONS	3-13
	9.0 CONCLUSIONS	3-14
4	LASER TECHNIQUES AND COMPONENTS	4-1 thru 4-8
	1.0 GENERATION OF A LASER BEAM	4-1
	1.1 COHERENT LIGHT GENERATION	4-1
	1.2 GENERATION OF LASER POWER	4-6
	2.0 LASER TECHNIQUES AND COMPONENTS	4-7
	2.1 GENERAL LASER MEDIA REQUIREMENTS	4-7
	2.2 OPTICALLY PUMPED SOLID-STATE LASER MEDIA REQUIREMENTS	4-7
	2.3 CLASSIFICATION OF LASERS	4-8
	3.0 REFERENCES	4-8
5	GENERAL LASER COMMUNICATION SYSTEM ANALYSIS	5-1 thru 5-25
	1.0 DELINEATION OF LASER SYSTEM COMPONENTS	5-1
	1.1 BLOCK DIAGRAM DESCRIPTION	5-1
	1.2 MULTIPLEX EQUIPMENT	5-1
	1.3 MODULATION EQUIPMENT	5-3
	1.4 GENERATION OF LASER ENERGY	5-3
	1.5 ANTENNA TRACKING	5-4

TABLE OF CONTENTS (Continued)

Section		Page
	1.6 TRANSMISSION MEDIUM	5-4
	1.7 DETECTION AND MULTIPLEX EQUIPMENT	5-4
	2.0 LASER COMMUNICATION SYSTEM ANALYSIS	5-5
	2.1 FREE SPACE LASER COMMUNICATION SYSTEMS	5-6
	2.2 THE USE OF LIGHT PIPED THROUGH METAL GUIDES	5-14
	2.3 FIBER OPTICS (MULTIPLE DIELECTRIC WAVEGUIDE)	5-16
	2.4 TRANSMISSION THROUGH METAL LIGHT PIPES	5-19
	3.0 GLOSSARY	5-22
	4.0 REFERENCES	5-25
6	PROPAGATION OF COHERENT LIGHT THROUGH ATMOSPHERE	6-1 thru 6-30
	1.0 ABSORPTION LOSSES	6-1
	1.1 ABSORPTION LOSS AT LASER WAVELENGTHS	6-1
	1.2 ABSORPTION LOSS CAUSED BY WATER VAPOR	6-3
	1.3 PROPAGATION THROUGH FOG	6-3
	2.0 LASER TRANSMISSION IN INCLEMENT WEATHER	6-7
	2.1 TRANSMISSION THROUGH FOG	6-7
	2.2 TRANSMISSION THROUGH RAIN	6-10
	2.3 TRANSMISSION THROUGH SNOW	6-14
	3.0 EXPERIMENTS IN DIFFUSE TRANSMISSION	6-14
	4.0 FOG DISPERSIVE TECHNIQUES	6-18
	4.1 VAPORIZATION OF WATER PARTICLES	6-20
	4.2 POSSIBLE SOLUTION TO TUNNELING	6-23
	4.3 TUNNELING EXPERIMENTS	6-23
7	MODULATION AND DEMODULATION	7-1 thru 7-19
	1.0 LASER MODULATION	7-1
	1.1 CHOICE OF MODULATION	7-1
	1.2 TECHNIQUES OF MODULATION	7-1
	1.3 PRACTICAL MODULATION MECHANISMS	7-4
	1.4 MODULATION OF SEMICONDUCTOR LASERS	7-6
	1.5 COMPARISON OF EXTERNAL AND INTERNAL MODULATION	7-6
	5.0 CONCLUSIONS	6-28
	6.0 REFERENCES	6-29

TABLE OF CONTENTS (Continued)

Section		Page
	2.0 LASER DEMODULATORS	7-7
	2.1 TYPES OF OPTICAL RECEIVERS	7-7
	2.2 THEORETICAL COMPARISON OF DEMODULATION TECHNIQUES	7-8
	2.3 AVAILABLE DEMODULATION TECHNIQUES	7-11
	3.0 REFERENCES	7-17
8	AIMING AND TRACKING IN LASER SYSTEMS	8-1 thru 8-41
	1.0 ATMOSPHERIC TURBULENCE EFFECTS	8-1
	1.1 EFFECTS OF ATMOSPHERIC TURBULENCE ON LASER PROPAGATION	8-1
	1.2 RECIPROCITY EFFECTS IN TRANSMISSION AND RETURN OF A LASER BEAM	8-5
	2.0 TRACKING ERRORS IN MOVING SYSTEMS (BRADLEY AND TRANSMIT TIME ERRORS)	8-5
	3.0 ACQUISITION TIME AND SEARCH RATES	8-7
	3.1 ANALYTICAL MODEL	8-7
	3.2 PRACTICAL CONSIDERATIONS	8-10
	4.0 DISCRIMINATION AGAINST UNWANTED RADIATING SOURCES	8-13
	4.1 BACKGROUND NOISE SOURCES	8-13
	4.2 DISCRETE NOISE SOURCES (FALSE TARGETS)	8-13
	4.3 DISCRIMINATION TECHNIQUES	8-14
	5.0 LASER ANTENNAS	8-14
	5.1 GENERAL APPLICATIONS	8-14
	5.2 SPECIFIC APPLICATIONS	8-16
	6.0 SCANNING AND ANTENNA TRACKING	8-19
	6.1 MECHANICAL TECHNIQUES	8-19
	6.2 PIEZOELECTRIC TECHNIQUES	8-20
	6.3 ULTRASONIC SCANNING	8-25
	7.0 DESIGN AND SYSTEMS CONSIDERATIONS	8-33
	7.1 ACQUISITION AND COARSE TRACKING SENSORS	8-34
	7.2 FINE TRACKING SENSORS	8-34
	7.3 MECHANICAL CONFIGURATIONS	8-35

TABLE OP CONTENTS (Continued)

Section		Page
	8.0 CONCLUSIONS AND RECOMMENDATIONS	8-40
	9.0 REFERENCES	8-41
9	PRIVACY OF LASER LINKS	9-1 thru 9-14
	1.0 PROBLEMS OF PRIVACY	9-1
	2.0 MECHANISMS FOR INTERCEPTION OP LASER BEAMS	9-1
	2.1 REPRACTIVE SCATTERING	9-2
	2.2 PARTICLE SCATTERING	9-2
	2.3 SCATTERING BY GLASS	9-6
	3.0 PRIVACY IN LASER SYSTEMS	9-6
	3.1 SPACE-SPACE LINKS	9-6
	3.2 GROUND-SPACE AND SPACE-GROUND LINKS	9-8
	3.3 AIR-AIR LINKS	9-9
	3.4 GROUND-GROUND LINKS	9-10
	4.0 REQUIREMENT FOR ENCRYPTION CONSIDERING VARIOUS MODULATION TECHNIQUES	9-11
	5.0 COUNTERMEASURES	9-13
	6.0 REPERENCES	9-13
10	CONCLUSIONS AND RECOMMENDATIONS	10-1 thru 10-5
	1.0 RECOMMENDED LASER APPLICATIONS	10-1
	2.0 LASER MATERIALS	10-3
	3.0 ATMOSPHERIC PROPAGATION	10-3
	4.0 MODULATION AND DEMODULATION TECHNIQUES	10-3
	5.0 AIMING AND TRACKING AND ANTENNA SYSTEMS	10-5
	6.0 PRIVACY	10-5
APPENDIX I	CHARACTERISTICS OF THE ATMOSPHERE	I-1 thru I-27
APPENDIX II	DESCRIPTION OF LASER PROPERTIES	II-1 thru II-23
APPENDIX III	THEORIES OF RAYLEIGH AND MIE SCATTERING	III-1 thru III-10
APPENDIX IV	DESCRIPTION OF LASER MODULATION TECHNIQUES	IV-1 thru IV-34
APPENDIX V	HEURISTIC DISCUSSION OF RECIPROCITY EFFECTS IN THE TRANSMISSION AND RETURN OF A LASER BEAM	V-1 thru V-15
APPENDIX VI	DIFFRACTIVE SCANNING	VI-1 thru VI-11

LIST OP ILLUSTRATIONS

Figure		Page
3-1	POWER RECEIVED PER UNIT POWER TRANSMITTED AS A FUNCTION OF ANTENNA RADIUS FOR A 15 MILE PATH	3-3
3-2	POWER RECEIVED PER UNIT POWER TRANSMITTED AS A FUNCTION OF ANTENNA RADIUS FOR A 20 MILE PATH	3-4
3-3	IMAGE MOTION AS A FUNCTION OF ELEVATION ANGLE	3-6
3-4	IMAGE MOTION AS A FUNCTION OF FREQUENCY	3-7
3-5	LINE OF SIGHT DISTANCE BETWEEN AIRCRAFT AND GROUND LOCATION AS A FUNCTION OF AIRCRAFT ALTITUDE	3-10
4-1	THREE-LEVEL ENERGY DIAGRAM	4-5
4-2	FOUR-LEVEL ENERGY DIAGRAM	4-5
4-3	HELIUM-NEON GAS LASER ENERGY DIAGRAM	4-5
5-1	LASER COMMUNICATION SYSTEM BLOCK DIAGRAM	5-2
5-2	NOISE DISTRIBUTION OVER FREQUENCY SPECTRUM	5-9
5-3	TRANSMITTER POWER REQUIRED AS A FUNCTION OF BAND-WIDTH FOR TRANSMISSION FROM GROUND TO SYNCHRONOUS SATELLITE	5-15
5-4	CONDITIONED PIPE LIGHT LOSSES IN VISIBLE RANGE	5-17
5-5	ATTENUATION OF COHERENT LIGHT IN FIBER OPTICS	5-20
5-6	THEORETICAL TRANSMISSION CHARACTERISTIC OF METAL LIGHT PIPES	5-23
6-1	ATMOSPHERIC LOSSES AS A FUNCTION OF WAVELENGTH FOR VARIOUS COMPOUNDS	6-2
6-2	WATER VAPOR ABSORPTION IN REGION NEAR 1.1525 MICRONS	6-4
6-3	WATER VAPOR ABSORPTION IN REGION NEAR 0.6328 MICRON	6-4
6-4	ATTENUATION AS A FUNCTION OF HUMIDITY FOR WATER VAPOR AND WATER VAPOR PLUS NITROGEN	6-5
6-5	ATTENUATION AS A FUNCTION OF WATER VAPOR PARTIAL PRESSURE IN MM	6-5
6-6	ATTENUATION AS A FUNCTION OF WATER VAPOR PARTIAL PRESSURE IN MICRONS	6-6
6-7	INFRARED ABSORPTION OF WATER	6-6
6-8	RADIUS OF DROPS OF MONODISPERSED FOG	6-9
6-9	TRANSMISSION LOSS THROUGH RAIN CAUSED BY SCATTERING AS A FUNCTION OF PRECIPITATION RATE	6-12
6-10	MAXIMUM TOLERABLE PRECIPITATION RATE AS A FUNCTION OF TRANSMITTED POWER	6-15
6-11	COMMUNICATION OUTAGES CAUSED BY RAIN AS A FUNCTION OF TRANSMITTER POWER	6-16

LIST OF ILLUSTRATIONS (Continued)

Figure		Page
6-12	REFRACTIVE COEFFICIENTS OF ICE AND WATER AS A FUNCTION OF WAVELENGTH	6-17
6-13	SUMMARY OF THE DIFFUSE TRANSMISSION OF THE TOTAL SPECTRAL REGION	6-19
6-14	BLOCK DIAGRAM OF ALL-WEATHER LASER CONCEPT	6-21
6-15	BLOCK DIAGRAM FOR EVALUATING FOG DISPERSIVE TECHNIQUES	6-25
6-16	RESULTS OF TUNNELING WITH RUBY LASER	6-26
6-17	RESULTS OF TUNNELING WITH INFRARED LAMP	6-26
7-1	POCKELS CELL LIGHT INTENSITY MODULATOR	7-4a
7-2	BASIC OPTICAL RECEIVER	7-7a
7-3	INFORMATION CAPACITY AS A FUNCTION OF FREQUENCY FOR VARIOUS LEVELS OF SIGNAL POWER	7-9a
7-4	INFORMATION EFFICIENCY COMPARISON OF HOMODYNE AND HETERODYNE RECEIVERS	7-9a
7-5	ABSOLUTE SPECTRAL CHARACTERISTIC OF VARIOUS CATHODE SURFACES	7-13a
7-6	DIAGRAM OF MICROWAVE PHOTODETECTOR	7-14a
7-7	DIAGRAM OF TRAVELING-WAVE DEMODULATOR	7-16
8-1	DEFOCUSING OF A PARABOLA	8-18
8-2	POSSIBLE CONFIGURATION FOR PIEZOELECTRICALLY DRIVEN MIRROR	8-21
8-3	ANGULAR DEFLECTION AS A FUNCTION OF FREQUENCY FOR CRITICALLY DAMPED SYSTEM AND CONSTANT DRIVE	8-26
8-4	PIEZOELECTRIC SCANNING OF DETECTOR FIELD OF VIEW	8-26
8-5	REFRACTION OF LIGHT IN AN ACOUSTICAL CELL	8-28
8-6	DIELECTRIC CONSTANT AND LOSS TANGENT AS A FUNCTION OF TEMPERATURE FOR KH_2PO_4	8-31
8-7	LASER COMMUNICATION TRANSCEIVER, CONFIGURATION A	8-36
8-8	TRANSMISSIVE AND REFLECTIVE PROPERTIES OF A TILTED, NARROW-BAND INTERFERENCE FILTER	8-37
8-9	LASER COMMUNICATION TRANSCEIVER, CONFIGURATION B	8-39
9-1	INTERCEPTION OF SCATTERED LIGHT	9-4
9-2	SCATTERING FROM A GLASS PLATE	9-7
9-3	INTERCEPTION OF MAIN BEAM BY BEAM SPLITTER	9-7

LIST OF TABLES

Table		Page
7-1	INFRARED DETECTORS	7-12a
8-1	DIELECTRIC PROPERTIES OF KDP AT 25°C (FIELD PARALLEL TO OPTICAL AXIS)	8-32
9-1	INTERCEPTION MODES REQUIRING ENCRYPTION	9-12

SECTION 1
INTRODUCTION

This report presents laser communication techniques that can be integrated into the AIRCOM System to satisfy unmet current and estimated Air Force requirements. This document constitutes the final report for AF Task 24, and is forwarded in response to a requirement for a final report.

The advent of the laser has aroused great interest among communication engineers because it affords use of a new spectrum millions of megacycles wide. Although the laser will have a great impact in certain areas of communication technology, its potential in any specific area must be carefully evaluated.

1.0 FAVORABLE CHARACTERISTICS

The characteristics of the laser that make it attractive for use in potential communication links are:

(a) Narrow beam width, 10^{-5} to 10^{-6} radians with suitable collimating optics

(b) High spectral radiance, allowing filtering of background noise and interference

(c) High carrier frequency, resulting in low percentage modulation for large modulation bandwidths

(d) Reasonably compact and economical.

2.0 PROBLEMS

The major problem areas that limit the usefulness of laser links at the present time include:

(a) Effects of the atmosphere and weather on propagation

(b) Need for improved wideband modulation and demodulation techniques

(c) Relatively low continuous wave output available at present, and low repetition rate attainable with pulsed lasers

(d) Necessity for extremely precise alignment of radiating and receiving elements.

3.0 TECHNICAL APPROACH

This study will present the characteristics and problems related to coherent light generation, laser communication through media other than

the atmosphere (free space, light pipes, fiber optics, and waveguides), modulators and demodulators, and aiming and tracking systems to determine possible areas of applications to Air Force communication. In addition, possible laser communication system applications, the privacy aspects of laser links, and the propagation of lasers through the atmosphere, which represents one of the most difficult of laser applications to realize, will be discussed. In connection with this latter consideration, a program of experimentation will be carried out to investigate methods for alleviating the dispersive and absorptive effects of fog on laser propagation through the atmosphere. Possible communication systems will be investigated and the applicability of lasers for use in support of transmission will be assessed.

SECTION 2
SUMMARY

The characteristics of lsser beams have caused considerable interest as to their potential use in support of Air Force communication requirements. The newer laser generating techniques, particularly semiconductor lasers, ensure that laser frequencies will be available over a continuous frequency range, ranging from the infrared through the visible portion of the spectrum. Laser techniques have already demonstrated considerable utility in fields other than communication. For example, areas such as lensless photography, surgery, welding, material analysis, and interferometry are under intensive study and show promise of providing a considerable number of industrial and research laser applications.

The study examines in detail those portions of laser systems that could bear on their use in support of Air Force communication requirements. To properly evaluate their potential application for a number of communication applications, a considerable amount of detail has been included concerning the various components of laser communication links. In many potential applications, lasers are attractive but they require additional development and somewhat complicated component design to counteract difficulties in transmission, encountered because of the frequency range of laser action. Laser techniques must compete with other existing and proposed communication techniques, which in many Air Force applications will perform aa well. The tradeoffs in these cases must be evaluated and decisions as to utility made on the basis of economic and relative performance considerations. There are, however, areas in which laser techniques seem to offer significant advantages over other techniques.

Section 3 of this report examines a number of specific communication link applications and assesses the potential applicability of laser techniques. The areas in which lasers show the most promise are generally those in which small antennas are required, and where the difficulties encountered because of propagation of the laser beam through the earth's atmosphere can be avoided. For other communication applications, laser techniques are also feasible; but they must compete with other communication devices using portions of the spectrum that do not require as much attention to atmospheric attenustion and refraction. Such devices are therefore simpler to implement. Laser use for atmospheric point-to-point links must be evaluated for individual, specific applications, and cannot be generally recommended as a useful technique.

Section 4 of this report considers the principles of laser action and reviews the techniques and materials for laser power generation. The research and development of lasers over the past few years has resulted in a large number of promising materials for laser power generation. At present, difficulties are still encountered in obtaining laser output on the order of watts of average power. Devices that can produce this power are available (for example, ruby lasers and semiconductor lasers), but they are inefficient in some cases (requiring light excitation) and require cooling in others. Because of the advances made in the area of laser power generation and the large number of promising techniques, the availability of laser power generation should not limit the realization of a laser communication system.

Section 5 analyzea the general laser communication system. Components are defined, and free space and various piped laser communication systems analyzed. Several examples of free space laser links are presented and required system parameters derived. Attenuation versus pipe length is presented for fiber optics, metal guides, and confined atmospheres within a metal pipe. The feasibility of free space and confined atmosphere links from the standpoint of available bandwidth is demonstrated although practical limitations prohibit the use of laser propagation in a confined atmosphere. Metal light pipes and fiber optics are not presently suited for laser transmission, although the potential utility of fiber optics for light weight cable makes further investigation worthwhile.

Section 6 considers laser propagation through the earth's atmosphere. Atmospheric attenuation of laser beams is examined under conditions of both clear and inclement weather. An analysis and experimental results of fog dispersing techniques using lasers, microwaves, and incoherent infrared radiation are presented. Although the clear atmosphere does not excesively attenuate light or laser propagation, fog, rain, and snow present a serious limitation to laser link performance. Fog dispersive

techniques do not show promise of significantly mitigating the effects of adverse weather unless considerable power is used. This would result in prohibitive system complications, both from the need for expensive fog dispersing equipment and from the turbulence effects arising from its use.

Section 7 examines available and proposed laser modulation and demodulation techniques. Laser modulators are presently in an experimental stage of development, although a number of promising modulation techniques have been proposed both external and internal to the laser cavity. Modulation of laser beams has been achieved at rates up to 10 gc; however, the modulation bandwidths obtained are considerably lower. Narrower modulation bandwidths (tens of megacycles) have been achieved and would suffice for many proposed laser communications applications.

Demodulation does not present as many difficulties as modulation. Fairly sensitive light detectors are available for limited portions of the visible spectrum. Although their efficiency drops, these detectors may be used in other portions of the spectrum. Heterodyning techniques require considerable development effort. The proposed and available techniques for light demodulation are presented.

Section 8 analyzes laser antennas, discusses aiming and tracking of laser beams, and suggests a number of techniques for effective aiming. The requirements of optical systems to cope with refraction and breakup of the laser beam arising from atmospheric turbulence are presented and approaches are suggested to reduce these effects. Proposed laser communication transceiver configurations are presented.

Section 9 considers the privacy aspects of laser links. Privacy is considered in terms of the inability of the interceptor to detect information on the lsser beam. For certain applications (space-space and air-air links), lasers csn ensure link privacy without encryption because of the unsvailability of the besm energy to an interceptor. Encryption is required where unavailaoility cannot be ensured (for example, where ground terminals sre required snd for space-ground links, depending on the degree of besm collimation). The svsilability of scattered light to sn interceptor is analyzed as is the possibility of sn interceptor having access to the main laser besm.

Conclusions snd recommendations regarding the applicsbility of lsser techniques to Air Force communication are presented in Section 10.

SECTION 3
POTENTIAL LASER COMMUNICATION SYSTEM APPLICATIONS

The potential capability of transmitting large information bandwidths with light and compact equipment makes laser communication systems extremely attractive for consideration in satisfying many communication requirements. Although many problems associated with laser communication still are to be solved, the manifold uses to which systems employing lasers could be put encourages considerable effort to overcome these difficulties and obtain operational systems.

In ground based usage, the information capacity, the narrow beamwidths and concomitant enhanced security, and the lack of interference between links make lasers attractive for tactical, as well as fixed, point-to-point systems. In mobile and other tactical situations, their potential simplicity and compactness along with the above features suggest many communication support systems that either are unattainable at present or are cumbersome because of equipment requirements.

However, effects such as atmospheric refraction, image motion, and quivering must be mitigated before laser communication systems become operational. Similsrly, methods must be found to overcome the effects of dispersive aerosols, such as fog and rain, on laser propagation. Considerable effort is required in these areas to produce operational systems. Furthermore, competing techniques, such as microwave radio relay in the case of fixed ground systems and millimetric-wave transmission in the case of mobile systems, lessen the relative sdvantage of laser systems and cast doubt on their economic competitiveness when considering propagation difficulties.

Nevertheless, areas do exist in which laser techniques have great potential. The prognosis for air-to-air private links that require only small antenna structures and that can support significant bandwidths becomes extremely good when laser techniques are considered. For example, for high altitude aircraft, many of the effects of atmospheric conditions on laser beams may be mitigated and implementation of workable systems would therefore become more straight-forward. At present, additional data on the effect of air heating and turbulence along an aircraft's skin

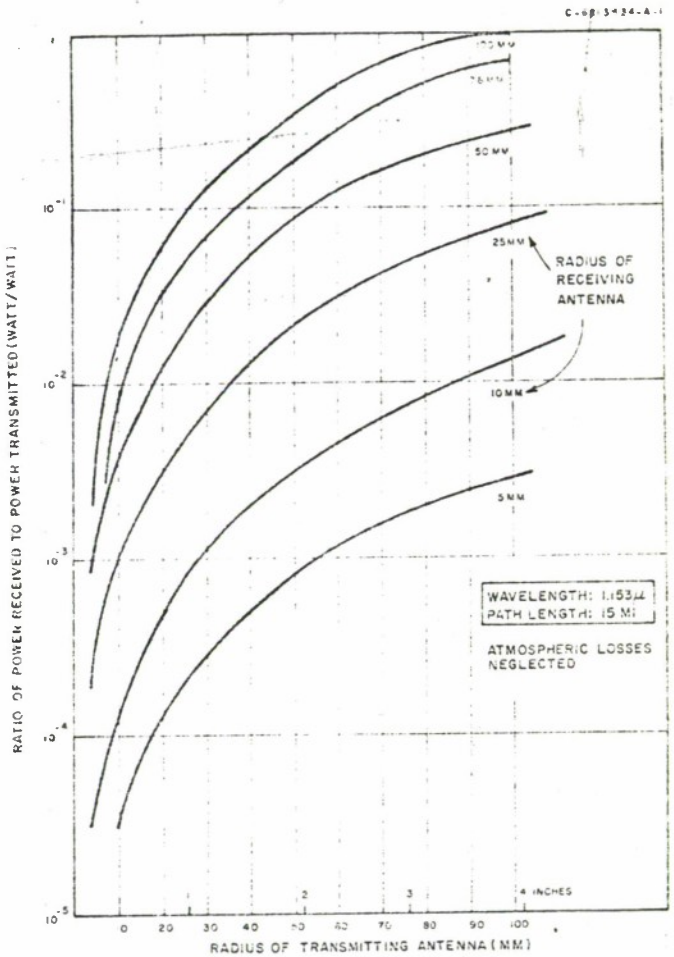
on laser propagation is required to better determine laser utility. Furthermore, present laser systems are generally bulky and, as a result, are unsuited for such applications. Development of lightweight laser systems is therefore required.

The main advantage in using laser techniques for aircraft applications is that of the small antenna structure needed to obtain a highly directive beam. It may be noted that millimetric waves do offer considerable competition in this area and that other advantages such as the potential high reliability and simplicity of laser systems become a more important factor in their favor as a result.

1.0 FIXED, GROUND-BASED POINT-TO-POINT APPLICATIONS

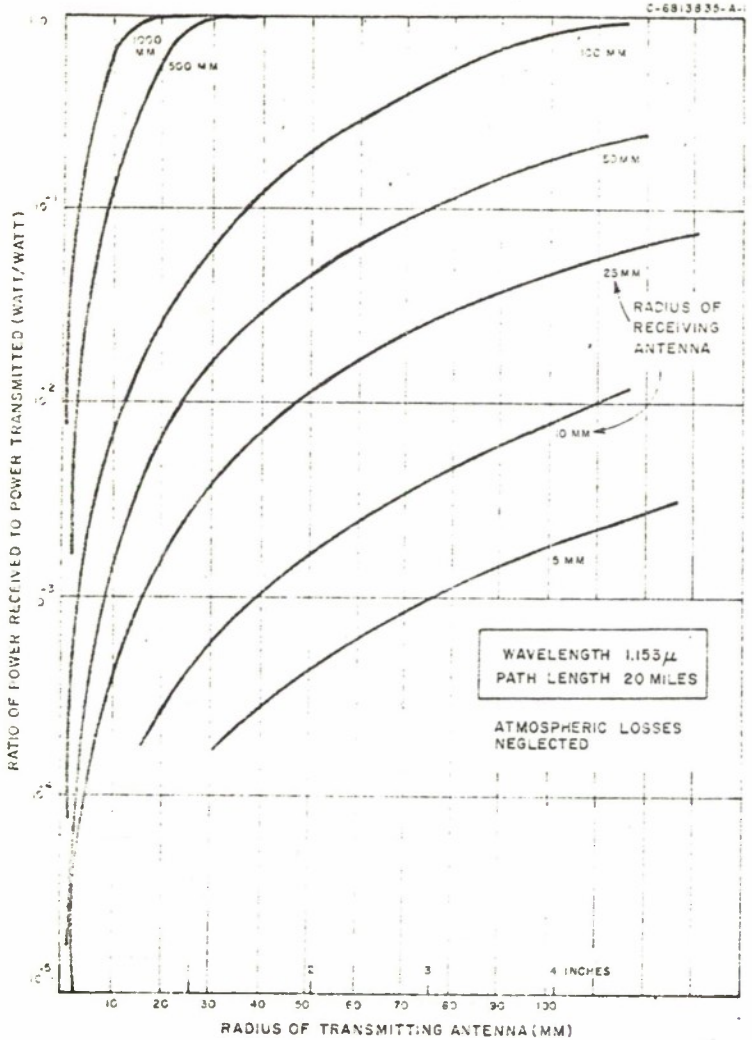
Because of the high frequency (10^{14} to 10^{15} cps) of laser carriers, bandwidths of several gigacycles are possible with bandwidths representing a relatively small percentage of the carrier frequency. In addition, the confinement of the beam should permit laser links to be set up almost at will without regard for mutual interference between laser systems at any given site. Thus a single frequency can be used for independent links at the same site.

Over a 15 to 20 mile path, essentially all of the energy transmitted by a laser, less that absorbed by the atmosphere, may be received by the receiver with optics of reasonable size. This arises from the narrow beam spread of a laser beam, which permits a small receiving antenna to intercept the entire solid angle of radiation from a transmitter. Figures 3-1 and 3-2 show the power received per unit of power transmitted as a function of the transmitter and receiver antenna sizes, neglecting atmospheric absorption, for a wavelength of 1.153 μ. From these curves it is evident that with receiver and transmitter antenna radii of 4 inches, essentially all the transmitted energy (less that absorbed by the atmosphere) may be intercepted by the receiver. With appropriate transmitter tracking of the laser beam, essentially non-interfering parallel links may be constructed by using a displacement of no more than a few feet. The high attainable directivity of the receiver along with the confinement of the laser beam should considerably alleviate problems of frequency allocation in crowded locations such as those presently encountered with microwave techniques. Additionally, because of the confinement of laser energy, the task of interception of information by an



POWER RECEIVED PER UNIT POWER TRANSMITTED AS A FUNCTION OF ANTENNA RADIUS FOR A 15 MILE PATH

FIGURE 3-1



POWER RECEIVED PER UNIT POWER TRANSMITTED AS A FUNCTION OF ANTENNA RADIUS FOR A 20 MILE PATH

FIGURE 3-2

enemy is made extremely difficult. General availability of the beam, however, would still require the use of encryption to ensure link privacy. The difficulties encountered with ground-based links are the most stringent of any of the possible laser links. Effects of atmospheric refraction, absorption, and dispersion caused by inclement weather are more pronounced for links of this type because of their proximity to the earth's surface. Transmission through the atmosphere under clear conditions can result in a loss of energy at the receiver of as much as 20 db. Adverse weather conditions increase these losses considerably, which can easily make the link inoperable.

In addition, image motion or twinkling creates serious tracking and aiming problems. Figure 3-3 shows effective image motion as a function of elevation angle for astronomical bodies as a function of visibility, and Figure 3-4 shows the image motion as a function of its frequency of variation.

To combat the effects of image motion, effective laser tracking systems must be devised. These must include tracking of the transmitter, since angular beam displacements (on the order of 100 microradians) at 20 miles can result in a physical beam displacement of approximately 10 feet, which would divert the energy past the antenna receiving area. The use of two way links coupled with the relative ease of aiming a light beam electronically, however, do make automatic tracking systems feasible. From Figure 3-4 it may be seen that a tracking transmitter with a response of 200 cps should be sufficient to reduce the apparent image motion for an elemental ray at the receiver to well below the beamwidth of the transmitting antenna.

Large diameter lenses produce wide coherent beams that will reduce the higher frequency effects, since these are due to the smaller disruptive volume in the beam. The result at the receiver is a beam that has variations in intensity across its wave front. If the receiver detects all the energy across the wave front, no energy is lost, although an upper limit of several gigacycles must be placed on the modulation of the laser beams because of difference in path length for components of the arriving wave. Atmospheric disturbances may cause fluctuations greater than the diameter of the aiming beam. The rate of these fluctuations, however, is generally below 10 cps so that tracking system requirements

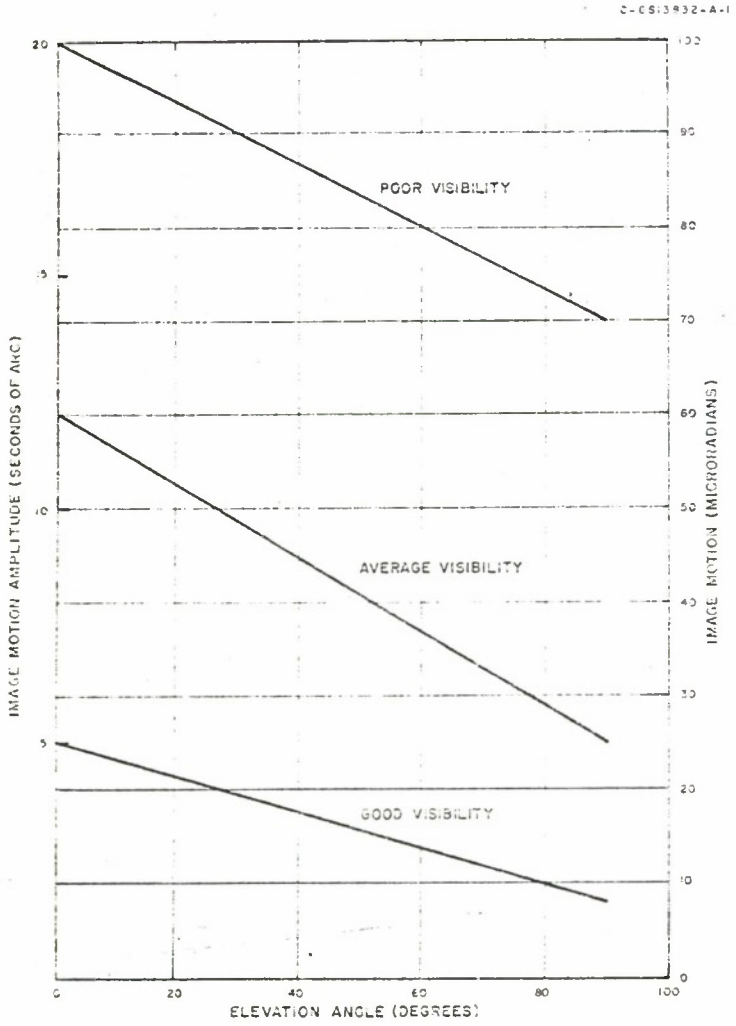


IMAGE MOTION AS A FUNCTION OF ELEVATION ANGLE

FIGURE 3-3

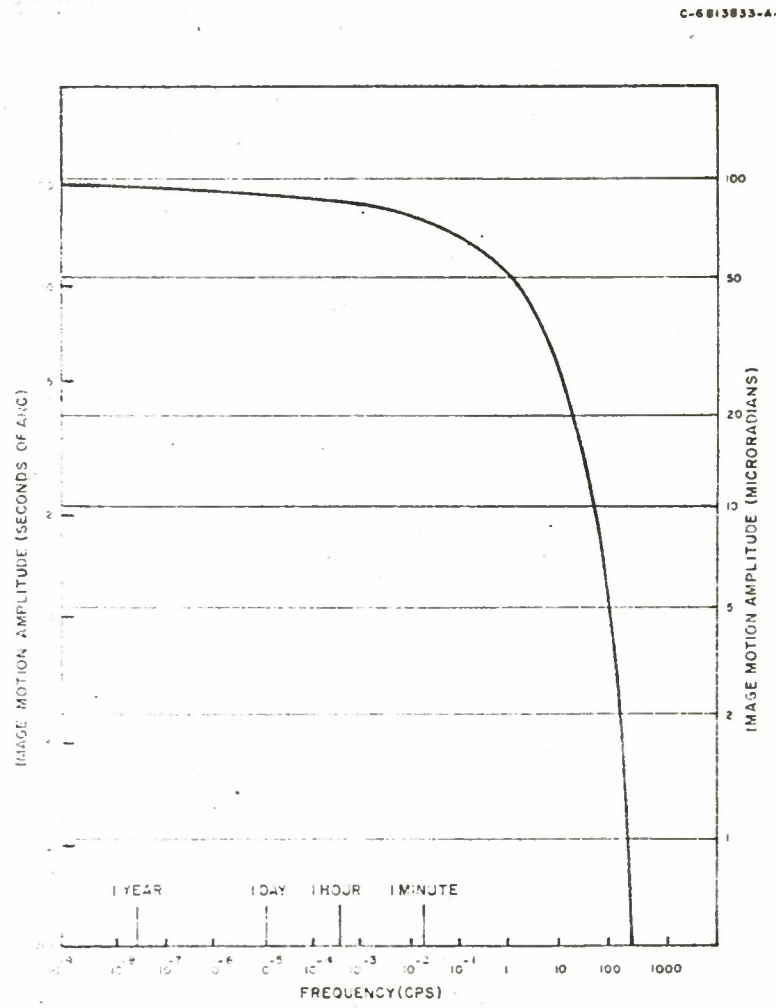


IMAGE MOTION AS A FUNCTION OF FREQUENCY

FIGURE 3-4

are less stringent. Thus, a combination of optics producing large diameter beams and tracking could effectively combat the effects of atmospheric turbulence.

The propagation characteristics of the atmosphere are more thoroughly treated in Section 6 of this report. As may be deduced from this section, proposed methods do exist for mitigating the effects of adverse weather conditions on laser propagation. These methods are still in the research stage, and considerable effort is required before their implementation. Additionally, complexity and cost may preclude their use if other techniques are considered.

Appendix I contains meteorological data relevant to laser transmission. Relationships between conditions and visibility are presented as are general characteristics of the atmosphere. It is shown that adverse weather conditions may persist for only small percentages of the year. These conditions, however, can persist for considerable periods and thus cause intolerable periods of communication outage unless fog dispersing techniques are used.

2.0 TACTICAL, GROUND-BASED POINT-TO-POINT WIDEBAND COMMUNICATION SYSTEM

The potentially light weight of laser communication components and the small antenna size suggest uses such as tactical battlefield video links, short range air-ground television, and other broadband applications. Although inclement weather would affect the operation of the laser link, tactical television would be used only under weather conditions similar to those favorable for laser transmission. Thus the laser transmission system should not by itself be the limiting parameter of a tactical television system. In this application other communication techniques, such as millimetric wave transmission, are strong competitors. Choice of a laser system must rest on a comparison between microwave, millimetric wave, and laser techniques with regard to complexity of equipment and suitability for use under a variety of operational conditions.

Other restrictions are imposed on laser links in a battlefield environment. Obtaining a line-of-sight path from laser transmitter to receiver may prove difficult because of interference from natural obstacles. Balloon, satellite, and hovering aircraft relays could all prove useful to some extent in overcoming these difficulties, but they increase the complexity of the system. Refractive and other atmospheric effects,

however, would still require transmitter tracking and thus further limit the operational utility. Requirements for light weight in the case of a tactical ground-ground system (perhaps carried by infantrymen) would in all probability prohibit the use of fog-dispersive techniques (described in Section 6) because of added weight and power requirements. Large lens techniques, providing a beam of wide diameter, might be used although they would increase the transmitter size and thus reduce the advantages accrued by compactness.

3.0 TACTICAL AIR-GROUND APPLICATIONS

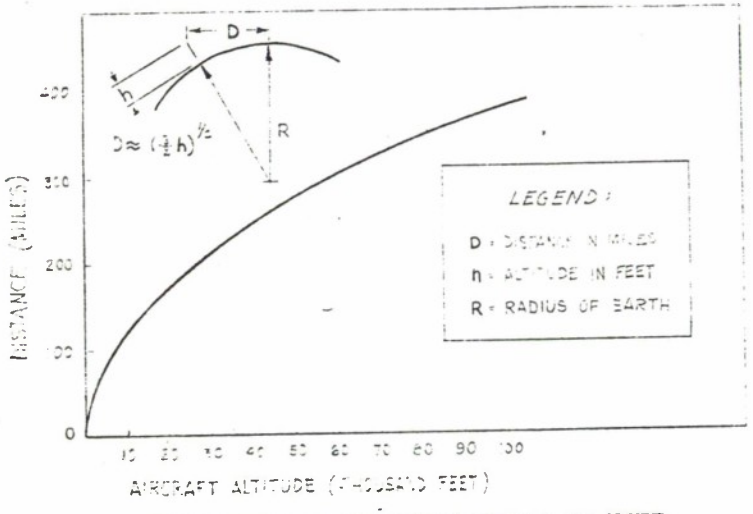
Real time transmission of video reconnaissance information from tactical reconnaisance craft to local command headquarters could prove yet another useful application of laser links. As shown in Figure 3-5, line-of-sight communication is theoretically possible within a radius of approximately 170 miles from a plane at an altitude of 21,000 feet transmitting to a ground receiver at sea level. At altitudes above 60,000 feet, the radius could be extended to more than 250 miles.

The small antennas necessary for a laser system could be designed to have a minimum aerodynamic effect on the aircraft and yet retain high directivity. Video bandwidths over an air-ground link are easily obtained with reasonable laser power output. Here, as in ground-based point-to-point usage, atmospheric attenuation in inclement weather is an important consideration. Transmission would be through an extensive segment of the earth's atmosphere, so that these effects are pronounced. In addition, diffraction and atmospheric turbulence effects would cause difficulties. Operation of a two way link to facilitate tracking would be difficult and fog dispersive techniques would be of limited use because of the ranges.

Despite these considerations, other limitations of certain tactical air-ground applications (for example, effective reconnaissance can only take place when weather conditions are favorable for light transmission) make laser transmission feasible for wideband air-ground links. Millimetric-wave techniques, however, are also favorable so that a comparison must be made of operational feasibility and design and economic considerations.

4.0 TACTICAL AIR-AIR APPLICATIONS

An extremely attractive area of utility for laser transmission exists in the requirement for secure intra squadron or intra airborne



LINE OF SIGHT DISTANCE BETWEEN AIRCRAFT AND GROUND LOCATION AS A FUNCTION OF AIRCRAFT ALTITUDE

FIGURE 3-5

mission communication support. Within the relatively close spacing of squadron aircraft, continuous, secure communications could be easily effected using laser transmission, since the total transmitted energy less that absorbed and scattered by the atmosphere can be received with small-diameter antennas. In addition, minimum beam spreading makes transmission extremely difficult to detect; therefore, continuous communication undetectable to an enemy could be maintained.

Since at high altitudes many of the deleterious features of atmospheric propagation are lessened, transmitter and receiver tracking and antenna syatem designs will be simpler. If this mode of operation is to be used at low altitudes, these considerations would become a factor once again. The nature of most low altitude missions, however, is such that short transmission ranges are usually required and thus should mitigate many of these effects. Additional data is required concerning the effects of high speed air flow at high altitudes on the propagation of light beams. The turbulence effects caused by the air flow alonside an aircraft may considerably limit the effectiveness of a laser link using an airborne terminal.

Secure command and control of rather widely spaced aircraft on short reaction time logistical missions is also a possibility using laser transmission techniques. Two aircraft at an altitude of 50,000 feet have a communication range of 500 miles so that spaced aircraft missions such as those involving large scale troop transfers could be supported.

5.0 AIRBORNE RADIO RELAY

From the previous discussion in paragraphs 3.0 and 4.0, it is evident that lasers would also prove useful in support of airborne radio relay systems, such as those used to erect or repair a communication network in emergency conditions. Similarly, laser links could be used with balloon relay stations to provide short reaction time tactical communication.

6.0 AIRCRAFT OVER THE HORIZON COMMUNICATION

Lasers provide the means whereby an effective communication link may be provided from an aircraft to a satellite for relay to ground control centers. The small size of laser transmitting antennas enables appreciable bandwidths to be transmitted to an orbiting satellite with

few aerodynamic effects on the aircraft. Since problems of locating and tracking random satellites would be difficult to solve, (handover and continuous tracking of the aatellite would be required) a synchronous satellite in this mode would be preferable from the standpoint of aircraft operation.

Also, the implementation of aircraft-satellite relay on an operational basis must be considered. If highly directive antennas (or optics) are used aboard the satellite, a complex aiming and tracking system must be used to locate and track a particular aircraft or group of aircraft. If, on the other hand, wide acceptance angles are used in satellite antennas, energy is received by the satellite from the earth's irradiance during sunlight hours. In addition to proper filtering, satellite multiple access techniques must be developed at laser frequencies to permit effective use of such a satellite relay. However, schemes such as RADA (Random Access Discrete Address) and other multiple access techniques have been devised for use in the microwave portion of the spectrum and could be extended for use with laser transmisaion.

Additional effects must be considered and examined, such as the effect on a beam of light by the highly turbulent air flow past a supersonic aircraft. However, these may be fixed effects that can be corrected since airflow patterns at high velocity should remain fairly constant. As was previously mentioned, additional experimental data in this area is required.

7.0 SPACE-SPACE, LINKS

The poasibility exists for the establishment of a laser link between a deep space vehicle and a station based either on the moon or on an earth satellite. This would probably be the most practical method for relaying information from a space probe to the earth using laser transmission. A laser link could be used between the probe vehicle and a satellite, and a microwave or another laser link could be used between the satellite and the earth. In this manner the problem of transmitting a laser beam from a deep space probe through the earth's cloud layer is circumvented.

Optical antenna gain limitations caused by atmospheric effects, such as dispersive beam broadening and short term atmospheric diffraction fluctuations, also make satellite based receiver stations attractive for deep space laser links. Dispersion effects can typically broaden an optical antenna beamwidth to 10 microradians, and fluctuations in atmospheric

diffraction at rates greater than 1 cps typically occur at amplitudes of 25 microradians at zenith. Servo system requirements to nullify these effects for the large astronomical mirrors that would be required to intercept appreciable amounts of energy from a probe are great so the 25 microradian figura presants a practical beam width limit for an earth based antenna. These effects are negligible in a lunar or satellite environment.

Considering atmospheric attenuation in addition to the above effects, a total of about 40 db may be saved in required satellite or deep space probe transmitter power by using a space or lunar based satellite receiver as opposed to an earth based receiver. This would result in corresponding weight savings in a deep space payload, although an extra satellite would be required. However, one such satellite or moon based station could serve a large number of missions.

8.0 PIPED LASER COMMUNICATION APPLICATIONS

Future developments may result in efficient laser transmission through optical "pipes" consisting either of fiber optics or physical pipes containing a controlled atmosphere. Of particular interest for military applications is the former technique whereby a cylindrical dielectric rod or fiber about one wavelength in diameter is used as an optical waveguide.

Fiber optical techniques allow the transmission of light through long, thin fibers of glass, plastic, or other transparent material. Light propagates through an optical fiber by a series of reflections from wall to wall. Injection of the light at a small angle to the axis of the fiber causes the light to be totally reflected at the inner surface thereby reducing the transmission loss to essentially the absorption loss within the fiber material itself. If parallel fibers are used, coupling between adjacent fibers may be prevented by insulating them with a thick jacket of transparent material with an index of refraction lower than that of the fibers. At present the losses are quite high, but future improvements may be anticipated.

For long distance applications, a cable containing amplifiers spaced at specific intervals would have to be used to overcome transmission loss. The optical fiber itself can act as a traveling-wave oscillator or amplifier. Laser action in fibers made of neodymium-doped glass features low

threshold powers and beam modes that are controlled by varying the cladding's index of refraction. At present these devices require optical pumping, limiting their use over long lengths of transmission.

Using fiber-optical techniques, cable of extremely lightweight and broadband characteristics is possible. Such a cable using fiber optics and laser amplifiers may provide a means whereby cable may be laid by helicopter or other aircraft and by fast lightweight vessels. This would permit the rapid implementation of point-to-point communication in contingency situations.

9.0 CONCLUSIONS

Lasers techniques are applicable to areas of communication where light weight, high directivity, and small antenna structures are required. In many of these applications, considerable competition will be offered by the advancing millimetric-wave technology, and further developments must be awaited in both areas to determine which technique will best fit communication requirements.

For fixed and mobile ground-based point-to-point applicstions, serious problems exist for laser applications. Although research in techniques such as fog dispersal may mitigate the adverse effects of weather on propagation, other portions of the spectrum such as microwaves and millimetric waves, that do not suffer the same propagstion effects may offer compsrable or better performance for most applications. Lasers thus show little promise of replacing these methods in ground-base point-to-point applications, slthough they may be used to augment existing or planned facilities. Although such laser links do show promise of being inherently secure, the general availability of ground-based point-to-point links to an enemy intercepter requires that security precautions such as encryption be used to ensure link privacy.

Similarly, tactical air-ground and ground-air laser systems suffer because the long line-of-sight path passes through the atmosphere. In addition, fog dispersive techniques are less effective at long ranges. Therefore, other propagation methods seem more attractive. The outstanding feature in favor of laser applications is the small size of the aircraft antenna that may be used to obtain a highly directive beam. Transmitted power, however, is not a critical consideration as in the case of an air-to-satellite link so that the degree

of directivity (requiring sophisticated tracking) obtainable with a laser beam is not generally required.

Lasers have a potential advantage in the implementation of tactical air-to-air, air-to-satellite, and aircraft radio-relay links. Small antenna structures capable of producing highly directive beams (required for security as well as power availability at the receiver) are advantageous in these applications, since required aerodynamic properties of the aircraft must be preserved. Additional information about the effects of atmospheric turbulence in close proximity to the aircraft is required.

Similarly in space-space applications, lasers will have much to offer for certain types of missions. Space conditions, however, do make the erection of lightweight stable antennas possible at microwave frequencies where photon noise does not limit system performance. Thus, the seeming advantage of lasers may not prove significant as new spacecraft antenna techniques become available.

Cables using fiber optics show promises of providing a lightweight submarine cable for military laser applications. At present, optical cable losses are high and considerable development is needed to make this technique feasible. Furthermore, the advantages to be accrued by furtherance of this development are contingent on the development of competing techniques such as satellite systems and other short reaction time communication techniques. The desirability of cable communication for certain Air Force applications ensures some degree of future applicability in conjunction with other systems and justifies the research needed to develop this communication technique.

SECTION 4
LASER TECHNIQUES AND COMPONENTS

1.0 GENERATION OF A LASER BEAM

The optical maser or laser is a device that amplifies and produces coherent light. The properties of the laser basically depend on the interaction of electromagnetic waves and matter.

Ordinary light radiation consists of photons released from atoms returning to a low energy state from which they were previously driven by an external source of energy. In ordinary thermal-type sources, atoms are energized by interatomic or intermolecular collisions and then spontaneously lose their energy (Reference 1). The resulting emitted energy is in the form of independent photons that differ in frequency, polarization, and direction of motion, and that distribute randomly in time. The radiation thus emitted has the general characteristics of wideband noise, with the average amplitude of radiation modulated by the random fluctuation of the number of photons emitted in a manner similar to that of the shot effect in a beam of electrons.

Laser radiation, on the other hand, exhibits coherency in that the emitted light is near monochromatic, the photons are emitted with spatial and phase coherence, and the average energy exhibits little noise-like amplitude fluctuation. Coherent light waves behave in the same manner as electromagnetic radiation occuring at lower frequencies. Thus, beam spread is determined by the physical relationships existing in the laser (cavity dimensions and light wavelength), resulting in extremely narrow radiation beamwidths with small structures. In the case of non-coherent light, the beam spread is determined by relationships between the size of the finite emitting source aod reflectors used to shape the light beam, resulting in a requirement for much larger structures. Furthermore, spatial coherence of such a source is considerably less than that of a laser beam, since there is non-uniformity of phase across the source.

1.1 COHERENT LIGHT GENERATION

Coherency in light may be obtained by a variety of methods. Optical specialists have been producing reasonable approximations to coherency for some time; for example, monochromaticity (phase and

frequency coherency) is obtained by using an optical filter with a narrow line width at the output of the light source. Spatial coherence is obtained by passing the light through a small pinhole to provide a point source. Since the power of the coherent signal is too small for any practical application, this method is useful only for laboratory experiments. Conversely, lasers produce useful power levels of coherent light.

1.1.1 Photon Concept

Laser action is obtained by causing the light radiation process, photons released from atoms returning to a low energy state from a high energy state, to be confined to several specific energy states of the atom. Thus all the energy released from the atom is due to the same quantitative loss in energy per photon, resulting in a single frequency of output. In understanding this process (the photoelectric effect) the concept of the photon is required.

A metallic surface emits electrons when illuminated by light of short wavelength. The number emitted in any time interval is proportional to the intensity of the light impinging on the surface, and their kinetic energy (E) is a linear function of the frequency (f) of the impinging photons. The kinetic energy of a single electron is given by:

$$E = h(f - f_1) \quad \text{joules} \tag{4-1}$$

where h = Planck's constant, 6.626×10^{-34} joule-sec

Thus, incident radiation is made up of bundles of photons, esch having energy hf. If hf exceeds hf_1, the energy necessary for an electron to cross the potential barrier at the surface of the metal, the electron is emitted with a kinetic energy corresponding to the excess $h(f - f_1)$. If hf_1 is not exceeded, the impinging energy is absorbed by the electron and it is raised to a higher energy state within the atom. The process is reversible, since an electron falling from a higher to a lower energy state emits radiation at a frequency given by:

$$f = \frac{\Delta E}{h} \quad \text{cps} \tag{4-2}$$

where ΔE is the difference in energy levels within the atom.

In a normal atom at thermal equilibrium, electrons may be in a number of discrete electric or magnetic energy levels. With two

energy levels E_1 and E_2 ($E_2 > E_1$) that have N_1 and N_2 electrons, each electron will pass from one state to the other and absorb or emit photons of electromagnetic energy $E_2 - E_1$ of frequency $f = (E_2 - E_1)/h$. At thermal equilibrium the distribution of electrons in the two states is given by Boltzmann's law:

$$\frac{N_2}{N_1} = \epsilon^{-(E_2 - E_1)/KT} \qquad (4\text{-}3)$$

where K = Boltzmann's constant, 1.3804×10^{-23} joule/K°

T = Temperature in degrees Kelvin

The higher energy state thus has the least electrons. The equilibrium is statistical, and the electrons comprising the system or population continually undergo transition from one state to the other. A specific electromagnetic energy density is obtained if this system is enclosed, say, by a cavity. The frequency is given by equation (4-2).

1.1.2 Population Inversion

In such an enclosed system, three distinct effects take place: production of radiation by spontaneous emission, amplification by induced emission, and attenuation by absorption. At equilibrium the attenuation is greater than the amplification, and equilibrium is maintained by the generation of new radiation by spontaneous emission. If it were possible to make N_2 larger than N_1, a population inversion would result and the incident radiation leaving the cavity would be more intense than the radiation entering, resulting in amplification. The basic problem of the laser is to create a population inversion sufficient to surmount the losses necessary to overcome the absorption (which are analogous to the losses in any physical system). Once this has been done, however, spontaneous emission constitutes an unfavorable factor since it tends to depopulate the upper level and thereby decrease the amplification.

1.1.3 Three and Four Level Energy Systems

A number of processes have been developed for obtaining population inversion. The processes using 3 or 4 energy levels invented by Professor N. Bloembergen in 1956 represents the most common one and is of general interest.

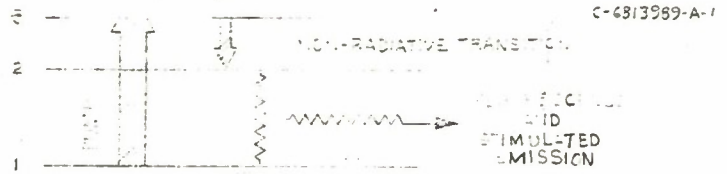
In the system having three energy levels (1, 2, and 3) as shown in Figure 4-1, illumination with radiation at a frequency of $(E_2 - E_1)/h$ can be best produce equal populations in the two levels because of the relationship between absorption and induced emission coefficients. If the system is illuminated with radiation at a frequency $(E_3 - E_1)/h$, however, an inversion in population can take place between levels 2 and 1 or between levels 3 and 2. For example, assuming the probability of transition from 2 to 1 is much smaller than that from 3 to 2 or from 3 to 1, the states of the atoms comprising the system will tend to accumulate in level 2 and an inversion can occur between 2 and 1. If, on the other hand, the probability of transition from 3 to 2 is smaller than the others, a good chance exists of being able to invert the population of 3 with respect to 2.

In the three level laser just described, the useful transition considered is that from level 2 to level 1, implying that level 1 is considerably depopulated; therefore, it has been pumped intensively. This dependence of the inversion on the pumping rate can be reduced considerably by the introduction of a fourth level as shown in Figure 4-2. In this case, if the probability of transition from 2 to 1 is high, the population of 3 will be easily inverted with respect to 2.

It is generally advantageous to widen the upper level and form an absorption band instead of a line, since high excitation power is difficult to obtain in a narrow frequency band. Such band widening can be obtained by inducing an electric field in the crystal, resulting in the Zeeman effect.

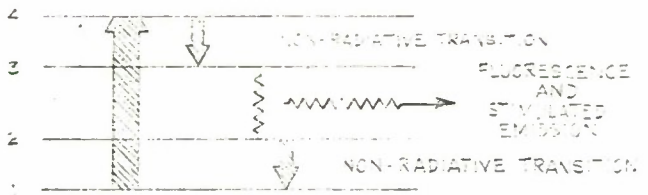
The actual fluorescence phenomenon in atoms is considerably more complex than just described. In general, numerous radiative ss well as non-radiative transitions are possible within the atomic structure, and likely candidates for lasing action must be evaluated by examination of the level diagrams of the atoms involved.

A simplified diagram of the helium-neon laser is shown in Figure 4-3. Helium electrons are excited to level 4 and give up their energy to the neon atoms by a collision process. The neon electrons then return to the ground state through radiative transitions from level 3 to level 2 and non-radiative tranaitions from level 2 to level 1. The collision transfer of energy from the helium to neon atoms is facilitated by the close correspondence of excited energy levels.



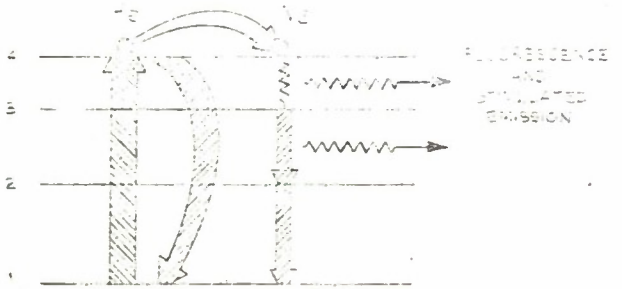
THREE-LEVEL ENERGY DIAGRAM

FIGURE 4-1



FOUR-LEVEL ENERGY DIAGRAM

FIGURE 4-2



HELIUM-NEON GAS LASER ENERGY DIAGRAM

FIGURE 4-3

1.2 GENERATION OF LASER POWER

Laser power is usually generated by containing the laser material within the walls of a cavity and exciting it until inversion occurs. The electrons will then return to the state of equilibrium through spontaneous emission of photons at a frequency given by equation (4-2).

Energy losses within the cavity may be defined in terms of the cavity Q factor by the following equation:

$$Q = \frac{f_0}{2\Delta f} = 2\pi f_0 T \qquad (4\text{-}4)$$

where Δf is one-half the bandwidth of the cavity, f_0 is the cavity center frequency, and T is the time required for the energy stored in the cavity to drop to $1/\epsilon$ of its initial value. In laser systems (as opposed to microwave systems) the bandwidth of the transition itself is much wider than the cavity resonance. As a result, the spontaneously emitted photons have the possibility, with variable probabilities, of exciting all those modes of the cavity with frequencies inside of the transition band. In those modes where the population inversion is sufficient to compensate for losses, an increasing enforcement of the mode is caused by induced emission. The excited modes of the cavity then compete, those with the greatest reinforcement tending to be those with the least losses and with frequencies nearest the center of the transition bandwidth.

In certain cases, it is possible to restrict oscillations to a single mode or a group of modes having very close characteristics. If a fraction of this mode radiates to the outside, a radiation that is coherent occurs since it has simultaneously the space and time coherence of the mode existing inside the cavity. The Q factor of the cavity is thus seen to be the determining factor of the coherence of the emitted wave.

Cavities used with lasers have dimensions that are extremely large with respect to the wavelength of the radiation (on the order of 10^5 to 10^6 wavelengths). One such optical cavity, which uses two confocal spherical mirrors to contain the radiation, is the optical cavity analogous to Fabry-Perot interferometers. Stationary waves are formed by superposition of spherical wave systems. Partial reflectivity of one of the walls allows radiation to the outside.

2.0 LASER TECHNIQUES AND COMPONENTS

2.1 GENERAL LASER MEDIA REQUIREMENTS

The main requirements (References 2 and 3) for a laser medium are:

(a) The laser medium should have as little absorption as possible, at the signal frequency, caused by factors other than the transition between the two direct lasing levels; such absorption tends to introduce additional loss in the optical cavity.

(b) The excited atoms must not absorb energy at the signal frequency. Such absorption not only causes loss in the cavity but also decreases the population of the upper laser energy level.

(c) The lifetimes of the lasing levels should enable a population inversion (Reference 2). In some cases the lifetime of the upper level does not have to be longer than that of the lower level (Reference 4).

(d) The natural linewidth ($\Delta\nu$) should be as small as possible, since the threshold pumping power to maintain laser oscillation is proportional to $\Delta\nu$.

(e) For continuous laser operation, the laser transition should enable the lower level to be depopulated, if necessary, by cooling.

2.2 OPTICALLY PUMPED SOLID-STATE LASER MEDIA REQUIREMENTS

For optically pumped solid-state lasers, additional requirements (Reference 2) are:

(a) The material should possess broad, strong absorption bands and reasonably high quantum efficiency.*

(b) The material should have narrow and sharp fluorescent lines.

(c) The material should be of sufficiently high optical quality that scattering caused by optical heterogeneities introduces negligible loss to the optical cavity system.

---

* Quantum efficiency is usually defined as the probability that the absorption of a pump photon will result in the emission of a signal photon.

2.3 CLASSIFICATION OF LASERS

Lasers can be classified according to type of material or method of excitation:

Type of Material	Method of Excitation
Gaseous	Collision Pumped
Cesium vapor	Electrically Pumped
Helium-Nitrogen	Explosively Pumped
Nobal gas	Laser Pumped
Liquid and Organic	Optically Pumped
Solid State	Solar Powered
Glass and optical fiber	
Rare earth	
Ruby	
Semiconductor (injection)	

Collision pumped lasers are excited by energy transferred electron-atom, atom-atom, or atom-molecule (molecular dissociation) collision. Explosively pumped lasers are pumped by the light from a shock wave caused by the detonation of a high explosive.

The brief description of laser properties given in Appendix II shows that a number of generation techniques are available and more are being developed. As a result, methods of generating laser power should become available over the entire light spectrum.

3.0 REFERENCES

1. Lasers; M. Pauthier; Electrical Communication, Vol 37, No. 4; 1962
2. The Laser; A. Yariv and J. P. Gordon; Proceeding of IEEE; Jan 1963
3. Lasers and Applications; Ohio State University; 1963
4. Optically Pumped Solid State Lasers; T. H. Maiman; Solid State Design; Nov 1963

SECTION 5

GENERAL LASER COMMUNICATION SYSTEM ANALYSIS

1.0 DELINEATION OF LASER COMMUNICATION SYSTEM COMPONENTS

Components of a laser system are generally the same as for any other radio relay link. The techniques for accomplishing certain of the communication functions (power generation, modulation, detection, etc) differ markedly from those used with lower frequency radio links, and comprise the areas in which considerable effort must be expended before embodiments of laser communication systems can be expected.

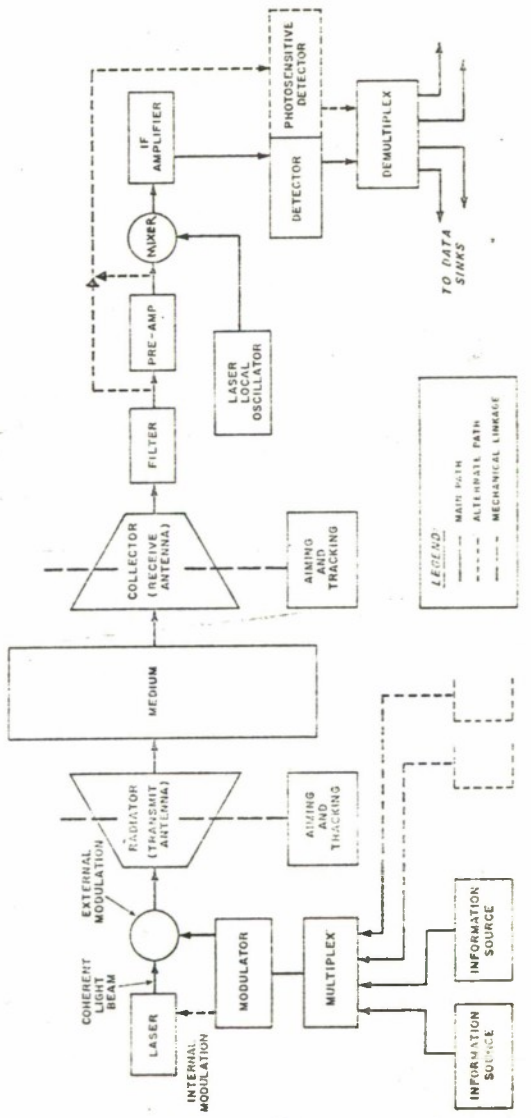
1.1 BLOCK DIAGRAM DESCRIPTION

As is shown in Figure 5-1, information sources are multiplexed to form a composite baseband modulating signal as is done for any communication link. The modulated signal is fed to a laser modulator that either modulates the laser beam within the laser cavity (internal modulation) or modulates the laser beam outside of the laser cavity (external modulation). The beam is then appropriately shaped by a transmitting antenna (or optics in the case of laser) and aimed at the receive antenna through a transmission medium. In certain of the media (for example, free space and the earth's atmosphere) aiming and tracking functions must be included at the transmitter and receiver, respectively. In atmospheric links, moreover, both functions may have to be included at both transmit and receive sites, depending on the choice of optics and the particular atmospheric conditions.

Laser energy from the receive antenna is filtered and fed to a preamplifier or photosensitive detector. The concept of a laser receiver may include local oscillators, mixers, and intermediate frequency (IF) amplifiers much the same as any radio relay receiver, although current laser techniques generally require an optical (or photosensitive) detector immediately after the filter or preamplifier. (Laser heterodyning techniques require additional research and development.) The resulting baseband signal is demultiplexed and sent to the data sinks.

1.2 MULTIPLEX EQUIPMENT

Multiplexing equipment for laser communication systems is generally no different from that used with any communication link for the same type of information to be transmitted. Short range laser systems



LASER COMMUNICATION SYSTEM BLOCK DIAGRAM

FIGURE 5-1

when used to their full potential (that is, a basebsnd modulation bandwidth of several gigacycles), however, require multiplexing techniques that can form a wideband composite signal. This same problem is encountered when high data rates are used by other transmission techniques, such as millimetric-wave relay, so that it is not unique to laser systems. For this reason, multiplexing is not thoroughly covered in this report.

1.3 MODULATION EQUIPMENT

Modulation of a laser beam presents many unique problems. Internal modulation of lasers (changing cavity parameters or pump power) results in a large degree of nonlinearity. Moreover, high tolerances are required on laser components. The potential bandwidths of modulation thus obtained are also limited by the high Q cavity. On the other hand, external modulation techniques thus far demonstrated require considerable input power (on the order of watts) and result in loss of laser output power. However, new materials show promise of reducing this power requirement considerably. The potential bandwidths obtainable with external modulation (10 gc subcarrier modulation has thus far been obtained showing the existence of the electro-optical effect at 10 gc), however, are much greater than those for internal modulation. One exception to the bandwidth restrictions on internal modulators is the gallium arsenide laser using pump power modulation. Laser modulators are more thoroughly treated in Section 7 of this report.

1.4 GENERATION OF LASER ENERGY

The laser itself usually takes the form of a very simple device. Depending on the techniques used and on the degree of coherency required, cooling devices may have to be used. When considerable power output is desired, maintaining low temperatures (about 20°K to 70°K for gallium arsenide) is extremely difficult because of losses encountered within the laser material. However, techniques of obtaining reasonable power outputs with room temperature devices do exist, and indications are that laser powers required for most communication purposes (on the order of watts) will be available. Laser power generation and techniques are discussed in Section 4 and Appendix II.

1.5 ANTENNA TRACKING

Because of the narrow beamwidth of laser transmission (which is perhaps its most attractive feature), aiming of the transmitted laser beam is extremely difficult. Tracking of receiver optics, however, should not present problems since in most applications receiver acceptance angles can be made quite large. If narrow angle receivers are required (as would be the case where a noisy background is encountered), tracking schemes could be used that are similar but are more precise than those used with present radio systems having directive antennas. Unique laser tracking problems occur in earth-based laser transmission systems where atmospheric effects cause high speed, unpredictable beam deflection. Here, tracking systems that allow transmitter tracking by a closed loop system would be required. Such a system requires transmission of tracking data to the transmitter from the receiver. Considerable effort will be required for such systems to be proven. Since earth-based systems will generally be short range, however, indications are that such systems are feasible. Aiming and tracking in laser systems is discussed in Section 8.

1.6 TRANSMISSION MEDIUM

The laser transmission medium varies with the application. The greatest difficulties are those encountered where ground-based laser terminals are used. Atmospheric effects on propagation, including refraction and attenuation, reduce the tracking ability and make adequate receiver power difficult to maintain. Transmission of laser radiation through the atmosphere is covered in Section 6.

1.7 DETECTION AND DEMULTIPLEX EQUIPMENT

Because of the difficulties in coherent mixing, current receivers directly detect the incoming light beam (dashed lines in Figure 5-1). A number of devices for direct detection of light beams are available with considerable bandwidth capability. Because of the use of these direct detection devices, laser receivers are fairly simple devices. The heterodyne receiver, on the other hand, is more complicated because of the necessity for control of the local oscillator and mixing. In certain applications where systems are power limited (for example, with deep space probes), however, their improved receiver noise characteristics warrant the additional complexity. Laser receiver considerations are presented in Section 7.

Demultiplexing of the received baseband aignal is similar to that used by conventional receivers for such wideband signals, and it generally will present no special considerations when applied to a laser communication system.

2.0 LASER COMMUNICATION SYSTEM ANALYSIS

The great interest aroused in the study of the application of lasers for communication systems is that these devices possess some unique characteristics with respect to other carrier generators. These characteristics are:

(a) Narrow beam spread
(b) High spectral radiance
(c) High carrier frequency
(d) Reasonably compact and economical systems

The narrow beam spread permits the realization of good capture of the beam energy at the receiving point; on the other hand, the utilizstion of this characteristic requires the use of sophisticsted direction and pointing accuracy control.

Theoretically, the achievement of a large information bandwidth is a simple problem in the case of lasers, as their carrier frequency is extremely high. For example, with respect to carrier frequencies of about 10^{14} cps, modulation bandwidths of 10 gc represent a bandwidth to carrier ratio of only 10^{-4}. In practice, modulation methods capable of achieving such bandwidths with desirable linearity and sensitivity have not been developed. Methods of superposition of various modulation subcarriers are rather cumbersome, and with their complexity reduce the advantages inherent in the application of laser communication systems.

At present, it can be stated that relatively narrow-band communication systems, consisting of as many as 20 or more television channels or an equivalent number of voice channels, are feasible with lasers.

The limitations for ground-based point-to-point usage are caused by signal fsding, which is produced by turbulence and heterogeneities of the atmospheric medium. These effects, which are well known to astronomers (twinkling of the stars), are more strongly in evidence when the propagation path is close to the ground. They result in noise intensity modulation, as well as in instability of the optical collimation and

focuaing accuracy. Space systems do not suffer from these effects and are only limited by the system tracking accuracy.

Laser communication systems (neglecting atmospheric transmisaion) may be treated in terms of two general communication system categories: transmiasion through free space and transmission through a contained medium such as a metal light pipe or fiber optics. Free space laser communication analysis presents essentially all the basic considerations of a laser link, similar to those of any free space radio link. A detailed treatment of laser transmission considerations imposed by transmission through the atmosphere is found in Section 6.

Laser transmission through a contained medium is covered by considering transmission through metal guides, fiber optics, and metal light pipes. Metal guides enclose a controlled atmosphere within which unperturbed free space transmission of laser beams can occur. Fiber optics provide waveguides for laser transmission by virtue of the difference in dielectric constant inside and outside the fiber. Metal light pipes form metallic waveguides where the propagation mode is one of multiple reflection along the pipe or guide. (These multiple reflections result in signal distortion.)

The following paragraphs analyze various laser communication links, free space systems, use of metal guides containing a controlled atmosphere, fiber optics systems, and metsl light pipes.

2.1 FREE SPACE LASER COMMUNICATION SYSTEMS (Reference 1)

2.1.1 Free Space Path Loss

Consider a laser transmitting a uniform distribution of power (P_t) over the solid angle (Ω_t), defined as A/R^2 where A is the area intercepted at the surface of a sphere of radiation and R is the radius of the sphere. The maximum sharpness of Ω_t is achieved in the diffraction limited case and is given by:

$$\Omega_t = \frac{\lambda^2}{A_t} \text{ ateradians} \qquad (5\text{-}1)$$

where λ is the radiation wavelength and A_t is the transmitter radiation area. The area illuminated at a distance R by such a transmitter is $R^2\Omega_t$. The signal power (P_r) picked up by a receiver at this distance is

determined by the fraction of the illuminated area intercepted by the receiver collector (A_r). Then

$$P_r = P_t \frac{A_r}{A} = P_t \frac{A_r}{R^2 \Omega_t} \text{ watts} \qquad (5\text{-}2)$$

$$P_r = \frac{P_t A_r A_t}{R^2 \lambda^2} \text{ watts} \qquad (5\text{-}3)$$

From equation 5-3 it is evident that for fixed aperture of the receiver and transmitter antennas, the higher the frequency (or the shorter the wavelength) of the radiation, the larger the power received. This result is significant in that relatively small aperture transmitting antennas can result in considerable receiver power because of the high frequencies used in laser communications.

2.1.2 Noise Limitations

The limitation on a laser communication system as with any other communication system is the presence of noise in the received signal. Aside from noise introduced by the receiver detection process, the noise contribution to the receiver arises from two sources: thermal noise of the transmitter background, and noise arising from the granular nature of the received signal (which is comprised of a stream of photons), which is referred to as quantization noise. In laser systems the latter noise source generally produces the most pronounced effect.

Background noise in free space arises from a superposition of extra terrestrial sources of which the sun is the most powerful single source. In general, the magnitude of this noise varies both with frequency and with the direction in which the receiving antenna is pointing. It is informative, however, to consider the contribution from a uniformly heated background, the temperature of which may be set corresponding to a level of radiance encountered in the sector of space that is of interest.

Assume a uniformly heated background with a spectral radiance S (a measure of power radiated per unit area per unit solid

angle per unit wavelength width). The noise picked up at the receiver due to this background will be proportional to the solid angle (Ω_r) intercepted by the receiver collector as seen from the noise source, the background area (A_b) intercepted by the solid angle of the receiver field of view (Ω_d), and the spectral width of the receiver filter of the preamplifier (F). The background noise power (P_{nb}) received would then be:

$$P_{nb} = FS\Omega_r A_b \text{ watts} \qquad (5\text{-}4)$$

or substituting $\Omega_r = A_r/R^2$, and $A_b = \Omega_d R^2$

$$P_{nb} = SA_r \Omega_d F \text{ watts} \qquad (5\text{-}5)$$

The background noise under this assumption is thus independent of the range. The signal-to-noise ratio (S/N) before detection under background limited conditions is, using (5-2) and (5-5),

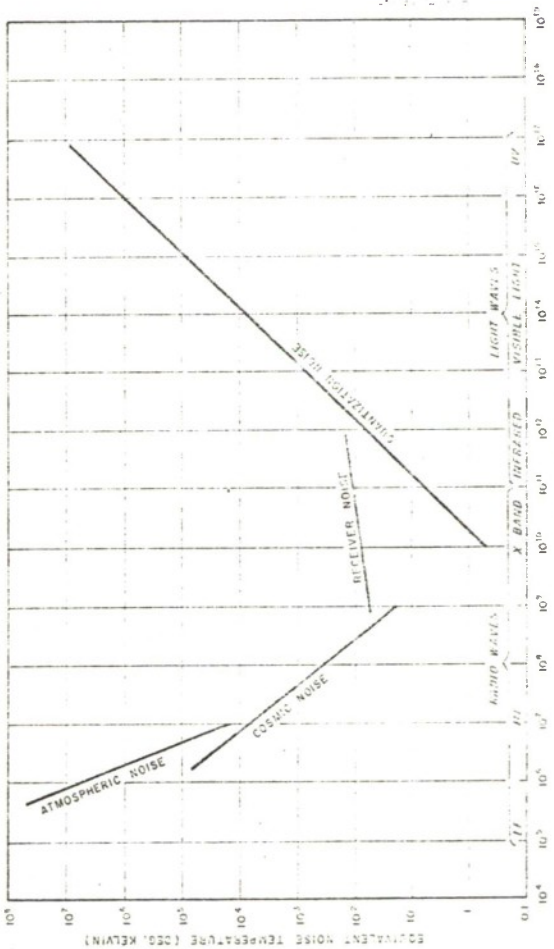
$$\frac{S}{N} = \frac{P_r}{P_{nb}} = \frac{P_t}{R^2 \Omega_t \Omega_d FS} \qquad (5\text{-}6)$$

or using (5-3) and 5-5)

$$\frac{S}{N} = \frac{P_t A_t}{R^2 \lambda^2 \Omega_d FS} \qquad (5\text{-}7)$$

Equations 5-6 and 5-7 indicate that the signal-to-noise ratio can be increased by limiting the receiver field of view. Obviously, this is no longer true if, as may be the case in outer space, the noise background consists of widely scattered discrete sources. In such cases a summation or integration over the background intercepted area (A_b) would be necessary.

Figure 5-2 shows the noise distribution over the frequency spectrum for free space. From this figure it is evident that at the frequencies of interest, background noise generally plays a minor



NOISE DISTRIBUTION OVER FREQUENCY SPECTRUM

FIGURE 5-2

role as opposed to quantization noise. This is no longer true when background radiation such as that resulting from radiation of clouds by sunlight is considered.

The quantum nature of radiation introduces a second type of noise. The energy of each photon is directly proportional to the radiation frequency (f) according to the expression E = hf, where h is Planck's constant (6.626×10^{-34} joule-sec). For a given radiation power there will be available only a corresponding number of photons per unit time, and as the carrier frequency is increased fewer photons become available to carry the information. Futhermore, the photons arriving at the receiver do so in a random manner. If a Poisson distribution of photon emission is assumed and $\bar{n}$ is the average number of photons per unit time arriving at the receiver, the root-mean-square deviation of photons at the receiver is:

$$n_{rms} = (2\bar{n}B_r)^{1/2} \quad \text{photons/sec} \tag{5-8}$$

where B_r is the receiver bandwidth.

The inherent noise power in the signal (P_{ND}) is then the rms number of photons/time multiplied by the energy of each photon:

$$P_{ND} = hfn_{rms} = hf(2\bar{n}B_r)^{1/2} \quad \text{watts} \tag{5-9}$$

Since the total power being received is:

$$P_r = \bar{n}hf \quad \text{watts} \tag{5-10}$$

$$P_{ND} = hf\left(2B_r \frac{P_r}{hf}\right)^{1/2} = (2hfP_r B_r)^{1/2} \quad \text{watts} \tag{5-11}$$

The noise power is therefore increased by both the bandwidth and the frequency of radiation as expected.

From (5-10) and (5-11), S/N can be determined, disregarding background noise:

$$\frac{S}{N} = \left(\frac{P_r}{2hfB_r}\right)^{1/2} = \left(\frac{\bar{n}}{2B_r}\right)^{1/2} \qquad (5\text{-}12)$$

All quantum detectors are square law detectors because the input power is proportional to the number of photons, which is also proportional to the detector current. The power output of the detector, however, is proportional to the square of the current. By this reasoning, in the case of an ideal detector, 100% quantum efficiency and no noise:

$$\left(\frac{S}{N}\right)_{out} = \left(\frac{S}{N}\right)^2_{in} \qquad (5\text{-}13)$$

Therefore, after detection (5-12) becomes:

$$\frac{S}{N} = \frac{P_r}{2hfB_r} \qquad (5\text{-}14)$$

or

$$\frac{S}{N} = \frac{\bar{n}}{2B_r} \qquad (5\text{-}15)$$

Substituting (5-2) in (5-14), the following general design equation of a photon noise limited laser communication link can be written:

$$\frac{S}{N} = \frac{P_t A_r}{R^2 \Omega_t \, 2hfB_r} \qquad (5\text{-}16)$$

or substituting (5-3) in (5-14):

$$\frac{S}{N} = \frac{P_t A_r A_t}{R^2 \lambda^2 \, 2hfB_r} \qquad (5\text{-}17)$$

As an example of an ideal deep space laser communication link, consider a space vehicle in the vicinity of Mars transmitting to an Earth satellite, a distance of approximately 4×10^{10} meters. A 10 mc modulation bandwidth is assumed for voice and television signals. The receiver has a collector area of 1 m^2, an ideal detector that introduces

no noise, and a 100% quantum efficiency. For proper signal reception a S/N of 10 will be imposed on the system. To ensure proper tracking and aiming of the transmitter and receiver with present-day techniques, Ω_t is restricted to 1.85×10^{-9} steradians, which corresponds to 10 seconds of arc beamwidth. From equation (5-1) and assuming a radiation wavelength of 1μ (3×10^{14} cps), this beamwidth would require a transmitter aperture of area:

$$A_t = \frac{\lambda^2}{\Omega_t} = \frac{(10^{-4})^2}{1.85 \times 10^{-9}} = 5.4 \text{ cm}^2$$

The designer now must find the required transmitter power to make such a system feasible. Assuming that the background noise at 10 mc is negligible compared to the photon noise, the following equation may be directly applied to find the required transmitted power:

$$P_t = \frac{(S/N)R^2 \, \Omega_t \, 2hfB_r}{A_r} = (10)(4\times10^{10})^2 \, (1.85\times10^{-9})(10^7)(4\times10^{-19}) \qquad (5\text{-}18)$$

$$\cong 120 \text{ watts}$$

At present, operational cw lasers, either gas or solid state, have outputs of only a few milliwatts, although higher powers have recently been obtained with semiconductor lasers. Pulsed ruby lasers exist with peak power capabilities of several megawatts for a few nanoseconds. Pulse repetition rates, however, are presently limited to only a few per second at these power levels.

2.1.3 Free Space Laser Communication System Examples

As a practical example of a free space laser link, consider transmission between a satellite and a desert-located ground station (Reference 1). The satellite laser link chosen for analysis consists of a laser transmitter (ground or satellite) that operates at 0.63μ, which is the visible line of the He-Ne gas laser, a video modulator, a transmitting telescope, a receiving telescope, a 0.001μ bandwidth optical receiver filter, and a photomultiplier tube with an S-20 response.

Data for a photomultiplier with an S-20 response yields a maximum quantum efficiency (q) of 0.18 and a dark current (i_d) of 0.3×10^{-15} ampere.

In a practical system, P_r incident on the phototube is given by:

$$P_r = P_t \frac{A_r \eta_t \eta_r T}{R^2 \Omega_T} = \frac{P_t \eta_t \eta_r D_r^2 T}{\theta_t^2 R^2} \text{ watts} \qquad (5\text{-}19)$$

where η_t and η_r are the efficiencies of the transmitter and receiver optics, respectively, D_r is the diameter of the receiver antenna, T is the transmittance of the atmosphere assuming clear weather and a minimum antenna elevation angle of 30°, and θ_t is the receiver field of view.

The noise power caused by background radiation has a maximum value of:

$$P_{nb} = \frac{\pi^2}{16} \eta_r F \theta_r^2 D_r^2 N_s \text{ watts} \qquad (5\text{-}20)$$

where N_s is the noise spectral density of the clear sky at 0.63μ (5×10^{-6} watts/cm^2-A°-steradian).

The dark current, i_d, of the phototube may be represented by an equivalent power at the input of the phototube:

$$P_d = \frac{i_d hf}{qe} \text{ watts} \qquad (5\text{-}21)$$

where e is the change on an electron.

The phototube currents generated by each of the above three input powers give rise to shot noise, which limits the system receiver bandwidth to:

$$B_r = \frac{qP_r^2}{2hf(S/N)(P_r + P_{nb} + P_d)} \text{ cps} \qquad (5\text{-}22)$$

If equations (5-19), (5-20), and (5-21) are substituted in (5-22) and the following parameters are assumed, the plot of transmitter power (P_t) as a function of receiver bandwidth (B_r) and receiver field of view (θ_r) is as shown in Figure 5-3.

S/N = 20 db	$i_d = 0.3 \times 10^{-5}$ amp
$\eta_t = 0.75$	$D_r = 80$ cm
$\eta_r = 0.75$	$R = 4.63 \times 10^8$ metera
$F = 0.001\mu$	q = 0.075 (non-optimum frequency in photodetector)
T = 0.01	$h = 6.62 \times 10^{-34}$ joule-sec
$f = 0.63\mu$	$e = 1.6021 \times 10^{-19}$ coulombs
$N_s = 5 \times 10^{-6}$ watts/cm^2-A°-steradian	

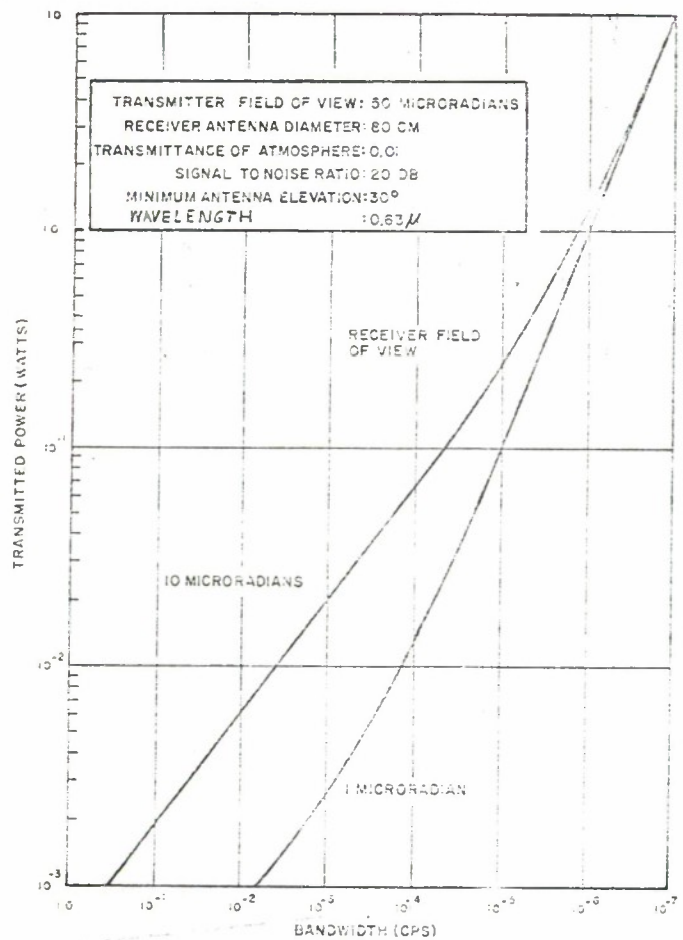
For transmissions from the earth, θ_t was chosen as 50 microradians, since atmospheric turbulence would limit system performance at narrower beam anglea. For transmissions from the satellite, the values for θ_t and θ_r are interchanged. Under these circumstances the received power is increased. If platform stability is important, the 1 microradian curve (diffraction limit for 80 cm optics) is used; if aiming accuracy is important, the 10 microsecond curve is used.

Transmission from a high altitude aircraft to a satellite would result in a lessening of atmospheric attenuation with a corresponding increase in bandwidth capability for a given power.

2.2 THE USE OF LIGHT PIPED THROUGH METAL GUIDES

It is well known that light is attenuated by the atmosphere, and under some conditions the attenuation may be severe. It hss been postulated that a metal pipe filled with s controlled atmosphere could be used to reduce the attenuation to a practical and constant value. Transmission around bends could be accomplished by prisms or other reflecting surfaces. Laser techniques are considered ideal for transmission under these conditions, since very narrow beams are readily possible and losses from the internal surface of the pipe can be reduced substantially.

Consider, for instance, a 100 km (54 nm) link established by tranamission through a 30 cm diameter pipe. The transmitted wavelength



TRANSMITTER POWER REQUIRED AS A FUNCTION OF BANDWIDTH FOR TRANSMISSION FROM GROUND TO SYNCHRONOUS SATELLITE

FIGURE 5-3

is 1μ ($f = 3\times10^{14}$ cps) from a gas laser that is operating in a single mode with near-coherent emission. Using a 30 cm diameter radiator, the beam is collimated to within 5 microradians with a suitable optical system. Assuming a modulation bandwidth (B) of 10 gc, a receiver collector area (A_r) of 706 cm^2 (30 cm diameter), a signal/noise ratio (S/N) of 100, and a detector quantum efficiency (η) of 0.01, the required transmitter power is:

$$P_t = \frac{(S/N)AB2hf}{\eta A_r} \qquad (5\text{-}23)$$

$$= \frac{(10^2)(1600\pi)(10^{10})(2)(6.6\times10^{-34})(3\times10^{14})}{(10^{-2})(2250\pi)}$$

$$= 2.8\times10^{-4} \text{ watts}$$

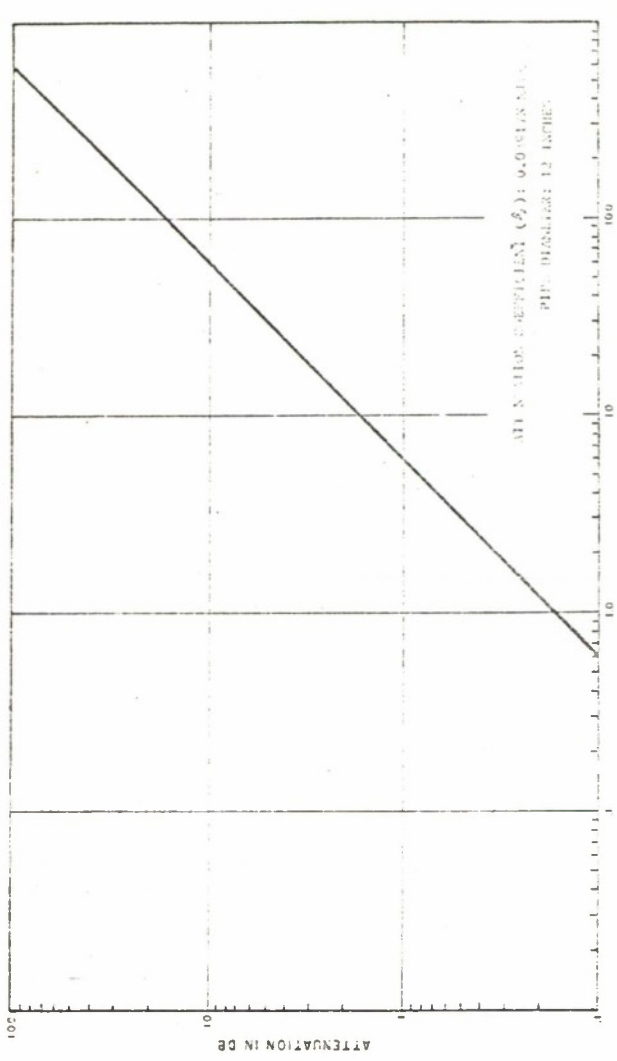
where A is the area of the transmitted beam at the point of interception by the receiving antenna. Thus less than 0.3 mw are required in such a system, well within today's capabilities.

In such a pipeline, mirrors must be used if bends are necessary. Mirrors introduce reflection losses and the problem of stabilizing the position of the mirror.

Unfortunately, factors limiting the normal use of a very long track of pipeline are the inevitable mechanical vibrations at the transmitting source and at the receiving terminal. These factors appear at present to limit the possible maximum single span length to 20 to 30 miles. Figure 5-4 shows the attenuation that may be expected for straight line propagation through a 12 inch (30.5 cm) diameter pipe.

2.3 FIBER OPTICS (MULTIPLE DIELECTRIC WAVEGUIDE)

Light may be guided in a manner similar to that used for guiding microwaves, that is, by multiple reflection of energy from the wall of the guide. As with microwave waveguide, there is a cut-off frequency below which no propagation occurs. Because the size is related to the wavelength, waveguides for light are microscopic; and the only way to increase the efficiency is to bind many of them together. This technique is known as fiber optics.



CONDITIONED PIPE LIGHT LOSSES IN VISIBLE RANGE

FIGURE 5-4

Each fiber is made with highly conductive optical glass, surrounded by a coating with a low refractive index to ensure internal reflection and to eliminate transverse coupling to neighboring fibers. Because of the small diameter of the individual fibers, the guide may be bent without loss of energy.

In the fiber optic theory, the total flux transmitted can be calculated, provided a transmission function (t) that depends on the properties of the fiber and the orientation of the ray is introduced:

$$F_t = \iint tI(\theta,\emptyset)\, dA_f\, d\Omega \qquad (5\text{-}24)$$

where,

F_t	= total flux transmitted
$I(\theta,\emptyset)$	= angular distribution of light intensity in fiber core, spherical coordinates
dA_f	= element of area in cross section of fiber at end of fiber
$d\Omega$	= element of solid angle
t	= transmission function of a given ray
$\theta,\emptyset$	= spherical coordinates

This formulation assumes that all rays are incoherent and there is no possibility of interference of any kind.

When a modulated laser beam is sent through a bundle of fibers, the amount of light detectable outside the bundle is practically zero for two reasons:

a. To reduce the amount of escaping rays from the external cylindrical wall, a second low refractive cladding is provided over the bundle of fibers.

b. To preserve the fibers against damage or dust, s plastic black cover is placed over the assembled fibers, so no light may be detected outside the bundle.

Maximum allowable attenuation depends on the sensitivity of the receiver, the noise threshold of the detector, and the light power introduced at the input. Although the first two parameters may improve with the state of the art; the third is determined by the quality of optical glass used in the fibers, the temperature of the bundle, and the method of coupling the light into the bundle.

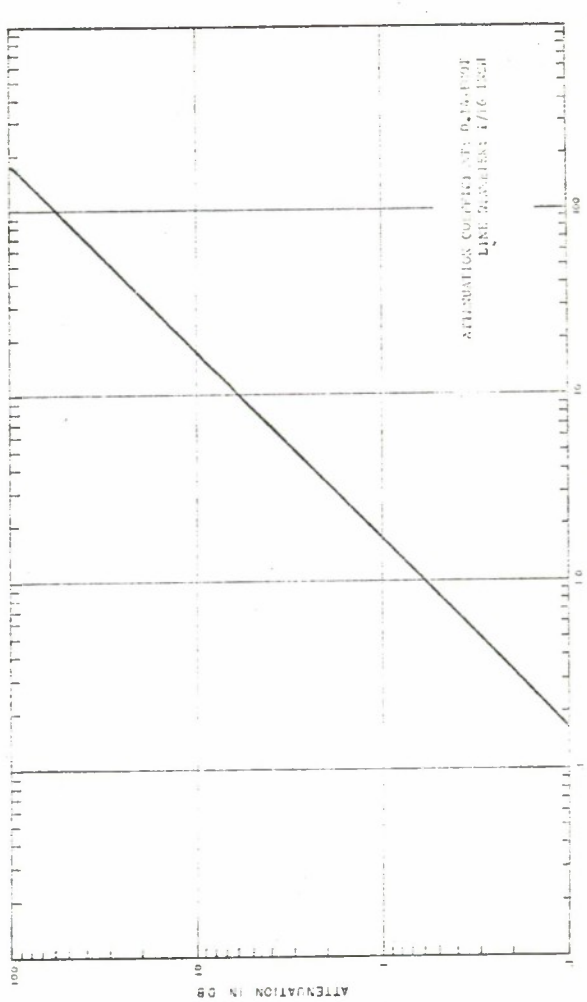
Figure 5-5 indicates the attenuation expected with light (or a laser beam) along an optical fiber path.

2.4 TRANSMISSION THROUGH METAL LIGHT PIPES

Of interest in certain applications is the transmission of light and infrared radiation through metal light pipes on waveguides (Reference 2). Metal light pipes to channel infrared radiation have been used as a simple means of transmitting radiation from one place to another. In the far infrared region of the spectrum, where energy is at a premium, a detailed examination of the transmission of these pipes is necessary to properly evaluate their usefulness. In some applications, such as transmission through an absorption cell or transmission from the exit slit of a spectrometer to a somewhat remote detector, the use of a light pipe instead of conventional mirror and lens optics may result in increased economy and simplicity of the apparatus. In the examination of the absorption properties of materials in strong magnetic fields and at low temperatures, where the radiation must pass through the material in a cryostat surrounded by an electromagnet, the use of conventional optics may not be convenient because of aperture restrictions. The latter are not present in the case of propagation through a light pipe.

A light pipe clearly is not image forming. In fact, the exit end of the pipe has the radiation flux almost uniformly distributed across its diameter. This effect is a disadvantage if the detector area is small in comparison to the pipe diameter. Since the inside diameter of the pipe cannot be made too small if acceptable transmission is to be obtained, only a fraction of the radiation at the end of the pipe is received by the detector under these conditions. This disadvantage may be reduced by the use of a cone condenser.

The expected percent transmission (T_t) through a light pipe can be calculated for askewed rays using the known relations for the reflectivity from metal surfaces and the number of reflections a ray at any particular angle must make before it reaches the end of the pipe. The results are a rough guide to the actual transmission, and are, in general, somewhat high because of values of received power, additional losses from surface imperfections, contamination in the pipe, and neglection of skewed rays. Skewed rays make more reflections, in general, than



ATTENUATION OF COHERENT LIGHT IN FIBER OPTICS
FIGURE 5-5

askewed rays, and thus are attenuated to a greater extent. Since an accuracy of only a few percent is required for this calculation, several mathematical approximations may be made to greatly simplify the work.

The reflection coefficients (R_s and R_p) of metal surfaces for far infrared radiation are well known. When they are expressed in terms of the grazing angle (α), and when the small angle approximation, $\sin \alpha \approx \alpha$, is made, they are given by:

$$R_s \approx 1 - 2x\alpha \tag{5-25}$$

$$R_p \approx \frac{2\alpha^2 - 2x\alpha + x^2}{2\alpha^2 + 2x\alpha + x^2} \tag{5-26}$$

where the subscripts s and p refer to the polarizations perpendicular and parallel to the plane of incidence, and x is defined by:

$$x = (2\epsilon_0 \omega\rho)^{1/2} = 0.18(\rho/\lambda)^{1/2} \tag{5-27}$$

where ω is the angular frequency in rad/sec, ρ is the resistivity in ohm-cm, ϵ_0 is the dielectric constant of free space, and λ is the wavelength in cm.

For unpolarized radiation entering the pipe and making n reflections, the reflection coefficient is defined as $R(\alpha,n) = (R_s^n + R_p^n)/2$. In the end result, the radiation does not have to be unpolarized since the plane of incidence assumes all orientations inside the cylindrical pipe.

When n is large and the small-angle approximation $\tan \alpha \tilde{=} \alpha$ is used, n can be written in terms of α, the length of the pipe (L) and its diameter (d) as $n \tilde{=} L\alpha/d$. And the discontinuous function $R(\alpha,n)$ can then be approximated by the continuous function $R(\alpha)$. Furthermore, in the region of interest x is much less than α. Thus with these approximations the following relations can be used:

$$(R_s)^n \approx e^{-2(xL/d)\alpha^2} \tag{5-28}$$

$$(R_p)^n \approx e^{-2(xL/d)} \tag{5-29}$$

Equations (5-28) and (5-29) show that both polarizations are exponentially attenuated down the pipe; parallel polarization is more rapidly attenuated than perpendicular polarization, and its attenuation is independent of α.

The percent total transmission of the pipe is easily found by weighting $R(\alpha)$ by the solid angle between α and $\alpha + d\alpha$ and integrating:

$$T_t = \frac{2}{\alpha_m^2} \int_0^{\alpha_m} \alpha R(\alpha)\, d\alpha \quad \text{percent} \tag{5-30}$$

where α_m is the maximum grazing angle of the incoming radiation; $\alpha_m = \frac{1}{2} F$, where F is the f/number of the incoming radiation. Letting $xL/d = q$:

$$T = \frac{e^{-2q}}{2} + \frac{(1 - e^{-q/2F^2})}{q} F^2$$

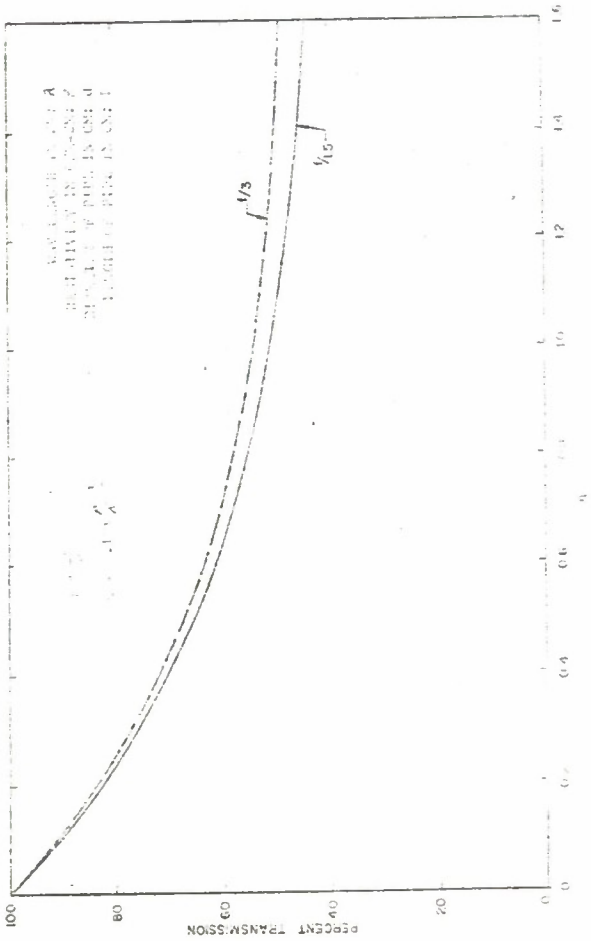
$$\approx \frac{1 + e^{-2q}}{2} - \frac{q}{8F^2} \quad \text{percent} \tag{5-31}$$

In Figure 5-6, T is plotted against q. From this graph the total transmission T may be computed as a function of the length L, the diameter d and the quantity x; for example, when $q = 1$, $T \tilde{=} 55\%$ at f/1.5.

Multiple reflections within a light pipe whose crosa-sectional dimension is many times the transmission wavelength cause signal distortion (similar to multipath interference), thus limiting the modulation frequency of a long pipe system. If the walls are made to absorb, reflective distortion may be eliminated; but the transmission losses will become quite high. For these reasons the usefullness of this technique for long transmission distances is severely limited.

3.0 GLOSSARY

- A area intercepted at surface of sphere
- A_b background area intercepted by receiver field of view
- A_r illuminated area intercepted by receiver antenna
- A_t transmitter radiation area or aperture
- B bandwidth
- B_r receiver bandwidth



THEORETICAL TRANSMISSION CHARACTERISTIC OF METAL LIGHT PIPES

FIGURE 5-6

D	diameter
e	charge on electron
F	f/number of incoming radiation or spectral width of receiver filter
F_t	total flux transmitted
f	transmitted frequency
h	Planck's constant
I	beam intensity
i_d	dark current
L	length
N_s	noise spectral density of sky
n_{rms}	root-mean-square deviation of number of photons
$\bar{n}$	average number of photons per unit time
P_d	power in terms of dark current
P_{ND}	noise power inherent in signal
P_{nb}	noise background power
P_r	received power
P_t	transmitted power
q	quantum efficiency
R	radius of sphere
R	reflection coefficient
R_p	parallel reflection coefficient
R_s	perpendicular reflection coefficient
S	spectral radiance
T	transmittance of atmosphere
T_t	percent transmission
t	transmission function
α	grazing angle
α_m	maximum grazing angle
ϵ_0	dielectric constant of free space
η_r	efficiency of receiver optics
η_t	efficiency of transmitter optics
θ	spherical coordinate
θ_r	receiver field of view

θ_t transmitter field of view

λ radiation wavelength

ϕ spherical coordinate

Ω solid angle

Ω_d solid angle of receiver field of view

Ω_r receiver solid angle

Ω_t transmitter solid angle

4.0 REFERENCES

1. Technological Extrapolation/Communication Application of Coherent Light During 1970-1975 Period; Hughes Aircraft Company, Communications Division; 8 February 1963; ITTCS Contract 480.103D, Task OG 1034 9469; 1911.3-TN-63-011

2. For Infrared Transmission Through Metal Light Pipes; R. C. Ohlmann, P. L. Richars, and M. Tinkham; Journal of Optical Society of America, Vol 43 and 44, August 1958

SECTION 6

PROPAGATION OF COHERENT LIGHT THROUGH ATMOSPHERE

The propagation of coherent light through the atmosphere is affected by various phenomena, such as absorption, scattering, and refraction, that modify the characteristics of intensity, phase, frequency, directivity, and collimation. The study of such phenomena and of the means for counteracting their effects is important for applications that involve atmospheric propagation over considerable path lengths.

In the following paragraphs the phenomena of absorption and scattering of coherent light by gaseous components, water vapor, or particles in the atmosphere are analyzed. In addition, methods of "tunneling" through fog by reduction of the scattering losses are discussed. Experimental results obtained in the laboratory using the propagation of a helium-neon (He-Ne) laser beam through a fog filled chamber are presented.

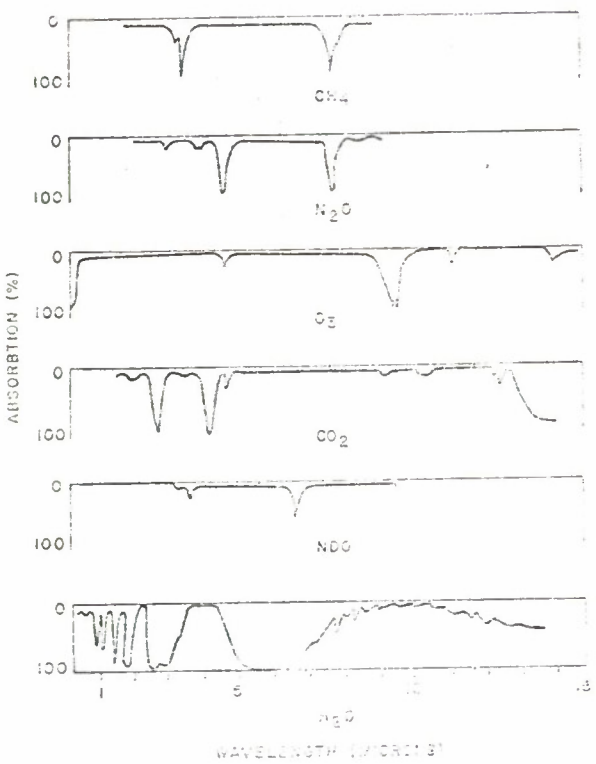
1.0 ABSORPTION LOSSES

The absorption losses that affect the propagation of optical and infrared radiation are caused by atomic and molecular resonance absorption by the atmospheric constituents water vapor (H_2O), carbon dioxide (CO_2), ozone (O_3), methane (CH_4), and nitrous oxide (N_2O). Plots of such losses as functions of the wavelength are shown in Figure 6-1. The absorption bands vary with the temperature and with the pressure, and are most important for H_2O, CO_2, and O_3. In general the losses produced by constituents other than water vapor are predictable with fair accuracy. On the other hand, the percent of water vapor varies strongly with weather conditions; and the corresponding absorption losses are accompanied by large scattering losses.

1.1 ABSORPTION LOSS AT LASER WAVELENGTHS

Although current technology in the generation of coherent light beams suitable for communication is expected to advance rapidly, only a few discrete wavelengths are presently used (Table II-1, Appendix II). For practical applications where cw beams are required, the He-Ne laser is at present most convenient.

The study of the absorption losses at frequencies primarily used by the He-Ne laser (1.15μ and 0.6328μ), therefore, is particularly important. As shown in Figure 6-2, a high resolution spectrographic



ATMOSPHERIC LOSSES AS A FUNCTION OF WAVELENGTH FOR VARIOUS COMPOUNDS

FIGURE 6-1

record of water vapor absorption in the region near the 1.152276μ, there are four wavelengths of interest. Figure 6-3 is a similar high resolution spectrographic record of the solar spectrum for the region near 0.6328μ. At this wavelength the only effect of interest is that caused by nickel absorption, and that caused by water vapor absorption is negligible.

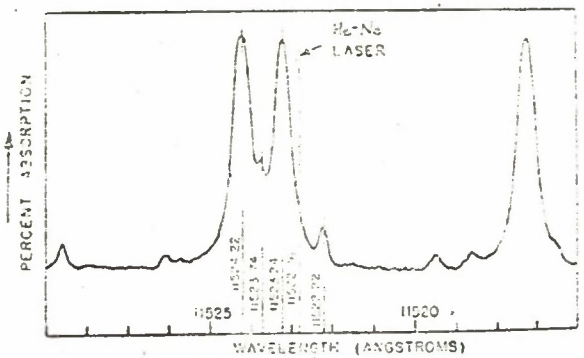
1.2 ABSORPTION LOSS CAUSED BY WATER VAPOR

The actual attenuation produced by water vapor at 1.15μ depends on temperature and pressure, since the shape and the width of the absorption lines vary with these parameters. As shown in Figure 6-4, the attenuation at 79°F, sea level, and 30% relative humidity (Reference 1), the attenuation is about 10 db/km. When the atmospheric pressure is decreased, as for example in the case of the proposed propagation of light in pipes, the line broadening and the attenuation are also decreased as shown in Figures 6-5 and 6-6, where the atmospheric pressure has been reduced to a value less than 0.1μ. Although the decrease of the absorption losses caused by water vapor is important to achieve suitable propagation conditions of laser beams, the existence of these losses constitutes one of the few means available for the reduction of scattering losses caused by fog particles. In fact, using the absorption interaction between radiation and water particles, the possibility exists that the latter may be vaporized, thus reducing their size and the corresponding scattering losses.

Study of the infrared absorption loss of liquid water shows that the absorption coefficient varies as shown in Figure 6-7 (References 2, 3, 4). A sizable attenuation occurs in correspondence of wavelengths larger than 1μ.

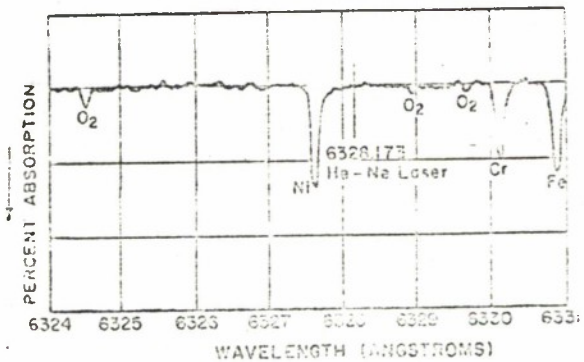
1.3 PROPAGATION THROUGH FOG

If the propagation of a beam of monochromatic, infrared radiation is through a fog medium, the complex phenomena of multiple scattering and of absorption occur. The attenuation caused by scattering decreases as the ratio λ/D, where λ is the radiation wavelength and D is the average diameter of the scatter particles. On the other hand, the absorption is relatively large for wavelengths above 1μ. Thus the percentage of energy absorbed increases as the wavelength is increased. In



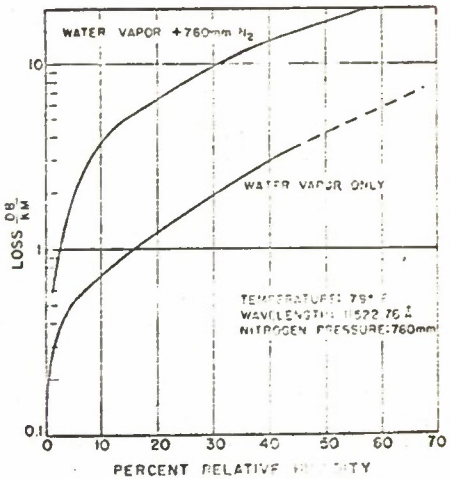
WATER VAPOR ABSORPTION IN
REGION NEAR 1.1525 MICRONS

FIGURE 6-2



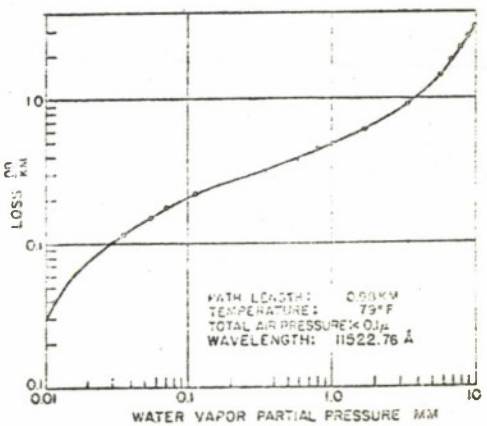
WATER VAPOR ABSORPTION IN
REGION NEAR 0.6328 MICRON

FIGURE 6-3



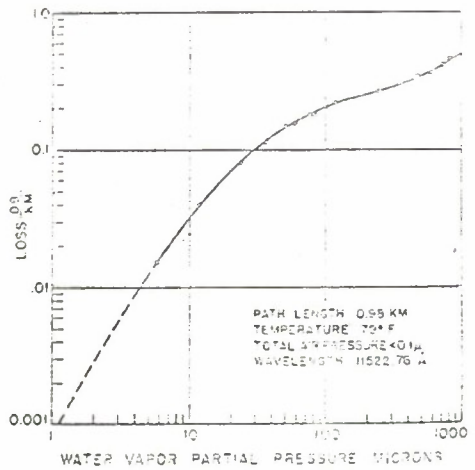
ATTENUATION AS A FUNCTION OF HUMIDITY FOR
WATER VAPOR AND WATER VAPOR PLUS NITROGEN

FIGURE 6-4



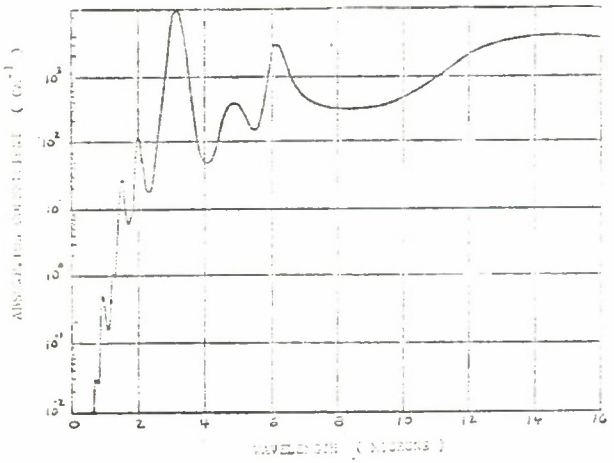
ATTENUATION AS A FUNCTION OF WATER
VAPOR PARTIAL PRESSURE IN MM

FIGURE 6-5



ATTENUATION AS A FUNCTION OF WATER VAPOR PARTIAL PRESSURE IN MICRONS

FIGURE 6-6



INFRARED ABSORPTION OF WATER

FIGURE 6-7

the study of methods of interaction that will decrease the attenuation losses through fog, these considerations are of particular importance. In the following paragraphs are described experimental investigations involving the messurement of the net attenuation of a laser beam with a wavelength of 0.6328μ through fog, where another beam of radiation of suitable wavelength is propagated along the same path. This experiment shows that when the latter wavelength is below 1μ (ruby laser) tunneling is difficult, and when the latter wavelength is above 1μ (high power tungsten lamp) the attenuation is decreased.

2.0 LASER TRANSMISSION IN INCLEMENT WEATHER

Inclement weather conditions are the most severe problem to overcome for reliable laser transmission through the atmosphere. The following paragraphs present a simplified analysis of laser transmission through fog, rain, and snow based on empirical data found in Appendix I. A theoretical treatment of Rayleigh and Mie scattering is contained in Appendix II.

2.1 TRANSMISSION THROUGH FOG

2.1.1 Transmission Loss

With a perfectly monochromatic, parallel beam, the received power is:

$$P_R = P_0 e^{-\beta R} \text{ watts} \qquad (6\text{-}1)$$

where R is the path length in miles, P_0 is the transmitted power, and β is the attenuation coefficient of a homogeneous medium. Since $e^{-\beta R} = 10^{-0.434\beta R}$ the transmission loss is:

$$L = 4.34\beta R \text{ db} \qquad (6\text{-}2)$$

For information transmission, assume operation in an absorption-clear window so that β is due entirely to scattering. Then β is related to the horizontal ground visibility (V) by the simple relationship, $\beta = 3.912/V$. Thus the transmission loss becomes:

$$L = 17 \frac{R}{V} \text{ db} \qquad (6\text{-}3)$$

where R has the same units as V. For a 10 mile path and a visibility of 5.5 miles, the loss from transmitter to receiver is 30 db.

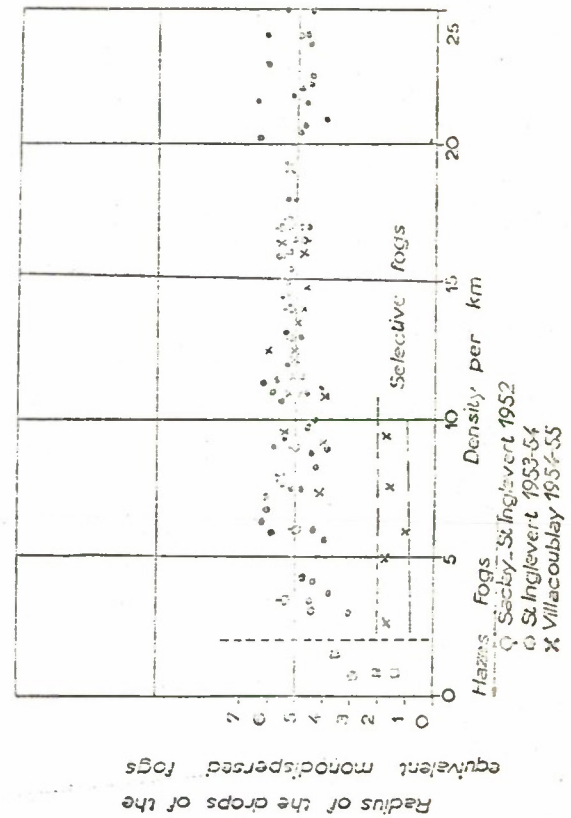
2.1.2 Loss Measurements

The derivation of equation (6-3) assumed homogeneous fog so that β was independent of the distance from the transmitter. In actuality this is not the case. Arnulf and Bricard (Reference 5) found that their chief difficulty in measuring transmission through fog and haze was a lack of homogeneity. They often experienced strong winds with a resultant rapid change in the attenuation coefficient. In addition, they sometimes found clouds close to the ground. To diminish these effects they employed the following method in making their attenuation-spectra measurements.

Spectrophotometric measurements were made simultaneously for each wavelength and for a reference wavelength, obtained by a second monochromatic visual photometer, set for green light of wavelength 0.55μ. Then to obtain a spectral curve, they recorded all wavelengths that corresponded to the same value of attenuation coefficient given by the reference photometer. They assumed that the number of the water droplets changed, but the relative distribution of the diameters of the drops remained constant, and made a Mie theory calculation of the spectral transmittance for compariaon with the experimental results. Good agreement was obtained between the theoretical calculations snd physical measurements.

It is also important to note that Arnulf and Bricard did not account for the absorption by atmospheric gases or water droplets, that is, their infrared measurements were made only in the transmission windows observed in Figure 6-1. Thus, for all practical purposes their so called absorption-spectra curves are really scattering-spectra curves. Figure 6-8 shows that most radii of the drops of infrared selectivity (sharpness of falloff of scattering coefficient with increasing wavelength) for 90 natural fogs or hazes are between 4.5μ and 6μ.

Taylor and Yates (Reference 6) during the course of their work measured the transmission of a fog mixed with light rain over a 3.4 mile path and found that the visual transmission was about 0.04% (34 db loss). Transmission at 3.64μ was 1.2% and at 11μ was 5.6%. Unfortunately no information on the characteristics of the existing fog or rain is given in their paper.



RADIUS OF DROPS OF MONODISPERSED FOG

FIGURE 6-8

2.2 TRANSMISSION THROUGH RAIN

2.2.1 Transmission Loss

Neglecting Rayleigh scattering and assuming an absorption-free window, the attenuation coefficient for homogeneous rainfall is:

$$\beta = \frac{NK\pi r^2}{6.21\times10^{-6}} \text{ miles}^{-1} \qquad (6\text{-}4)$$

where r is the radius of a raindrop in centimeters, N is the number of drops per cubic centimeter, K is a constant, which is a function of the ratio of the radius of the drop to the wavelength, and 6.21×10^{-6} converts centimeters to miles.

For transmission at Laser frequencies, K = 2 so that equation (6-4) becomes:

$$\beta = 1.01\times10^{6}\, r^2 N \text{ miles}^{-1} \qquad (6\text{-}5)$$

The number of raindrops per cubic centimeter is given by:

$$N = \frac{M}{\frac{4}{3}\pi r^3 \rho} \text{ drops/cm}^3 \qquad (6\text{-}6)$$

where M is the concentration of precipitation in grams per cubic centimeter and ρ is the density of water ($1 g/cm^3$). If the units are M kilograms per cubic meter and r meters, ρ equals 10^3 kg/m^3 and N is measured in drops per cubic meter.

Substituting equation (6-6) into equation (6-5):

$$\beta = \frac{0.242\times10^{6}\, M}{r\rho} \text{ miles}^{-1} \qquad (6\text{-}7)$$

Using the relationships in Appendix I, $M = 0.708\times10^{-7}\, h^{0.893}$ g/cm^3 where h is the precipitation rate in millimeters per hour. The updraft wind velocity is assumed to be negligible compared to the raindrop velocity. For severe thunderstorms, however, this assumption may not be valid. Considering only the median raindrop radius $r_0 = 0.045\, h^{0.21}$ cm, and substituting these equations in equation (6-7):

$$\beta = \frac{0.38\, h^{0.683}}{\rho} \text{ miles}^{-1} \qquad (6\text{-}8)$$

Substituting equation (6-8) in equation (6-2), the transmission loss is:

$$L = \frac{1.65R\, h^{0.683}}{\rho} \text{ db} \qquad (6\text{-}9)$$

where ρ equals 1 g/cm^3 if the units of R are centimeters and h are millimeters per hour.

Figure 6-9 is a plot of the transmission loss through rain for a 10 mile path. Notice that up to a moderate rain the transmission loss is tolerable (about 40 db). Of course, the actual tolerable level is determined by the available transmitter power and the receiver noise and sensitivity.

2.2.2 Bending of Laser Beam

Another problem experienced in laser transmission through rain is the bending of the beam, which could result in severe aiming problems. One way to minimize bending is to transmit a wide beam so that a good fraction of the energy is always concentrated at the receiver. As shown in Section 8, the random variation of raindrops can result in some degree of recombining at the receiver. Also, because of the randomly varying paths from transmitter to receiver at each instant of time, some of the light rays have "clear-through" paths to the receiver.

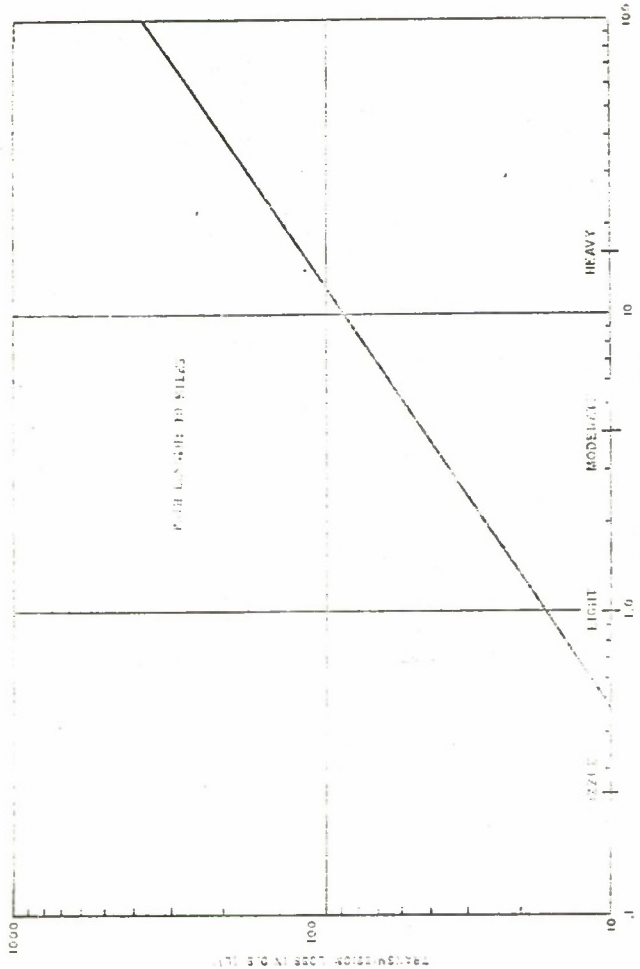
2.2.3 Tolerable Precipitation Rate

The maximum acceptable transmission loss is a function of the transmitted power (P_t), the wavelength (λ), the information bandwidth (B), the photonic efficiency of the receiver ($\emptyset$), and the attenuation caused by divergence of the beam. The minimum detectable power is affected by λ, B, and $\emptyset$.

Reference 7 shows that for bandwidths above 10 megacycles, the minimum detectable power is:

$$(P_r)_{min} = \frac{k_1\, fB}{\eta} \text{ watts} \qquad (6\text{-}10)$$

where k_1 is Planck's constant (6.6×10^{-34} joule-sec), f is the carrier frequency in cps, B is the receiver bandwidth in cps, and η is the photonic efficiency of the receiver.



TRANSMISSION LOSS THROUGH RAIN CAUSED BY SCATTERING AS A FUNCTION OF PRECIPITATION RATE

FIGURE 6-9

With the wavelength (λ) in microns, equation (6-10) becomes:

$$(P_r)_{min} = \frac{2\times10^{-19}\ B}{\lambda\ \eta} \qquad (6\text{-}11)$$

For example, if the wavelength is 0.5μ, the photonic efficiency is 10^{-3}, and the bandwidth is 10^{10} cps, the minimum detectable power is 4 microwatts.

Assuming zero loss caused by beam divergence, the maximum acceptable transmission path loss is:

$$L_{max} = -10 \log_{10} \frac{(P_r)_{min}}{P_t} = -10 \log_{10} \left(\frac{2\times10^{-19} B}{\lambda\ \eta}\right) - \log_{10} P_t \qquad (6\text{-}12)$$

where P_t is the transmitted power.

For the above conditions where the minimum detectable power is 4 microwatts:

$$L_{max} = 54 + 10 \log_{10} P_t$$

Thus, if laser beam has an output power of 10 watts, the tolerable transmission loss would be 64 db. In terms of the precipitation rate (h) and the path length (R) the maximum acceptable path loss is:

$$L_{max} = 1.65 h_{max}^{0.683} R \qquad (6\text{-}13)$$

Substituting equation (6-13) for L_{max} in equation (6-12)

$$1.65 h_{max}^{0.683} R = -10 \log_{10} \left(\frac{2\times10^{-19} B}{\lambda\ \eta}\right) - \log_{10} P_t \qquad (6\text{-}14)$$

and solving for h_{max} yields:

$$h_{max} = 14.6 \left[\frac{- \log_{10} \left(\frac{2\times10^{-19} B}{\lambda\ \eta}\right) + \log_{10} P_t}{R}\right]^{1.465} \text{ millimeters per hour.}$$

Equation (6-14) is important in that it gives the precipitation rate above which the signal is no longer useful. For example, if B is 10^{10}, λ is 0.5μ, η is 10^{-3}, and R is 10 miles:

$$h_{max} = 0.5(5.4 + \log_{10} P_t)^{1.465} \qquad (6\text{-}15)$$

Figure 6-10, a plot of equation (6-15), gives the precipitation rate above which the signal cannot be detected as a function of the transmitted power for a 10 mile path.

Figure 6-11 gives the approximate percentages of time during an average year when communication outages caused by rain would be experienced for a 10 mile path at Washington DC. This interesting curve shows that a 1 watt transmitter system would experience outages 0.4% of the time, which corresponds to 35 hours a year.

2.3 TRANSMISSION THROUGH SNOW

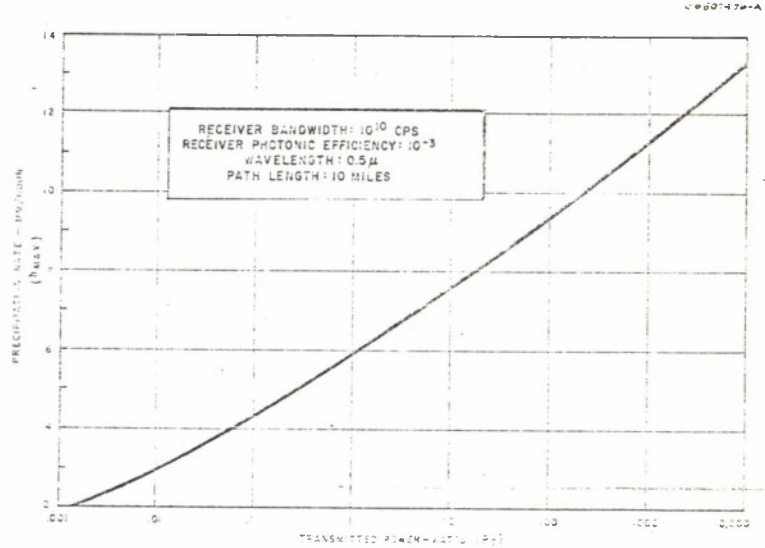
The scattering properties of snow are complex. Snow may occur in a great variety of forms of either single ice crystals or aggregate of such crystals. In general the attenuation by dry snow is a small fraction of that caused by rain of an equivalent precipitation rate. Wet snow, however, both scatters and attenuates appreciably more than rain.

Wet snow falls slowly; hence, many more particles are present than in an equivalent rain. Furthermore, the thin water coating distributed over the non-spherical shape of ice may scatter a higher proportion of incident energy than will water spheres of the same size. (Although this is true at microwave frequencies, it may not be true at optical frequencies.)

As shown in Figure 6-12, for identical frequencies, the real and imaginary parts of the refractive index for ice are, in general, different from those for liquid water. Consequently, the influence of each part on an unknown mixture is difficult to determine.

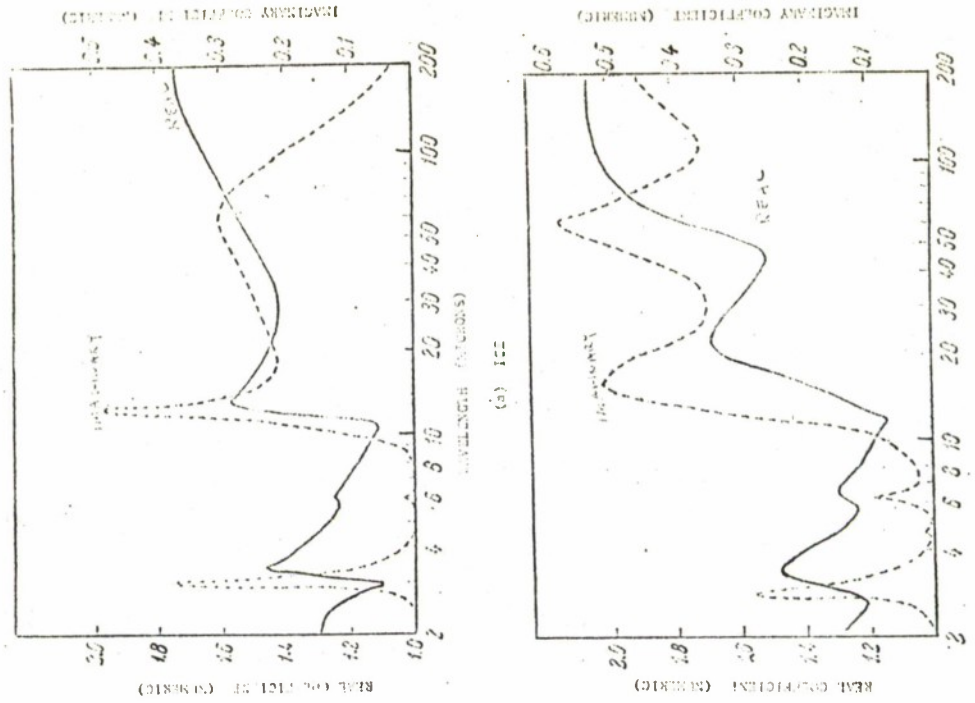
3.0 EXPERIMENTS IN DIFFUSE TRANSMISSION (Reference 8)

Theoretical work is usually limited to simple, ideal models. Because of this limitation, an empirical solution is sought to the problem of the diffuse transmissions through real atmospheres. Experimentally, intense pulses of light were observed by the wide-angle detectors at slant ranges from 0.5 to 9 km. These pulses of light emanated at



MAXIMUM TOLERABLE
PRECIPITATION RATE AS A FUNCTION OF TRANSMITTED POWER

FIGURE 6-10



REFRACTIVE COEFFICIENTS OF ICE AND WATER AS A FUNCTION OF WAVELENGTH

FIGURE 6-12

heights from 30 to 1600 meters above the ground-level detectors and from 70 to 2500 meters below the airborne detectors. Measurements were made under a variety of weather conditions over a period of almost 2 years.

Experimental diffuse transmission may be divided into three main categories: transmission through haze, transmission through cloudy atmospheres, and transmission with the source near a diffusely reflecting surface. The curves summarized in Figure 6-13, are a least-square fit to the experimental data taken in several nights under similar weather conditions. These curves indicate in a general manner the transmission of the atmosphere under a variety of meteorological conditions. The concept of a virtual source intensity is presented with some doubts, but the trend indicated by the apparent extinction coefficients over the slant ranges for the available experimental data is real. Data was taken from a number of sources, and the slope of the curves is indicative of the attenuation coefficients.

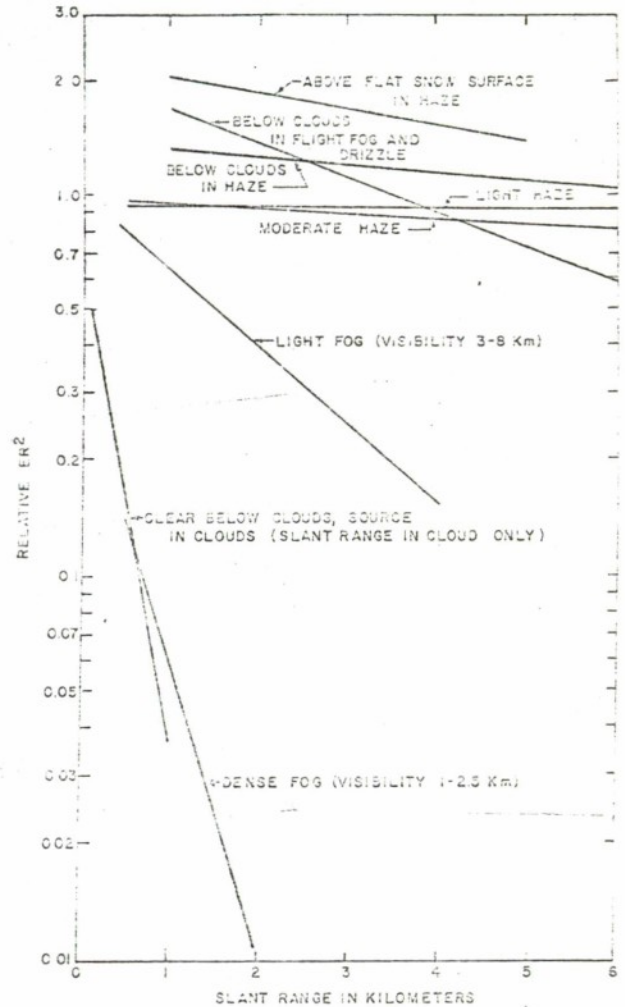
Within the limitations of the measurements, the data fit the simple mathematical form:

$$ER^2 = I_o \times 10^{-kR}, \quad 0.5 \text{ km} < R < 9 \text{ km} \qquad (6\text{-}16)$$

where E is the observed flux density normalized to unit source strength at unit distance in a vacuum, R is the path length, I_o is the source intensity, and k is the attenuation coefficient. Equation (6-16) was chosen because the quantity log ER^2 versus R usually formed a straight line when plotted.

4.0 FOG DISPERSIVE TECHNIQUES

The previous paragraphs illustrate the characteristics of the light propagation through the atmosphere, with reference to absorption and to scatter losses. In practical circumstances, the conditions that minimize the extinction coefficient must be determined before establishing the design of a laser communication system. This problem is complex because the phenomena of absorption and scatter interact, resulting in loss of coherence, random fluctuations of amplitude and phase, etc. A general conclusion from the analysis in Appendix III is that the absorption cross-section is minimum for light in the visible range, and the scatter



SUMMARY OF THE DIFFUSE TRANSMISSION OF THE TOTAL SPECTRAL REGION

FIGURE 6-13

cross-section for a fixed wavelength decreases as the size of the scattering particle decreases. On the basis of these observations, a convenient design is obtained by selecting the wavelength within the visible spectrum, and by vaporizing water particles to reduce their size.

4.1 VAPORIZATION OF WATER PARTICLES

Water could be vaporized by an auxiliary radiation beam that follows the same path as the communication beam, but which has a wavelength that couples a suitable amount of energy to the fog particles. Figure 6-14 shows such a system.

The selections of wavelength and power characteristic of the auxiliary beam are critical; in the ideal case the wavelength should be in the infrared range, above 2 microns. For example, Figure 6-7 shows a large absorption coefficient at a wavelength of 3.4μ. Unfortunately, only low power laser beams are available around this wavelength. The only high power laser beams are those obtained from ruby (0.6943μ) and from neodymium-doped glass (1.06μ). The small absorption coefficient at these wavelengths indicate that a small fraction of the energy is coupled to the fog particles.

4.1.1 Energy Required For Vaporization

The energy density required to vaporize the particles of a uniform fog may be computed from basic physical constants. From equation (6-6), the concentration of precipitation is:

$$M = N \frac{4}{3} \pi r^3 \rho \quad g/cm^3 \qquad (6\text{-}17)$$

where ρ is the density of water (1 g/cm^3), N is the number of particles per cubic meter, and r is the particle radius in meters.

With an initial temperature of the fog particles of 20°C the heat energy required to raise the temperature of water to 100°C to produce vaporization, must be computed. To raise the temperature of 1 g of water from 20°C to 100°C a quantity of heat equal to 80 calories is required, and to vaporize 1 g of water at 100°C 540 calories are required. Hence, a total of 620 calories per gram is required to vaporize one gram of water initially at 20°C.

The transfer of heat to the fog particles achieved by a collimated beam of radiation of the proper wavelength. If the collimated beam has a diameter D, the total mass of water in this beam per unit beam length is:



BLOCK DIAGRAM OF ALL-WEATHER LASER CONCEPT

FIGURE 6-14

$$M' = \frac{\pi D^2}{4} M = \frac{\rho\pi^2 D^2 Nr^3}{3} \text{ g/cm} \qquad (6\text{-}18)$$

Hence, if M' is in grams per centimeter, the energy required is:

$$H = 4.19 \frac{620\rho\pi^2 D^2 Nr^3}{3} \text{ joules/cm} \qquad (6\text{-}19)$$

where 4.19 converts calories to joules.

4.1.2 Sample Computation of Vaporization Energy

As an example assume that the radius a is 5μ and that the diameter D is 1m. The required energy per water droplet is obtained as follows: concentration of each droplet (M) is 5.25×10^{-13} kg/m^3; heat energy per droplet (h) is 1.36×10^{-6} joules; volume of 1m long path (V) is 0.785 m^3; and number of droplets per meter path (NV) is 0.785N, where N has units of m^{-3} for this example. Therefore the energy per meter path:

$$H = 0.785Nh = 1.07Nx10^{-6} \text{ joules/m}$$

The density of droplets (N) is one of the characteristic parameters of the fog. A typical vslue corresponding to the case of high density fog may be taken as 10^{10} m^{-3}. Correspondingly, the energy required is for the above example:

$$H = 1.07 \times 10^4 \text{ joules/m}$$

Referring this quantity to unity cross-section:

$$H/S = 1.36 \times 10^4 \text{ joules/m}^2$$

If the absorption cross-section of the fog particles is C_{abs}, the energy that is coupled into the water is $C_{abs} H_0/S$, where H_0/S is the energy of the interacting beam. Letting $C_a H_0/S = 1.36 \times 10^4$ joules/m^2:

$$\frac{H_0}{S} = \frac{1.36 \times 10^4}{C_a} \text{ joules/m}^2 \qquad (6\text{-}20)$$

Since the maximum value of C_a is unity, the minimum beam energy density is 13.6k joules/m^2. A pulsed laser beam provides

high power pulses of duration variable from few nanoseconds to about 1 ms. The energy per pulse is generally on the order of joules, and in special cases it may reach 100 to 1000 joules. Assuming that the collimated laser beam has a diameter of 1 cm, the corresponding energy density per pulse is about 10^4 times the net energy per pulse. Clearly, if the absorption coefficient is close to unity, the energy density is sufficient to cause vaporization. Unfortunately the absorption cross-section is small for wavelengths of 0.69μ and 1.06μ. Therefore, a large number of laser pulses would be required to transfer the necessary energy to the fog medium. When the heat transfer occurs over an extended length of time, more complex phenomena caused by cooling, medium turbulence, heat transfer within the fog medium, etc, take place, and accurate computation of the heat energy required is complex.

4.2 POSSIBLE SOLUTION TO TUNNELING

Clearly, the ideal solution of the tunneling problem is to use high power, high energy laser pulses with wavelengths larger than 2μ, which would momentarily clear a narrow path through the fog.

A practical solution that might be feasible in certain cases, especially when drifts and turbulence are absent, is to use incoherent infrared beams of suitable wavelength. In this case, the absorption cross-section may be made large; and since the efficiency of beam generation is also large, the energy density is only limited by the collimation. For example, a searchlight beam, assuming a beam cross-section of 1 m^2, would be required to produce about 1.36×10^4 joules for the numerical example given in paragraph 4.1.2. This result is practical in view of the above limitations. An incoherent infrared beam having a divergence angle of 1 degree may be realized by suitable selection of the source dimension and the focal length of the collimator, since the beam angle is given by d/f where d is the source lateral dimension and f is the focal length.

4.3 TUNNELING EXPERIMENTS

The tunneling effect caused by laser and infrared incoherent beams has been verified in laboratory experiments with a fog chamber.

Fog may be produced by fine sprays or by rapid condensation of water vapor. In the first case, difficulties may arise because of the recombination of water particles and the formation of "wet" fog;

In the second case a good condensation is obtained, but a limited control of the size and density of the fog is realized. Because of the time limitation a study was not made of the optimum means to simulate fog. Fog in the laboratory experiments was produced by rapid condenaation of superheated water vapor in a cylindrical fog chamber of 1 m length and 0.15 m diameter. A copper coil, through which liquid nitrogen was passed, was placed within the chamber. Suitable pyrex windows were installed at both ends of the chamber.

A block diagrsm of the experimental set-up is shown in Figure 6-15. The fog chamber was supplied inputs of superheated steam from a pressure chamber and liquid nitrogen. Dry gaseous nitrogen was flushed near the windows to avoid condensation and frosting. A He-Ne laser beam of wavelength 0.6328μ was passed through the fog; its intensity was monitored at the input by a photomultiplier and at the output by a monochromator. Measurements with a microscope were made of the average size of the fog particles by allowing the particles to be formed on glasswool. Diameters on the order of 10μ were observed.

Measurements were made of the energy density provided by different interacting beams.

(a) Ruby Laser

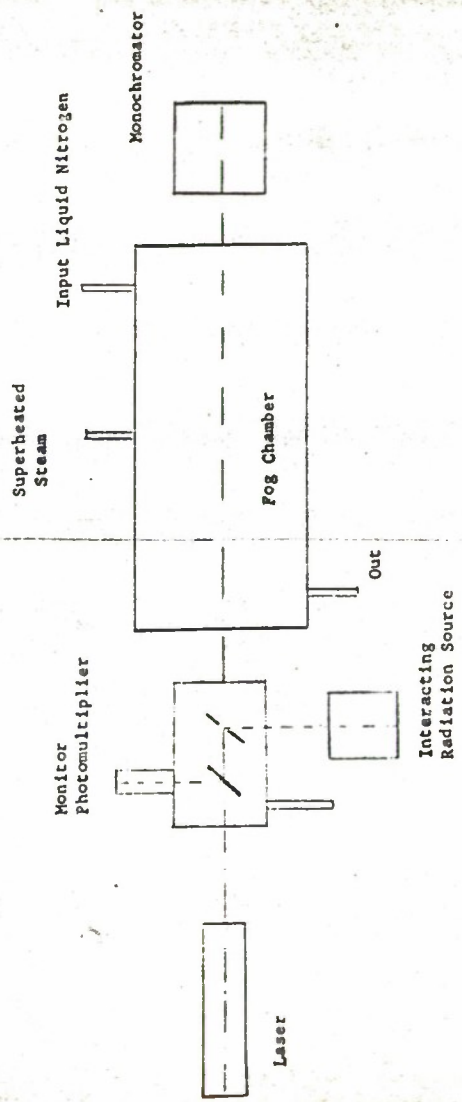
A ruby laser beam with an energy of 2 joules per pulse and a beam diameter of about 1 cm, to facilitate the coincidence of the communication beam path and the interacting beam path, was pulsed at a rate of 1 per minute over a half-hour period. Intially, a dense fog was produced in the chamber and allowed to decay slowly; measuring the variation of the attenuation of the laser beam with time, the intensity (I) varied with time (t):

$$I = I_0 \epsilon^{\alpha t} \qquad (6\text{-}21)$$

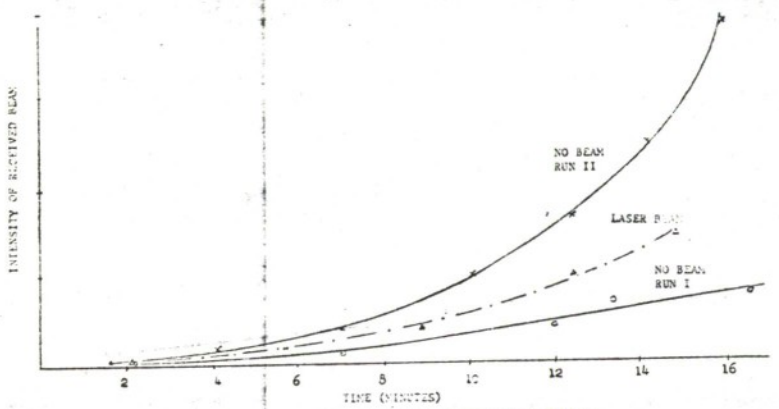
where α is 0.22 to 0.29 per minute snd I_0 is the initial intensity. When the interacting ruby laser beam was applied, no change in the attenuation versus time was noted. See Figure 6-16.

(b) Infrared Incoherent Beam

Another experiment was conducted using an infrared source consisting of a tungsten lamp (Sylvania SN 50,189). Measurement of the total output power from this lamp gave 22.9 watts of actual infrared power.

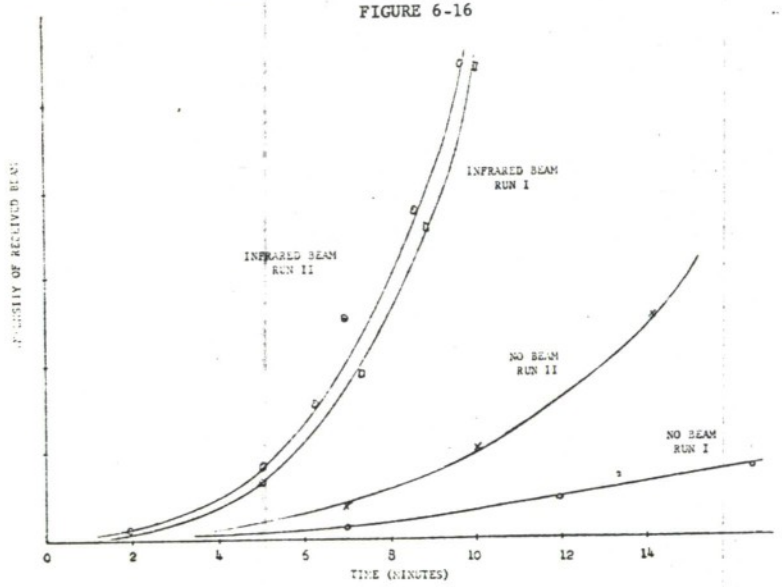


BLOCK DIAGRAM FOR EVALUATING FOG DISPERSIVE TECHNIQUES
FIGURE 6-15



RESULTS OF TUNNELING WITH RUBY LASER

FIGURE 6-16



RESULTS OF TUNNELING WITH INFRARED LAMP

FIGURE 6-17

Because of losses in the beam size, from the optical collimation arrangement at the chamber, the net radiated power entering the fog chamber was found to be 0.71 watt. Repeating the measurement of the attenuation versus time with and without the effect of the interacting beam, the attenuation varied according to equation (6-21), except that α was approximately 0.5 per minute. See Figure 6-17.

The experiment showed some success, although a close correlation with theoretical calculations cannot be made because of uncertainties in the value of the net absorption cross-section for the wide spectrum of the infrared source.

(c) Microwave Interacting Beam

Since water has a strong absorption band at approximately 3 cm, it is possible to couple energy to the fog particle using a microwave beam of such a wavelength. An experiment was conducted by passing through the fog chamber a microwave beam with a peak power of 6 kw and pulsed at 2000 cps. The average power of this beam was 3 watts. The experimental result was negative, that is, no variation in attenuation was detected when the microwave interaction was applied. Theoretical computations based on data available agree with this result.

The magnitude of the Poynting vector $|P|$ of the microwave beam varies with the total cross-section (Q) of each fog particle (sum of absorption cross-section and scatter cross-section:

$$|P| = P_0 \epsilon^{-\beta \ell} \qquad (6\text{-}22)$$

where β equals Qn (n is the density of fog particles) and ℓ is the length of the path.

The total cross-section of each fog particle may be expressed as follows:

$$Q \cong \frac{4\pi^2}{\lambda} cr^3 \qquad (6\text{-}23)$$

where

$$c = \frac{6\,\epsilon_2}{(\epsilon_1 + 2)^2 + \epsilon_2^2} \qquad (6\text{-}24)$$

ϵ_1, ϵ_2 are the real and the imaginary parts of the complex dielectric constant of the fog medium, λ is the wavelength, and r is the mean radius of the particle. Combining equation (6-23) and the relation $\beta = Qm$:

$$\beta = \frac{4\pi^2 ncr^3}{\lambda} \qquad (6\text{-}25)$$

For example, assume $n = 8.33 \times 10^7\ m^{-3}$, $r = 5\mu$, $\lambda = 0.03m$, $\epsilon_1 = 59$, $\epsilon_2 = 38$, and $c = 0.0485$:

$$\beta = 1.25 \times 10^{-4}\ m^{-1}$$

Hence, the absorption coefficient is very small and the microwave power coupled into the beam is not sufficient to provide vaporization of the fog particles.

5.0 CONCLUSIONS

Atmospheric attenuation of the laser beams during periods of inclement weather can degrade link performance to intolerable levels. Laser transmission without fog or rain dispersing devices would not be feasible at most locations.

The fog dispersing techniques investigated do not generally show promise of being able to provide clear communication for point-to-point laser links. For effective fog dispersion using a high power laser beam, the following conditions must be satisfied:

(a) The absorption coefficient must be large (close to unity).

(b) The energy coupled to the beam in a given time must be sufficient to vaporize the fog particles.

(c) The time in which the vaporization energy is transferred must be short with respect to the average drift time of the fog, as well as with respect to the time constant of cooling.

The ideal solution would be obtained using a high power laser beam having a wavelength such that the absorption coefficient is close to unity. In this case, the required vaporization energy would be transferred to the fog in a very short time, and the difficulties caused by drift and cooling would be overcome.

As shown in the course of the experimental investigation, the above conditions are not realizable at the present time. Results using laser and microwave fog dispersing beams are generally unsatisfactory, as may be seen in Figure 6-16. An incoherent infrared beam resulted in reduced

attenuation through the fog, but required minutes of continuous energy to effect appreciable reductions. Motion of fog and rain would probably negate these beneficial effects.

Further difficulties would be encountered in the aiming and tracking of a laser beam propagating through a clear area formed by the fog dispersing beam. Atmospheric turbulence created by evaporation along the path would result in effects that are discussed in greater detail in Section 8.

In many areas, however, inclement weather would limit performance only during a small part of the year. Thus on a statistical basis, by varying the laser communication link bandwidth, service could be maintained between point-to-point terminals. Figure 6-11 shows that a suitably designed laser link with a power of 1 watt could provide service of 10^{10} cps bandwidth for 99.6% of the time. By dropping the bandwidth to 10^6 cps, 99.8% availability is ensured.

Implementation of ground-based point-to-point laser links from the standpoint of atmospheric attenuation is thus dependent to a large degree on location and on the link reliability requirements. As a backup device lasers may provide a useful medium despite the losses encountered during inclement weather. However, turbulence effects occurring in clear weather, considered in Section 8, militate against their use because of the resulting complications in aiming and tracking techniques required to ensure adequate link performance.

6.0 REFERENCES

1. Symposium on Laser and Applications; R. K. Long and T. H. Lewis; Ohio State University; Nov 1962
2. The Near Infrared Absorption Spectrum of Liquid Water; J. A. Curcio and C. C. Petty; Journal Optical Society of America, Vol 41; 1951
3. Infrared Absorption of Liquid Water from 2 to 42 Microns; E. K. Plyler and N. Acquista; Journal Optical Society of America, Vol 44; 1954
4. Absorption of Atmospheric Radiation by Water Films and Water Clouds; J. E. McDonald; Journal of Meteorology, Vol 17; 1960
5. Transmission by Haze and Fog in the Spectral Region 0.35 to 10 Micron; A. Amulf and J. Bricard; Journal of Optical Society of America, Vol 47, No. 6; June 1957

6. Atmosphere Transmission in the Infrared; J. H. Taylor and H. W. Yates, Journal of Optical Society of America; Vol 47, No. 3; March 1957

7. Principal Use of Coherent Light; H. D[illegible] Electrical Communications, Vol 37; 4 Nov 1962

8. Diffuse Transmission Through Real Atmospheres; R. C. E. Loridge and J. C. Johnson; Journal of Optical Society of America, Vol 48, No. 7; July 1958

SECTION 7

MODULATION AND DEMODULATION TECHNIQUES

1.0 LASER MODULATION

1.1 CHOICE OF MODULATION

In the design of a communication link, it is important to select the most suitable modulation method for a given situation. Some essential factors that affect the choice are:

(a) Type of information, digital or analog

(b) Requirements of performance, signal-to-noise ratio, fidelity, error rate, bandwidth (or response time), etc

(c) Noise characteristics of channel, additive or multiplicative

(d) Peculiarities of equipment, limitations of transmitter and receiver, pulse or continuous wave (CW) operation, size, weight, power supply, etc

The choice between digital or analog modulation for a laser link is dependent on the type of laser transmitter to be used as well as on the type of information to be relayed. Techniques have been developed for digitizing all types of information such as audio and video. Such methods can result in all-digital transmission for lasers should the appropriate laser technique for the application require it.

How well each type of laser can be adapted to specific requirements of the type of communication system at hand must also be evaluated. The required performance dictates the desired properties of the laser being used, and vice versa.

Perhaps, the equipment limitations are of the greatest interest in making a decision on the type of modulation to be used. Both pulsed and CW laser sources have the potentiality for either analog or digital modulation. The pulsed laser can be adapted readily for pulse modulation (pulse amplitude, pulse width, pulse position, and pulse code modulation).

1.2 TECHNIQUES OF MODULATION

The techniques of light modulation can be divided into two classes: external modulation (or indirect modulation), and internal modulation (or direct modulation). An analysis of modulation techniques is given in Appendix IV.

1.2.1 External (Indirect) Modulation

In principle, external modulation techniques are based on the variation of the light transmission charecteristics of certain crystals or liquids owing to the electro-optical effect, the magneto-optical effect, and the ultrasonic pressure-optical effect. A brief description of the basic phenomena involved is given in paragraph 1.0, Appendix IV.

In attempting to select an optical modulator external to a laser, there are many characteristics that must be considered. Because of the large number of characteristics, there is unfortunately no ideal modulator for all communication systems. Some of the characteristics are discussed below, and it is evident that significant trade-offs must be made.

(a) Diameter of Aperture.

Large diameters permit large beams and lower beam intensity, but they increase thermal problems.

(b) Modulating Field in Electro-Optical Material

The field should be uniform to have uniform modulation across the beam diameter; this uniformity is difficult to attain at higher modulation frequencies, and the problem becomes worse with higher dielectric constant material.

(c) Angle of Incidence

Some electro-optical crystals require extreme precision in alignment between light beam and crystalline axis. The problem is compounded when the axis wanders in the crystal.

(d) Optical Power Loss

Long modulators generally absorb more optical power than short ones, and also degrade spatial coherence. Losses as high as 6 db have been experienced in modulators. (Reference 1)

(e) Optical Scattering

Electro-optical materials generally scatter optical radiation; scattering results in optical power loss and degradation in spatial coherence.

(f) Electrical Power Loss

Electro-optical materials are invariably lossy electrically, and the loss generally increases with increasing modulating frequency. The losses generally create a thermal gradient in the material, induce stress, and distort the optical beam.

(g) Temperature

Electro-optical materials may be sensitive to temperature and some will operate best over a limited range. Both ambient and rise in internal temperatures require consideration.

(h) Linearity of Modulation

Most electro-optical modulators do not provide distortion-free performance over a wide dynamic range of power or voltage unlike a conventional microwave amplifier. Acceptable linearity can be obtained perhaps over a 5 db range when properly biased. With a digital system, however, the lack of linearity is a minor problem.

(i) Subcarrier Modulation Frequency

For a given information bandwidth, the percentage bandwidth becomes smaller if the subcarrier frequency is increased. System components often perform in terms of percentage bandwidth instead of cycles of bandwidth; thus a higher subcarrier frequency appears desirable. However, as discussed above, higher modulation frequencies, such as microwave frequencies, increase dielectric loss and stipulate smaller optical aperture.

(j) Chemical Stability

Some electro-optical materials are hygroscopic and require special coatings; these coatings if not properly applied may affect spatial coherence. Other materials degrade gradually under the effect of strong electric fields.

(k) Intense Optical Beams

Under the influence of high optical intensities, some materials have produced Stokes and anti-Stokes line shifts. Also optical harmonic frequencies have been generated in certain materials. These contribute to optical loss and produce spurious radiation. This may not be a problem if the peak optical power is small, as would be expected in a communication system.

(l) Pulsed and Continuous Duty

Some electro-optical modulators are limited by thermal effects so that increased performance in terms of bandwidth can be achieved during a short pulse. Pulse or burst transmission service may be of value under special communication applications.

(m) Size and Weight

Although some electro-optical modulators may be compact, the required auxiliary optical components plus modulator power supply may not be. If a pulse or burst service is desired, the modulator dc power supply needs to provide the average and not the peak power load, provided there is sufficient peak capacity.

1.2.2. Internal Modulation (Direct Modulation)

In internal modulation, an operational parameter involved in the generation of the coherent radiation, such as the level of pumping power, the tuning of the cavity, the population level of the laser transition levels, and the position of the laser transition levels, is modified. Obviously, the modulation process takes place inside the laser resonator.

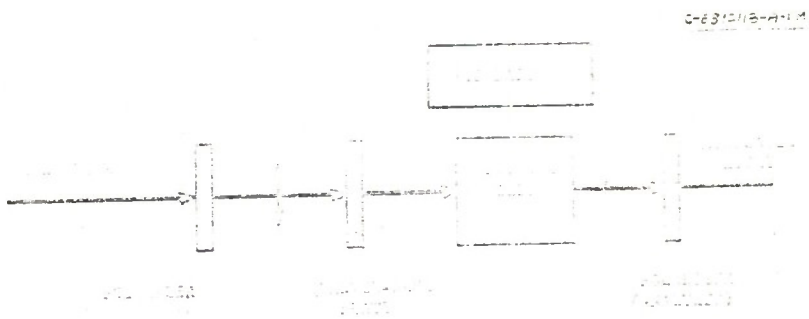
The principles suggested for external modulation can be used for internal modulation. The methods employed can be classified as regeneration modulation, pump-power modulation, Zeeman and Stark modulation, and geometry-variation modulation. A brief outline of such techniques is provided in paragraph 2.0, Appendix IV.

1.3 PRACTICAL MODULATION MECHANISMS

Most of the recent developments in laser modulation exploit the electro-optical properties of Pockels cells, which provide the largest modulation bandwidth and percent modulation for the lowest amount of power.

The Pockels cell can be used as a light intensity modulator by using a linearly polarized light beam input and a polarization analyzer at the output. To obtain a linear operating condition a 1/4 wavelength retardation plate may be inserted between the cell and either of the polarizers as shown in Figure 7-1.

To achieve high modulation rates the cell must be housed in a microwave structure. Blumenthal used a high Q re-entrant coaxial line resonator to modulate light at 800 mc (Reference 2). Kaminow (References 3 and 4) modulated light at 10 gc with a 10 mc bandwidth and a 0.34 radian retardation with 5 watts power by matching the microwave traveling wave with the velocity of light as it passes through the cell. A practical modulator was developed (Reference 5) and tested over a frequency range from 30 to 1 gc, a rather wide bandwidth. The modulator consists of two 40-inch long brass rods separated by a stack of ammonium dihydrogen phosphate (ADP) crystals (2 x 4 x 56 mm in size). The required power is 10 watts. In addition,



POCKELS CELL LIGHT INTENSITY MODULATOR

FIGURE 7-1

the development of a traveling wave type modulator has been reported (Reference 6); this consists of a parallel plate transmission line where a portion of the dielectric is ADP or potassium didentenium phosphate (KDP). In this case, the optic axis of the crystal was perpendicular (instead of parallel as in the former modulators) to the direction of the light beam. This device provides gigacycle bandwidths and a power requirement of only 12 watts for 100% modulation. Another modulator design uses a slow wave serpentine structure around a CuCl rod that modulates at 10 gc frequency and dissipates only milliwatt power (Reference 7). The use of a Fabry-Perot interferometer containing an electro-optic material has also been suggested (Reference 8) as a possible wideband modulator.

The direct modulation of a He-Ne gas laser has been achieved (Reference 9) by modulating the pumping rf power supplied by a conventional transmitter. The gas laser with a confocal resonator, emitted wavelengths of 1.153μ. A small percent of total pump power, modulated by a 1kc signal, resulted in sinusoidal light modulation. One experimental communication system for a single audio channel has been built with such a modulation concept. However, recent work (Reference 10) reports pulsed laser de-ionization times of 1 to 2 μs, implying a modulation capability of 500 kc.

Recent work (Reference 11) on a perovskite ($KTa_xNb_{1-x}O_3$) called KTN appears to be promising for an electro-optical modulator operating at high modulation frequencies with low power requirements. With a driving voltage from 16v to 80v, the power dissipated ranges from 15mw to 200mw. A dc bias voltage is required for linearity, and the light direction is perpendicular to the electric field. A modulation bandwidth in the gigacycle range seems probable.

KTN has a high electro-optical effect at room temperature, and it is not sensitive to temperature. Since the dielectric constant (ϵ) is high (up to 20,000), large samples of KTN cannot be used, thereby restricting the size of the optical aperture for high modulation frequencies. Field distortion effects can be avoided if the KTN size is less than about $\lambda_\epsilon/30$, where λ_ϵ is the modulation wavelength in the dielectric. The relationship between free-space modulation wavelength λ_0 and λ_ϵ is:

$$\lambda_\epsilon = \frac{\lambda_0}{\sqrt{\epsilon}} \qquad (7\text{-}1)$$

Therefore, the size of KTN (ϵ = 20,000) should be less than $\lambda_0/4200$.

1.4 MODULATION OF SEMICONDUCTOR LASERS

The semiconductor laser is uniquely suited for amplitude modulation (AM) since the output light is related to the input current. However, the optical power-current characteristic is not linear; and distortion-free AM can only be accomplished at low modulation percentages, which waste optical power.

Also, AM should be avoided because of the noise introduced by multiplicative propagation disturbances, that is, scintillation (produced by scatter), beam angle deviations, and beam break-up. By using frequency modulation (FM) or phase modulation (PM), these disturbances can be minimized. In addition, the signal-to-noise (S/N) ratio may be improved by increasing the bandwidth, provided a threshold signal level is exceeded. Unfortunately, FM techniques, which are as simple as AM techniques, do not exist for the junction laser. However, there is a modulation scheme, termed AM-FM, that possesses the advantages of both AM and FM. In this scheme, the radio frequency subcarrier, frequency modulated by the information signals, amplitude modulates the laser output. This modulation scheme has the following advantages:

(a) A high degree of distortion in the AM process can be tolerated.

(b) The demodulated AM signal at the receiver can be limited in amplitude to remove the effects of multiplicative disturbances.

(c) The output S/N ratio can be increased by increasing the bandwidth.

(d) The system can be implemented with devices and techniques that are presently available.

1.5 COMPARISON OF EXTERNAL AND INTERNAL MODULATION

The advantages and disadvantages of external and internal modulations are as follows:

Advantages	Disadvantages
External Modulation	External Modulation
Large bandwidths	High power requirements
Linear response to information signal	Additional transmission loss

Advantages	Disadvantages
Internal Modulation	Internal Modulation
Modulation is enhanced by laser cavity	Higher tolerances for all components
Power requirements small	Nonlinear response (in most cases) of level of oscillation to a change in cavity parameters.
No optical power loss, can handle high laser beam powers	Bandwidth is limited by high Q of optical cavity

The methods of modulation discussed in Appendix IV will provide amplitude modulation as well as frequency or phase modulation. Techniques of internally pulsing modulating the laser beam are also mentioned.

1.6 FREQUENCY MULTIPLEXING

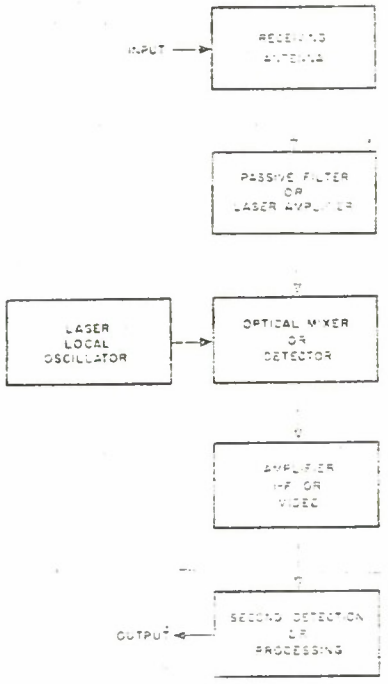
The efficient use of large bandwidths usually implies frequency multiplexing of many independent signals into a wide frequency region. Various techniques for effective multiplexing are possible. For example, subcarriers can be used that are phased in such a manner as to produce different degrees of left- or right-handed polarization of the same light beam. Care must be taken not to have different sidebands overlap.

As indicated in Reference 12, a method has been developed for producing single-sideband, suppressed carrier modulation at optical frequencies. The modulator consists of two electro-optical crystals to which the modulation signal has been applied with a 90° phase shift with respect to one another. The merging light then has left-hand polarization components that are rejected by a right-circular polarizer and right-hand components that carry the upper sideband frequency only. It has been used successfully at audio frequencies. Such modulation can not only improve the S/N ratio, but it can also conserve the bandwidth. In addition, it provides a laser frequency without introducing additional frequency components.

2.0 LASER DEMODULATORS

2.1 TYPES OF OPTICAL RECEIVERS

To establish a basis for the comparison of different types of optical receivers, it is convenient to adopt the generalized block diagram of a basic receiver shown in (Figure 7-2). The major components are an



BASIC OPTICAL RECEIVER

FIGURE 7-2

active preamplifier or a passive filter, a coherent mixer or video detector, an intermediate frequency (IF) or video amplifier, and a second detector or other signal processor such as a frequency discriminator. Receivers are classified as either crystal-video or optical-superheterodyne and are used with or without an active optical filter (laser preamplifier).

(a) Crystal-Video
- Passive optical filter, or none
- Photosensitive detector
- Video amplifier

(b) Optical-Superheterodyne
- Passive optical filter, or none
- Coherent local oscillator
- Photosensitive mixer
- IF amplifier
- Second detector or processor

The basic components of the optical receivers exist today in more or less advanced forms. It is of interest to analyze some of the basic limitations and advantages of the different types of receivers.

2.2 THEORETICAL COMPARISON OF DEMODULATION TECHNIQUES

The ability to transmit information in the infrared and visible light range is often limited by quantum noise rather than by thermal noise, as is the case at lower frequencies. The transition region occurs at approximately the frequency (f) where $kT \approx hf$, but depends also on the received signal power (S). The purpose of the following paragraphs is to compare various types of infrared and optical receivers according to the theoretical rates at which they can transfer information. The results of this comparison (Reference 13) indicate that in the frequency range of interest and for relatively low ratios of signal power to hfB (B is the bandwidth), binary counters can transfer energy more efficiently than homodyne receivers which, in turn, are more efficient than either coherent preamplifier or superheterodyne receivers. At high S/h2B ratios, however, the amplifier or mixer receivers, or both, is more efficient.

Shannon (Reference 14) defines information as prescribed entropy and information capacity as the rate at which entropy is received. The total received power, however, is signal plus noise power so that the useful

information capacity of a receiver channel is the total entropy rate less the entropy rate of the noise itself. Reference 14 also shows that the information capacity of a channel can be maximized by modulating the carrier so that the signal has the statistical properties of white noise. The presence of this type of modulation is one of the assumptions made by Reference 13. The noise power is assumed to be white even though it may be "colored" (peaked in frequency) because it is relatively flat over the bandwidth of the receiver, which is generally narrow compared to the carrier frequency, when a large frequency range is considered.

The maximum information capacity can be used to compare receiver capabilities regardless of the carrier frequency. Because the maximum capacity is to be determined, the carrier is assumed to be white-noise modulated. The entropy rate is given by:

$$R = B \log_2 \left(1 + \frac{P}{hfB}\right) + \frac{P}{hf} \log_2 \left(1 + \frac{hfB}{P}\right) \qquad (7\text{-}2)$$

where P equals the power received.

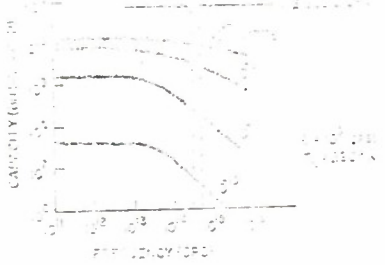
The maximum information capacity can be determined by subtracting the value of R when P = N (the entropy rate of the noise alone) from the value of R when P = S + N (the entropy rate for the entire wave). The result is the upper limit of the information capacity in the wave (C_{wave}) for a signal of average signal power (S) in the presence of average noise power (N):

$$C_{wave} = B \log_2 \left(1 + \frac{S}{N+hfB}\right) + \frac{S+N}{hf} \log_2 \left(1 + \frac{hfB}{S+N}\right) - \frac{N}{hf} \log_2 \left(1 + \frac{hfB}{N}\right) \qquad (7\text{-}3)$$

Equation (7-3) is plotted in Figure 7-3 for B equals 1 gc, T_N ($N = kT_N$) equals 290° K, and for several values of total power (P). If the information capacity of a receiver, which is influenced by the noise the receiver adds, is designated by C, then an appropriate figure of merit is the efficiency defined by C/C_{wave}.

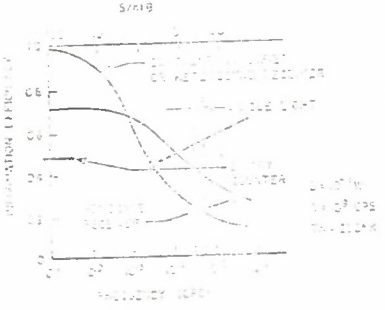
Equation (7-3) is consistent with the usual value given for C_{wave} in the classical limit (correct for frequencies up to the far infrared) where N is much greater than hfB:

$$C_{wave} = B \log_2 \left(1 + \frac{S}{N}\right) \qquad (7\text{-}4)$$



INFORMATION CAPACITY AS A FUNCTION OF FREQUENCY FOR VARIOUS LEVELS OF SIGNAL POWER

FIGURE 7-3



INFORMATION EFFICIENCY COMPARISON OF HOMODYNE AND HETERODYNE RECEIVERS

FIGURE 7-4

Equation (7-4) is obtained by expanding Equation (7-3) in terms of $\frac{hfB}{N}$ and $\frac{hfB}{S+N}$ and then retaining only the first term.

The information capacity efficiency of a coherent laser or parametric amplifier receiver, a superheterodyne receiver, a homodyne receiver, and a quantum counter receiver are shown in Figure 7-4 as a function of frequency for a particular value of received power. The coherent amplifier curve was obtained by adding the amplifier noise contribution, KhfB to N in equation 7-3. K is a constant that has a minimum value of 1 for an ideal (noiseless) amplifier. The superheterodyne curve was obtained by adding the shot noise of the mixer (hfB/ϵ) to N; ϵ is the quantum efficiency of the photodiode used as a mixer and has a value of 1 for the ideal case. The amplifier and superheterodyne curves, both plotted for ideal devices, are thus identical. The homodyne receiver (Reference 15) curve was obtained by substituting the appropriate calculated S/N ratio, which yields:

$$C_{homodyne} = \frac{B}{2} \log_2 \left(1 + \frac{2S}{N + \frac{1}{2\epsilon} hfB}\right) \qquad (7\text{-}5)$$

where N is the average received noise in the frequency bandwidth (B). Finally, the quantum detector efficiency curve was obtained from a detailed consideration (Reference 14) of the probability distribution for the various numbers of received photons resulting from the transmission of some known number of photons. In the case where $S \gg hfB$, the quantum counter extracts half the available energy in the wave.

As a result of the study, the following conclusions were drawn by Reference 13:

(a) When the received signal or noise power is much larger than hfB, where f is the center frequency of the wave and B the bandwidth, a receiver using an ideal coherent amplifier or an ideal heterodyne converter can extract essentially all the information that can be incorporated in the wave while an ideal quantum counter receiver is limited to about half the capacity of the wave. The ideal homodyne converter is intermediate between these two.

(b) When P is much less than hfB, a binary quantum counter can extract essentially all the information that can be incorporated in the wave, while the other types of receivers become increasingly less efficient.

(c) For a given power and bandwidth, the upper limit to the information that can be incorporated in a wave begins to drop off fairly rapidly when f increases beyond P/hB. Thus for a given frequency and bandwidth, there is a threshold for received power below which the information capacity of a communication channel drops off rapidly. When external noise is present, this power level is about hfB.

2.3 AVAILABLE DEMODULATION TECHNIQUES

The basis for a demodulation system, considering present techniques (that is, non-heterodyne), is the radiation detector. There are three major considerations in choosing a detector for a laser beam: spectral response, sensitivity, and bandwidth or response time. Also two classes of light detectors can be distinguished:

(a) Particle-counting or quantum detectors.

(b) Energy-integrating or thermal detectors.

2.3.1 Quantum Detectors

Quantum detectors detect the existence of the photon of radiation, but not its energy. In the detection process, a photon is absorbed by the detector surface, which releases a single free electron. The detection of the photon by this one-to-one photon-electron conversion can take place only if the photon energy exceeds the threshold level, which is a characteristic of the photoelectric or photoconductive material used as the detector. Since photon energy decreases as the frequency of the radiation signal decreases, there is a photon-energy frequency level below which radiation cannot be detected by a quantum detector. For a detector material having a threshold level (work function) slightly less than the individual quantum energy of the incoming radiation, the number of free electrons can at best be equal to the number of incoming photons; that is, its quantum efficiency is less than one.

Since photons are counted without considering their frequency-dependent energy, the power sensitivity of the radiation detector is frequency dependent; it decreases with increasing frequency. Quantum detectors are square-law detectors, the output power is proportional to the square of the input power.

Quantum detectors, although limited by frequency sensitivity, are being used exclusively at present in optical receiver systems because of their larger bandwidth capacity. Detection at several gigacycle modulation rates has been reported (Reference 16). Three basic quantum detectors are in use: photoconductive, photovoltaic, and photoemissive:

(a) Photoconductive Detectors

In photoconductive detectors, the absorbed photon causes electrons in the valence band or impurity levels to move to the conduction band, thus increasing the conductivity of the semiconductor material. The build-up and decay times for these excess particle concentrations depend on the minority carrier lifetimes in the particular semiconductor. These times range from a few nanoseconds to hundreds of microseconds, and the set limits to the highest modulation frequencies to which the cell will reset limits to the highest modulation frequencies to which the cell will respond. The fastest cells of the photoconductive type are p-n junction photocells, whose voltage-current characteristic changes with illumination.

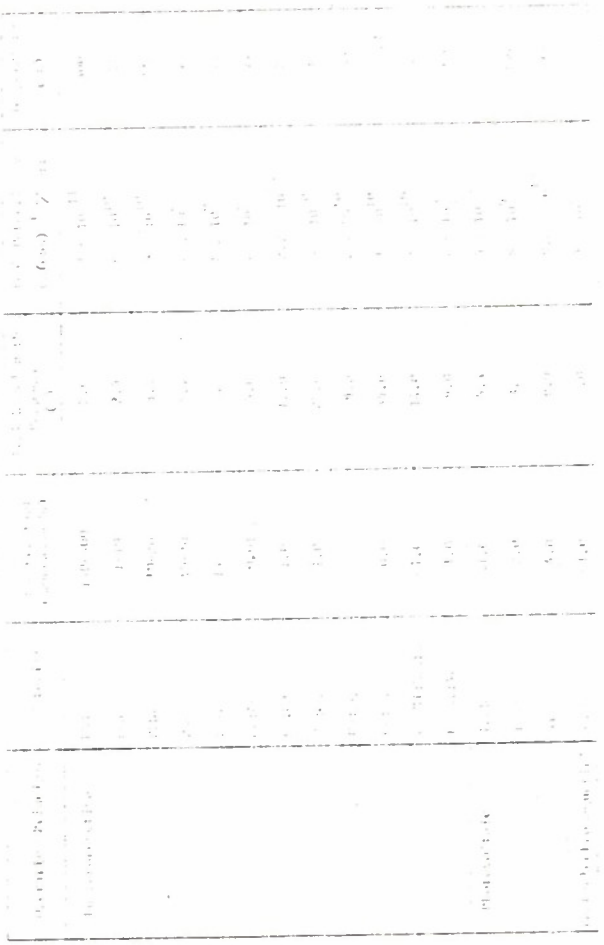
A PIN-diode (Reference 17) has been used to detect a ruby laser modulated above 10 gc; a silver-bonded germanium parametric diode (Nippon Electric's type GSB-1, Japan) can also be used to obtain similar results. Presently, the cesium gas laser, which emits at 7μ, has such a long wavelength that indium-antimony (In-Sb) detector appears to be the most sensitive cell at this frequency.

Characteristics of some infrared detectors are given in Table 7-1.

(b) Photovoltaic Detectors

In photovoltaic detectors, incident photons produce free carriers at the junction of p-n diodes so that a potential difference is developed. These cells generate their own electromotive force and can be used in circuits without any external bias supply. The most promising photovoltaic cells are the silicon (Si) and germanium (Ge) diffused junction devices discussed in Reference 18. Conversion efficiencies of about 7% or 8% are delivered. The germanium p-n junction extends its sensitivity much further in the infrared (about 2μ) than does silicon. Bell Telephone Laboratory is reportedly developing a germanium diode with an essentially flat response to about 2 gc, with the possibility of being extended to 20 gc.

TABLE 7-1
INFRARED DETECTORS



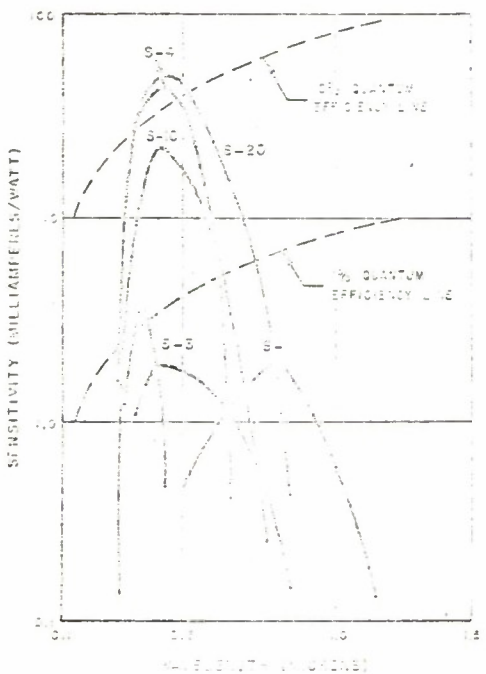
(c) Photoemissive Detectors

In photoemissive detectors, absorbed photons cause electrons to be freed from the detector surface. Phototubes, photomultipliers, and traveling-wave microwave phototubes are of this type. They are the most sensitive and fastest detectors in the ultraviolet and visible region of the spectrum.

Photocathode sensitivities are initially dependent on the wavelength of the incident light. In Figure 7-5, the relative sensitivities of various types of surfaces are presented as a function of wavelength. The most sensitive and efficient photocathodes are of the cesium-antimony (Cs-Sb) type, especially after suitable oxidation. In the special region of 0.40 to 0.42μ, surfaces of this type are capable of a quantum efficiency of 25%. The emission is reduced to threshold values, however, if the incident radiation increases to about 0.7μ. Typical Cs-Sb cathodes (S-4) yield sensitivities of 30 to 60 μamp/lumen. Thus, the Cs-Sb photocathode exhibits its best performance in the blue portion of the visible spectrum. The Bi-Ag-O-Cs photocathode (S-10) has an extended long wavelength response in the visible region. Surfaces of this type maintain quantum efficiencies of 3% to 8% in the range from 0.4 to 0.6μ. Its sensitivity is typically above 30 μamp/lumen. It has longer wavelength response than the Cs-Sb surface at the expense of total quantum efficiency. The Ag-O-Ce surface cathode (S-1) has the most extended long wavelength response; it shows a peak quantum efficiency of about 0.5% at 0.85μ in the near infrared region. The S-1 surface can be used to detect the He-Ne laser radiation at 1.153μ, but with a very low quantum efficiency of only about 0.03%.

2.3.2 Thermal Detectors

Thermal detectors convert the incoming radiation energy into heat, the variation of which is then translated into a current or voltage variation. The performance of such detectors is governed by their ability to absorb energy, which depends on the radiation frequency and their thermal time constant. They are also square-law detectors. The advantage of thermal detectors over quantum detectors is their sensitivity to wide



ABSOLUTE SPECTRAL CHARACTERISTIC
OF VARIOUS CATHODE SURFACES

FIGURE 7-5

radiation frequencies. Their main disadvantage is a very high time constant (on the order of 1 ms), which make them of little practical use for data transmission. Sensitivity, especially in the infrared, is comparable or better than that of quantum detectors.

2.3.3 Direct Demodulation

Three major classes of detectors can be used as straight demodulators for intensity modulated light beam: photomultipliers, semiconductor photodiodes, and traveling-wave microwave phototubes.

(a) Photomultiplier

The photomultiplier is a sensitive optical detector that can be used up to about 200 mc. The principal factor limiting the frequency response is the spread in transit time through the secondary-emission multiplication chain. Thus extremely short pulses at the input become longer pulses at the output.

A photomultiplier that does not, in principle, spread the transit time uses crossed electric and magnetic fields (Reference 19). These photomultipliers have been used to detect light modulated at microwave frequencies.

A typical photomultiplier is the RCA 7102 with eleven stages of multiplication. Amplifications of 10^7 or higher are easily attained. The tube is capable of detecting input pulses having durations shorter than 0.01 μs, and with an S-1 response covers a spectral range of 0.42 to 1.1μ. Peak detectivity is about 0.8μ. For low dark current, cooling is required. Power supplies of several thousand volts are necessary to operate this photomultiplier.

(b) Semiconductor Photodiodes

Semiconductor photodiodes can be coupled to mechanisms that allow detection and amplification of the modulated signal. High-Q coupling, needed because of the minute signal quantities, can be done by coupling the photodiode to a tuned resonator (Reference 17) or by using the parametric amplifier structure shown in Figure 7-6 (Reference 20). The diode mainly used as the photo-sensing elements is employed as a variable capacitor. The pumping signal provides an ac voltage across the diode, which in turn varies the width of the diode depletion layer at the pumping frequency.

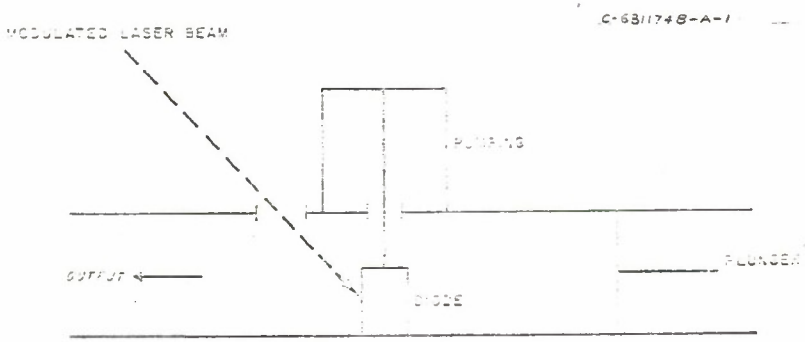


DIAGRAM OF MICROWAVE PHOTODETECTOR

FIGURE 7-6

(c) Traveling-Wave Microwave Phototube

A traveling-wave microwave phototube, described in (Reference 16), can be used as a broadband light demodulator. It consists of a photosensitive cathode followed by a traveling-wave tube structure as shown in Figure 7-7. Sylvania is presently marketing a version of this tube (SY-4302) with a 1.5 gc to 4.5 gc frequency range. Photomultipliers provide high gain, but operate only in the visible and near infrared regions of the spectrum and have low response times. Semiconductor photodiodes provide no gain, but operate over much wider regions of the spectrum (through the infrared) and have inherently faster response times. Traveling-wave phototubes, though, provide high gain and operate only in the visible region, but are limited in bandwidth by the microwave structure.

2.3.4 Optical Heterodyne Demodulation (References 21 through 24)

If heterodyne methods are used, an increase in sensitivity and in S/N ratio can be realized. The modulated light beam and the local oscillator light beam must be exactly cophasal over the entire surface of the photodetector. This requires sophisticated control of the optics involved.

As in radio frequency applications of heterodyne detectors, the output signal has an amplitude proportional to the product of the amplitudes of the input signal and of the local oscillator signal. A critical area is that of maintaining the proper frequency relationship between the signal and the local oscillator. This problem requires high frequency stability and is still under study. As a possible solution, homodyne detection can be used, that is, make the local oscillator frequency identical to that of the unmodulated laser.

A He-Ne gas laser with a single optical frequency output has been recently announced by Reference 25. This laser should be particularly useful for the local oscillator in a heterodyne detector (Reference 26). The single frequency output is a consequence of the short (2 inch) gas cell having a small bore.

The tracking of the incoming optical signal by the local oscillator poses a problem that is treated in References 27 and 28.

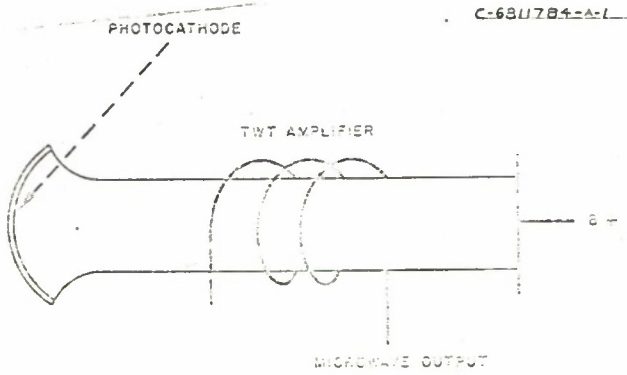


DIAGRAM OF TRAVELING-WAVE DEMODULATOR

FIGURE 7-7

The severe cophasal requirement of an optical heterodyne detector takes on additional magnitude when the laser beam propagates through a turbulent atmosphere. A special technique to reduce the cophasal difficulties is discussed in Reference 29. Another possible method of avoiding the cophasal problem is to transmit simultaneously over the laser beam both signal and local oscillator frequencies. The cophasal relationship should be maintained even when the laser beam is transmitted through some turbulent atmosphere. Suitable means for modulating the laser beam require invention and development.

Since a diplexer is necessary in a heterodyne detector, an optical arrangement to accomplish diplexing is needed. A proposed optical diplexer is given in Reference 30.

3.0 REFERENCES

1. Gigacycle Bandwidth Coherent Light Traveling-Wave Phase Modulator; C. J. Peters; Proceedings of IEEE, Vol 51; Jan 1963.

2. Design of a Microwave-Frequency Light Modulator; R. H. Blumenthal; Proceedings of IEEE, Vol 50, No. 4; April 1962.

3. Microwave Modulation of Light by the Electro-Optic Effect; I. P. Kaminow; Nerem Record, Vol 3, 1961.

4. Microwave Modulation of the Electro-Optic Effect in KH_2PO_4; I. P. Kaminow; Physics Review Letters, Vol 6; 15 May 1961.

5. Wideband Laser Modulator; Microwaves; Nov 1961.

6. Wideband Coherent Light Modulator; C. J. Peters; Nerem Record, Vol 4; 1962.

7. Laser Modulator is More Efficient; Electronic Design; 12 Oct 1962.

8. The Fabry-Perot Electro-Optic Modulator; E. I. Gordon and J. D. Rigden; Nerem Record, Vol 4, 1962.

9. Direct Modulation of a He-Ne Gas Laser; E. J. Schiel and J. J. Bolmarcich; Proceedings of IRE; June 1963 (correspondence).

10. Pulsed Helium-Neon Gas Laser Applications; L. L. Antes, J. Goldsmith, and W. McMahan; IEEE Transactions on Military Electronics, Vol MIL-8; Jan 1964.

11. Electro-Optic Properties of Some ABO_3 Perovskites in the Paralectric Phase; J. E. Geusic, S. K. Kurtz, L. G. Vsn Uitert, and S. H. Wemple; Applied Physics Letters, Vol 4; 15 April 1964.

12. Single-Sideband Suppressed-Carrier Modulation of Coherent Light Beams; C. F. Buhrer, V. J. Fowler, and L. R. Bloom; Proceedings of IRE, Vol 50, No. 8, (correspondence); Aug 1962.

13. J. P. Gordon; Proceedings of IRE, Vol 50, No. 9; Sept 1962.

14. The Mathematical Theory of Communication; C. E. Shannon and W. Weaver; University of Illinois Press; 1949.

15. I. Dolrowolski; Journal of Optical Society of America, Vol 49; Aug 1958.

16. Photomixing Experiments with a Ruby Optical Master and a Traveling-Wave Microwave Phototube, B. J. McMurty, and A. E. Siegmem; Applied Optics; Jan 1962.

17. Microwave Photomixing of Optical Maser Outputs with a PIN-junction Photodiode; H. Inaba and A. Siegman; Proceedings of IRE, Vol 50, No. 8; Aug 1962.

18. A New Si P-N Junction Photocell for Converting Solar Energy into Electric Power; Journal of Applied Physics, Vol 25; 1954.

19. A Microwave Frequency Dynamic Crossed-Field Photomultiplier; O. L. Gaddy and D. F. Holshouser; Proceedings of IEEE, Vol 51; Jan 1963.

20. Detection and Amplification of the Microwave Signal in Laser Light by a Parametric Diode; S. Saito et al; Proceedings of IRE, Vol 50, No. 11; Nov 1962.

21. The Optical Heterodyne; S. Jacobs; Electronics; 12 July 1963.

22. Heterodyne Receivers for R-F Modulated Light Beams; D. J. Blattner and F. Sterzer; RCA Review; Sept 1962.

23. Advances in Lasers; L. M. Vallese; Semiconductor Products; Aug 1963.

24. Lasers; Electronic Design; 2 Aug 1963.

25. Single Frequency Gas Laser at 6328 Å; E. I. Gordon and A. D. White; Proceedings of IEEE, Vol 52; Feb 1964.

26. Optical Heterodyning Using Point Contact Germanium Diodes; C. K. N. Patel and W. M. Sharpless; Proceedings of IEEE, Vol 52; Jan 1964.

27. AFC Optical Heterodyne Detector; P. R. Rabinowitz, J. LaTourrette, and G. Gould; Proceedings of IEEE, Vol 51; May 1963.

28. Optical Heterodyne Detection of Microwave-Modulated Light; R. Targ; Proceedings of IEEE, Vol 52; March 1964.

29. Optical Heterodyning With Noncritical Angular Alignment; W. S. Read and D. L. Fried; Proceedings of IEEE, Vol 51; Dec 1963.

30. Lossless Beam Combination For Optical Heterodyning; A. E. Siegman and B. J. McMurty; Proceedings of IEEE, Vol 52; Jan 1964.

31. Communications Technology; DCA R&D Objectives Guide, Vol 1; 1963; AF Contract 19(626)-5, CCN1.

SECTION 8

AIMING AND TRACKING IN LASER SYSTEMS

The problem of tracking and acquisition will determine the ultimate limits of an optical communication system. The main advantage of lasers as radiating sources over microwave sources is their ability to transmit energy within solid angles that are defined by the diffraction limits of optical antennas (for example, mirrors). To use this property to its fullest capability, pointing and tracking accuracies on the receiver part are required which by far exceed those of comparable microwave systems. The problem is aggravated by atmospheric propagation effects that are considerably more serious in the optical region than at microwave frequencies. On the other hand, optical radiation detectors are quantum counters with noise characteristics (sensitivities) much inferior to microwave detectors. Thus, a careful analysis of all components and environmental conditions is required in order to determine the potential and practical limits of optical communication. This section presents a thorough discussion of the above problem areas together with analytical and numerical examples

1.0 ATMOSPHERIC TURBULENCE EFFECTS

1.1 EFFECTS OF ATMOSPHERIC TURBULENCE ON LASER PROPAGATION

The effects of atmospheric turbulence on a light beam, and the description of the turbulence itaelf are extremely complex subjects. In addition the atmosphere is far from simple, so that the entire topic is rather confusing.

Consider a narrow beam of light traversing a portion of the atmosphere. As it passes through the atmosphere it is deflected in a random manner so that the beam is seen to dance about. After some distance the diameter of the beam exceeds the size of the turbulent elements and the beam not only dances, but it is also broken up. The large deflections occurring at a great distance from the receiving end are not seen, as they miss the receiving aperture completely, giving rise to scintillation, while the image in the focal plane will be affected by the atmosphere near the receiver, giving rise to a dancing image.

The size of the elements causing the deviations and the amplitude of the deviations, is of course critical. But no single correlation

distance can be given as the atmosphere is not uniform. Turbulence can be caused by a number of factors, the effect of each being quite different. Near the ground there is, of course, turbulence in the boundary layer arising simply from atmospheric shear.

However, even with no wind the atmosphere transfers heat up from the ground during the day, and vice versa at night. This can be a very large effect, and is apparent in the daytime formation of clouds. Other different sources of turbulent effects must also be noted. There is turbulence in the free atmosphere away from the boundary layer, and under some conditions during the night bubbles of warm air from the surface break away and rise leading to strong refractive effects. The interaction of these effects is extremely complex. For example, in early evening with a mild wind, thermal turbulence can be quite strong, but if a strong breeze arises there is much better mixing of the air and the scintillation decreases.

Consider observing a star; instead of discussing the statistical complexities of turbulence theories examine the meteorological mixing length (ℓ) as a measure of the size of turbulent elements. The mixing length is a function of the wind velocity ($\bar{u}$) and from dimensional arguments

$$\ell = k \frac{\frac{d\bar{u}}{dz}}{\frac{d^2\bar{u}}{dz^2}}$$

where experimentally k is about 0.4. Since u(z) has an approximately logarithmic profile, it follows that to a first approximation $\ell \propto z$. Actually, in lapse conditions the increase is more rapid with height, and with inversions it is less rapid.

One thus expects the turbulent elements to increase in size as one moves away from the boundary layer to some height z. Hence in looking at a star, large deviations caused by small elements near the telescope, with weaker deviations caused by larger elements further away, are observed. One notes also that the telescope itself does some weighting in thst large deviations caused some distance from it will not be

observed. It is usually considered that the major protion of the deviation is caused within the first few hundred meters of the telescope. Wind shear near the tropopause or an inversion layer also causes turbulence, but because of the great distance from the observer only scintillation is observed from this source. Deviations are also much smaller because of the decreased density.

One of the difficulties in reconciling the data is the use of a monotonic correlation function. This in actual practice is not what is observed, as turbulence arises at different levels from different sources, both thermal and wind shear being involved. Thus in the astronomical case, there is a tendency for disturbances arising near the observer to be independent of scintillation, which arises at or near the tropopause. However this situation is not true in the case of a horizontal path.

The scintillation modulation, which is of basic importance in the ease of a communication system, depends on a number of factors. It is well known that it will be a minimum at sunset and sunrise when thermal equilibrium is attained, and that it will be at its worst in the daytime. Thus the temperature gradient has a strong effect on scintillation. The scintillation is more simply a function of the Richardson number (Ri) changing little with numbers above 0.35 and 0.4 for the same temperature gradient. But with Ri's below 0.35 the percent scintillation per unit temperature gradient increases approximately inversely as the Richardson number. Up to several kilometers the percent scintillation will also be proportional to path length. Measured slopes vary from 0.8 to 0.9, so the increase is not quite proportional to path length, but this does make a good approximation. The spectrum of the scintillation depends on many factors, but in all cases dies out above a few hundred cycles. Scintillation at 1 kc is usually several orders of magnitude lower than that between 1 and 100 cps. The point at which the spectrum begins to decrease rapidly varies with the receiving aperture, the wind, path length, and other conditions. For apertures on the order of 10 cm the break point is usually between 10 and 100 cps, with the tendency being toward the lower frequencies. Percent modulation varies roughly inversely with the aperture as long as the beam is reasonably larger than the aperture, although it will not drop to zero with an aperture much larger

than the beam since there is scattering out of the beam at large angles. Typical modulation percentage for an 8 cm beam and a 8 cm aperture would be about 15% for a 100 meter path. For a point source (for example, a star) under the same conditions the modulation percentage would be on the order of 60%. Increasing the aperture to 20 cm would typically give 5% modulation for an 8 cm beam and 20% modulation for a star. These figures are for a summer night with moderate to strong breezes and clear sky, so that they apply to reasonably good conditions.

Because the turbulent elements near the observer tend not to scatter light completely out of the receiver they introduce little scintillation. However, they do introduce phase shifts in the wave fronts that cause tha effects gathered under the heading of scintillation. Deviations caused by small elements on the order of centimeters in size can be as high as 10 seconds or more under reasonably good conditions at night. There are also smaller deviations, an image typically having a Gaussian distribution with a width at half-power points of 2 seconds. Much of this effect seems to be caused by larger elements, possibly on the order of 10 cm in size. From the standpoint of a communications system some compensation may be possible for these phase shifts since they are equivalent to a linear displacement of the image.

Humidity has been suspected of having a strong effect on scintillation in some cases, but this occurs primarily at very high (> 60 to 70%) humidities, and could either be due to humidity fluctuation, or, more likely, to the effects on other meteorological parameters, such as radiation balance.

It is quite difficult to predict how a given system will operate, but in order to minimize scintillation effects one should get above the first few meters of atmosphere, to say 10 meters height, and then use large diameter optics. Beams should never be so narrow that it is possible for beam dancing to carry them out of the receiver - at night this dancing could be 10 seconds of arc for a narrow beam; in the daytime it could be much larger. If small angular beam divergences were to be used (by small, order of 10 to 30 seconds), the transmitter beam diameter should be large enough to average over the small local elements, which may be assumed to be of the order of a centimer in size. Thus the transmitter beam diameter probably should be larger than 10 cm.

1.2 RECIPROCITY EFFECTS IN TRANSMISSION AND RETURN OF A LASER BEAM

The existence of reciprocity between antennas is a basic theorem commonly applied at radio frequencies. Reciprocity also applies at optical frequencies provided the transmission medium is isotropic and constant such as in free space. In a turbulent atmosphere the stated conditions are not met and thus reciprocity begins to fail under certain situations. The degree of reciprocity failure is large when (a) beam, transmitter, and receiver sizes are large compared to the turbulent elements, which are typically about 1 cm and (b) distance between transmitter and receiver is large compared to aperture size. In other words, reciprocity can exist in a turbulent atmosphere if either the distance between transmitter and receiver is very small compared to aperture size, or the beam diameter is small compared to that of the turbulent element.

Invariably the turbulent elements are much larger than the optical wavelength, and under this condition the turbulent elements can produce angular deviations of the beam which are of the same order of magnitude as the beam divergence. Thus because of atmospheric inhomogeneities, the total beam arriving at the receiver may be broken up into many portions with each portion arriving from slightly different directions.

Reciprocity can be attained in a turbulent atmosphere if a reflected (or return) wave could be transmitted that would match simultaneously both phase and amplitude distribution across the aperture; otherwise reciprocity failure will result. In practice, this return wave will originate from a single source that will normally produce a single-valued phase and amplitude distribution across the aperture so that full reciprocity cannot be assured under dynamic conditions of a turbulent atmosphere.

A heuristic discussion of these effects is presented in Appendix V.

2.0 TRACKING ERRORS IN MOVING SYSTEMS (BRADLEY AND TRANSIT TIME ERRORS)

Two types of time errors are of importance in a communication system between vehicles that are separated by great distances and moving at high relative velocities. These are the Bradley error (or astronomical aberration) and the transit time error. The Bradley error results from

the fact that received energy appears to come from a direction that is determined by the resultant of the propagation velocity vector and the tangential velocity vector components of the receiving vehicle orientated perpendicular to the direction of propagation. A mechanical analog of this effect is the case of vertically falling raindrops exhibiting a horizontal velocity component when observed from a moving platform. The transit time error is simply given by the angular position change of the transmitting or receiving vehicle, or both, during the finite propagation time.

Neither of these errors is of any consequence on the receiver performance as it will always track the apparent transmitting source. However, extremely narrow beam systems may require that tracking information be used to change the transmitter's pointing direction in order to correct for the above errors. The transmitter may otherwise miss the communicating station entirely even though receiver and transmitter are perfectly aligned and a message is being received.

The maximum Bradley error (α) occurs when the receiving vehicle's tangential velocity (V_T) is perpendicular to the direction of the incoming radiation:

$$\alpha_{max} = \frac{V_T}{C} \tag{8-1}$$

where C is velocity of light.

The maximum transit time error occurs when both vehicles separated by a distance (R) move with velocity (V_T) in a direction perpendicular to the geometric line of sight. The transit time is then:

$$t_R = \frac{R}{C} \tag{8-2}$$

during which time the transmitting vehicle moves a distance (D)

$$D = V_T t_R = \frac{V_T R}{C} \tag{8-3}$$

Thus, the maximum angular transit time error (β) is given by:

$$\tan \beta_{max} = \frac{D}{R} = \frac{V_T}{C} \tag{8-4}$$

Comparing equations (8-1) and (8-4), the transit time error for this case is in effect the Bradley error, which is independent of separation.

The maximum pointing error occurs for the case of communication between a low flying satellite in an equatorial orbit with an east-to-west heading and a ground station at the equator. In this case the errors for both atations are additive:

$$\tan \alpha \simeq \alpha = \frac{1}{C} (V_{TS} + V_{TE}) \qquad (8\text{-}5)$$

where V_{TS} and V_{TE} are tangential velocities of satellite and earth respectively and both tangential velocities are referred to the center of gravity of the earth. Thus, equation (8-5) becomes

$$\alpha \simeq \frac{1}{C} \left[\left(\frac{GM}{R_S} \right)^{1/2} + \omega_E A \right] \qquad (8\text{-}6)$$

where G is the gravity constant, M is the mass of the earth, ω_E is the angular velocity of the earth, A is the radius of the earth, R_S is the radius of satellite orbit, and C is the velocity of light.
For $R_S = A + 150$ km, from equation (8-6):

$$\alpha_{max} \simeq 2.76 \times 10^{-5} \text{ radians}$$

$$\simeq 5.7 \text{ seconds}$$

The above number corresponds to the diffraction limited beam divergence of a 2.3 cm radiating aperture at λ equal to 0.63μ. Thus, under extreme cases such as the above example, and for very narrow-beam systems it will be necessary to compute the transmitter lead-angle from the receiver tracking data according to equations (8-5) or (8-6). With this information the transmitter servo can then be programmed accordingly.

3.0 ACQUISITION TIME AND SEARCH RATES

3.1 ANALYTICAL MODEL

There are two related but different search problems that have been considered in previous literature. The first of these problems is the optimum distribution of search effort. The techniques developed in

this area have found application to such problems as searching a large area of ocean for submarines, lost aircraft, or returned spacecraft. In these applications the techniques result in search patterns for aircraft.

The second problem area that has received a great deal of attention is the radar acquisition problem. Here, the scanning is usually defined by some cyclic pattern. The techniques that have been developed for radar define the probability of acquiring a target that enters into this scan pattern. The published techniques for radar, however, concentrate on the noise characteristics of microwave systems.

The laser communication system search problem is related to both the above problems. However there are stronger ties with the first in that it appears likely that a non-fixed search pattern will be more useful than the fixed scan usually considered in the radar acquisition problem. Further, the noise characteristics of a laser system must include quantum noise, which is of little consequence in the radar problem. The radar concepts are of value, however, in pointing out the approach to the relationship of system noise and the probabilities of detection and false alarm.

In the design of a laser search and acquisition system, the primary problem is the narrow beamwidth and the resulting low probability of hitting a target with this beam while searching. It is not enough to know the optimum method, or pattern, in which to scan the beam. This pattern may be the best for a given system operating in a given environment. However, the time required to follow this pattern until acquisition may be much greater than other system constraints, such as transceiver motion, will tolerate. Similarly, it is not enough to know probabilities of detection for a given laser system in a given environment, for again the time required may be completely out of line with other system constraints. With this in mind, an analytical model has been developed at the General Electric Spacecraft Department that yields the average search time for a given laser communication system in a given environment. This technique uses the detection and false alarm probabilities of the laser system, the searching mode of the receivers, the scanning mode of the transmitter, and the initial probability distributions for the locations of the transceivers. This expected (or average) search

time allows a direct observation of the effect of changes in laser system gain characteristics and search and scanning methods in terms of a parameter (average search time T_S) that is critical to the basic feasibility of the laser communication link. The expressions obtained are in series form and are quite general in nature. They can be applied directly to a given situation without modification.

The general expression for average time for acquisition is:

$$E\left(T_S\right) = \sum_{K=0}^{\infty} \sum_{n=KM+1}^{(K+1)M} P_{n-KM} \left(1 - \sum_{j=1}^{M} P_j\right)^K \left(K \sum_{i=1}^{M} \tau_i + \sum_{i=1}^{n-KM} \tau_i\right) + E\left(T_{FA}\right) + I \tag{8-7}$$

where $E\left(T_S\right)$: average time for acquisition, $E\left(T_{FA}\right)$: average time spent in processing false alarm signals, I: time spent in signal integration, τ_i: time spent examining the i^{th} resolution element, M: number of resolution elements per scan, P: probability of the search being successful in the element indicated in the subscript, K: number of the scan.

In general, the approach to the calculation of the probability of the search being successful in the element i, P, is to consider the probabilities affecting this single resolution element. Here the probability of a successful search will be considered for the case of station No. 1 searching for station No. 2. The establishment of a communication link will usually require that station No. 2 also search for station No. 1, but this can be handled in the same manner that is about to be described. The probability of a successful search can be defined as the probability that station No. 1 is looking at station No. 2 and that station No. 2 is transmitting to station No. 1 and that the transmitted signal is detected by station No. 1. In terms of conditional probabilities this statment is equivalent to the following equation:

$\Pr(\text{successful search})_i = \Pr(\text{station No. 1 looking at station No. 2})_i \Pr(\text{station No. 2 transmitting to station No. 1/station No. 1 looking at station No. 2})_i \Pr(\text{station No. 1 detects signal/station No. 1 is looking at station No. 2 and station No. 2 is transmitting to station No. 1})_i$

or:

$$\Pr(SS)_i = \Pr(L)_i \Pr(T/L)_i \Pr(D/LT)_i = P_i \tag{8-8}$$

In this expression, Pr(L) refers to the searching approach of the receiver; $\Pr(T/L)_i$ refers to the scanning approach of the transmitter; and $\Pr(D/TL)_i$ is the probability of detection for the system ignoring the search problem. Therefore, the system can be broken down into segments for individual consideration.

In determining the probability of detection for this analytical model, the transmitter power, transmitter beamwidth, system bandwidth, and receiver signal-to-noise (S/N) ratio are considered. It is here that the model allows an easy comparison of such questions as beam focussing versus beam scanning and image detectors versus point detectors.

In considering the initial probability distribution for the location of the transceivers, all information initially known about the locations can be employed in the analytical model. This includes such things as preliminary radio frequency acquisition and trajectory data that is available by analysis or earlier tracking. In the usual case, a normal probability distribution for the location of the transceivers will result from the combination of factors contributing to the initial information. This, in turn, specifies the desirability of a spiral scan and search. It follows that $E(T_S)$ will be smallest when the greatest probabilities are multiplied by the smallest times. The analytical model also allows for a variable [illegible] scan in τ_i is specified for each resolution element. In cases of initial probability distributions that are particularly nonuniform, this mode of scanning has advantage of decreasing $E\left(T_S\right)$ in the same manner of multiplying the greatest probabilities by the smallest times.

3.2 PRACTICAL CONSIDERATIONS

No particular problem should be encountered in tracking and communicating with space vehicles from the ground since, on a deep-space mission for example, the vehicles position, velocity, and trajectory

must always be known to a very high accuracy. The problem, thus, reduces to one of mere computation and accurate pointing.

If no or very limited information on the flight data of the space vehicle is available, such as in the case of vehicle-to-vehicle communication, it may be necessary to scan a large solid angle. For a given search volume or total field of view (Ω) it is then important to determine the size of the instantaneous field of view (resolution element, ω) which enables acquisition in a minimum of time while maintaining a minimal S/N ratio. If the subscripts T, R, refer to "transmitter" and "receiver" respectively, the four different scanning situations result:

(a) Case I. $\omega_T < \Omega_T$; $\omega_R < \Omega_R$

(b) Case II. $\omega_T = \Omega_T$; $\omega_R < \Omega_R$

(c) Case III. $\omega_T < \Omega_T$; $\omega_R = \Omega_R$

(d) Case IV. $\omega_T = \Omega_T$; $\omega_R = \Omega_R$

3.2.1 Case I

This situation is the most general because in its limits it contains all subsequent cases. It also constitutes the most difficult situation. Both receiver and transmitter are scanned over their entire solid angle. Complete coverage, however, will only be obtained (in the simplest manner) if the transmitter of station No. 1 scans its entire field while the receiver of station No. 2 moves to the next resolution element or vice versa. Such a process can be expressed analytically as:

$$\frac{d\Omega_R}{dt} T_A = \Omega_r \qquad (8\text{-}9)$$

and

$$\frac{d\Omega_T}{dt} T_A = \frac{\Omega_T \Omega_R}{\omega_R} \qquad (8\text{-}10)$$

where T_A is the acquisition time. From equations (8-9) and (8-10):

3.2.4 Case IV

This case is trivial and applies only under the condition of accurate prior knowledge of each vehicle's position, velocity, etc. No scan is required and acquisition time is at minimum.

This study is concerned with a wide range of possible applications. Thus, no one numerical example will be of representative value. For specific types of spacecraft mission, however, numerical data has been gathered in accordance with the above equations (Reference 1).

4.0 DISCRIMINATION AGAINST UNWANTED RADIATING SOURCES

4.1 BACKGROUND NOISE SOURCES

In tracking as in communication, noise sources place sensitivity limitations on receivers attempting to extract information from the arriving signal. However, since the actual information bandwidth required for tracking is usually several orders of magnitude less than that of the transmitted information, a system designed for adequate reception of information will produce more than sufficient power for the tracking system to operate. A thorough treatment of laser communication systems is presented in Section 5 of this report.

During acquisition of the laser beam, the high scanning speeds required to reduce acquisition time may introduce system bandwidth requirements which approach that of the transmitted information. In this case a compromise must be made with respect to acquisition time.

4.2 DISCRETE NOISE SOURCES (FALSE TARGETS)

The previous discussion has been concerned with background noise, appearing to come from an extended and uniform source. After acquisition has been accomplished and the receiver field is very narrow, this contribution may be of little concern for the receiving channel. For the tracker, however, a more serious problem arises. Discrete noise sources such as stars and planets. During night time operation with wide acceptance angle and/or increased sensitivity (for example, by cooling) the detector may no longer be tube noise limited. In this case, bright stars might be mistaken for real transmitters by the tracker.

As an example, Anderson (Reference 1) has calculated that a ruby laser with an output of 10^0 watts focussed into a solid angle of 32 sec

by 32 sec will appear as bright as a 9^{th} magnitude star. Employing a narrow-band filter with a total star-power-to-passband-power ratio of 10^3, the same laser will appear as a 2^{nd} magnitude star. There are only a few stars which are comparable in brightness to 2^{nd} magnitude, however, compared with the output power of continuous wave gas laser there will be a large number of stars comparable in brightness. Thus, the application of discrimination techniques during the acquisition phase will become a necessity.

4.3 DISCRIMINATION TECHNIQUES

Because stars and planets are black body radiators as compared to the monochromatic transmitter sources, spectral discrimination by means of filtering becomes the first and most obvious method. Two cases of importance arise.

(a) Case I, transmitter wavelength(s) is (are) known

(b) Case II, transmitter wavelength(s) is (are) not known

Case I simply requires fixed filters in the tracking receiver. Case II calls for two separate detectors where the available spectrum is equally divided between them (for example, with a two-color beam splitter) and for comparing the two outputs. Instead of two detectors, one detector and an oscillating filter (frequency smaller than the scan rate) can also be used.

In addition to spectral discrimination, means of temporal discrimination are available. During the acquisition phase the scanning transmitter can be programmed to radiate a modulated signal in such a way that correlation processing techniques can be employed.

Pure amplitude modulation will not be the most desirable mode as the transmitted signal is to be compared against noise source of random amplitude fluctuations. Subcarrier frequency modulation or pulse code modulation (PCM) are much more promising approaches. Applicable techniques that fall within this area can be directly adopted from well developed microwave and radar practices.

5.0 LASER ANTENNAS

5.1 GENERAL APPLICATIONS

Laser antennas are generally refracting or reflecting telescopes. Actually, at microwave frequencies a great many of the antennas

are also essentially refracting or reflecting telescopes. Another basic type of antenna, the array, may be desirable at optical frequency when two or more lasers are used to transmit simultaneously. Optical frequencies imply much smaller dimensions for a given gain; they also imply much smaller tolerances. Further, at optical frequencies the problem of coherence is of much greater importance than at radio frequencies.

With a highly coherent source such as a helium-neon gas laser, the antenna parts must be of the highest quality. The coherence of the light tends to reveal small imperfections in optical parts, such as grinding marks on lenses. In general, tolerances on lenses, reflectors, optical flats, prisms, and so forth must be such that the deviation of the actual optical path length from the nominal equals a small portion of a wavelength. Further, this includes the effects of temperature and any scanning motion. Thus, the effect of any heat source (for example, the sun or the laser output) must be examined to make sure that unequal heating of optical parts does not cause beam distortion. (Heating causes thermal expansion, change of refractive index and also strain.) A. E. Blume and K. F. Tittel (Reference 2) discuss thermal effects in solid state lasers; most of the conclusions are applicable to optical parts. All of these thermal effects can cause optical path length changes. It may be necessary to place the antenna in a temperature controlled cavity. The dynamic and static effects of any scanning motion or change of position must also be considered because of possible structural distortion.

If rapid beam scanning is desired, it can be achieved over small angles by the use of a piezoelectric crystal or some such device acting to move the effective radiating center of the telescope feed system laterally at a high rate. As long as the beam motion achieved by this means is only a few beamwidths the beam distortion will not be large. Rapid scanning of more than a few beamwidths is a much more complicated problem and will not be considered in this study.

Two types of sources are being considered for the transmit function. One is the helium-neon gas laser, which radiates in a highly coherent manner over a round aperture. This radiation is relatively easy to manipulate for feeding a telescope of almost any size. An optically pumped solid state laser that radiates with reasonably good

spatial coherence over its output aperture could be handled in the same manner. The electrically pumped semiconductor laser, such as gallium arsenide, is a more difficult problem. First, its radiating aperture is oblong; second, the spatial coherence presently tends to be poor, since it will often radiate in sequence from various small regions of its aperture. However, spatial coherence may improve with further understanding and development of these devices. The oblong aperture can be used to feed a round or square aperture by first passing the radiation through a cylindrical lens that causes the beam divergence in the plane normal to the junction to be the same as in the plane parallel to the junction.

It appears desirable to consider the use of one antenna to both transmit and receive in which case the transmit signal must be kept out of the receive channel. If the transmit and receive frequencies are unique a frequency filter could be used as the isolation device. As the two frequencies will probably be the same or close, other means must be found. The most obvious isolation technique is to transmit and receive with different polarizations and use a polarization filter. Either circular or linear polarizations could be used.

5.2 SPECIFIC APPLICATIONS

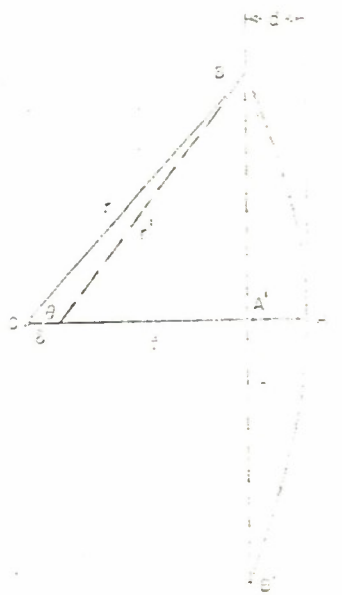
It would be advantageous to have c[illegible]n specific features for the antennas considered in this study. In particular, it would be desirable to have a controllable beamwidth, varying from perhaps the diffraction limit of λ/D to two or possibly three orders of magnitude larger, with an aperture that might be 4 to 12 inches in diameter. In addition, transmit rapid scan properties should be independent of the beam diameter. The large aperture is needed for operation close to the ground in order to average out any atmospheric turbulence. However, an aperture of 4 inches will have a diffraction limit of 10^{-5} radian, whereas about a 10^{-2} radian beamwidth may be necessary in some situations. Defocusing has been proposed as a simple means of increasing the beamwidth from a fixed aperture. Though analysis of defocusing has not been performed, it appears that it will not work very well. The best guess at present is that if the antenna feed is moved axially toward the lens or reflector, a reasonably good broad radiation pattern may be obtained for

some feed positions, but in general the radiation pattern will be poor. Analysis and computation in some detail would be necessary to prove or disprove this estimate, or, alternatively, it may be possible to perform an experiment for the same purpose. This experiment would involve using very small lenses so that the far-field or Fraunhofer distance would be in the order of 10 meters. Thus the effects of defocusing on the far-field pattern could be determined at ranges so short that atmospheric effects would be small.

Unfortunately, if defocusing does not work, there is no alternative immediately apparent to produce a beam divergence variable over a wide range of angles. It is possible to produce a beam much larger than the diffraction limit by shaping the output reflector or lens although the beamwidth cannot then be varied. It is fairly simple to increase the beamwidth by using an iris to change the effective aperture. A large aperture would then produce a small beam and vice-versa. This, unfortunately, defeats the primary purpose of the large aperture; to overcome atmosphere turbulence. It may be seen, then, that the whole problem is a difficult one which needs considerable study.

Tolerances of many kinds need be considered, as discussed above. Heating effects on optical parts do not seem to be much of a problem, because power levels will not be very high for most communication applications. The bottlenecks will probably be the smallest lenses, where the power densities will be the highest. Mechanical tolerances must also be considered. One obvious tolerance will be on the allowable motion of the feed point relative to the lens or reflector. Lateral motion caused, for example, by vibration will deflect the beam an amount roughly equal in radians to the deflection divided by the focal distance. Thus if the beam is one milliradian, the allowable deflection would be about 10^{-4} times the focal distance. Longitudinal deflection will defocus the beam and the allowable amount for a collimated beam can be readily calculated. Consider the geometry of a defocused parabola, as shown in Figure 8-1, where O is the focus of the parabola, OA = f and OB = r. The depth of the parabola is d. From the definition of a parabola:

$$r = f + d \quad \text{(this implies collimation)}$$



DEFOCUSING OF A PARABOLA

FIGURE 8-1

If the feed point is moved a distance δ toward the parabola, then a phase error is introduced, since $r' \neq f + d - \delta$.

$$r'^2 = r^2 + \delta^2 - 2\delta r \cos\theta$$

Neglecting δ^2

$$r'^2 \doteq r^2 - 2\delta r \cos\theta = r^2 \left(1 - \frac{2\delta}{r} \cos\theta\right)$$

$$r' \doteq r \left(1 - \frac{\delta}{r} \cos\theta\right) = r - \delta \cos\theta$$

$$r - r' = \delta \cos\theta$$

Thus the path length of a ray from the feed point to point B has changed by $\delta \cos\theta$, whereas the path length of a ray from the feed point to A and back to A' has changed by δ. Previously these rays had exactly the same path length. Now a phase error of magnitude δ (1-cos θ) has been introduced because of the difference in the new path lengths. The phase error over the entire radiating aperture BA'B' will have approximately a quadratic shape. Only about $\lambda/4$ phase error can be tolerated, so that the allowable δ will be roughly λ, or about 10^{-6} meters. This is a very tight tolerance that depends on the focal length-to-diameter ratio and will not change appreciably for a lens system. Thus careful mechanical design plus temperature control of the enclosure will be necessary.

6.0 SCANNING AND ANTENNA TRACKING

6.1 MECHANICAL TECHNIQUES

Two types of scanning operations must be considered for the purpose of optical communication.

(a) Low speed, large angle scan of the whole transceiver system for tracking and acquisition.

(b) High speed, small angle scan of transmitter or receiver beam, or both, to correct for the various propagation errors that have been discussed previously.

For the first type, it is obvious that, due to the masses involved, only mechanical systems are applicable. All necessary information

regarding tracking rates, accuracies, and associated servo problems is readily available from current radar technology. Thus, no detailed description of mechanical tracking systems will be given here.

As far as accuracies and stabilities are concerned, a comparison with state-of-the-art infrared (missile) tracking systems is in order. Pointing accuracies of 3 seconds of arc (for the gimballing system) are current practice with readout accuracies of the order of 10 to 20 seconds. Short-term stabilities are fractions of a second. Astronomical star tracking systems, of course, achieve greater accuracies at the expense of size and weight. Thus, it appears that the above listed numbers are well within the diffraction limited beam width of practical sized antennas.

The second type covers the situation where an optical beam of small aperture (on the order of 1 cm) is scanned within the (fixed) antenna system. Such a technique, however, is limited to angular deviations of a few times the antenna beam width, because of the obvious abberation problem. The following discussion is concerned only with techniques that fall under this category.

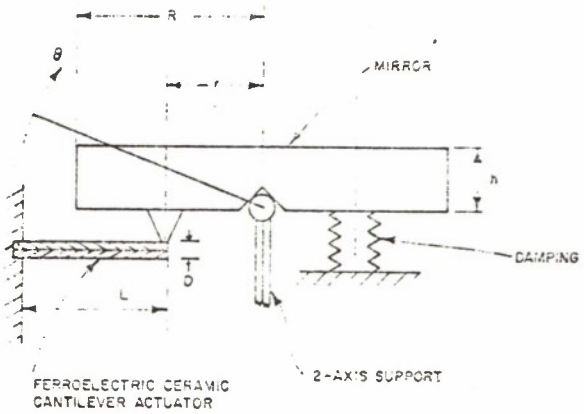
Again, the purely mechanical systems can be separated out as much literature is available on methods such as rotating wedges, and spinning prisms (Reference 3). For scan angles of 1 degree or less, electronic techniques are clearly superior.

For reasons of simplicity the following discussions are concerned with one dimensional scanning systems only. The results obtained, however, are general enough in nature to be extended to systems with 2 or 3 degrees of freedom.

6.2 PIEZOELECTRIC TECHNIQUES

The piezoelectric or magnetostrictive properties of ferroelectric ceramics can be utilized in a number of ways for the generation of small, controlled angular motions of optical reflectors such as mirrors and prisms. One typical configuration is shown in Figure 8-2. Two independent ceramic actuators (of the type in Figure 8-2), operating in two perpendicular planes will provide the required two-dimensional scanning operation.

A ferroelectric ceramic has a high dielectric constant, usually above 1000, at temperatures below the critical Curie point. Above the



POSSIBLE CONFIGURATION FOR
PIEZOELECTRICALLY DRIVEN MIRROR

FIGURE 8-2

Curie temperature, the material tends to lose its high dielectric constant and its piezoelectric properties. Therefore a Curie temperature well above maximum operating ranges is necessary. An example of actuator design, using simplified approximate calculations follows. The design utilizes the properties of PZT-4, a ferroelectric ceramic suited for high energy density, whose Curie temperature is approximately 350°C.

The ceramic is formed by sintering at temperatures above 1000°C, in pressed or molded forms. When removed from the kiln, it has the characteristic high-dielectric constant, but will not produce electrical charge at its surfaces when pressed and so is not piezoelectric. However, when metal electrodes are attached on two faces and a charge is applied, the resultant electric field aligns bound charges within the ceramic. And the ceramic lengthens slightly in the direction of the applied field while shortening slightly in the perpendicular directions. The strain is proportional to the square of the bound charge polarized by the applied field.

The square-law effect is called electrostriction. The ceramic also exhibits dielectric hysteresis, retaining a portion of its induced polarization when the applied field is removed. For piezoelectric use, the ceramic is subjected to a very high field while cooling from high temperatures. The heat and field cooperate to produce saturation polarization, a large portion of which is retained after cooling and removal of the field.

Ceramic that has been poled by this process exhibits piezoelectricity, producing charge and field along the poled axis when mechanically stressed. If the remnant polarization from poling (P_0) and a small additional polarization signal (P) is induced, the electrostrictive strain is proportional to the total, squared:

$$(P_0 + P)^2 = P_0^2 + 2P_0P + P^2 \qquad (8\text{-}14)$$

Because P_0 is much larger than any signal component P that can be induced at temperatures well below Curie,

$$P_0^2 \gg 2P_0P \gg P^2 \qquad (8\text{-}15)$$

The strain component corresponding to P_0^2 is thus unaffected by signal, that corresponding to $2P_0 P$ is directly proportional to signal, and that corresponding to P^2 is negligibly small. The linear correspondence between signal components of strain and polarization is piezoelectric coupling.

For design purposes, an algebraic representation of the linear signal properties is needed. The strain (S) is linearly dependent on applied stress (T) and applied field intensity (E). Mathematically:

$$S = \frac{T}{Y} + dE \qquad (8\text{-}10)$$

where Y and d are constants of proportionality, Y is the elastic (Young's constant) modulus, and d is the piezoelectric strain constant. For a well-poled PZT-4 ceramic bar, the values applicable to mirror actuator operation are:

$$Y = 1.28 \times 10^{7} \text{ psi}$$

$$d = 4.33 \times 10^{-9} \text{ inch per volt}$$

When PZT-4 is clamped to prevent motion and strain, an applied field (E) produces a stress of magnitude

$$dYE = 5.60 \times 10^{-2} E \text{ psi}$$

Maximum useable field is of the order of 20,000 volts per inch (20 volts per mil), corresponding to an induced clamped stress of 1120 psi. This is well under the tensile strength of the ceramic.

The simplest mirror actuator would be a longitudinally expanding rod. For the desired magnitude of motion, however, such a design would require an unduly long ceramic rod.

A much more practical design is that of a laminated cantilever as shown in Figure 8-2. The ceramic bar is anchored to a solid support and bearing against the mirror force (F). The bar is formed of thin ceramic laminations, arranged so that an applied positive voltage induces contraction in the upper half of the bar and expansion in the lower half. These longitudinal stresses act to bend the bar upwards when voltage is applied. The laminations are connected electrically in parallel, so that a high field can be produced by a relatively small voltage. The choice

linear displacement (y) ≈ ±0.0055 inch and $f_{res} \approx 33$ cps. Thus, for the chosen configuration the deflection angle is $\theta_{res} \approx \pm 38$ minutes. If critical damping is applied, the frequency characteristic of such a system is shown in Figure 8-3.

From the foregoing discussion it is readily seen what the possible trade-offs between scan angle and scan frequency are.

The concern here has been with wideband systems only as this will be the requirement for a variable-frequency scan. For a fixed-frequency scan, however, much higher rates can be achieved. The same basic algebra applies for this case and transducer displacement has to be multiplied by the mechanical Q of the system. No estimates on behalf of this Q-factor can be made, however, without a detailed knowledge of all design parameters.

A practical method to scan the field of view of the receiver is shown in Figure 8-4. Two narrow slits are mounted in crossed position where each slit is operated by a cantilever ceramic bar as described above. The slits are in the focal plane of the receiver optical system and the effective angular field depends on the magnification. The masses involved are much smaller than in the mirror case discussed above. Thus, a higher frequency response can be expected.

6.3 ULTRASONIC SCANNING

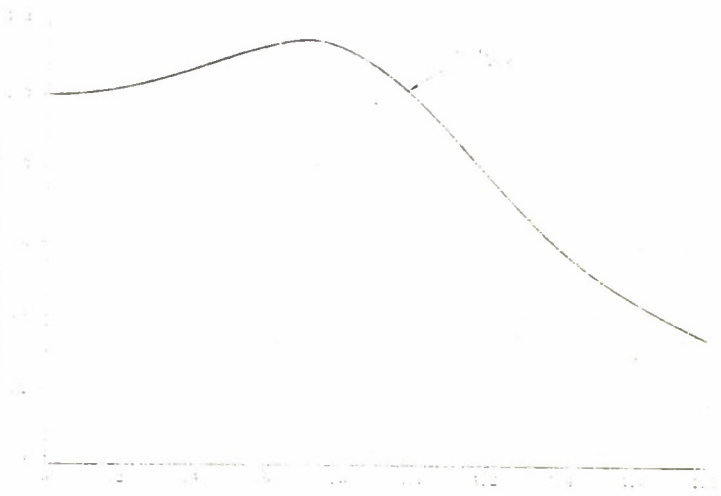
In ultrasonic scanning the direction of a light beam is changed as it passes through a medium supporting ultrasonic waves. Either of two optical phenomena, refraction or diffraction, may be basically involved.

6.3.1 Refractive Scanning

A standing ultrasonic wave produces a sinusoidal variation of the refractive index in the propagation medium. A plane optical wavefront incident normally on this medium is refracted, see Figure 8-5. If the light wave is incident at a node and its width is much less than the acoustical wavelength, then the light beam is deflected first to one side of the normal and then to the other; it scans at twice the frequency of the ultrasonic wave.

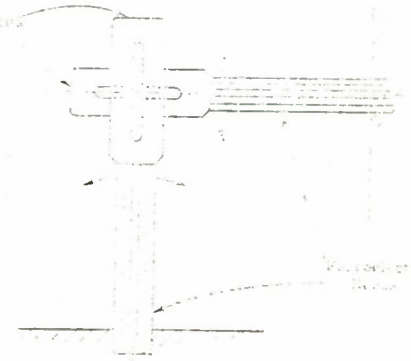
The angle through which the beam scans is given by:

$$\theta_t = \frac{2\pi \Delta N_r d}{\lambda} \cos ft \quad \text{degrees} \qquad (8\text{-}23)$$



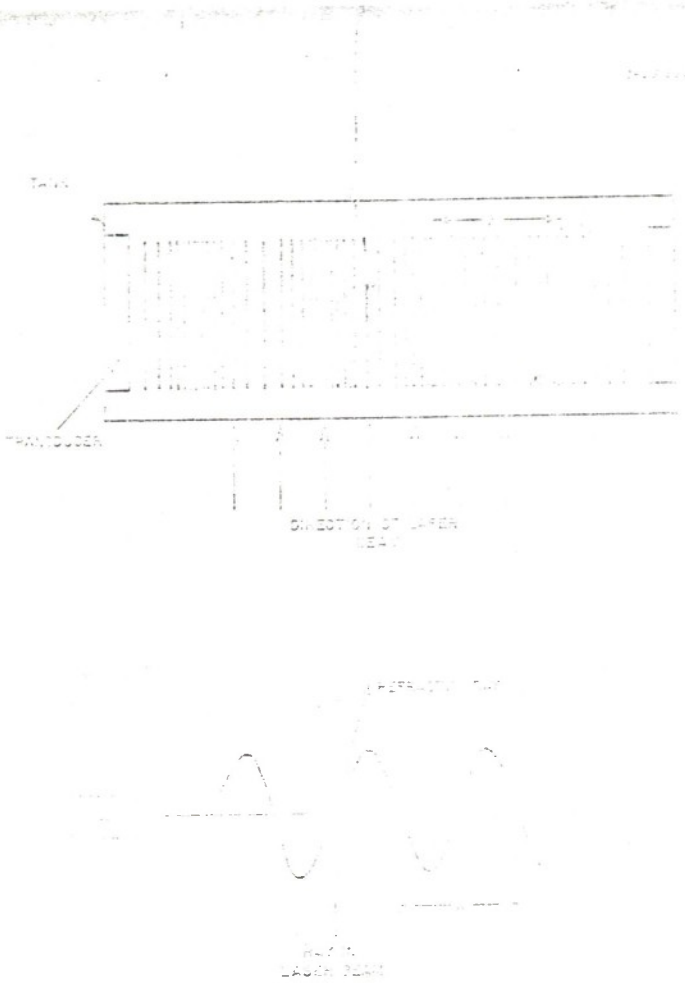
ANGULAR DEFLECTION AS A FUNCTION OF FREQUENCY FOR CRITICALLY DAMPED SYSTEM AND CONSTANT DRIVE

FIGURE 8-3



PIEZOELECTRIC SCANNING OF DETECTOR FIELD OF VIEW

FIGURE 8-4



REFRACTION OF LIGHT IN AN ACOUSTICAL CELL

FIGURE 8-5

where ΔN_0 is the amplitude of the acoustic wave that has frequency f, wavelength λ, and width d. The maximum value for θ_t, found to date, is 1.4 degrees. Larger angles should be possible if the amplitude of the propagated ultrasonic wave can be increased. However, at higher power levels the harmonic content of the ultrasonic wave degrades the optical beam.

The scan frequency is limited by the requirement that the width of the light beam must be much greater than the ultrasonic wave length (λ). Hence, for an optical beamwidth of 1 mm, λ must be about 1 cm. Therefore, the maximum acoustical frequency or half the scan rate is $f = v/\lambda = 1.5 \times 10^6$ cps, where v is the velocity of the sound wave and is about 1.5×10^5 cm/sec for most liquids. Higher scan rates could be achieved by using solids, where the velocity of sound is greater, but then the angular deflection is down by an order of magnitude.

This technique enables an optical beam to scan through about 1 degree at rates up to a few megacycles.

6.3.2 Diffractive Scanning

Diffractive scanning appears to be much more promising even though it is plagued with difficulties. Some are inherent to the basic phenomena involved, others are experimental. A theoretical description of the physical phenomena is given in Appendix V. It is shown that large angular deflections are possible; these are gained only at the expense of the intensity. Thus, with presently available transducers, production of 10 degree scan angle reduces the intensity to the threshold of possible measurement and seemingly too low to be useful. Only significant improvement in the amplitude of the acoustical waves that can be propagated will relieve this situation. Further, the scan rates are not limited electronically but by the resolution required. It is possible that shear waves might give rise to a slight enhancement, as the acoustical velocity is smaller.

6.3.3 Electro-Optical Scanning

The angle of refraction (θ) for a plane wavefront of light incident on a boundary between two dielectrics of refractive indices n_0 and n is given by Snell's law:

$$\sin \theta = \frac{n}{n_0} \sin \theta_0 \qquad (8\text{-}24)$$

or for small angles:

[illegible]

where θ is the angle of incidence. [illegible] in liquids (for example. The electro-optic effect provides a means of obtaining changes in the index of refraction as a function of an applied electric field. These changes are typically 10^{-5} at room temperature and [illegible] dielectric breakdown). Two possibilities exist:

(a) Enhancement of Pockels effect

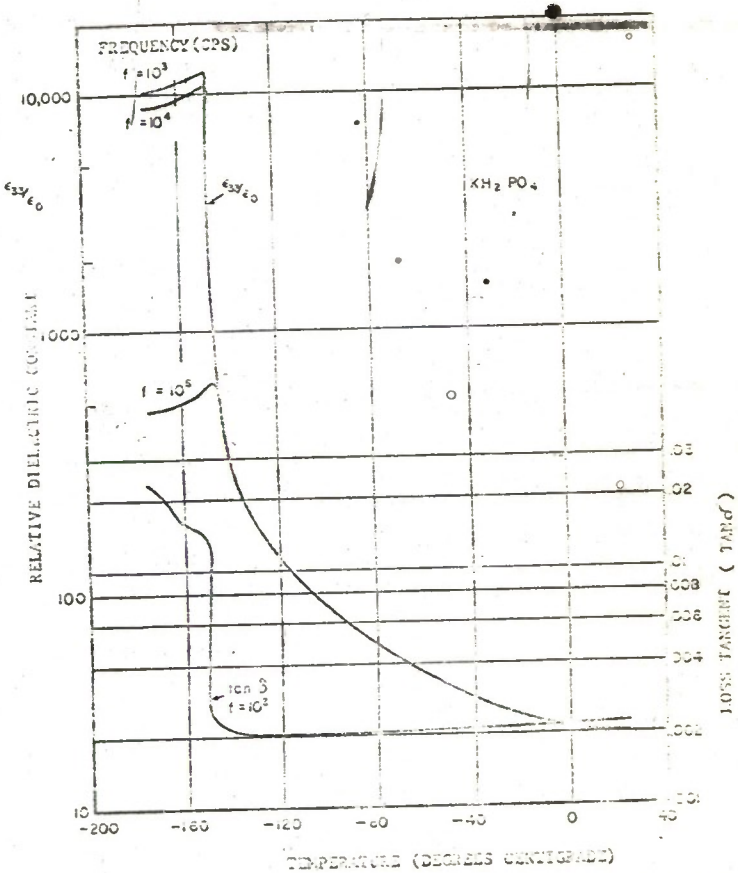
The most promising materials are KH_2PO_4 (KDP) and KD_2PO_4 (DKDP). It can be shown that, for those two materials, the ratio

$$\frac{r_{63}}{\epsilon_{33}\epsilon_0} = \text{constant} \qquad (8\text{-}28)$$

is an essentially temperature-independent constant, where ϵ_{33} is the effective dielectric constant along the optic axis. The Pockels constant (r_{63}) can therefore be written as:

$$r_{63}(T) = \frac{2.1\times10^{-7}}{T - T_c} \qquad (8\text{-}29)$$

where r_{63} is in m/v with T in °K, T_c is the Curie temperature (= 122°K for KDP and = 222°K for KDP*). The temperature dependence of r_{63} for KDP is plotted in Figure 8-6 (Reference 5). Note the temperature variation of r_{63} is much greater than that of ϵ_{33}. The dielectric properties of KDP are listed in Table 8-1 (Reference 5).



DIELECTRIC CONSTANT AND LOSS TANGENT AS A FUNCTION OF TEMPERATURE FOR KH_2PO_4

FIGURE 8-6

TABLE 8-1

DIELECTRIC PROPERTIES OF KDP AT 25°C (FIELD PARALLEL TO OPTIC AXIS)

f (cps)	10^2	10^3	10^4	10^5	10^6	10^7	10^8
ϵ_{33}/ϵ_0	21.4	20.7	20.5	20.3	20.2	20.2	20.2
tan $\delta \times 10^4$	170	24	<20	<5	<5	<5	<5

Figure 8-6 and equation (8-27) indicate that a significant increase in the electro-optical effect can be gained by operating at temperatures close to the Curie temperature.

(b) Enhancement of Angle Dependence on Changes in Refractive Index by Operating at Large Angles of Incidence.

At the General Electric Company, Electronics Laboratory, a method for electro-optical beam deflection has been developed (Reference 6) that is a combination of both possibilities of increasing electro-optical effects. This method calls for a special configuration of two KDP (or KDP*) crystals where the electric field is applied along the direction of propagation. If d is the linear aperture and ω the ordinary index of refraction of the crystal, it can be shown that the included scan angle (θ) is given by:

$$\theta \simeq \frac{2}{d} \omega^3 r_{63} V \quad \text{degrees} \qquad (8\text{-}28)$$

where V is the voltage along the crystals. No distortions, other than those caused by material imperfections, are experienced by the emerging beam.

Because the device works equally well for light polarized in two orthogonal directions, multiple passes through the same scanner element can be made separable by virtue of polarization. Thus, for cascading of up to three elements the total scan angle becomes:

ILLEGIBLE

A low f-number, folded Cassegrainian telescope with parabolic primary mirror represents the best compromise with respect to the above requirements as a universal optical system.

The simplest design configuration, of course, is the use of separate optical systems for each of the four described functions. This, however, does not meet the requirement of light weight and compactness (small inertia). It also introduces serious boresight problems. In the following discussions attempts have been made to combine a maximum number of, if not place all, functions in one telescope with a minimum of interference and loss in efficiency.

As the transmission and reception functions have been previously discussed they will not be repeated here.

7.1 ACQUISITION AND COARSE TRACKING SENSORS

The acquisition problem is the most difficult one as it imposes enormous bandwidth and scanning speed requirements. Also, because loss of contact is very likely to occur during the initial acquisition phase, a detector memory is required.

A vidicon or image orthicon would be the best solution to this problem. The accuracy of the target coordinates can be estimated to be of the order of one resolution element of the electronic scan. For a 525 line scan and a 15 degree field of view this would be about 4 minutes of arc.

7.2 FINE TRACKING SENSORS

A resolution on the order of minutes is not adequate for precise determination of position and tracking of a narrow laser beam. Two methods are available to overcome this problem:

(a) Narrowing the image orthicon trackers field of view after acquisition has been accomplished.

(b) Using a second detector for the precision tracking.

From the standpoint of reliability and complexity, it appears at this time that the second alternative will be the more promising. A variety of star trackers are known with accuracies of the order of seconds of arc (Reference 8). Depending on the way the error signal is generated, these devices fall into two categories.

7.2.1 Quadrature Detectors

The image plane of a photomultiplier (or thin film detector for applications requiring low sensitivity) is divided into four sectors. By comparing the energy in the four sectors, the angular position of the object can be determined. Elegant solutions featuring photomultipliers with divided cathodes are currently being developed (Reference 9).

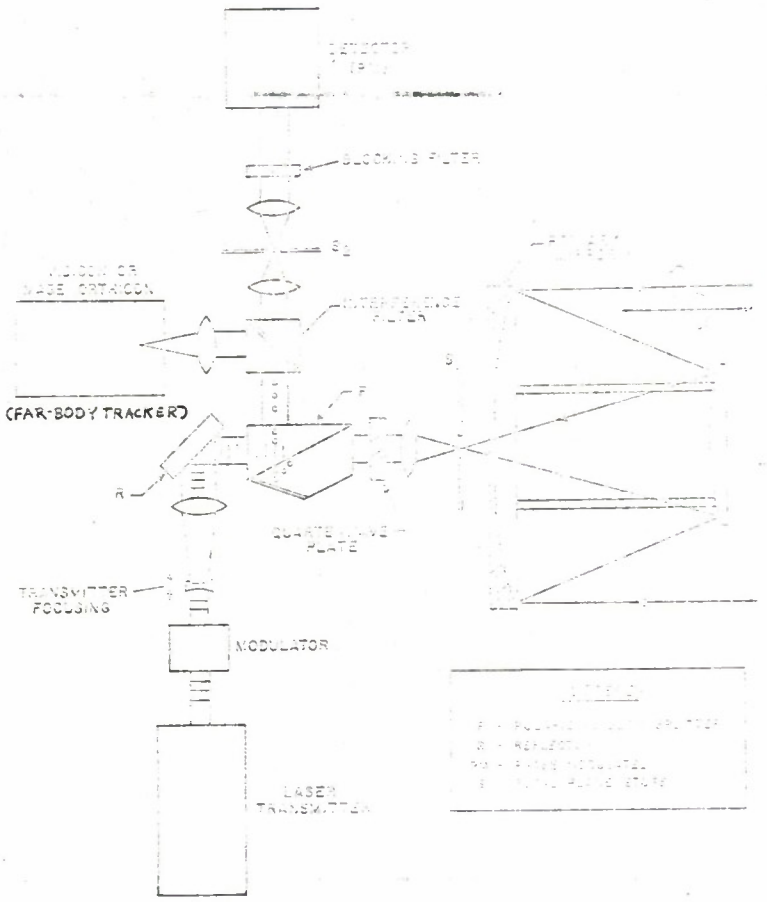
7.2.2 Revolving Reticle Detectors

The reticle is placed in the focal plane and angular target information is obtained in the form of either amplitude or frequency modulation of the incoming energy.

Both types of precision trackers have their advantages, depending on specific systems requirement. Their common feature is, however, that they use the same type of photodetector as the communication receiver. Thus, the obvious question arises whether the two functions can be combined in one detector. Anderson has shown (Reference 1) that for slow scan speeds (on the order of 100 cps) the interference between tracker and communication channel is negligible for all practical purposes. The advantage of such a combination is not only its simplicity, but also the additional background discrimination that can be gained for the communication receiver because of the shutter effect.

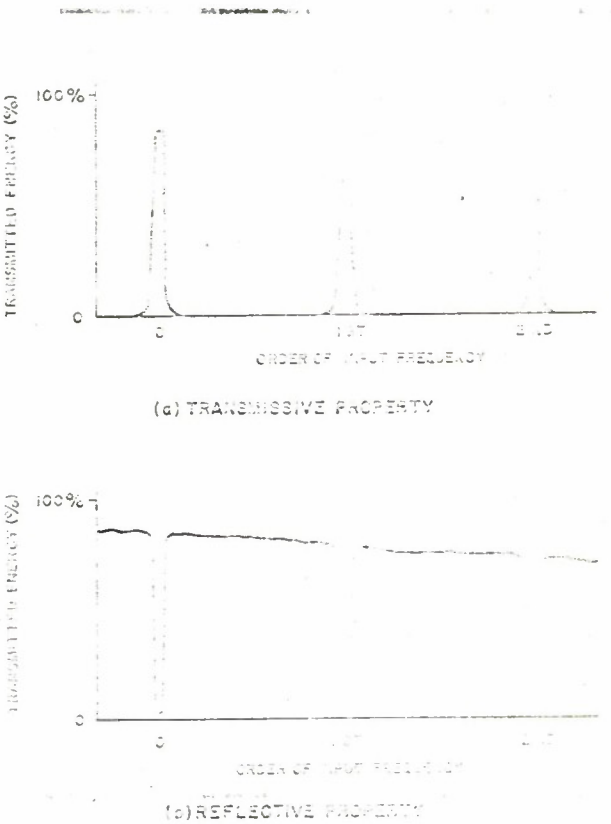
7.3 MECHANICAL CONFIGURATIONS

One potential solution to the problem of combining all functions of the communication link in one telescope is shown in Figure 8-7. Receive and transmit channels are separated utilizing linear polarization. The isolator is a polarizing beam splitter, P (for example a Foster-Seeley prism) that should give at least 50 db of isolation. The linearly polarized laser output is converted into circular polarization by means of a quarter-wave plate. If both stations transmit right-handed circularly polarized radiation, then the transmitted and received signal will be crossed polarized at the beam splitter and, thus, be separable without losses. Another lossless way of isolating the receiver (plus time tracker) from the far-body tracker is proposed through the use of a tilted narrow-band interference filter. The reflection and transmission properties of such a filter are shown in Figure 8-8.



LASER COMMUNICATION TRANSCEIVER, CONFIGURATION A

FIGURE 8-7



TRANSMISSIVE AND REFLECTIVE PROPERTIES OF A TILTED, NARROW-BAND INTERFERENCE FILTER

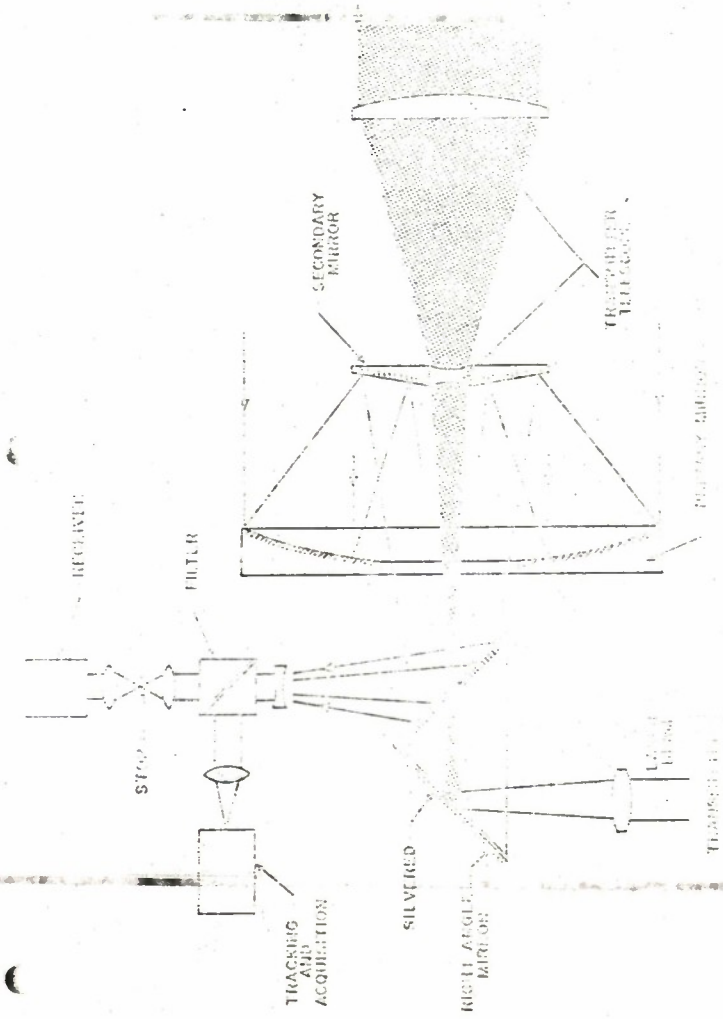
FIGURE 8-S

Because only a very small portion of the total incident spectrum contains the wanted information, the remainder can effectively be utilized for coarse tracking purposes. The two focal plane stops S_1 and S_2 ($S_1 > S_2$) are adjustable and define the field of view for tracker and receiver respectively. Coarse tracking of the antenna is accomplished by mechanically gimballing the whole, integrated system. Fine tracking (scanning) within a fixed antenna orientation of the transmitter or receiver, or both, is independently done by using one of the techniques described in Paragraph 6.2 (for example, piezoelectrically with the reflector, R, and the aperture, S_2). The optical system past the secondary antenna mirror is only one of several possible configurations.

The system has the advantage, (for operation at high altitudes or under conditions where reciprocity can be established simply by a large enough transmitting antenna) that a perfectly symmetric and boresighted link can be established. It has the disadvantage that the receiver will be sensitive to transmitter radiation that is scattered from clouds and haze. This is because polarization is expected to be preserved for backscattering within this particular region of Mie scattering. Backscatter may not be a problem for most practical cases, however, and can also be eliminated for pulsed operation by proper gating of the receiver.

The tracking and acquisition requirements determine the minimum acceptable transmitter beam divergence that will always be much larger than the diffraction limit of a large (for example 24 inch) receiving paraboloid. Thus, pruposeful defocussing becomes necessary. To circumvent this difficulty (Paragraph 5.0), the specific radiation pattern of Cassegrainian systems can be utilized as shown in Figure 8-9. Since the innermost cone of the reflecting system is blanked by the secondary mirror, it could contain the (refractive) transmitter telescope. By proper choice of secondary optics (see Figure 8-9) no received energy is lost at the right angle mirror which isolates transmitter and receiver. Additionally, effects caused by near-zone scattering are small.

It is felt that configurations A and B represent the two most practical fundamental systems. Several combinations and internal variations thereof are possible and it is not intended to describe these in



LASER COMMUNICATION TRANSCEIVER, CONFIGURATION B

FIGURE 8-9

detail. For example, tracking sensor and/or star trackers that are normally very small and compact could be mounted externally to (for example on the front of the secondary mirror) the reflecting telescope.

8.0 CONSLUSIONS AND RECOMMENDATIONS

The problems of tracking, aiming and acquiring have been discussed from both the components and systems standpoints. In general, feasibility has been shown for a medium range optical communication link under a variety of conditions. Solutions to specific problems have been given, and block diagrams of workable systems presented. Other problems have only been listed, due to the uncertainty of assumptions and also due to the limited time available for this study. Areas requiring further investigation and development, however, are clearly defined. These are:

(a) Atmospheric Propagation Effects

Much additional information is needed on the validity of the principle of reciprocity under varying conditions of turbulence and other disturbances. Also relatively unknown are the propagation effects for coherent radiation with respect to phase, amplitude, polarization, path length and aperture size.

(b) Components

This is of particular importance in the area of reception and includes the following items:

(1) Photodetectors with higher sensitivity and fast response in the region from 0.8 to 1.5 microns.

(2) Optical filters with band-pass of the order of 1×10^{-4} microns with high peak transmission, temperature stability and large field of view.

(3) Lightweight reflective or refractive elements (plastic) having high precision.

(4) Small size, high resolution tracking sensors.

(c) Systems

A great deal of analytical work is required in order to fully understand the component implementation of specific systems requirement. One particular aspect, which calls for extensive developmental work, is the demand for a high speed, wide angle, electronically controlled optical beam scanner.

9.0 REFERENCES

1. R. F. Anderson; Technical Documentary Report ASD-TDR-62-733; AD No. 293452.
2. Thermal Effects in Laser Amplifier and Oscillators; A. E. Blume and K. F. Tittel; Applied Optics, Vol 3; April 1964.
3. M. R. Holber and W. L. Wolfe; Proceedings of the IRE, Vol 47; 1959.
4. B. Zwicker and P. Scherrer; Helv Phys Acta, Vol 17; 1944.
5. T. R. Slicker and S. R. Durlage; Journal of Applied Physics, Vol 37; 1963.
6. I. N. Court and F. K von Willisen; GE Technical Information Series R64ELS-1; Jan 1964.
7. J. E. Geusic et al; Applied Physics Letter, Vol 4; April 1964.
8. F. Stephens; SAE Journal, Vol 69; 1961.
9. The Quadrant Multiplier Phototube; M. Rome; March 1963.

SECTION 9

PRIVACY OF LASER LINKS

1.0 PROBLEMS OF PRIVACY

Privacy involves the following three factors:

(a) Before an interceptor can detect a signal, he must find its source. To do this he must have a detector at the right wavelength pointed in the right direction at the right time; otherwise, he will not know a communication link exists.

(b) Once the detector locates the signal, it must intercept sufficient power to detect a message.

(c) Merely intercepting a signal of adequate strength is not satisfactory; the message must be deciphered. This can be guarded against through the use of traffic encryption, much the same as is done with other links carrying secure traffic.

In the following paragraphs the first of these problems (a above) is assumed to have been solved; that is, the interceptor knows the location of the source, the time of transmission, and the correct frequency. It is in the second problem that the potential advantages of laser communication links lie. In many applications, the confinement of laser energy to extremely narrow beamwidths, which is easily accomplished using laser techniques, can deny to an interceptor sufficient power to adequately detect a message being carried by the beam. If this can be accomplished, then recourse to encryption techniques to prevent deciphering traffic becomes unnecessary.

A secondary consideration in traffic privacy is that, in most cases, the interceptor must perform his task without alerting the user to the fact that the interceptor is at work.

2.0 MECHANISMS FOR INTERCEPTION OF LASER BEAMS

The primary mechanism by which laser beams may be available to an interceptor is by scattering. Scattering can be divided into three major categories: that due to atmospheric refraction; that due to airborne particles such as dust, snow, smoke, and aerosols; and that produced by glass through which the beam is transmitted. Most scattering produces phase shifts, which generally will destroy the phase coherence of the received light.

2.1 REFRACTIVE SCATTERING

Atmospheric refraction is the bending experienced by a beam as it passes through turbulent regions in which there are small variations of air temperature and pressure. Measurements show that the beam can be bent through an angle of as much as 1 milliradian, at scintillation frequencies between 10 cps and 1 kc. Experimental observation indicates that the beam can be detected at angles exceeding 10 milliradians, although this has not been measured. Detection at large angles is estimated to occur for only for short times, during which bursts of data might be intercepted; but this phenomenon cannot be relied on for interception of the beam for long periods of time.

2.2 PARTICLE SCATTERING

Particles in the air establish a major limit on the operation of any optical system. Fog, snow, dust, or water vapor can cause scattering of up to 100% of the signal at ranges as short as 100 meters. This form of scattering has little effect on the shape of the main beam, other than attenuation. Scattered light goes into the "side lobes."

Each particle radiates the light it scatters as a spherical wave; and since scattering particles have a random distribution, there is no preferred direction to the scattered light. An exception to this is the light scattered from plane-faced crystals such as snow. In this case, each plane face on which the beam falls reflects a large portion of the light specularly. Since such crystals can fall with a preferred orientation, the scattered light can concentrate in conical beams.

Another exception to spherical scattering is the transparent sphere that is large with respect to the wavelength of the light, such as raindrops. Internal reflections produce focusing effects resulting in preferred directions depending on wavelength. Examples of this phenomenon are the scattering of sunlight by ordinary clouds, the sun-dogs and rings around the sun produced by scattering from clouds of ice crystals, and the rainbows produced by scattering from rain drops.

Practical application of scattering of electromagnetic waves is made in radio tropospheric scatter. Here teletype, voice, and even television signals are transmitted well beyond the horizon. The scattering of light beams in this manner has also been used for years by Naval and

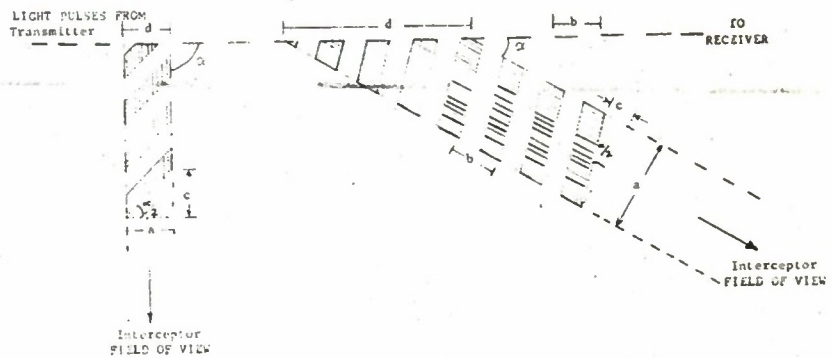
Maritime services for communicating over the horizon, or over intervening land. The signalman merely points his searchlight upward and blinks the light in the conventional way. The beam can be seen for miles, depending on the condition of the atmosphere. A brief treatment of scattering is given in Reference 1.

Whether successful interception of a laser beam can be achieved depends on a number of factors dealing with the laser system. For instance, a limit could be that a significant number of photons must be received per bit of information. If an interceptor cannot receive at least that number of photons per bit, then it would not be able to decipher a message.

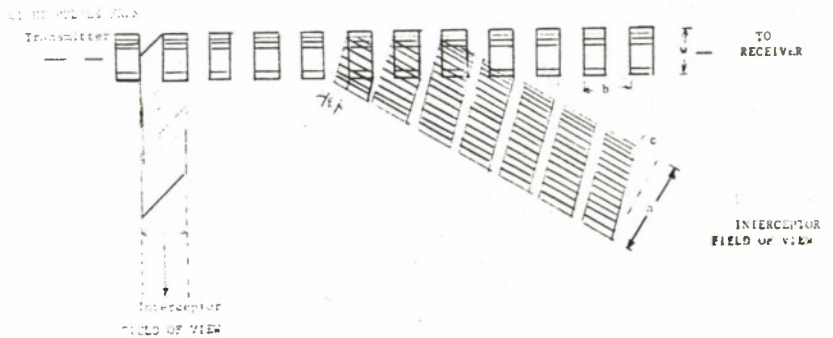
2.2.1 Interception of a Narrow Beam

Another limit on the interceptor could be the physical length of a bit in space. To receive a useful number of photons by atmospheric scatter, the interceptor must observe the beam over some length (d) with a receiver beam width (a) at the scattering area, as shown in Figure 9-1a. The look angle between the laser beam and the interceptor beam is α. The interceptor beam was drawn in Figure 9-1a with parallel sides; this would introduce minor distortion since it is not anticipated that the interceptor can be placed close to the main beam. The interceptor observes bundles of scattered light spread out in both time and space. If the distance $c = a \tan \alpha/2$ is greater than half the bit length (b), one end of one bundle will arrive at the receiver before the opposite end of the previous one. Thus the interceptor receives triangular pulses if square waves are transmitted, the triangles overlap if c is greater than b/2. If the width of the beam (a) is increased to improve the S/N ratio, nothing is gained since the time overlap of successive pulses at the receiver is also increased. This causes "blurring" or "smearing" of the light bits and hence of the signal. The only remedy available to the interceptor is to reduce the look angle (α) by either increasing the range of observation or decreasing the distance between the interceptor and the beam.

For example, assume a narrow pencil beam ($\alpha = 90°$), b equal to 1 meter (a bit rate of 300 mc), and transmitter duty cycle (Du) of 0.5. Then to determine the value of a that will produce a maximum ac



(a) From Narrow Beam



(b) From Broad Beam

INTERCEPTION OF SCATTERED LIGHT

FIGURE 9-1

signal at the interceptor. As c gets longer, the triangular component of the signal increases; when c = b/2, overlap commences and there is no further increase in the ac component of the signal. Therefore, since c = a tan α/2 and tan 45° = 1, a = b/2 or 0.5 meter.

As another example, assume a narrow pencil beam (α = 30°), b equal to 1 meter, and Du equal to 0.5. To determine the value of a that would produce a maximum ac signal at the interceptor, c = b/2 and tan 15° = 0.2679; therefore, c = 0.2679a. Since c = 0.5 meter and a = 1.87 meter, the length of beam that can be observed is 3.74 meters.

2.2.2 Interception of Wide Beam

The discussion in the above paragraphs assumes the beam has little width. Consider now the situation where the beam width (w), or diameter, is significantly large as shown in Figure 9-1b. The main beam travels in bundles, having leading and trailing edges. Light scattered towards the interceptor at the leading edge of the bundle at one side must travel a different path than that scattered from the leading edge at the other side. This serves to lengthen each light bit that the interceptor can detect. This lengthening (f) is determined by the relation f = sin α/2. If f is equal to the "dark" space between light bits, the interceptor receives a continuous signal instead of the transmitted square waves. As the angle α is reduced, the spreading is also reduced, as it must be, since the intended receiver must see no spreading.

For example, assume a large diameter beam (α = 90°), and b and w equal to 1 meter. Interception without overlap at the receiver is not possible if scattering is assumed uniform throughout the illuminated volume. If Du equals 0.5 and the width (a) is increased from zero, the dc level of the signal increases and the triangular portion varies in phase and amplitude but the maxima never exceed the value when a = b/2.

As another example, assume a large diameter beam (α = 90°), b and w equal to 1 meter, and Du equal to 0.5. Determine the maximum angle (α) at which detection can be achieved with no overlap with a 1 meter aperture (a). The sum of c + f must be less than b/2, therefore, a tan α/2 + w sin α/2 is less than b/2. Then tan α/2 + sin α/2 is less than 0.5, and α is approximately 29°.

2.3 SCATTERING BY GLASS

When light passes through glass, some light is scattered at both surfaces and source is scattered within the glass as shown in Figure 9-2. A laboratory comparison was made of the light scattered by a piece of glass to that in the main laser beam. Roughly 1% of the power of the beam was scattered, and about 5% was specularly reflected. This phenomenon might be useful to an interceptor in two ways: the scattered light can be observed from either the transmitter lenses or the receiver lenses; or in some limited cases, it can be observed from a piece of transparent material held in the beam, somewhere mid-range. Since only about 1% of the signal is scattered in this manner, the user of the laser system would not be aware of the interference. However, once again the subject of signal strength versus bit rate must be considered. If only 1% of the signal is scattered, and this is scattered uniformly in all directions, the interceptor will not receive a large percentage of the scattered signal. For instance, let us consider the light scattered from the transmitter lens (about 1%) is detected by a $10^{-2} m^2$ detector located at a distance of 1 km. Since the light is scattered spherically, the light that reaches the receiver is uniformly distributed over a sphere whose area is $4\pi x10^6$ m^2. The received signal will be

$$(10)^{-2}(10)^{-2}/(4\pi)(10)^6 = 8x10^{-12}$$

of the transmitted signal, or -111 db.

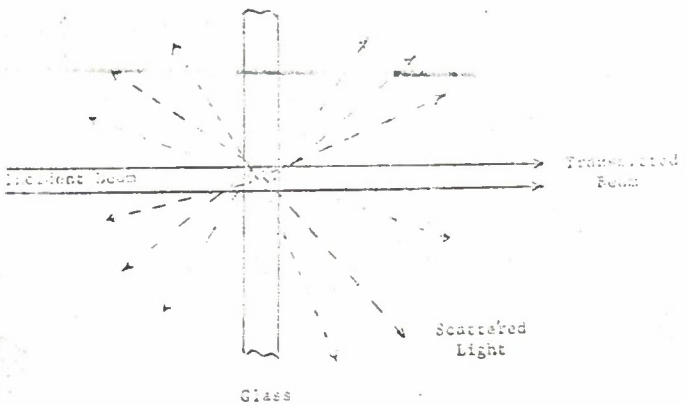
Should the interceptor be in a position where it is possible to use scattering by glass, he can improve his S/N ratio by rotating the transparent plate so that it acts like a beam splitter (see Figure 9-3), which would then provide a few percent of the signal, depending on the index of refraction and surface condition.

3.0 PRIVACY IN LASER SYSTEMS

Laser communication systems can be placed in the following broad categories: space-space, space-ground, air-to-air, and ground-ground. The chances for interception in each case varies, so they are discussed separately.

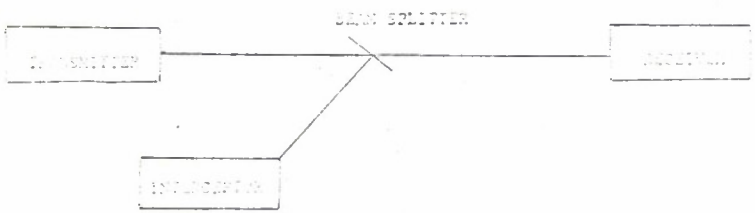
3.1 SPACE-SPACE LINKS

Two space vhicles that are in communication with each other can be separated by distances from zero to millions of kilometers. Such



SCATTERING FROM A GLASS PLATE

FIGURE 9-2



INTERCEPTION OF MAIN BEAM BY BEAM SPLITTER

FIGURE 9-3

links must use accurately pointed beams, and where the separation is great, the beam would be as narrow as possible to conserve power and improve the S/N ratio. Beam widths of about 10 microradians are feasible. Such a beam would spread to a 10 kilometer diameter at a distance of one million kilometers. Obviously no receiver, either that of a friend or foe, can intercept or obstruct a large fraction of such a beam. It is therefore possible that an interceptor could be in position to collect as much energy as the desired receiver, without obstructing receiver energy and so being detected.

In space, although light travels in straight lines, vehicles must travel along curves, with the result that three vehicles are difficult to keep in a straight line for very long. For this reason, interception of the main beam is not feasible except for short durations. Continuous interception can therefore be achieved only from the scattered portions of the beam. If the laser system is designed to reduce possible interception and to conserve power, it will transmit only enough energy to permit satisfactory operation of the receiver within the main beam. Any receiver outside the main beam will therefore be unable to collect enough energy, unless it compensates for the loss of signal by using a significantly larger receiver aperture. The only scattered energy useful to the interceptor is that scattered directly by the transmitter, since there are few scatterers in space and the receiver vehicle intercepts only a small portion of the transmitted energy. Thus space-space systems are inherently private.

3.2 GROUND-SPACE AND SPACE-GROUND LINKS

Interception can be achieved at several points in this system, depending on the direction of flow of information.

3.2.1 Ground-Space Links

Interception in ground-space systems might be achieved from space in the vicinity of the space vehicle, from the air in the vicinity of the transmitter, or from the ground looking at atmospheric scattered light.

Interception from space involves having a vehicle in line with both receiver and transmitter, and as mentioned in paragraph 3.1 this can be achieved only under special conditions.

The use of an aircraft is feasible only under severely limited conditions, and involves probable knowledge of the aircraft mission by personnel at the transmitter.

Looking upward from the ground intercepting light scattered by the atmosphere might seem a good method, but if the information rate is high the intercepted information will be garbled as discussed in paragraph 2.0.

3.2.2 Space-Ground

The feasibility of intercepting a space-ground transmission depends on the parameters of the system. A well collimated beam, say 10 microradians, covers a ground area of no more than 50 to 60 feet in diameter if transmitted from a vehicle at 1000 miles altitude. However, at longer ranges this radius would increase, compromising the system. As mentioned elsewhere, space interception is not likely. Atmospheric scattering is not effective. The only two intercept means left are those that place the interceptor close to the user's receiver or those that can use scattered signal from the transmitter. The first of these, being within the beam on the ground, could be accomplished easily for space vehicles at long range;and the other, using the scattered signal, requires the interceptor to track the space vehicle and to have a large receiver aperture. Space-ground links thus are not inherently private.

3.3 AIR-AIR LINKS

Among the more difficult problems for interception are those of the aircraft system. Two aircrsft flying in formation could communicate with relative ease, assuming the pointing of the transmitter and receiver antennas is accurate. The likelihood that these messages could be intercepted is extremely small. The laser beam can have such a narrow angle that the receiving sircraft obstructs the entire main beam. In addition, sssuming that two-way communication is to be maintained, the two transmitters could be adjusted to produce only an adequate signal level to assure reliable communicstion, thereby reducing the possibility thst side-lobe or scattered light could be intercepted usefully. Also, the interceptor would have to maintain a position from which it could observe the scattered light, which would require an sircraft following the communicating pair.

Under some tactical situationa, air-ground communication could be maintained by lsaers. This would require that the aircraft remain visible to the ground aite at sll times. The interceptor, in this csse, might be able to detect scattered light, ss discusaed above in paragraph 3.3, but sgain if the signal level is kept low, little can be done with the intercepted light. The radius of the beam at the receiver would be small so that interception of the msin beam is not feasible.

3.4 GROUND-GROUND LINKS

Interception of laser communication between two atations on the ground preaents peculiar problems, some of which are discussed in paragraph 2.0. Since the trsnsmitter csn limit its output beam to s 0.01 milliradisn, an interceptor could not be expected to plsce a receiver in the beam path without being detected, except as diacusaed in paragraph 2.3. In that case, it ia likely that, with a good telescope such as the Questar, the uaer could aee light scattered by the besm splitter, and so determine that an interceptor ia present.

The methods of interception most likely to aucceed are those using acattered or reflected signal from either the tranamitter or the receiver lenaes, or from smoke, dust or stesm generated by the interceptor near mid-range. (In the latter case, the user might not recognize that the cloud waa generated for the purpose of interception.) Because of the general availability of the laser beam in these methods, privacy without encryption csnnot be enaured.

Permanent ground stations might be linked by optical beams made independent of the weather by being transmitted through a pipe. Such a pipe might take three forms: light fibers using internal reflection, a hollow pipe with reflective wall, or a hollow pipe with non-reflecting wslls.

Interception of the beam from a system using either of these methods is difficult, but possible. Such pipes would probably be buried, and the interceptor would be forced to dig to the pipe snd insert a fiber into the pipe to conduct a small but useful portion of the energy to his detector. Careful monitoring of the received signal level might be used quite successfully to gusrd against this kind of interception, but such vigilance ia not likely, unless the uaer haa such monitoring equipment in place.

In general, piped laser systems cannot be considered any more secure or free from tampering than a wire line. As a result, encryption would be required over such a link for secure traffic.

4.0 REQUIREMENT FOR ENCRYPTION CONSIDERING VARIOUS MODULATION TECHNIQUES

Aside from main beam interception, the only effective technique for interception of laser beams exists in the atmosphere, where scattering takes place.

Consider now modulation techniques that may be used to prevent demodulation of the message by an interceptor. The scattering process lengthens the period of any modulation on the beam, which is observed off to the side of the main beam. This is due to a multipath phenomenon where the possible path lengths are different. Consider pulse modulation of the main beam with 50% duty cycle. As the angle of the interceptor's beam with respect to the main beam is increased from zero the pulse duration in the interceptor's beam lengthens. At an angle of 90° and if the intercept of the interceptor's beam and the main beam is a line whose length is longer than or equal to the length of a cycle of pulse modulation, then a steady amplitude signal will be received at the interceptor and no information can be decoded. Therefore to prevent the interceptor from receiving the information, it would be advisable to modulate at as high a rate as possible to cause this blurring or smearing at small angles. This may be done by sending information at a very high rate, in which case the separate information bits would overlap and cause scrambling of the information bits.

Another technique of blurring the signal off axis would be to modulate a microwave subcarrier with the information bits that may have any desired bit rate. The optical beam is then modulated with the microwave subcarrier. The interceptor's beam subtending many microwave wavelengths would, at fairly small angles, receive a reduced S/N ratio because of the blurring of the microwave signal.

Another phenomenon of scatter that may be used to avoid the interceptor's demodulation of the information has to do with the phase angle of scattered light. Small particles are assumed to scatter coherently in time. For large transparent particles, some of the light will enter the particle and undergo internal reflections; a portion of the light will be

diffracted and the net result is considerable degradation in spatial coherence. Since the particles are randomly located in space, the effect is further degradation in spatial coherence. Therefore, the energy received at a ~~point off~~ the ~~main axis~~ of the beam is the superposition of many phasors having independent random phases and thus is incoherent.

If coherent phase modulation is used, the beam can transmit information provided the scatter process is coherent. The interceptor's beam must be essentially coincident or cophasal with the main beam to be able to receive a coherent signal. The user's receiver must operate under this same restriction; however, the user has an advantage because he knows where to point. If the user has a heterodyne receiver, there is a further pointing requirement because of the necessity for matching the phase of the local oscillator and the received signal over the photodetector surface. When scattering and atmospheric turbulence are present, such a heterodyne receiver may be useless because of this requirement. A phase demodulator that may circumvent this difficulty has recently been presented (Reference 2).

Table 9-1 gives the interception modes (scatter, side lobe pickup, or sampling main beam) that require encryption under different kinds of modulation.

TABLE 9-1

INTERCEPTION MODES REQUIRING ENCRYPTION

Modulation System	Main Beam Diameter	Interception Mode: Scatter	Side Lobe Pickup	Sample Main Beam
Optical-Phase	Any	No	Yes	Yes
Low Frequency Subcarrier	Small	Yes	Yes	Yes
	Large	No	Yes	Yes
High Frequency Subcarrier	Small	No	Yes	Yes
	Large	No	Yes	Yes

5.0 COUNTERMEASURES

There is one countermeasure that can be used against nearly all attempts at interception depending on scattering of the beam. Since scattering involves only a small portion of the signal, scattered in all directions, an obvious solution is to trsnsmit only enough signal power to provide reliable signal at the receiver. However, necessary margin in link design may preclude this approach. Under this operational procedure, it is relatively certain that the interceptor can receive adequate strength only by using an extremely large aperture (a minimum of 10^4 to 10^5 times as large as that of the user); however, this will generally result in a scrambled message.

To reduce possibilities of interception of side lobes or glass-scattered light, the transmitter should have an aperture only large enough to pass the main beam, snd not so small that some of the main beam is reflected from its edges. With wide aperture transmitters required in the atmosphere, this will have limited effectiveness.

An important countermeasure to interception for readily accessable links will be alertness on the part of the user, both at the transmitter and at the receiver. To intercept a significant portion of the transmitted light, an interceptor must expose a large-aperture receiver to some portion of the beam. If the operators of the system maintain careful surveillance of the beam path and if all regions from which a line of sight to either transmitter or receiver exists, an attempt at interception can be detected in all cases except that using particulate scattering along the beam. In the latter case, a countermeasure might be to prevent detection by using a beam splitter to divide the beam in such a way that two beams are adjacent in space, close enough that they would be difficult to separate from the side, but not from the receiver. These two beams could be modulated out of phase (zero on one beam with one on the other), so that from the side the interceptor can only detect a continuous signal.

6.0 REFERENCES

1. Atmospheric Scattering in the Visible and Infrared; J. A. Curcio, G. L. Knestrick, and T. H. Cosden; NRL Report 5567; Jan. 1961.

2. Demodulation of Microwave Phase-Modulated Light; S. E. Harris and C. F. Buhrer; No. FC11, 1964 Spring Meeting, Optical Society of America, Washington, DC; 1-3 April 1964.

SECTION 10

CONCLUSIONS AND RECOMMENDATIONS

Considerable developmental effort is still required before laser techniques can be used for Air Force communication. There are certain communication requirements that presently cannot be satisfied because of restrictions arising from the size of components necessary to ensure adequate received power. In addition, characteristics of the laser beam, such as the confinement of the besm to small (10^{-5} to 10^{-6} rad) angles of transmission, can provide certain communication links with privacy that can only be obtained by conventional communication techniques with complex encryption. Moreover, the available spectrum in a laser link, resulting from the high carrier frequency, makes spread-spectrum techniques of modulation feasible where required, while using other portions of the spectrum may prohibit their use because of bandwidth limitations.

Although present laser equipment is generally bulky, lasers show promise of providing small, reliable, and simple communication system components. In certain applications, however, techniques for transmission in other parts of the spectrum, such as those for millimetric waves, can compete in bandwidth and size of components. A logical choice of technique in these instances must await further development in both lasers and millimetric waves.

Since most laser techniques are still in a research stage, it is generally not feasible to recommend specific techniques in support of Air Force communication requirements. The conclusions and recommendations that follow therefore assess the suitability of laser techniques with regard to the specific applications presented in Section 3, and outline necessary effort based on the technological studies presented in the other sections that are germane to the application being considered. Additional recommendations assessing techniques for generating the laser beam, propagation through the atmosphere, aiming and tracking, and privacy are also presented.

1.0 RECOMMENDED LASER APPLICATIONS

Of the Air Force communication applications discussed in Section 3, lasers show promise of providing a primary communication technique in the following areas:

(a) Tactical air-air communication

(b) Airborne radio relay

(c) Air-satellite links for over the horizon aircraft communication

(d) Space-space links

(e) Fiber optical laser communication for lightweight cables.

For items a, b, and c above, the possibility of lightweight, small antenna structures for aircraft that can be made steerable makes lasers an attractive technique for communication. For tactical air-air communication, the inherent privacy of the laser link as discussed in Section 9 eliminates the need for encryption for use with intra-squadron or intra-mission communication. Similarly, the same considerations hold for airborne radio relay. In considering air-satellite links, lasers may provide the only technique for delivering appreciable information bandwidths to a satellite from an aircraft.

For these three applications, lasers in aircraft operating at high altitudes should not experience atmospheric effects to the extent of those experienced in ground-based point-to-point usage. However, additional data is required (and should be obtained) to ascertain these atmospheric effects at high altitude before feasibility can be demonstrated. In addition, implementation of airborne laser systems must await development of tracking techniques that are applicable to the conditions encountered.

Space-space links should make considerable use of advanced laser techniques. The extent of their application depends in large measure on the development of suitable aiming and tracking techniques.

For lightweight cable applications using fibre optics, considerable effort is required to reduce losses and develop fibre optics laser techniques prior to any definite recommendation. However, since alternate techniques do not presently exist for construction of such lightweight cables, the necessary development is warranted.

Communication applications that use lasers as a secondary or backup link can include line of sight atmospheric links. Atmospheric applications at sites that have predominantly clear weather are feasible, contingent on development of appropriate aiming and tracking systems. In inclement weather conditions lasers do not show much promise of providing a useful technique.

The use of lasers for specific missions must be assessed with regard to the effect of loss of transmission because of atmospheric conditions. Thus for photographic reconnaisance missions, loss of laser transmission may occur simultaneously with loss of the ability to receive video or other information, in which case the laser by itself does not provide the system limitation.

2.0 LASER MATERIALS

Numerous materials show promise of providing the necessary medium for production of laser power for communication. These are reviewed in Section 4. Lasers using liquids, solids, or semiconductors appear most useful since a low volume unit is feasible. Semiconductor lasers, in particular, seem to offer a material that is easily modulated. However, at present, such devices require cryogenic cooling (20° - 70°K) to achieve reasonable power output.

Indications are that with the development effort as described in Section 4, a considerable choice of materials for laser generation will be available.

3.0 ATMOSPHERIC PROPAGATION

Atmospheric disturbance presents a major impediment to laser propagation, primarily during inclement weather. Thus, if a high reliability laser link is desired, fog dispersing techniques must be developed. However, these techniques would introduce problems caused by increased turbulence resulting from their use.

Experiments with fog dispersive techniques showed that some improvement in transmission could be obtained. However, this improvement was marginal. Furthermore, extension to a link would require prohibitive equipment investment, making this technique unattractive when compared with other ground-based point-to-point techniques (that is, microwave and millimetric wave).

4.0 MODULATION AND DEMODULATION TECHNIQUES

4.1 MODULATION

A number of techniques have been demonstrated for external modulation of laser beams that can potentially achieve modulation bandwidths of several gigacycles. At present the most promising of these techniques uses the electro-optical effect where a 10 gc subcarrier modulation was

obtained. As much as 17 mc of modulation bandwidth has thus far been obtained using piezoelectric effects. Magneto-optical effects seem less promising because of necessary compromises of bandwidth and percent modulation for crystal thickness and heating.

A number of the problems associated with external modulators are outlined in Section 7 of this report. These include: thermal problems, necessity for uniform fields, precision in alignment, optical power loss, scattering, electrical losses creating thermal gradients in materials, temperature sensitivity, non-linearities, necessity for high subcarrier frequencies, chemical stability, effects arising from intense optical beams that contribute to optical losses, and relatively large bulk.

Many of the same electro-optical, magneto-optical, and piezoelectric effects have been proposed for internal modulation. As of yet, bandwidths obtained have been lower than those for external modulation. Moreover, with internal laser modulation, the ultimate limit on modulation bandwidth is determined by the Q of the laser cavity, which is not the case with external modulation. Additionally, the internal modulation bandwidth can also be limited by the stimulated emission relaxation time constant.

In addition to the above effects, pump power modulation shows some promise of providing a method for modulation, which may provide up to 500 kc of modulation bandwidth.

Modulation of the semiconductor laser at a 2 gc rate has been reported, although bandwidths this high have not been demonstrated. This device therefore shows promise of providing an effective means for direct or internal modulation of laser beams.

4.2 DEMODULATORS

At present several techniques for direct demodulation exist, which can support laser links in most applications. Heterodyning techniques show promise of improving S/N ratios by permitting coherent modulation and demodulation, and should be investigated further. One method of overcoming cophasal considerations is to send a local oscillator signal along with the transmitted information. This and other techniques require further investigation.

5.0 AIMING AND TRACKING AND ANTENNA SYSTEMS

Indications are that for laser transmission in the atmosphere the laser source should be made as large as possible (that is, a large diameter collimated beam) to avoid the effects of atmospheric turbulence, such as changes in shape of the beam cross-section and in light intensity distribution within the cross-section (breakup of the beam). However, experimental data is necessary to determine the degree of reciprocity in the atmosphere that would ascertain the feasibility of constructing tracking systems to overcome beam bending effects.

Aiming and tracking of laser beams between moving vehicles present problems similar to those presently encountered using microwave techniques, with the exception that accuracy requirements are more stringent. Because of this higher accuracy requirement, the acquisition mode for laser systems presents considerable difficulty. Several techniques present themselves for electro-optical beam deflection and should be studied further. At present separate detectors for acquisition and precision tracking are indicated.

Several techniques for laser system tracking are presented in Section 8, which should be further investigated. Effort should be devoted to achieving high speed, electronically controlled optical scanners.

6.0 PRIVACY

Indications are that in a significant number of laser applications, privacy of the communication link without using encryption is feasible. In particular, communication between mobile users (for example, local space-space and tactical air-air) can be made private, since interception of main beam energy becomes extremely difficult because of the confinement of the laser beam to extremely small angles of propagation. In fixed point-to-point communication through the atmosphere, laser modulation mechanisms can be formulated that will make it extremely difficult for an enemy to detect transmitted information. Because of general availability of the laser beam, however, encryption would still be required. Lasers used in cable or piped systems are generally as vulnerable to interception as any other cable carried signal.

APPENDIX I

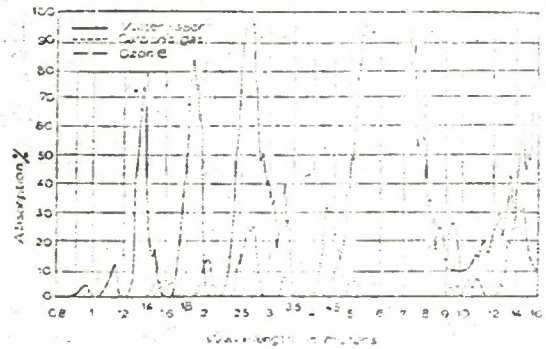
CHARACTERISTICS OF THE ATMOSPHERE

1.0 GENERAL

The various physical properties of the atmosphere have been treated extensively in the literature and will not be dwelt upon here. Transmission losses in the atmosphere are due to two sources: energy absorption by the atmospheric gases (that is, water vapor, carbon dioxide, oxygen, etc) water droplets; and losses due to scattering by the various atmospheric particles, both natural and manmade, which include water droplets, smoke particles, dust particles, and gas molecules.

Absorption by gas molecules is insignificant in the visible spectrum as compared to scattering. In the infrared region, however, this is no longer true. Figure I-1 shows the infrared absorption regions for the atmospheric constituents water vapor, carbon dioxide, and ozone. The spectra for water droplets will be approximately the same shape as that of the water vapor.

From the aborption spectra (Figure I-1), the water vapor high absorption windows are defined in Table I-1 with the relative intensity normalized to 100% for the window at 2.7μ. Also shown in Table I-1 are the defined low absorption windows.



ABSORPTION SPECTRA OF WATER VAPOR, CARBONIC GAS AND OZONE PRESENT IN THE EARTHS ATMOSPHERE

FIGURE I-1

TABLE I-1

WATER VAPOR ABSORPTION DEFINITIONS

Dark Windows (High Absorption) Definition:
IA: 0.78μ, for H_2O vapor, 0.02 - Relative Intensity
IIA: 0.94μ, for H_2O vapor, 0.05 - Relative Intensity
IIIA: 1.13μ, for H_2O vapor, 1.2 - Relative Intensity
IVA: 1.38μ, for H_2O vapor, 0.74 - Relative Intensity
VA: 1.8 to 1.95μ, for H_2O vapor, 0.85 - Relative Intensity
VIA: 2.56 to 2.8μ, for H_2O vapor, 1.0 - Relative Intensity
VIIA: 5.7 to 7.0μ, for H_2O vapor, > 1.0 - Relative Intensity
VIIIA: 14.5 to 15.8μ, for H_2O vapor, 0.75 - Relative Intensity

Clear Windows (Low Absorption) Definition:[a]	
I: 0.72 to 0.94μ	V: 1.90 to 2.70μ
II: 0.94 to 1.13μ	VI: 2.70 to 4.30μ
III: 1.13 to 1.38μ	VII: 4.30 to 6.0μ
IV: 1.38 to 1.90μ	VIII: 6.0 to 15.0μ

Note: [a]Taken from Reference 1

The energy loss due to atmospheric scattering is a function of the refractive index of the air, the radii and number of scattering particles (or molecules) per unit volume of air, and the wavelength of the transmitted signal. Table I-2 lists the size and number density of typical atmospheric scatterers.

TABLE I-2

SIZE AND NUMBER DENSITY OF TYPICAL ATMOSPHERIC SCATTERERS

Type of Scatterer	Radius (μ)	Number of Particles per cm³
Condensation Nuclei	0.005 to 0.05	2×10^{4}
Haze Particles	0.1 to 0.5	5×10^{2}
Dust Particles	0.2 to 1.0	10^{-2}
Rain Drops	625	2.4×10^{-7}

When a light beam traverses the Earth's atmosphere, it will be attenuated through scattering and absorption with a residual part being received by the detector. The total value of attenuation is called extinction, so that:

$$\text{Extinction} = \text{Scattering} + \text{Absorption}$$

Examples of inhomogeneities in the atmosphere that cause scattering are water droplets and dust particles; if the density is low enough (the distance between scatterers is at least three times their diameter), the scatter of each particle may be studied independently of that of the other particles. This is generally true as even in a very dense fog consisting of droplets 1 mm in diameter and through which light can penetrate only 10 meters, there is about 1 droplet per cm^3; that is the mutual distance is some 20 times the radii of the drops. For simplicity in the calculations, let us suppose all droplets have the same size (monodispersed) and distributed uniformly through the fog or the cloud. The extinction of the beam is related to the complex refractive index of the droplets

$$m = (\xi - i\frac{4\pi\sigma}{\omega})^{1/2} \qquad \text{(I-1)}$$

where ξ is the dielectric constant of the water, σ the electrical conductivity and ω the angular frequency. Writing

$$m = r - ir' \qquad \text{(I-2)}$$

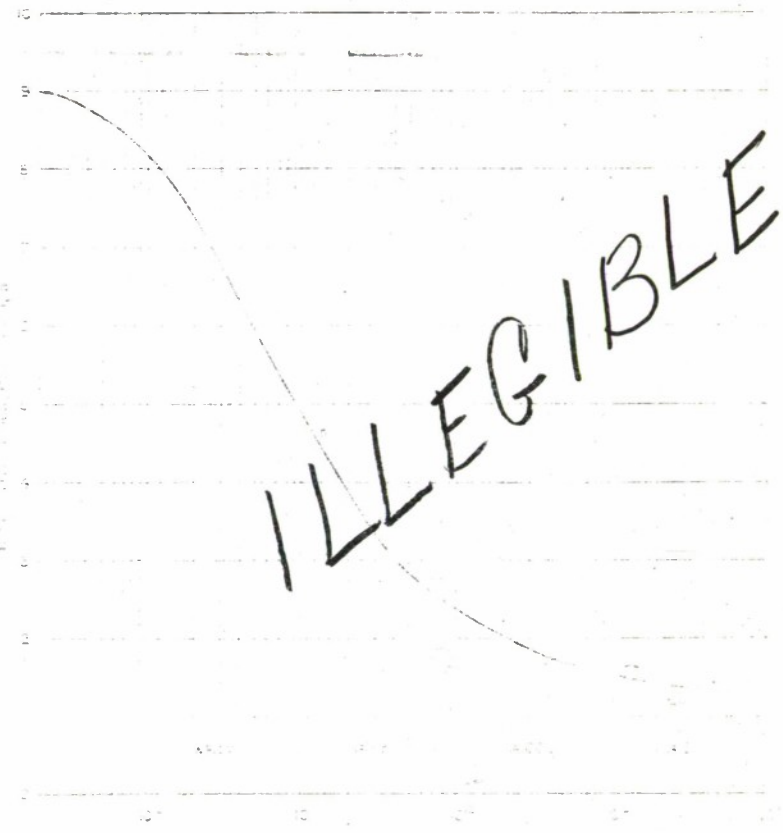
we have

$$r^2 - (r')^2 = \xi \qquad \text{(I-3)}$$

$$2rr' = \frac{4\pi\sigma}{\omega} \qquad \text{(I-4)}$$

For water droplets the refractive index is real in the visible range; that is, $r' \cong 0$, but, it is complex in the infrared and microwave ranges. Hence, while in the visible range scattering predominates in infrared and microwave ranges scattering as well as absorption take place.

Figures I-2 and I-3 show the real and imaginary parts of the complex index of refraction of water droplets as a function of frequency. Figures I-4 and I-5 show the real and imaginary parts of the complex dielectric constant of water droplets as a function of frequency. Figure I-6 shows the real part of the resulting attenuation coefficient through

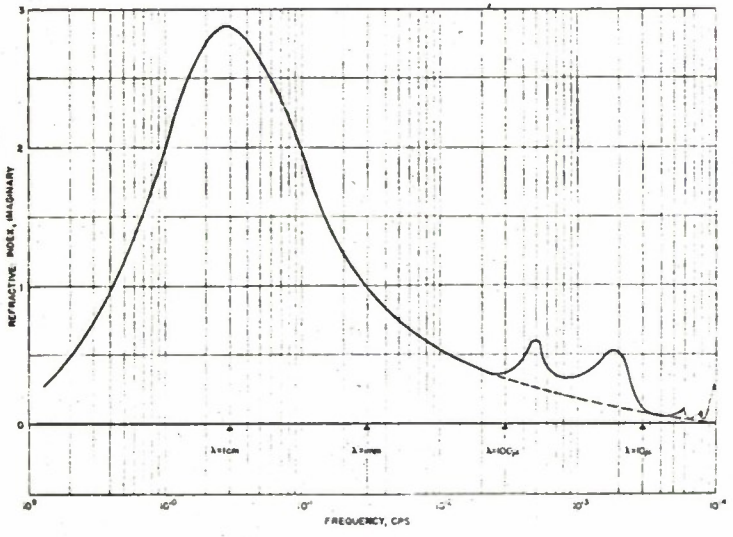


REAL PART OF COMPLEX INDEX OF REFRACTION
OF WATER DROPS VERSUS FREQUENCY

FIGURE I-2

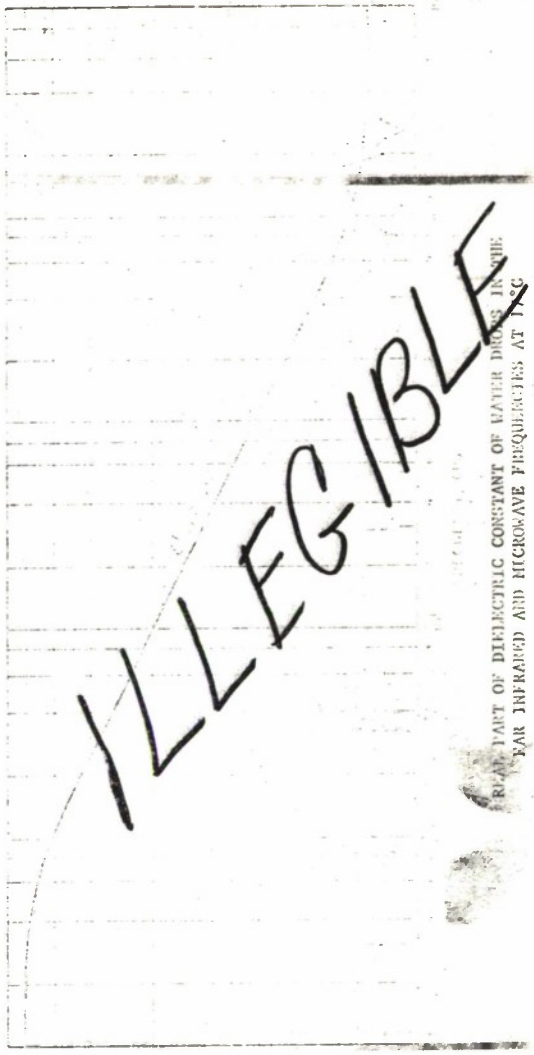
...ARY PART OF COMPLEX INDEX OF REFRACTION OF WATER VERSUS FREQUENCY

FIGURE I-3



IMAGINARY PART OF COMPLEX INDEX OF REFRACTION OF WATER VERSUS FREQUENCY

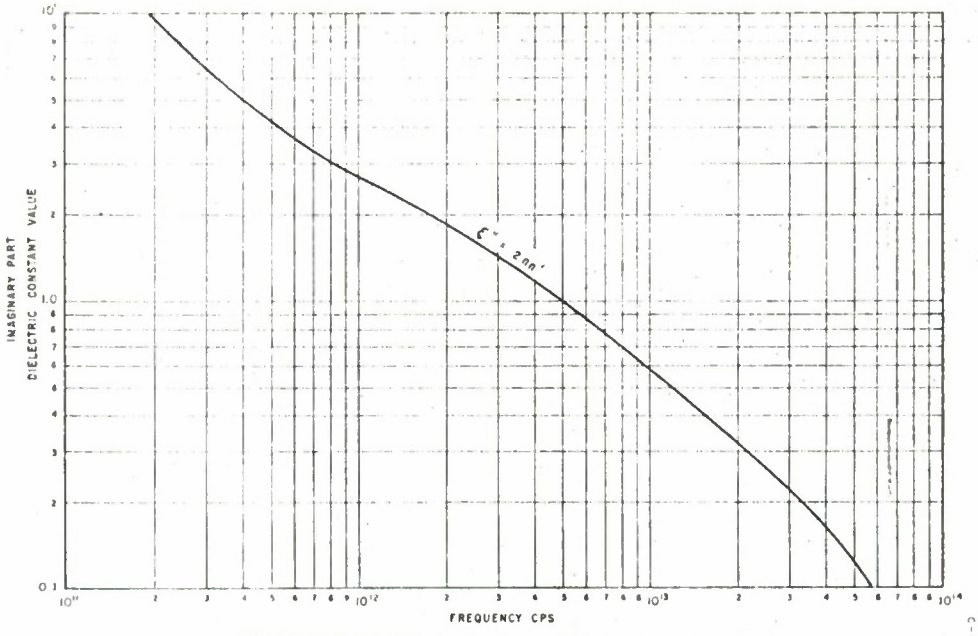
FIGURE I-3



...PART OF DIELECTRIC CONSTANT OF WATER DROPS IN THE FAR INFRARED AND MICROWAVE FREQUENCIES AT 1°C

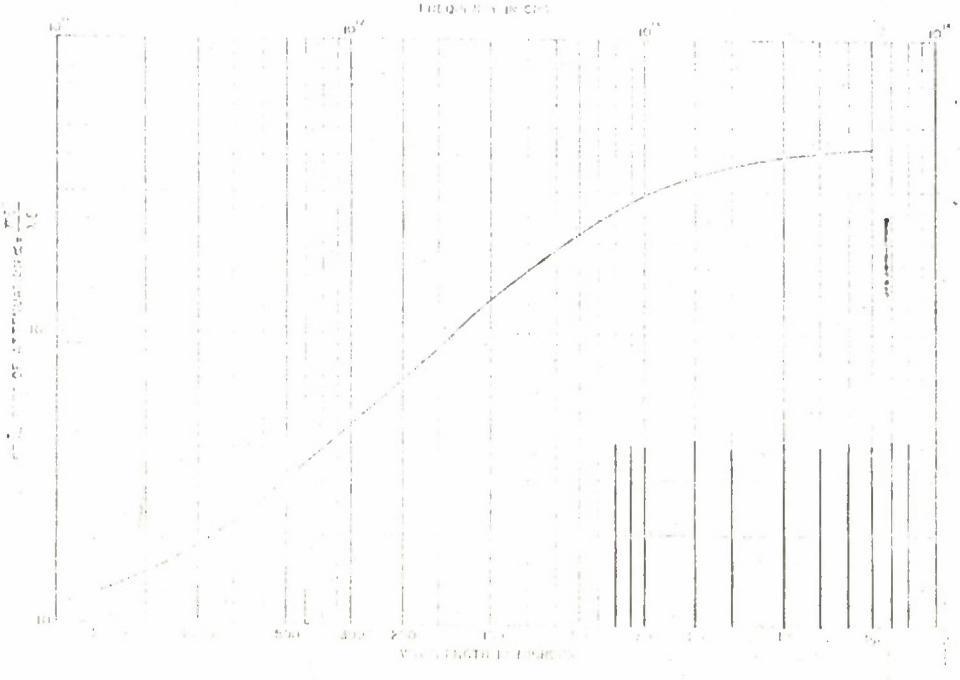
FIGURE I-4

ILLEGIBLE



THEORETICAL VALUES OF $4\pi\sigma/\omega = 2NN' = \xi''$ WATER DROPS
IMAGINARY TERM OF DIELECTRIC CONSTANT $\xi = M^2 = \xi' - i\xi''$

FIGURE I-5



APPROXIMATE VALUE OF THE REAL PART OF THE ATTENUATION
OF A PLANE WAVE THROUGH A WATER LAYER

FIGURE I-6

a layer of water as a function of frequency and Figure I-7 shows the conductivity of water droplets as a function of frequency.

2.0 FOG AND VISIBILITY

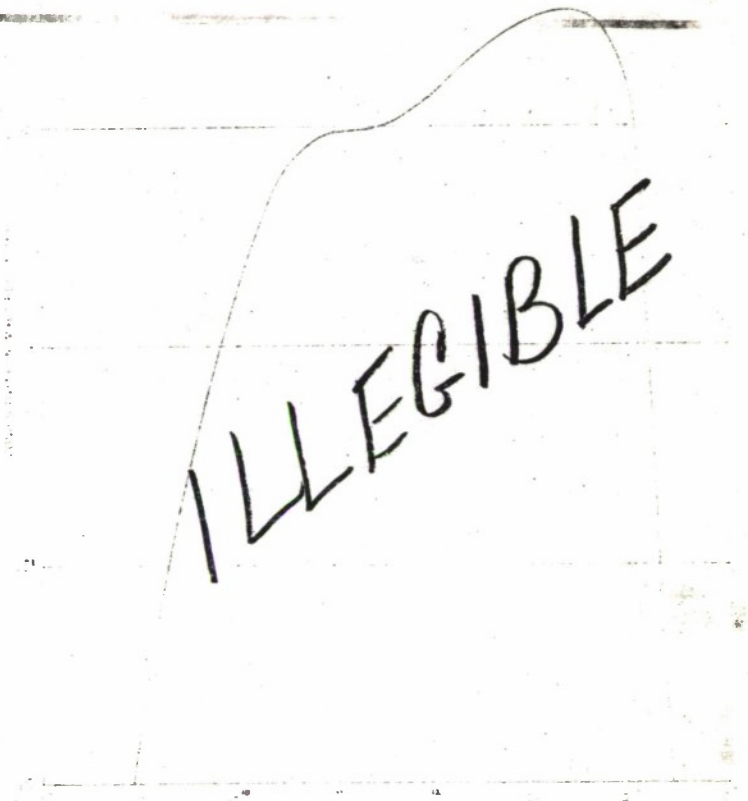
2.1 PHYSICAL CHARACTERISTICS OF FOG*

A fog is a cloud of particles, usually water droplets (water fog) but sometimes of ice crystals (ice fog). There is no essential distinction between fogs and free-floating clouds in the atmosphere. Fogs seldom produce precipitation, if any at only very small rates; in this respect they are similar to many of the free clouds seen in the sky that are not giving precipitation. Fogs and those clouds which do not tend to develop precipitation are said to be colloidally stable; that is, there is no marked tendency within them for the size of some of the droplets to grow rapidly at the expense of the other drops. Clouds (fogs) of this type are characterized by relatively small-sized drops, predominantly much less than 100μ in diameter (rain drops are 400-1,000μ), and also their drop-size spectrum (more or less bellshaped in general) has a smaller range than found in colloidally unstable or precipitating clouds. But the size distribution, median and modal size, etc, in fogs vary greatly from case to case. The variations being related to the method of formation; history of the fog; its age; the wind, temperature, and radiation conditions; thickening, or thinning tendency; admixture of smoke or other "foreign" aerosols; effects of rain or snow falling into it from above; etc. Theory and certain experiments suggest that initially a fog formed by a simple adiabatic** expansion should have a fairly uniform drop size, assuming sufficient uniformly effective condensation nuclei are present (often the case in nature). Because observations on fogs rarely show this uniform size, it must be assumed that considerable coalescence of droplets takes place with time, through collisions due to turbulence and the faster falling of the resulting larger droplets.

---

* Taken from the Encyclopedia Britannica; 1957; Vol. 9, p 436

** Adiabatic - A body is said to undergo an adiabatic change when its condition is altered without gain or loss of heat. The line on the pressure volume diagram representing the above change is called an adiabatic line.



VALUE OF CONDUCTIVITY (σ) OF WATER DROPLETS
AT 17°C AT DIFFERENT FREQUENCIES

FIGURE I-7

Normally water fogs form and persist at relative humidities of 100%; but many cases are reported with humidities between 95% and 100%, presumably because special nuclei effective somewhat below 100% are present, or because of pollution. However, NaCl particles deliquesce at about 70% relative humidity and this effect probably explains the fogs and hazes reported at sea with humidities ranging from 75% to 95%.

The concentration of droplets in fog rarely exceeds 100 per cubic centimeter, and the liquid water contents are usually of the order of hundredths of a gram per cubic meter and less (whereas rain and many warm, unstable clouds have 0.1 to 3 grams per cubic meter). Fogs, however, often appear to be denser than any clouds, because a large number of small drops is a more effective light-absorbing medium than a smaller number of larger drops.

Table I-3 shows the various fog-producing and fog-dissipating processes. It must be realized that many of the processes enumerated are commonly operating together in dependent fashion and in different amounts.

Figure I-8 shows the distribution of water droplets radii in haze and fog as measured by Arnulf and Bricard (Reference 2). In their experiments they used very fine spider threads, the finest having a diameter on the order of magnitude of a few hundredths of a micron. A picture showing some captured water droplets is shown in Figure I-9; some of the threads are invisible because they are too fine. For various fogs the radius of the drops of the equivalent monodispersed fog was determined and it was found that most fogs had a rather constant equivalent radius varying between 4.5 and 6μ.

The various types of fogs considered were:

(a) Hazes. - Attenuation coefficient (β) in the visible range is less than 2.5 miles^{-1}.

(b) Small-drop fogs. - Attenuation coefficient (β) is less than 12.5 miles^{-1}.

(c) Evolving fogs. - Have changing distributions of water droplets diameters.

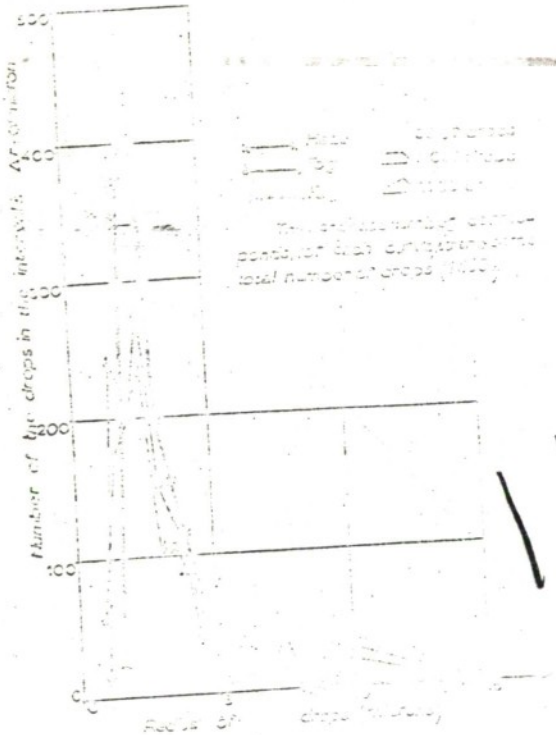
(d) Nonevolving fogs. - Distribution of water droplets diameters remains constant.

TABLE I-3[a]

FOG-PRODUCING AND DISSIPATION PROCESSES

Fog-Producing Processes	Fog-Dissipation Processes
(a) Evaporation from:	(a) Sublimation or condensation on:
(1) Rain that is warmer than the air (rain-area fog or frontal fog)	(1) Snow with air temperature below freezing (excepting ice-crystal fogs)
(2) Water surface that is warmer than the air (steam fog)	(2) Snow with air temperature above freezing (melting snow)
(b) Cooling because of:	(b) Heating because of:
(1) Adiabatic upslope motion (upslope or orographic fog)	(1) Adiabatic downslope motion
(2) Flow of air across the isobars toward lower pressure (isobaric fog); effect negligible	(2) Flow of air across isobars toward higher pressure (effect negligible)
(3) Falling pressure (isallobaric fog; unimportant)	(3) Rising pressure (unimportant)
(4) Radiation from the underlying surface (radiation fog)	(4) Radiation absorbed by the fog or the underlying surface
(5) Advection of warmer air over a colder surface (advection fog)	(5) Advection of colder air over a warmer surface
(c) Mixing:	(c) Mixing:
Horizontal mixing unimportant by itself, and strongly counteracted by vertical mixing	Vertical mixing (important in dissipating fogs and in producing stratus clouds)

[a] Source: Weather Analysis and Forecasting; Sverre Petterssen; McGraw-Hill; 1940.



DISTRIBUTION OF THE RADIUS OF DROPS
FIGURE I-8

ILLEGIBLE



WATER DROPLETS ON SPIDER THREADS
FIGURE I-9

2.2 VISIBILITY THROUGH FOG

The visual range (visibility) of an object is defined as the horizontal distance for which the apparent contrast between an object and its surroundings becomes equal to the threshold contrast of the human eye where the background is the horizon.

The limited visibility that one experiences on a foggy day is due primarily to the extremely high scattering coefficient associated with the high concentration of tiny water droplets. Figure I-10 shows the density of the water droplets as a function of the visibility. In the transmission of signals in the infrared region, however, the losses are due both to scattering and absorption. The ratio of the two losses depend on the transmitted wavelength (that is, whether or not we are at a window in the frequency spectra).

If a parallel beam of light intensity (I_o) travels a distance (X) through an absorbing or scattering medium, its intensity is reduced according to Lambert's Law

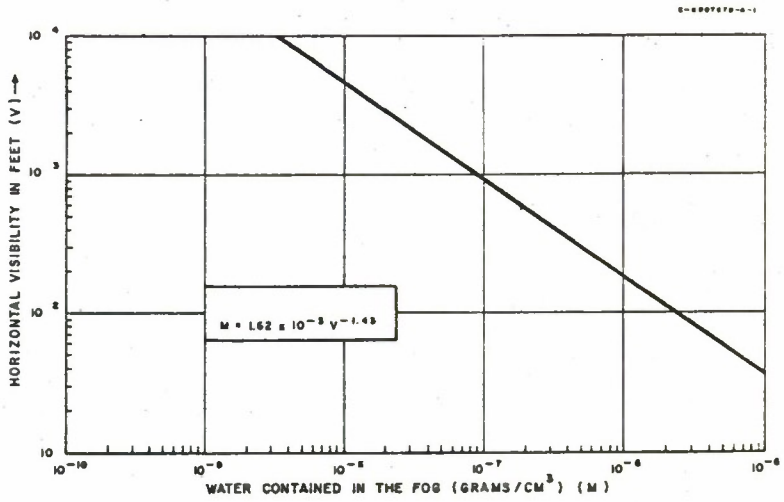
$$I = I_o e^{-\beta X} \qquad \text{(I-5)}$$

where β is the absorption of scattering coefficient depending on the mechanism involved.

Condon (Reference 3) shows that the horizontal visibility (V) is inversely proportional to β

$$\beta = \frac{3.912}{V} \qquad \text{(I-6)}$$

In the visual range we can assume that β is due solely to scattering. Table I-4 gives the total scattering coefficient versus the horizontal visibility at the ground based upon this assumption.



WATER CONTENT IN FOG AND VISIBILITY RELATIONSHIP

FIGURE I-10

TABLE I-4

TOTAL SCATTERING COEFFICIENT VERSUS HORIZONTAL VISIBILITY

Horizontal Visibility (miles)	Total Scattering Coefficient β_s (miles^{-1})
1/16	62.59
1/8	31.30
1/4	15.65
1/2	7.824
1	3.912
1-1/2	2.608
2	1.956
3	1.304
5	0.7824
10	0.3912
20	0.1956
30	0.1304

The total scattering coefficient actually is the sum of the Rayleigh scattering coefficient (β_m) which is used for small particles and the Mie scattering coefficient (β_p) which is used for large particles. The expressions are

$$\text{Rayleigh: } \beta_m = \frac{14.35}{N\lambda^4} \text{ miles}^{-1} \qquad \text{(I-7)}$$

where

N = number density of air (cm^{-3})

λ = wavelength (cm)

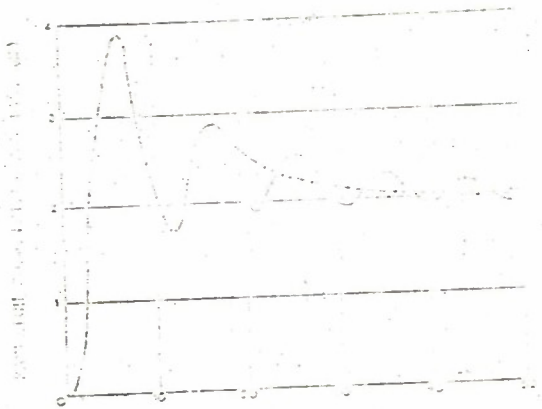
$$\text{Mie: } \beta_p = \sum \frac{\pi^2 N K}{6.21 \times 10^{-6}} \text{ miles}^{-1} \text{ for } r \geq .05 \qquad \text{(I-8)}$$

where

r = the radius of particle (cm)

N = the number of sphere of radius r per cubic centimeter of air

K = a constant, which is a function of the refractive index of the particle and the ratio of the radius of the particle to the wavelength. Its variation is shown in Figure I-11.



DIFFUSION FUNCTION, AFTER HOUGHTON AND CHALKER

FIGURE I-11

In the visual range, in the case of fog, the Mie coefficient far exceeds the Rayleigh coefficient. Figure I-12 shows the variations of the Rayleigh coefficient with wavelength over the region from 0.1 to 1000μ. The variations of the Mie coefficient with visibility is shown in Figure I-13.

3.0 RAIN

The frequency at which given rates of precipitation occurs and the associated distributions of various precipitation parameters must be taken into account in any laser communication system through the atmosphere.

As evidenced by ones' ability to see long distances when it is raining indicates that at optical frequencies the attenuation due to rain is less than that due to fog.

In the visible range transmission losses are due primarily to scattering. In the infrared region the losses are due to absorption by the gases and rain drops and scattering by the rain drops.

Atlas and Kessler (Reference 3) show some very useful empirical relationships for rain.

These are

$$V_D = 2.78 \times 10^3 \, M^{0.12} \qquad \text{(I-9)}$$

$$h = 3.6 \times 10^4 \, M \, V_D \qquad \text{(I-10)}$$

$$r_o = .045 \, h^{.21} \qquad \text{(I-11)}$$

where

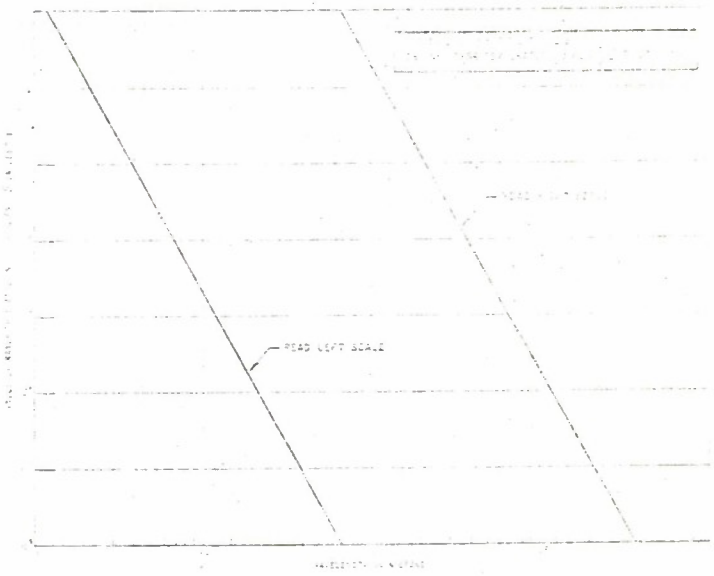
V_D = raindrop velocity (cm/sec)

h = precipitation rate (mm/hr)

M = concentration of precipitation (grams of water per cubic centimeter of space)

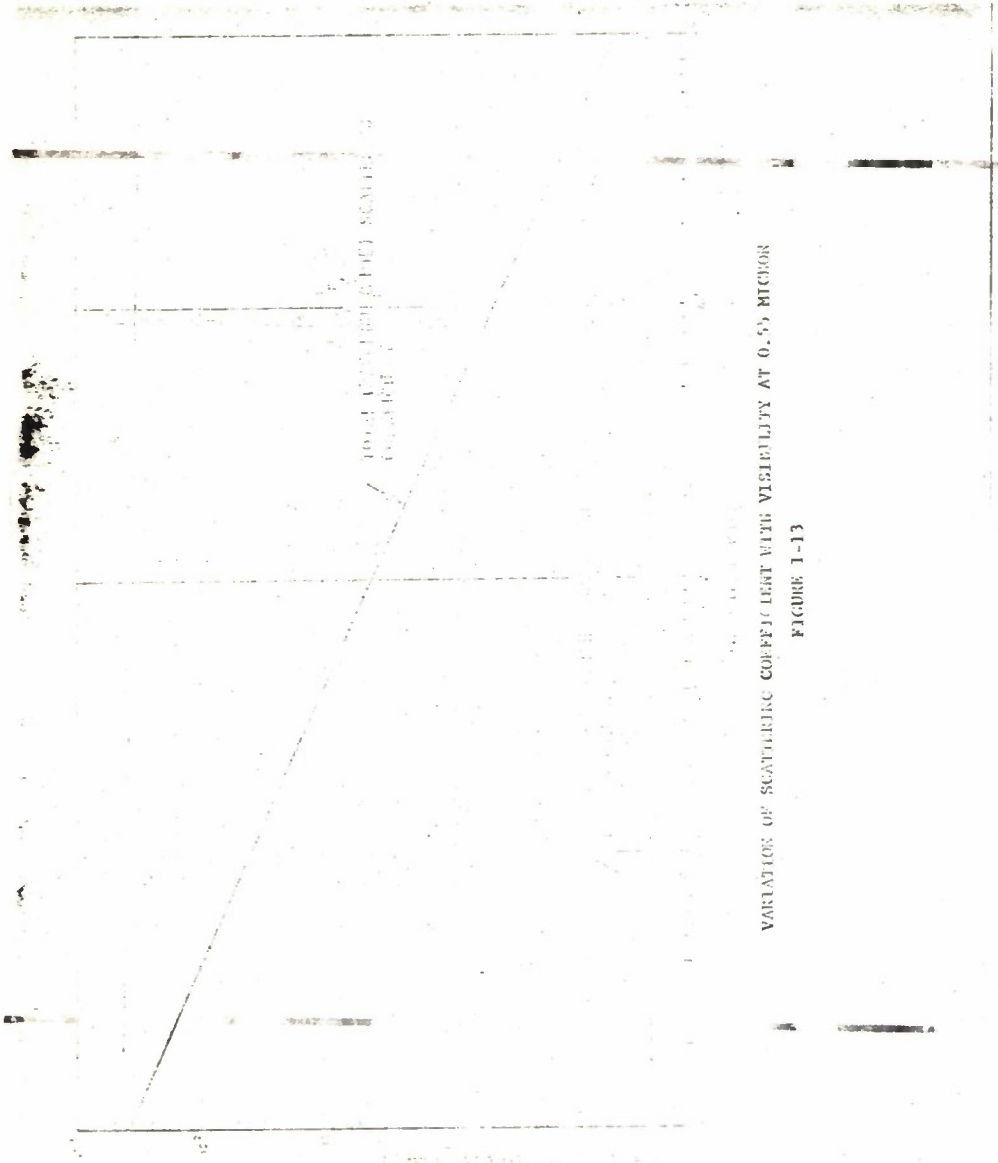
r_o = median raindrop radius (cm)

Steady-state conditions with respect to water distributions do not exist when updrafts equal or exceed the fall velocity of the particles. Such strong updrafts exist locally for periods of about 5 to 15 minutes in thunderstorms and can lead to high local concentrations of water substance. There is evidence that occasional severe thunderstorms may be briefly associated with local water concentrations as high as 70 grams



VARIATION OF RAYLEIGH SCATTERING COEFFICIENT WITH WAVELENGTH

FIGURE I-12



VARIATION OF SCATTERING COEFFICIENT WITH VISIBILITY AT 0.55 MICRON

FIGURE I-13

per cubic meter, as compared to about 1 gram per cubic meter for an ordinary heavy rainfall.

Figure I-14 shows a plot of the median raindrop diameter based upon equation (I-11). The terminal fall velocity for distilled water droplets in stagnant air is shown in Figure I-15.

The usual classification of precipitation rates are:

(a) Drizzle. - $h \leq 0.25$ mm/hour

(b) Light rain. - $h \leq 1$ mm/hour

(c) Moderate rain. - $h \leq 4$ mm/hour

(d) Heavy rain. - $h \leq 16$ mm/hour

Figure I-16 shows the approximate percentages of time during an average year when various instantaneous rates of precipitation are equalled or exceeded at Washington DC.

4.0 SNOW

Less than 1% of all precipitation, falling at rates equal to or exceeding 3 mm/hour fall in the form of snow.*

Table I-5 shows the approximate variation of the terminal fall speed of snow crystals and flakes with temperature.

TABLE I-5

TERMINAL FALL SPEED VERSUS TEMPERATURE

Temperature Range (°C)	Fall Speed (cm/sec)
≤ -8	50
-8 to 0	50-100**
0 to 2	100-140**

Atlas and Kessler (Reference 3) show that the median radius for snow particles can be written as

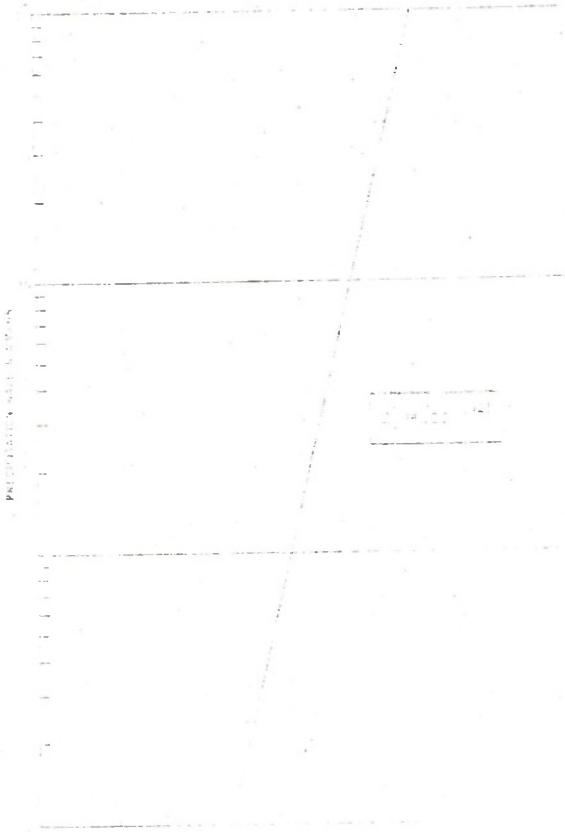
$$r_o = 0.07\, h^{0.48} \text{ cm} \qquad \text{(I-12)}$$

where

h = precipitation rate (mm/hr)

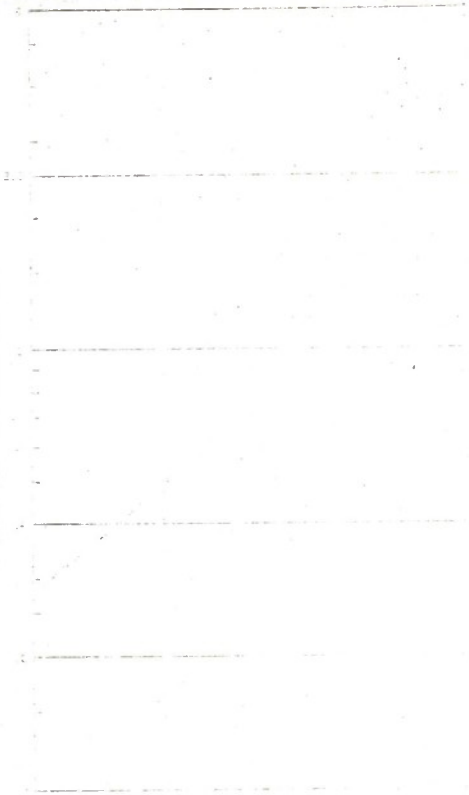
* Handbook of Geophysics: Based on extensive data taken at four stations in the Northwest United States.

** Linear relationship



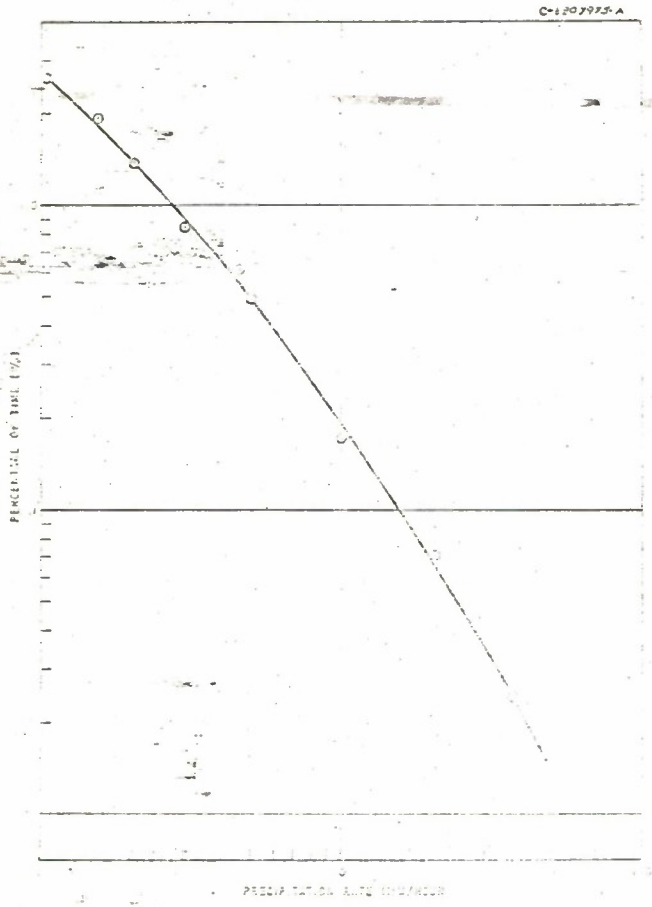
MEDIAN DIAMETER OF RAIN DROPS FOR
DIFFERENT PRECIPITATION RATES

FIGURE I-14



TERMINAL VELOCITY OF FALL FOR DISTILLED
WATER DROPLETS IN STAGNANT AIR

FIGURE I-15



APPROXIMATE PERCENTAGES OF TIME DURING AN AVERAGE YEAR WHEN GIVEN INSTANTANEOUS RATES OF PERCIPITATION ARE EQUALLED OR EXCEEDED AT WASHINGTON DC

FIGURE I-16

Also work of Rigby, Marshal and Hitschfeld (Reference 4) has shown that the distribution of particle sizes in snow may be given by

$$N_D = N_o e^{-3.67 \frac{D}{D_o}} \qquad \text{(I-13)}$$

where

N_D = the number of particles per cubic centimeter size range (cm^{-4})

D = melted diameter of snow particles

D_o = median diameter of snow particles

and that

$$N_o = 3.8 \times 10^{-2} \, h^{-0.87} \, cm^{-4} \qquad \text{(I-14)}$$

To treat theoretically the actual scattering behavior of snow is very complicated due to the fact that the snowflakes are very irregular in shape tending to appear as thin crystals. Also, as the flakes fall, partial melting occurs, the degree of which depends greatly on the ambient temperature.

5.0 REFERENCES

1. Atmospheric Transmission in the Infrared; J. H. Taylor and H.W. Yates; Journal of the Optical Society of America; March 1957; Volume 47, Number 3.

2. Transmission by Haze and Fog in the Spectral Region 0.35 to 10 Microns; A. Arnulf and J. Bricard; Journal of the Optical Society of America; June 1957; Volume 47, Number 6.

3. Handbook of Geophysics, Revised Edition; prepared by the Geophysics Research Directorate of the Air Force Cambridge Research Center; published by the Macmillan Company; 1960.

4. The Development of the Size Distribution of Raindrops During Their Fall; E. C Rigby, J. S. Marshall, and W. Hitschfeld; Journal of Meteorology; 1954; Vol. 11.

APPENDIX II

DESCRIPTION OF LASER PROPERTIES

1.0 SOLID-STATE LASERS

1.1 RUBY LASERS (References 1 and 2)

Ruby (Al_2O_3 doped with Cr^{3+}) lasers, first developed by Maimem in May, 1960, have undergone a great deal of improvement. These lasers can be operated either at room temperature or at lower temperatures by cooling the system. The emission frequency will vary slightly with the change in temperature (Reference 3). The output wavelength usually observed is 0.6943μ (Reference 4). Other wavelengths usually (References 5 and 6) obtained are at 0.6929, 0.6934, 0.7010, 0.7040, and 0.7670μ.

The spectral bandwidth of the laser line is less than 10^{-6}μ and beamwidths approaching diffraction limits of 1 microradian have been measured (Reference 7).

Peak power outputs of 14 megawatts have been observed (Reference 7) by varying the Q of the optical cavity with a Kerr Cell (Figure I-1). Burst energy of the order of tens of joules can be obtained from long (for example, 20 cm) lasers. Recently, a device (Reference 1) capable of generating peak power pulses of 50 to 100 megawatts has been developed. It is further reported (Reference 1) that peak powers in the 500 to 1000-megawatt range have been produced by cascading the giant pulse laser oscillator with a laser amplifier (that is, a laser-laser system).

Another way of increasing the power output is to obtain single-mode operation;[1] it has been reported that, in some recent experiments, a single-mode emission well above threshold has already been obtained (Reference 8). High threshold powers are necessary. The threshold energy ranges from about 1,500 to 3,150 joules (Reference 2).

Optical pumping is employed. High-powered mercury srcs are most commonly used for the CW case and Xenon arcs are most prevalent in pulsed applications. These high intensity lamps emit radiation over a rather broad spectrum, generally covering the region from about 0.3000μ

1 At room temperature, the ruby laser oscillates usually in several longitudinal modes, placed several hundred mc apart.

to 1.2000μ. The absorption band of ruby is not nearly this broad, so a large fraction of the pump light is wasted. Thus, the overall efficiency is not very high, typically 1% or less; 5% to 10% efficiencies are predicted with optimum pumping conditions (Reference 1) and ruby rod of improved optical quality.

For CW operation, (Reference 5) ruby crystals of a trumpet-like shape have been grown and operated at liquid N_2 temperature with an output less than 10 ma at 0.6934μ and beam angle 0.07 degree. A solar-powered laser with this trumpet geometry is [illegible].

1.2 RARE EARTH LASERS (References 4 and 5)

Rare earth ions being tested for laser applications are Er^{3+}, Tm^{3+}, Ho^{3+}, Yb^{3+}, Dy^{2+}, Gd^{3+}, En^{3+}, Sm^{2+}, Nd^{3+}, and Pr^{3+}. Host crystals commonly used are fluorides such as CaF_2, BaF_2, SrF_2, LaF_3; tungstates, $CaWO_4$, $SrWO_4$; molybdenates, $CaMoO_4$, $SrMoO_4$, $PbMoO_4$; and silicate class.

Nearly all rare earth doped materials, except a few, emit light at wavelengths in the infrared region. The ion Sm^{2+} in host crystals CaF_2 and SrF_2 provides, at liquid helium temperature (4.2°K), laser output of 0.7083μ and 0.6937μ in the visible region.

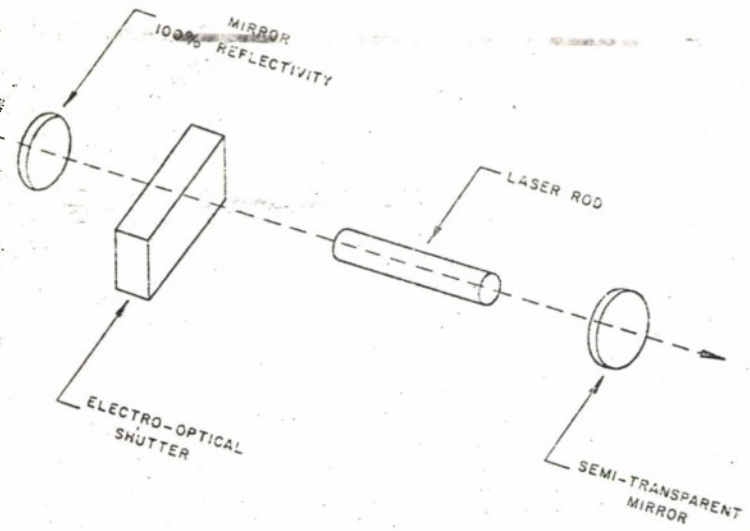
Dy^{2+}: CaF_2 looks like a promising material for use in communications; the crystal has run CW with output power about 2 mw and an efficiency of 3×10^{-4}%, furthermore, the undesirable "Spiking" disappears at liquid helium temperatures. For CW operation, U^{3+}: BaF_2 and Nd^{3+}: $CaWO_4$ can also be used.

Most rare earth lasers require cooling and relatively low threshold power. Recently (Reference 9) a new laser host crystal, $Ca(NbO_3)_2$ has been reported; experiments were performed with Nd^{3+}, Ho^{3+}, Pr^{3+}, Er^{3+}, and Tm^{3+}.

1.3 GLASS AND OPTICAL FIBER LASERS (References 4, 10, and 11)

The first glass fiber laser was built by American Optical Company with Nd^{3+} doped in barium crown glass. A 1.06μ emission wavelength was observed at room temperature with a rod of 32μ diameter, 3 inches long.

Light propagates through a long, thin optical fiber, of glass (or plastic) or other transparent materials, by a series of reflections from wall to wall. Only those rays are propagated that enter the end of the fiber at an angle small enough to cause total reflection from the



Q-SWITCHED LASER, SCHEMATIC DIAGRAM
FIGURE II-1

walls. Glass fibers have been built (Reference 12) to support light beams from the ultraviolet to the infrared region (0.33μ to 10μ). As the fibers are made thinner and their diameters become comparable to the wavelength of light, optical geometrical analysis no longer applies, and the fibers behave as dielectric waveguides, exhibiting waveguide transmission modes (References 13 and 14). It is then possible to calculate the waveguide modes that can be established and deduce the conditions for their excitation. Because of this capability to sustain a limited number of modes and due to low attenuation, fibers extracted from suitable laser materials should be expected to laser without using an external resonator, essential in other types of lasers.

An inexpensive method of drawing glass fibers has been reported (Reference 14). In the future, intensive research is expected in this field. Potential uses of these in communication systems as filters, light amplifiers, repeaters, etc. are obvious.

Most of these lasers are of the pulsed type except Nd^{3+} - glass lasers. The light output wavelengths lie between 0.3125μ to 1.95μ; that is, from near ultraviolet to near infrared. Output energies in excess of 50 joules and efficiencies over 2% have been reported for pulsed operation of Nd^{3+} - glass (Reference 4).

1.4 SEMICONDUCTOR LASERS

1.4.1 Description

As a functional unit in a communication system, the semiconductor (junction) laser is a solid-state device that is energized by an electric current producing an output beam of coherent radiation. In contrast with other solid-state lasers, the conversion process involves no intermediate steps such as optical pumping.

1.4.2 Summary of the Physical Processes in Junction Lasers

A junction laser consists of a specially prepared p-n junction constructed in one of a limited number of semiconducting materials. Both the junction geometry and the semiconductor material must meet the requirements discussed below.

When an electric field is applied to a p-n junction (such that electrons in the n-type material and holes in the p-type material move toward the junction), the electrons recombine with holes upon arriving at the junction. Each recombination yields a quantum of

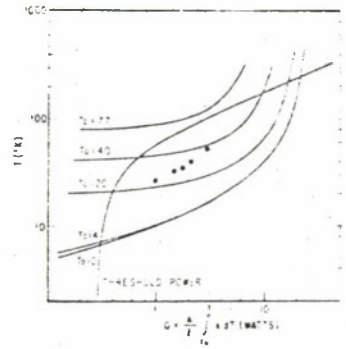
energy approximately equal to the band gap energy for the particular semiconductor in question. In indirect materials such as silicon and germanium, this energy is carried away from the junction primarily by phonons. In direct materials such as gallium arsenide (GaAs), the recombination process is primarily radiative and the energy is carried away from the junction by photons.

When an electron reaches the region where the radiative transition takes place, it may exist there for a finite average lifetime before the spontaneous recombination process takes place. Under this condition the radiation is not coherent. As the rate at which electrons arrive at the transition region increases, the probability for stimulating the recombination process increases. Each photon arising from a stimulated recombination is an exact duplicate of the initiating photon.

As it is usually desirable to generate a directional beam of light, plane parallel reflecting surfaces are used to return some fraction of those photons with the desired frequency and directional characteristics to the transition region. The reflecting surfaces may be obtained by either polishing the surface of a crystal in planes perpendicular to the junction plane, or by cleavage of the crystal along its naturally occurring cleavage planes. These enhance the further production of photons with the desired characteristics. Other optical geometries are also being studied. It is essential for the junction to be a uniform, flat, plane.

1.4.3 Environmental Requirement

Although junction lasers have been operated at room temperature with very low average power (Reference 15), high power application requires low temperature. The highest average power yet reported, 3.2 watts (Reference 16) continuous, has been achieved by careful "thermal packaging" of a GaAs laser crystal. A plot of the junction temperature of the diode as a function of input power with the base of the package held constant yields a thermal characteristic curve for the package. A family of thermal characteristic curves for different values of base temperature is shown in Figure II-2. By plotting the threshold power on the same graph, it is evident that continuous laser action can only be accomplished when the base of the diode package (of this design) is held below 50°K.



THERMAL CONDUCTIVITY INTEGRAL OF
GaAs FOR A VARIETY OF BASE TEMPERATURES

FIGURE II-2

It is true that the dc laser package was designed for low temperature operation and that other materials may be expected to perform better at higher temperatures. However, the design of a higher temperature package is considerably more difficult for two reasons: the threshold power increases rapidly with temperature, and the thermal conductivities of materials generally decrease with temperature.

1.4.4 Optical Characteristics

Coherent light has been observed from junctions prepared in several compounds, some of which are:

Compound	Wavelength (μ)
GaAs (References 17, 18)	0.84
$GaAs_{.8}P_{.2}$ (Reference 19)	0.71
InP (Reference 20)	0.9
$In_{.65}Ga_{.35}As$ (Reference 21)	1.77
$In_{.75}Ga_{.25}As$ (Reference 21)	2.07
InAs (Reference 22)	3.14
InSb (Reference 23)	5.2

Coherent light has also been observed from SiC (Reference 24), but it has been questioned if it was a result of true laser action (Reference 25). All of the compounds tabulated above are members of the III-V family of semiconducting compounds. As indicated, some of these mixtures produce emission at intermediate wavelengths. If all possible tabulated mixtures were to exhibit laser action, then it is possible that a laser, of any wavelength between spproximately 0.7μ to 5.2μ, may be constructed at will. Recent interest is being focused on the II-VI compounds thst hold the possibility of making junction lasers emit visible light.

The greatest amount of development effort to date has gone into the GaAs junction laser.

The spectral output of a GaAs junction laser consists of one or more very narrow spectral lines spaced 1 to 2 Å ($1x10^{-4}$ to $2x10^{-4}$ μ) apart in the vicinity of 0.845μ. In addition, there is a low level incoherent background radiation. Various efforts have been made to determine the spectral line width, but most hsve been instrument limited. The lowest upper limit based on experimental evidence so far reported is about 0.007 Å, corresponding to 310 mc (Reference 16). Theoretical

considerations indicate that it may be as low as 15 kc at 20°K (Reference 26). This theory assumes that the width is due to thermal oscillations of the resonant cavity. Such oscillations may be expected to produce a 15 kc frequency modulation on the laser beam. It has been suggested that coupling to a longer, higher Q resonator would reduce the modulation frequency, hence narrow the line width.

Optical harmonic generation in GaAs junction lasers has been observed and reported (References 27, 28). The amount of power found in the harmonics is very low and not of great consequence in this discussion.

The size of a typical GaAs junction laser is a line source about 1 to 5μ wide and up to 0.5 mm long. Because of the small size of the source, diffraction effects cause the light to fan out. The divergence of the beam in the plane normal to the junction is about 15°. In the plane of the junction the divergence varies from a few degrees to as much as 15°, depending on the length and uniformity of the cavity excitation.

1.4.5 Electrical Characteristics

The GaAs junction laser behaves electrically much like any other semiconductor diode rectifier. The dynamic forward resistance is about 0.1 ohms above 1.5 volts.

The General Electric JL-10 (Reference 29) is the highest power dc operated laser available. Laboratory prototypes of this device have exhibited efficiencies as high as 46 per cent. Typical low frequency junction capacitance for the JL-10 is 250 pf at 0 volts. At operating voltages this is expected to become insignificant compared with the "package" capacitance of 3 to 4 pf. It is evident then that the junction laser is typically a very low impedence circuit element and requires special consideration to obtain a proper match to other standard high frequency components.

1.4.6 Modulation Considerations

The upper frequency limit for direct modulation of the junction laser has not been established. Though the minority carrier lifetime is short, about 10^{-9} seconds (Reference 30) in GaAs, it becomes even shorter when the recombination is stimulated in the lasing mode of operation.

The highest modulation frequency observed and reported is 2 gc (Reference 31).

Measurement of the delay between the initiation of current and the emission of light indicates that modulation frequencies of 5 gc should be possible (Reference 32).

There are several methods of direct modulation to be considered. The most obvious is modulation by current. The variation of intensity with current for a typical GaAs junction laser is shown in Figure II-3. It is evident that, by operating about some point in the region of greatest slope, a large signal gain may be realized.

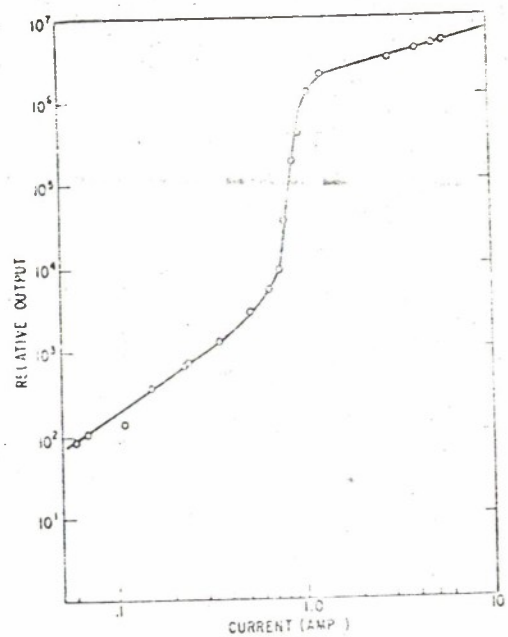
A modified GaAs junction laser has been used to demonstrate that small signal amplification can be achieved (Reference 33). When driven by another GaAs junction laser operating below threshold, gain in excess of 1000 was realized. In the work reported, the Q of the cavity was decreased by modifying the reflective surface of the laser. The result was a broadly tuned amplifier.

The output wavelength of the GaAs junction laser is also temperature dependent. The temperature characteristic is shown in Figure II-4. Because the thermal time constant of the junction laser can be made to be very low (about 1 μsecond), it is feasible to consider temperature modulation. Because current is a source of heat in a less than 100 per cent efficient diode, current modulation (at frequencies < 1 mc) inherently induces a frequency modulation.

The output wavelength of the junction laser is also pressure dependent as shown in Figure II-5. This suggests that coupling of the laser crystal to a piezoelectric device would provide a means of pressure modulation.

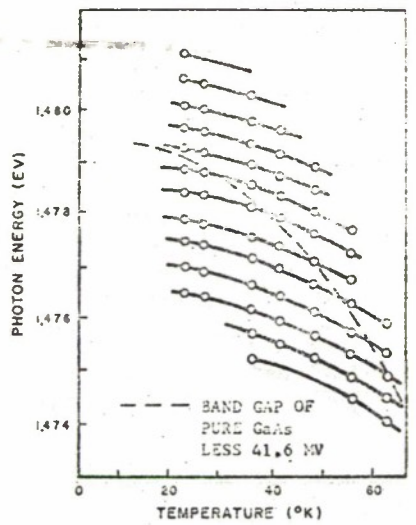
The dependence of the output of an InAs laser on the magnetic field has been reported. The effect of the magnetic field is two-fold. It changes the threshold current as shown in Figure II-6, and the wavelength as shown in Figure II-7.

In the propagation of information on the output of the junction laser, one may consider pulsing the diode to achieve higher peak power. The high power dc laser has an inherently short thermal time constant. Therefore, power pulses at widths greater than about 1 microsecond cannot exceed the average dc power handling capability. Higher than



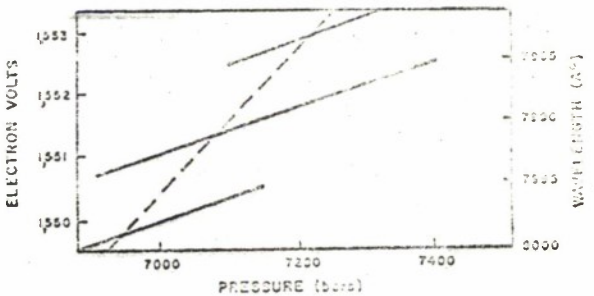
VARIATION OF PEAK AMPLITUDE WITH CURRENT

FIGURE II-3



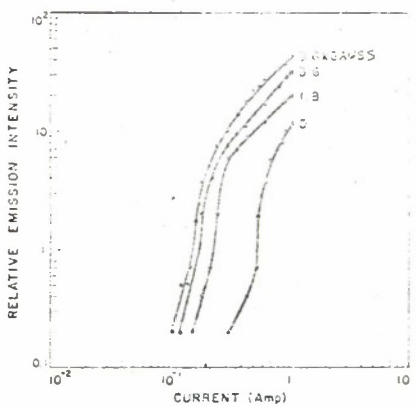
POSITIONS OF CAVITY MODES AND OF COHERENT OUTPUT

FIGURE II-4



VARIATION WITH PRESSURE OF THE PEAK ENERGY OF
THREE MEMBERS OF A FAMILY OF STIMULATED EMISSION MODES

FIGURE II-5

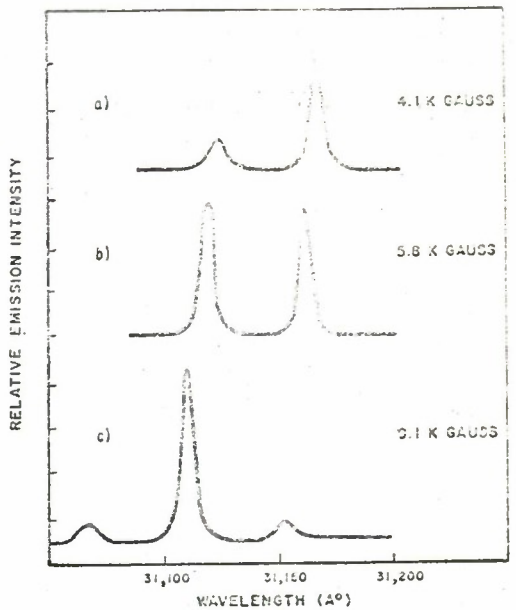


PULSE DURATION: 0.4 microseconds
TEMPERATURE: 4.2°K

PULSE RESULTS THAT ILLUSTRATE THE REDUCTION OF THE CURRENT THRESHOLD AS A FUNCTION OF MAGNETIC FIELD PERPENDICULAR TO THE DIRECTION OF CURRENT FLOW

FIGURE II-6

C-6611733-B-AM



NOTE:

SPECTRA FOR THREE DIFFERENT VALUES OF MAGNETIC FIELD PERPENDICULAR TO THE DIRECTION OF CURRENT FLOW. THE DIODE FORWARD CURRENT WAS 220 MA DC.

SPECTRA OF CW EMISSION FROM InAs DIODE LASER AT 4.2°K

FIGURE II-7

average peak power may be expected at pulses less than a microsecond, but experimental data on the sub-microsecond pulse capability are not yet available.

1.4.7 Conclusions and Recommendations

The requirement of low temperatures for the operation of junction lasers should not be a deterrent to its use in a communications system. When the junction laser is coupled to one of the increasing numbers of low temperature, closed-cycle mechanical refrigerators, the resulting system is a room temperature system. There are at least two machines presently being marketed: the Cryogem by Norelco, and the Cryomite by Malakar. Others are under development by Cryonetics, General Electric, and Hughes Aircraft.

Though the shortest output wavelength yet reported for junction lasers is in the neighborhood of 0.7μ, there is evidence that junction lasers emitting in the visible spectrum are forthcoming.

Many problems associated with obtaining a narrow clean output from a junction laser exist. Thus, laser action along the junction is irregular, causing unevenness of output along the junction.

Current modulation seems to be the best choice for applying information to the output of the junction laser. To do so requires careful consideration to obtain efficient coupling at high modulation frequencies.

The recent reports of successful amplification in a p-n junction of light from an external source encourages one to speculate on the usefulness of such an amplifier on both the transmission and receiving terminals of a light communication link.

2.0 LIQUID AND ORGANIC LASERS

Morantz reported (Reference 34) laser action in an aromatic molecular species (benzophenone and naphthalene) in rigid glass with emission wavelength 0.47μ in the visible blue region at 77°K. However, this laser emission has not been confirmed by other investigators. Terbium doped in a propriatary organic type liquid is said (Reference 35) to emit in the green between 0.53μ and 0.55μ. Under study are the ferromagnetic liquids that can be easily modulated by external magnetic fields.

There are rare-earth ions that preserve their fluorescence in solutions. These are good candidates for laser materials, so are organic and

metal-organic compounds, especially chelates. In the chelates, a central metal ion is attached to a number of organic liquids. The organic groups can absorb energy over a wide band and transfer the excitation to the metal ion. This transfer of excitation from one organic group to another is a well-known phenomenon. Four kinds of chelate lasers have been reported in the visible region (≈ 0.613μ).

Liquids (and gases) allow almost complete freedom from the problems of solid-state single crystal growth and shaping. Liquids permit a reasonable concentration of active material in a given volume, and large usable samples of convenient sizes are easily obtained.

Solution of the difficult cooling problem is greatly facilitated by the possibility of circulating the working fluid; a laser container of required dimensions can be provided with an outlet and an inlet and the liquid circulated between the laser and a heat exchanger.

3.0 GASEOUS LASERS (References 5, 36, 37, and 38)

The output of a continuously operating gaseous optical maser is capable of exhibiting a high degree of coherence and frequency purity; that is, relatively high monochromativity. The main disadvantage is low gain per unit length as compared to solid-state lasers. This requires the present gas lasers to be quite long (100 cm in most cases). However, it has been reported that a new Hg-He laser has been developed with high gain.

The basic structure of the device is inherently simple. It consists of a cylindrical discharge tube placed within a simple optical cavity consisting of two plane parallel or spherical mirrors. Recently, resonators containing one plane and one spherical mirror have been used to ease the problem of collimating them.

The oscillation frequency is determined by the length of the interferometer. Thus, depending on the required degree of frequency stability, the mechanical rigidity of the structure of the device becomes of prime importance.

A number of gases have been used to achieve laser oscillations, such as He-Xe, He-Ne, Noble gases (Helium, Neon, Argon, Krypton, and Xenon), and a mixture of oxygen and argon or neon.

The power output of the presently operating continuous wave gaseous lasers is generally in the range of tens of milliwatts. Recently, the

operation of a He-Ne laser with a power output in the range of hundreds of milliwatts has been announced (Reference 39). In pulsed operation, peak powers of the order of hundreds of watts have been reported in He-Ne discharge (Reference 40) as well as in a discharge containing nitrogen gas (Reference 41).

An optically pumped cesium vapor laser has been developed (Reference 42). The pump is an rf powered helium lamp with strong radiation at 0.3888μ. The light output has been observed at both 7.18μ and 3.20μ. The output beam power is about 50 μw.

4.0 LASER-PUMPED LASERS

Lasers can be used as pumping sources to both maser and lasers. H. Hsu (Reference 43) has recently extended the concept of parametric interactions in nonlinear systems to optical frequencies. The successful generation of optical harmonics utilizing the nonlinearity in the electric susceptibility of piezoelectric crystals (Reference 44) is a demonstration of the parametric interaction of coherent photons. Hsu envisions lasers as sources of coherent radiation to pump a paramagnetic medium and obtain a coherent optical oscillator in a similar fashion as present day microwave parametric amplifiers (Reference 45); generation in the far infrared at tunable frequencies would thus be possible.

Another type of laser-pumped laser has been reported to use Raman-active gases in laser systems to achieve scattering of coherent light to new wavelengths. By illuminating organic gases with a pulsed ruby laser at 0.6943μ, researchers (Reference 46) at Ford Motor Co., Michigan, were able to obtain laser light at 0.3231μ. This ultraviolet emission was produced by hydrogen, which simultaneously scattered blue, deep blue, and green. Raman scattering of coherent light was previously observed only from liquids.

Table II-1 lists the frequency range (and the materials used) of various lasers. Table II-2 lists chemical symbols of elements used in lasers.

TABLE II-1

LASER FREQUENCIES
(MICROWAVES, JAN. 1964)

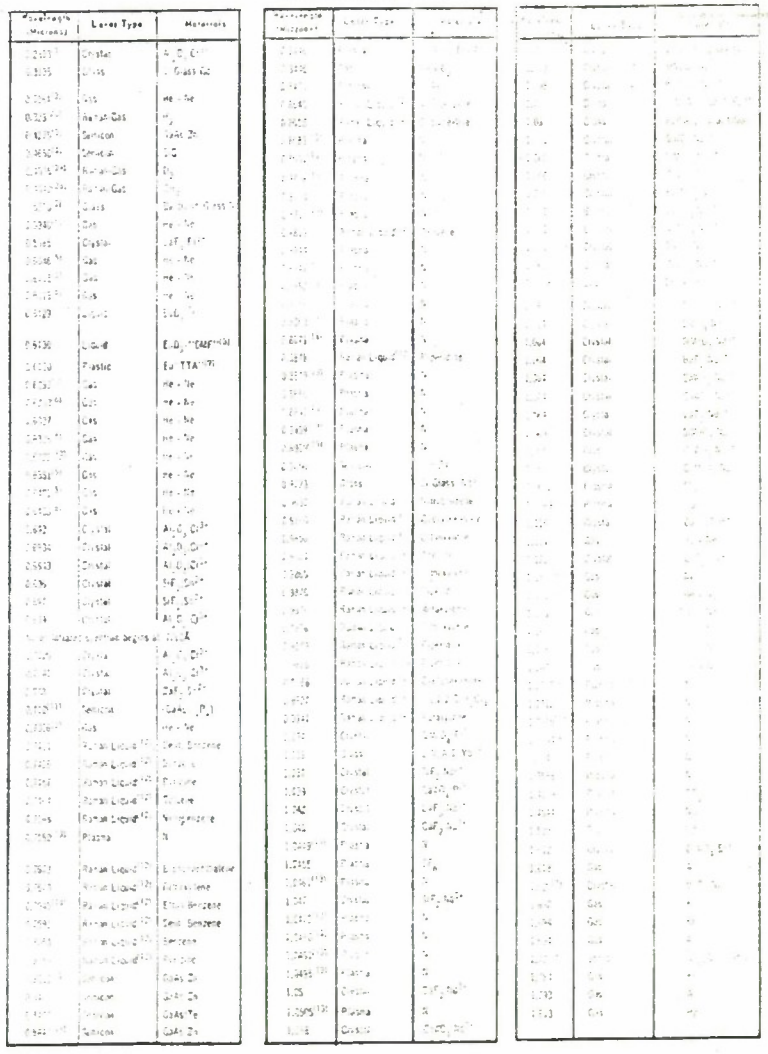


TABLE II-1 (Continued)

LASER FREQUENCIES

Wavelength (Microns)	Laser Type	Materials
[illegible]	[illegible]	[illegible]

Wavelength (Microns)	Laser Type	Materials
[illegible]	[illegible]	[illegible]

Footnotes

(1) Produced as a third harmonic from ruby's second harmonic of 0.3170 μ. Ford has also produced many lines between 0.2313 and 2.5 μ by four-photon techniques, by frequency mixing, and by a combination of the two methods.
(2) Second harmonic coherent emission.
(2a) Achieved through Raman scattering induced by coherent pulses from a 50-kW ruby laser. The figure shown is the shortest wavelength component of an output spectrum which includes several other frequencies.
(3) Cw version of IBM's pulsed semiconductor lasers. The 0.4175-μ second harmonic has been detected by IBM directly from the junction.
(4) Whether this is an actual laser emission is still unresolved at this time.
(5) Achieved through mechanical suppression of unwanted oscillations in a multi-mode laser.
(6) Mechanically tuned.
(7) Europium ion in trisbenzoylacetonate molecule, a chelate in alcohol form. Also described as an adduct of piperidine and benzoylacetonate.
(8) Europium dibenzoylmethide chelate with dimethylformamide.
(9) Phenoyl trifluoro acetonate chelate in polymethyl methacrylate plastic, reportedly a laser material.
(10) One version emits on 1.150 and 3.39 μ.
(11) Also operated at several hundred wavelengths down to 0.6060 μ, and several crystals of reacting fusion μ; emission wavelengths of semiconductor lasers are temperature dependent.
(12) Coherent emission resulting from Raman scattering induced by pulsed ruby laser emission [illegible] on [illegible].
(13) One of many wavelengths produced from polyatomic molecules through dissociation excitation transfer, first used by BTL and indicated here by "plasma."
(14) Principal wavelength among 7 Raman lines.
(15) This is an ion fluorine device.
(16) More than [illegible] other wavelengths have been produced [illegible] lines at BTL; these range in Ne from [illegible].55 μ; A, 1.61 to 26.9 μ; Kr, 1.45 to 7.07 [illegible].26 to 18.506 μ; and He, 2.06 μ.
(17) Radiative transition is phonon assisted.
(18) Different compounds of (InGa)As are believed capable of emitting [illegible] from 0.81 to 3.1 μ.
(19) Also magnetically shifted to 2.125 μ.
(20) Achieved with a Q-spoiling filter on TRG's 7.15-[illegible] optically pumped laser.
(21) Operates only in a magnetic field but is magnetically tunable.
(22) Highest microwave maser frequency.

TABLE II-2

CHEMICAL SYMBOLS OF ELEMENTS USED IN LASERS

Symbol	Element	Symbol	Element
A	Argon	La	Lanthanum
Al	Aluminum	Li	Lithium
As	Arsenic	Mg	Magnesium
B	Boron	Mo	Molybdenum
Ba	Barium	N	Nitrogen
Br	Bromine	Nd	Neodymium
C	Carbon	Ne	Neon
Ca	Calcium	Ni	Nickel
Ce	Cerium	O	Oxygen
Cl	Chlorine	P	Phosphorus
Cr	Chromium	Pb	Lead
D	Deuterium	Pr	Praseodymium
Dy	Dysprosium	S	Sulfur
Er	Erbium	Si	Silicon
Eu	Europium	Sm	Samarium
F	Fluorine	Sr	Strontium
Ga	Gallium	Te	Tellurium
Gd	Gadolinium	Tm	Thulium
H	Hydrogen	U	Uranium
He	Helium	W	Tungsten
Hg	Mercury	Xe	Xenon
Ho	Holmium	Yb	Ytterbium
In	Indium	Yt	Yttrium
Kr	Krypton	Zn	Zinc

5.0 REFERENCES

1. Optically-Pumped Solid State Lasers; T. H. Maiman; Solid State Design; Nov. 1963.
2. A Comparison of the Energy Output of Various Solid-State Laser Materials; W. Ruderman and F. Gould; Lasers and Applications. Edited by W.S.C. Chang, Ohio State University.
3. Thermal Timing of Ruby Optical Maser; I.D. Abella and H.Z. Cummins; Journal of Applied Physics; June 1961; Vol. 32, No. 6.
4. Laser Materials and Devices; R.D. Haun; Electro-Technology; Sept. 1963.
5. The Laser; A. Yariv and J.P. Gordon; Proceedings of the IEEE; Jan. 1963.
6. Ruby Laser Operation in the Near IR; E.J. Woodbury and W.K. Ng; Proceedings of IRE; Nov. 1962; Vol. 50, No. 11.
7. Giant Optical Pulsations from Ruby; F.L. McClung and R.W. Hellwarth; Journal of Applied Physics; March 1962, Vol. 33.
8. Observations Relating to the Transverse and Longitudinal Modes of a Ruby Laser; V. Evtuhov and J. Neeland; Applied Optics; June 1962.
9. Calcium Niobate $Ca(NbO_3)_2$ - A New Laser Host Crystal; A.A. Bellman, S.P.S. Porto, and A. Yariv; Journal of Applied Physics; Nov. 1963.
10. Optical Maser Action of Nd^{3+} in a Barium Crown Glass; E. Snitzer; Physical Review Letter; Dec. 1961; Vol. 7.
11. Rectangular Optical Dielectric Waveguides as Lasers; Bird, Carpenter. McDermott, and Powell; Laser and Applications, Edited by W.S.C. Chang, Ohio State University; 1963.
12. Fiber Optics for Electronic Engineers; G.V. Novotny; Electronics; June 1962.
13. Cylindrical Dielectric Waveguide Modes; E. Snitzer Journal of Optical Society of America; May 1961; Vol. 51, No. 5.
14. Observed Dielectric Waveguide Modes; E. Snitzer and H. Osterberg; Journal of Optical Society of America; May 1961; Vol. 51, No. 5.
15. G. Burns and M.I. Nathan; IBM Journal of Res. and Dev. 7; Jan. 1963.
16. W.E. Engeler and M. Garfinkel; G.E. Report No. 64RL(3547G).
17. R.N. Hall et al; Physical Review Letter; Nov. 1962; Vol. 9.
18. M.I. Nathan et al; Applied Physics Letters; Nov. 1962; Vol. 1.
19. N. Holonyak, Jr. and S.F. Bevoiqua; Applied Physics Letters 1962; Vol. 1.
20. K. Weiser and R.S. Levitt; Applied Physics Letters; May 19
21. I. Melngoilis et al; Proceedings of the IEEE; August 1963;
22. I. Melngoilis; Applied Physics Letters; May 1963; Vol. 2.
23. R.J. Pelan et al; Applied Physics Letters; Nov. 1963; Vol.
24. L.B. Griffiths et al; Proceedings of IEEE; Oct. 1963; Vol.
25. R.N. Hall; Proceedings of the IEEE; Jan. 1964; Vol. 52.
26. R.N. Hall; Solid State Circuits Conference; Feb. 1964.
27. M. Garfinkel and W.E. Engeler; Applied Physics Letters; No Vol. 3.
28. J.A. Armstrong, M.I. Nathan, A.W. Smith; Applied Physics L 1963; Vol. 3.
29. Engineering Specification, JL-10; General Electric Company
30. R.J. Carbone, P.R. Longaker; Applied Physics Letters; Jan. Vol. 4.
31. Microwave Modulation of a GaAs Injection Laser; B.S. Golds J.D. Welch; Proceedings of the IEEE.
32. K. Konnerth and C. Lanza; Applied Physics Letters; April 1 Vol. 4.
33. J.W. Crowe and R.M. Craig, Jr.; Applied Physics Letters; F Vol. 4.
34. Simulated Light Emissions by Optical Pumping and by Energy in Organic Molecules; Morantz, White, and Wright; Physical Letter; Jan. 1962; Vol. 8, No. 1.
35. The Many-Faceted Laser Scramble; A. Corneretto; Electronic Sept. 1962.
36. Lasers and Applications; W.S.C. Chang; Published by Ohio S University; 1963.
37. Gaseous Optical Masers; C.K.N. Patel; Lasers and Applicati Edited by W.S.C. Chang; Chap. 2.
38. Gaseous Optical Masers; A. Javan; Solid-State Design, Nov.

39. Laser Operation at 3.39μ in a He-Ne Mixture; A.L. Bloom, W.E. Bell, and R.E. Rempel; Applied Optics; Mar. 1963; Vol. 2, No. 3.

40. H.A.H. Boot, et al; Nature; May 1963.

41. L.E.S. Mathias and J.T. Parker; Applied Physics Letters; July 1963; Vol. 3.

42. Continuous Optically Pumped Cs Laser; P. Rabinowitz, S. Jacobs, and G. Gould; Applied Optics; July 1962; Vol. 1, No. 4.

43. Three-Dimensional Parametric Interactions of Waves and Quasi-Particles; H. Hsu; Proceedings of IRE; Sept. 1962; Vol. 50, No. 9.

44. Generation of Optical Harmonics; P.A. Franken et al; Physical Review Letter; 1961; Vol. 7.

45. Parametric Photon Interactions and their Applications; H. Hsu and K. Tittel; Laser and Applications, Edited by W.S.C. Chang, Ohio State University; 1963.

46. The Industry; Electronic Design; Dec. 1963.

APPENDIX III

THEORIES OF RAYLEIGH AND MIE SCATTERING

1.0 RAYLEIGH SCATTERING

Consider initially the propagation of a plane polarized light wave of wavelength λ through a medium consisting of a uniform distribution of small spherical particles of dielectric material having dielectric constant $\epsilon' - j\epsilon''$ and radius a. If the incident wave is

$$\bar{E}_0 \, \epsilon^{j\omega t} \tag{III-1}$$

the induced dipole moment per each sphere is

$$\bar{P} \, \epsilon^{j\omega t} \tag{III-2}$$

where $\bar{P} = \alpha \bar{E}_0$ and α is the polarizability of the spheres. The induced dipole moment radiates a field which at distance $r \gg \lambda$ is expressed as follows

$$E = \frac{k^2 P \sin\gamma}{4\pi\epsilon_0 r} \, \epsilon^{-jkr} \tag{III-3}$$

where $k = \frac{2\pi}{\lambda}$ and γ is the angle between the direction of $\bar{r}$ and that of $\bar{P}$ as shown in Figure III-1. The intensity of the electromagnetic field varies as $\sin^2\gamma$ and therefore the maximum radiation occurs at right angles to the axis of the dipole. The average Poynting vector per each sphere is

$$P_r = \frac{1}{2} \mathrm{Re} \left(\bar{E} \times \bar{H}^* \right) = \frac{\mu_0 \omega^4 P^2 \sin^2\gamma}{32\pi^2 r^2 C} \tag{III-4}$$

The total power radiated in all directions is obtained integrating over a sphere of radius r

$$P_{total} = \int P_r ds = 2\pi \int_0^{\pi} P_r r^2 \sin\gamma \, d\gamma = \frac{\mu_0 \omega^4 P^2}{12\pi C} \tag{III-5}$$



DEFINITIONS OF θ AND ρ

FIGURE III-1



PROPAGATION THROUGH PLANE-PARALLEL CLOUD MEDIUM

FIGURE III-2



POLAR DIAGRAM OF SCATTERED INTENSITY

FIGURE III-3

Hence, the total power scattered is proportional to the square of the pole moment and to the fourth power of the frequency, or inversely pr portional to the fourth power of the wavelength. The phenomena of sc tering can be represented in terms of a scattering matrix. In genera if the incident field has polarized components $E_{\ell o}$ and E_{ro}, we can rep sent the relationships between these components and those of the scat tered field E_ℓ, E_r as follows

$$E_\ell = A_2 E_{\ell o} + A_3 E_{ro} \qquad \text{(III-}$$

$$E_r = A_4 E_{\ell o} + A_1 E_{ro} \qquad \text{(III-}$$

The coefficients A_i are complex numbers and define a transformation m trix, which may be written as follows

$$A_i = S_i(\theta_i) \frac{e^{-jkr}}{jkr} \qquad \text{(III-}$$

where S_i are complex "scattering" coefficients. In the above relatio ship θ is the angle between the direction of scattering and that of incident light, and ρ is the azimuth angle. In the case of spherical scatterers and of plane incident waves the scatter phenomena are ind pendent of ρ; this case is illustrated in Figure III-1 where $\overline{P}$ is the induced dipole moment and γ the angle between the direction of $\overline{P}$ and direction of scattering. In equations (III-6 and III-7) E_ℓ and E_r ar respectively the parallel and the perpendicular components of the el tric field vector. The amplitude functions are defined as follows

$$\begin{pmatrix} E_\ell \\ E_r \end{pmatrix} = \begin{pmatrix} S_2 & S_3 \\ S_4 & S_1 \end{pmatrix} \frac{1}{jkr} \begin{pmatrix} E_{\ell o} \\ E_{ro} \end{pmatrix} \qquad \text{(III}$$

We note that, if the medium is isotropic, $\overline{P}$ is parallel to $\overline{E}_0$ a the polarizability α is a scalar quantity. The angle γ is thus rela to θ so that, for the perpendicular field component (r - component) $\gamma = 90°$; for the parallel component (ℓ - component) $\gamma = 90° - \theta$. He

the scattering matrix is expressed as follows (from equations III-3 and III-4)

$$\begin{pmatrix} S_2 & S_3 \\ S_4 & S_1 \end{pmatrix} = -j\frac{k^3}{4\pi\epsilon_o}\begin{pmatrix} \cos\theta & 0 \\ 0 & 1 \end{pmatrix} \qquad \text{(III-10)}$$

for the case of spherical particles. If a comparison is made between the phenomena of scatter from a single sphere and that from a cloud of particles, each acting independently of the others, it can be shown that the interference phenomena resulting in the second case reduce to the consideration of the amplitudes of the various scattering terms only.

In fact, if the scatter phenomena are referred to a common origin, the individual scatterers provide different values of the phase shift and amplitude of the scattered field in a given direction. However, these phenomena are of a random nature because the spherical particles move randomly and the light is itself totally or partially incoherent. For this reason the interference phenomena resulting from superposition of the fields scattered from various particles of a cloud may be expressed simply as the sum of the amplitudes of the various contributions, disregarding the phases. There follows that the resulting Poynting vector is the sum of the magnitudes of the individual Poynting vectors

$$P_{res} = \sum P_i$$

The effect of a scattering cloud on the propagation of a light wave may be considered equivalent to the presence of a complex refractive index of the medium. In fact, as pointed out previously, if the incident wave is

$$u_0 = E_0\, \epsilon^{j\omega t} \qquad \text{(III-11)}$$

the resultant wave in the forward direction ($\theta = 0$) is

$$u = u_0 + \sum E_i\, \epsilon^{j\omega t} \qquad \text{(III-12)}$$

where E_i are the scattered field components. Assume that the cloud consists of a homogeneous medium of thickness d, with N particles per unit volume. Then extending the summation over the cloud, one has for the forward direction, see Figure III-2

$$u = u_0\left[1 + S(0)\int_v \frac{1}{jkr}\,\epsilon^{-jk(x^2+y^2)/2r}\,dx\,dy\right] \qquad \text{(III-13)}$$

where the integral is extended over the volume of the cloud; integrating, one has

$$u = u_0\left[1 - \frac{2\pi}{k^2} Nd\, S(0)\right] \qquad \text{(III-14)}$$

If a plane wave is propagated in a medium of propagation constant k, one has for the path length d, $u = u_0\, \epsilon^{-jkd}$; on the other hand, if the propagation constant is k', one has

$$u = u_0\, \epsilon^{-jk'd} \qquad \text{(III-15)}$$

Letting $\bar{n}$ equal the equivalent complex refractive index of the cloud medium, the change of the amplitude of the wave in propagating through the cloud is proportional to $\epsilon^{-jk(\bar{n}-1)d}$. From equation (III-13) one has

$$\epsilon^{-jkd(\bar{n}-1)} = 1 - \frac{2\pi}{k^2} Nd\, S(0) \qquad \text{(III-16)}$$

that is, approximately, letting $\epsilon^{-jkd(\bar{n}-1)} \cong jkd(\bar{n}-1)$

and

$$k\bar{n} \cong \frac{2\pi}{jk^2} Ns(0) = k \qquad \text{(III-17)}$$

The corresponding formal refraction index of the cloud medium is

$$\bar{n} = 1 - j\frac{2\pi}{k^3} NS(0) = n' - jn'' \qquad \text{(III-18)}$$

This quantity represents the complex contribution of the scattering medium. There follows

$$n' = 1 + \frac{2\pi N}{k^3} \text{Im } S(0) \qquad \text{(III-19)}$$

$$n'' = \frac{2\pi N}{k^3} \text{Re } S(0) \qquad \text{(III-20)}$$

The quantity n' and n", respectively, determine the phase lag and intensity of the propagating wave. It is noted that for spherical particles the scattering coefficients S_3 and S_4 are zero. For an arbitrary scattering direction θ we have

$$E_r = S_1(\theta) \frac{e^{-jkr}}{jkr} E_{ro} \qquad \text{(III-21)}$$

$$E_\perp = S_2(\theta) \frac{e^{-jkr}}{jkr} E_{io} \qquad \text{(III-22)}$$

The corresponding intensity of light is obtained taking the squares of the amplitudes and is expressed as follows for perpendicular polarization

$$P_\perp = \frac{S_1^2}{k^2 r^2} P_o \qquad \text{(III-23)}$$

for parallel polarization

$$P_p = \frac{S_2^2}{k^2 r^2} P_o \qquad \text{(III-24)}$$

for non-polarized light

$$P_n = \frac{1}{2k^2 r^2} (S_1^2 + S_2^2) P_o \qquad \text{(III-25)}$$

There follows that in general for non-polarized incident light the total intensity of the scattered light is

$$P_n = \frac{(1 + \cos^2\theta) k^4 |a|^2}{2r^2 (4\pi\epsilon_o)^2} P_o \qquad \text{(III-26)}$$

This relationship is illustrated in Figure III-3 where the solid lines denote the total intensity and the dotted lines denote the intensities of the polarized components. The scattering cross-section (C_{Scatt}) is defined as the area on which the flux of incident light is equal to the total flux of scattered light. Considering the direction $\theta = 0$ we have integrating over a sphere of radius r

$$C_{Scatt} = \frac{P_{total}}{P_o} = \frac{k^4 |a|^2}{6\pi\epsilon_o^2} \qquad \text{(III-27)}$$

Note that P_{tot} is given by equation (III-5) and $P_o = \frac{1}{2} E^2 \left(\frac{\epsilon_o}{\mu_o}\right)^{1/2}$

2.0 MIE SCATTERING

The general problem of scattering of a plane wave from a spherical particle of radius a is treated by application of Maxwell's equations and solution of the boundary value problem obtained satisfying the continuity equations at the surface of the spheres. Letting E_i, H_i and E_r, H_r respectively equal the incident and the scattered fields, one has for the total field at any point outside the sphere

$$E = E_i + E_r \qquad \text{(III-28)}$$

$$H = H_i + H_r \qquad \text{(III-29)}$$

Assuming that the external medium is lossless and letting P_a and with P_s respectively equal the total power absorbed and scattered by a sphere, one finds that the scattered power is expressed as follows

$$P_s = \left(\frac{\pi E_o^2}{k^2}\right) \left(\frac{\epsilon_o}{\mu_o}\right)^{1/2} \sum_{n=1}^{\infty} (2n + 1) \left(|a_n r|^2 + |b_n r|^2 \right) \qquad \text{(III-30)}$$

where k is the propagation constant of the external medium and ϵ_o, μ_o are its permittivity and permeability, respectively. The coefficients

a_n^r and b_n^r are expressed in terms of spherical Bessel functions; the general relationships are given in the literature [1]. If the dielectric constant of the spherical particle is much larger than that of the external medium one has approximately

$$a_n^r \cong - \frac{j_n(ka)}{h_n(ka)} \qquad \text{(III-31)}$$

$$b_n^r \cong - \frac{[ka\, j_n(ka)]'}{[ka\, h_n(ka)]'} \qquad \text{(III-32)}$$

where $j_n(r)$ and $h_n(r)$ are respectively spherical Bessel functions and spherical Hankel functions.

The absorbed power is obtained from the expression

$$P_a + P_s = \left(\frac{\pi E_o^2 \, Re}{k^2}\right) \left(\frac{\epsilon_o}{\mu_o}\right)^{1/2} \sum_{n=1} (2n+1)(a_n^r + b_n^r) \qquad \text{(III-33)}$$

From the above quantities one can compute the corresponding scattering and absorption cross-section, that is

$$C_{Scatt} = \frac{P_s}{P_o}, \quad C_{abs} = \frac{P_a}{P_o}, \quad C_{total} = C_{Scatt} + C_{abs} \qquad \text{(III-34)}$$

where

$$P_o = \frac{1}{2} E_o^2 \left(\frac{\epsilon_o}{\mu_o}\right)^{1/2} \qquad \text{(III-35)}$$

In general the numerical evaluation of the above expressions is cumbersome. A simplified case occurs when the ratio a/λ is large with respect to unity. In fact one has for large values of the arguments

$$j_n(\rho) \cong \frac{1}{\rho} \cos\left(\rho - \frac{n+1}{2}\pi\right) \qquad \text{(III-36)}$$

1. Electromagnetic Fields; J. A. Stratton; Mc Graw Hill; 1941.

$$h_n(\rho) \cong \frac{1}{\rho} (-j)^{n+1} \epsilon^{j\rho} \qquad \text{(III-37)}$$

Substituting into the expressions for a_n^r and b_n^r one finds letting $N = \frac{K_i}{K}$ = complex index of refraction of the spheres

$$a_n^r \cong j^n \epsilon^{-jka} \frac{\sin x - N \cos x \tan y}{1 - jN \tan y} \qquad \text{(III-38)}$$

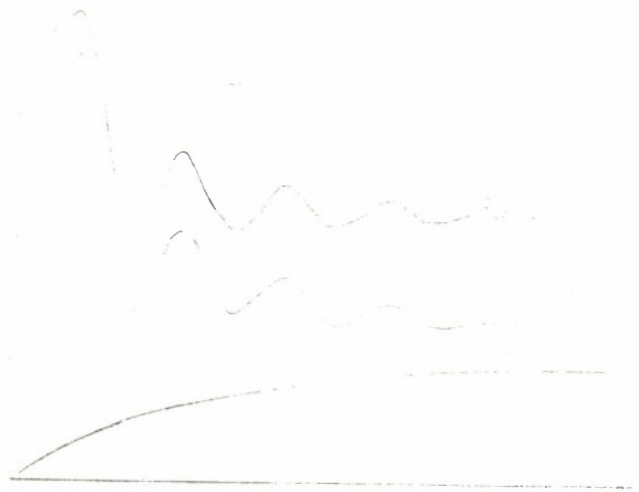
$$b_n^r \cong -j^{n+1} \epsilon^{-jka} \frac{\cos x \tan y - N \sin x}{\tan y + jN} \qquad \text{(III-39)}$$

where $x = ka = \frac{n+1}{2}\pi$, $y = ka(N-1)$

The coefficient a_n^r and b_n^r are thus oscillating functions of ka and n.

The computation of the scattering and absorption cross-section follows straightforwardly from the above relationships. The absorption losses of the spheres may be computed and measured on the basis of the complex index of refraction of the cloud medium.

An example of computation of scatter, absorption and total cross-section for a wavelength of 3.5μ is shown in Figure III-4.



SCATTER, ABSORPTION, AND TOTAL CROSS SECTION COMPUTATIONS FOR 3.5-WAVELENGTH

FIGURE III-4

DESCRIPTION OF LASER MODULATION TECHNIQUES

1.0 DESCRIPTION OF EXTERNAL MODULATION TECHNIQUES

In principle, external modulation techniques are based on the variation of the light transmission characteristics of certain crystals or liquids due to the field effects of (References 1 and 2):

(a) Electro-optic effect: Pockels effect, Kerr effect, and conductivity effect

(b) Magneto-optic effect: Faraday effect

(c) Ultrasonic pressure-optic effect: Photolastic effect

A brief description of the basic phenomena involved follows.

1.1 ELECTRO-OPTIC EFFECT

The variation of the refractive properties of an optical medium by the application of an electric field is called the electro-optic effect. In a crystalline medium, with the field parallel to the light propagation, this is named the Pockels effect; in a liquid medium, with the field normal to the light propagation, the effect is designated the Kerr effect as shown in Figure IV-1. When an isotropic solid or liquid is subject to a strong electric field it becomes doubly refracting; light with different polarization will travel with different velocity, that is, one component is retarded relative to the other and the light beam emerging from the cell is elliptically polarized. If the emergent beam is passed through a polarization analyzer the energy transmitted will vary with the polarization resulting from the field produced by the applied voltage. Thus, the beam can be modulated by use of an ac voltage, the output from the cell being phase or polarization modulated and the final output beam through the polarization analyzer (polaroid or prism) intensity modulated.

The strongest effect of this sort and by far the most widely applied for laser beam modulation is the Pockels effect. Crystals which display such effect are KDP (potassium dihydrogen phosphate), ADP (ammonium dihydrogen phosphate), KDP (potassium didentenium phosphate), KDA (potassium dihydrogen arsenate), ADA (ammonium dihydrogen arsenate), RbH_2PO_4, $NaClO_3$, Zn_2S, and CuCl, that is, piezoelectric and ferroelectric crystals.



SCHEMATIC ARRANGEMENT OF POCKELS (OR KERR) CELL MODULATOR
FIGURE IV-1

The dihydrogen phosphates have relatively high electro-optic constants[1] but light transmission for these crystals, (for example, KDP and ADP which are often used cells) falls off rapidly beyond 1.3μ whereas CuCl is transparent to infrared radiation up to 15μ.

The electro-optic effect is connected with a modification of the optical properties of certain piezoelectric crystals as a result of the application of an external electric field; crystals of about twenty different symmetry classes exhibit the effect. For example, crystals of class 42m (V_d), such as KH_2PO_4 (KDP) and $NH_4H_2PO_4$ (ADP), have been found to exhibit a large electro-optic effect. Because of birefringence, the optical aperture is very limited and the electric field must be applied in the direction of the propagation of light for maximum effect. Crystals of cubic symmetry, class 43m (T_d) such as CuCl, ZnS, and Hexamethylenetetramine (HMTA) provide larger optical apertures and permit the application of the electric field in a direction perpendicular to that of propagation of light. The largest electro-optic effects are exhibited by KDP crystals, and by HMTA crystals.

In general, the birefringence of crystals can be expressed in terms of the index ellipsoid

$$\frac{x^2}{n_x^2} + \frac{y^2}{n_y^2} + \frac{z^2}{n_z^2} = 1 \qquad \text{(IV-1)}$$

where n_x, n_y, n_z are the three principal refractive indexes with the crystalographic axes as the optical axes. In crystals of T_d class, $n_x = n_y = n_z = n_0$.

For simplification purposes, reference will be made to the latter case. When an electric field having components E_x, E_y, E_z is applied, the index ellipsoid is modified as follows

$$\frac{(x^2 + y^2 + z^2)}{n_0^2} + 2r_{41}(E_x\,yz + E_y\,zx + E_z\,xy) = 1 \qquad \text{(IV-2)}$$

[1] Electro-optic constant is defined as a measurement of optical phase retardation per unit of applied voltage.

By recourse to a rotational transformation of the coordinate axes, the latter equation can be transformed to a canonical form

$$\frac{x'^2}{n_x'^2} + \frac{y'^2}{n_y'^2} + \frac{z'^2}{n_z'^2} = 1 \qquad \text{(IV-3)}$$

where the new three principal indexes are obtained as roots of the characteristic equation

$$\begin{vmatrix} \frac{1}{n_0^2} - \eta, & r_{41} E_z, & r_{41} E_y \\ r_{41} E_z, & \frac{1}{n_0^2} - \eta, & r_{41} E_x \\ r_{41} E_y, & r_{41} E_x, & \frac{1}{n_0^2} - \eta \end{vmatrix} = 0 \qquad \text{(IV-4)}$$

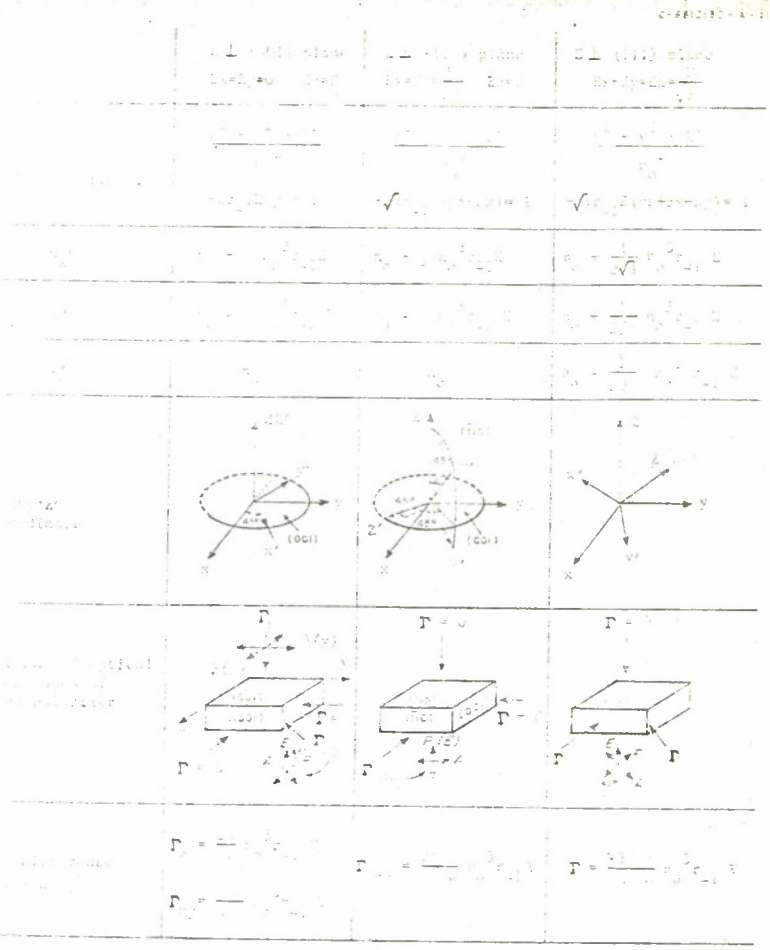
For example, Namba (Reference 3) has computed the solutions for the case of ZnS crystals when the electric field is respectively perpendicular to (001), to (110), or to (111) planes; these results are summarized in Figure IV-2 where d and ℓ are the thickness of the crystal in the direction of the field and of the light respectively; Γ_z is the phase retardation of light traveling in the direction of the applied field; and Γ_{xy}, Γ_{max}, and Γ are the phase retardations for light traveling perpendicularly to the direction of the field. Values of the electro-optic coefficient for various crystals are listed in Table IV-1.

In crystals, the electro-optic effect is generally linear in the applied field, that is the direction of polarized beam of light is rotated by an angle

$$\theta = \Gamma E \ell \text{ radians}$$

where $$\Gamma = \left(\frac{2\pi}{\lambda}\right)\left(\frac{\Delta n}{E}\right) \qquad \text{(IV-5)}$$

where E is the applied electric field and ℓ the optical path length within the crystal. The frequency dependence of the effect is limited by the dielectric losses, which increase with the frequency (for example, of the order of 0.01 in KDP at 300° K and 15 gc).



ELECTRO-OPTIC PROPERTIES OF ZnS CRYSTAL

FIGURE IV-2

TABLE IV-1

ELECTRO-OPTIC CONSTANTS OF VARIOUS CRYSTALS

Crystal	Symmetry-Class	Electro-optic Coefficient (cm/v)	Index Refraction (n)
CuCl	T_d	$r_{41} = 6.1\times10^{-10}$	1.93
ZnS	T_d	$r_{41} = (1.6 - 2.1)\times10^{-10}$	2.36
$NaClO_3$	T	$r_{41} = 0.4\times10^{-10}$	1.513
KDP	V_d	$r_{63} = 11\times10^{-10}$	1.51
KDP		$r_{41} = 8.6\times10^{-10}$ (IV-6)	
ADP	V_d	$r_{63} = 8.3\times10^{-10}$ (IV-7a)	
		$r_{41} = 21.9\times10^{-10}$ (IV-7b)	
HMTA	T_d	$r_{41} = 7.3\times10^{-10}$ (IV-8)	

Electro-optic effects also occur in certain liquids, such as CS_2; however, these are smaller than those in crystals and vary as the square of the electric field. If a suitable dc bias field is applied, the resultant effect is linear. For example, for CS_2 the corresponding electro-optic coefficient, B, (Kerr constant) is found from $\theta = 2\pi BE^2\ell$; if $E = E_0 + \Delta E$, $\Delta\theta = 4\pi BE_0\Delta E\ell$ and $B = 0.36\times10^{-11}$ cm/v^2. Pershan and Bloembergen (Reference 4) have pointed out some of the technical difficulties and limitations encountered in the application of the electro-optic modulator. With reference, for example, to a KDP crystal in which the light is propagated parallel to the E field, the angle θ of rotation of the direction of polarization is

$$\theta = \frac{\pi E \ell n_0^3 r_{ij}}{\lambda_0} \qquad \text{(IV-9)}$$

where r_{ij}, is the electro-optic coefficient and n_0 is the index of refraction for $E = 0$. When the crystal is placed between two perfect Nicols, (Figure IV-3) the average intensity of the modulated light is $\theta^2 I_0/2$ where I_0 is the intensity of the incident light. In certain crystals, a leak of light occurs because of anisotropy and because of imperfections. For example, in KDP, light not exactly parallel to the axis gets depolarized and contributes to the leak. For practical applications, it is necessary to minimize these depolarization effects with respect to the controlled phenomenon. As previously pointed out, crystals of cubic symmetry (such as HMTA, CuCl, and ZnS) behave more favorably in this respect. A transmission line modulator design based on the application of the electro-optic effect is discussed next (Reference 5).

A polarized light beam is propagated between two crystals having their optic axes traverse to the conductors (Figure IV-4). With reference to the dimensions shown in Figure IV-4, the total phase variation per section of transmission line is

$$\phi = \frac{\omega(w - a)}{c} + \frac{\omega a}{c'} \qquad \text{(IV-10)}$$

where ω is the angular frequency of the radiation, c is the velocity of light in free space and c' is the velocity of light in the crystal. If E_z is the traverse electric field of the modulation wave, the corresponding variation of c' is

$$\Delta c' = \frac{1}{2} crn^2 E_z \qquad \text{(IV-11)}$$

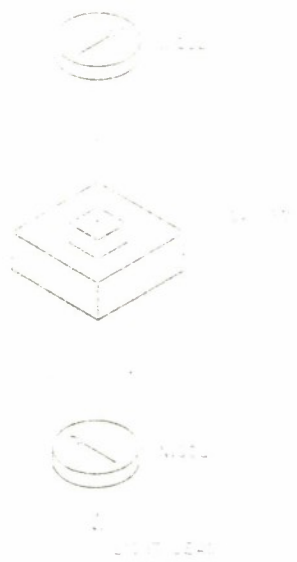
where r is the electro-optic coefficient and n is the index of refraction.

The variation of the phase of light per line section caused by the variation $\Delta c'$ is

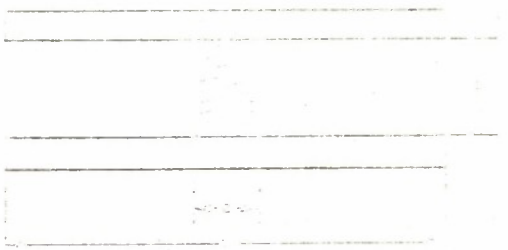
$$\Delta\phi = \left(\frac{w - a}{c'^2}\right)\left(\Delta c'\right) \qquad \text{(IV-12)}$$

Equating the velocities of propagation of light and of the modulation wave, one has:

$$c' = c\left(\frac{w - a + a\epsilon_r}{w}\right)^{-\frac{1}{2}} \qquad \text{(IV-13)}$$



ELECTRO-OPTIC EFFECT MODULATOR
FIGURE IV-3



SECTION OF TRANSMISSION LINE MODULATOR
FIGURE IV-4

where ϵ_r is the relative permittivity of the cryatal. It follows, letting $n = c/c'$, that

$$w = \frac{a(\epsilon_r - 1)}{(n^2 - 1)} \qquad \text{(IV-14)}$$

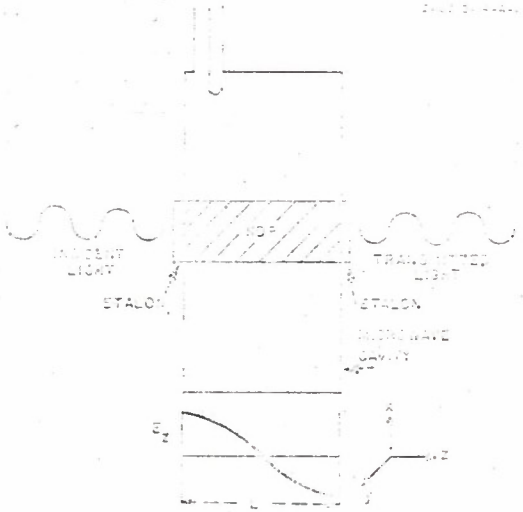
The dimension a is determined by fabrication requirements (for example a = 2 mm), so that w follows from Equation (IV-14). On the other hand, the dimension b may be selected to provide a desirable value of characteristic impedance Z_0 in accordance with the relationship:

$$Z_0^2 = \frac{\mu_0 b^2}{w\epsilon_0 (w - a + a\epsilon_r)} \qquad \text{(IV-15)}$$

where μ_0 is the permittivity of free space, ϵ_0 and ϵ_r are the dielectric constants of free space and the crystal material respectively.

In practice, crystals of dimensions 2 mm x 4.3 mm x 5.6 mm have been used with a line modulator of 50-ohm characteristic impedance. Modulation sensitivities of 12 watts for 100% modulation were obtained with a total light attenuation per pass of 6 db.

Detection of the phase modulation must be obtained by mixing with an unmodulated light beam having the same frequency. Another realization of electro-optic modulation has been described by E. I. Gordon and J. D. Rigden (Reference 6). The design is based on the use of an electro-optic crystal inside a Fabry-Perot etalon, which is tuned to the optical frequency (Figure IV-5). As the light beam makes many back-and-forth passes through the crystal, it is possible to increase effectively the modulation senaitivity. The etalon is placed within a microwave cavity, the frequency of which is chosen to have the value c/2Ln where L is the etalon spacing and n is the index of refraction of the crystal. The bandwidth of the modulator coincides with the bandwidth of the cavity. As an example, a light beam of wavelength 0.6328μ, and a modulator having a microwave frequency of 10 gc was built; the reflectivity of the etalon mirror was $\gamma^2 = 0.9$ and the Q of the cavity was 150. The conversion of the light phase modulation to amplitude modulation can be obtained by means of crossed Nicola or by heterodyning. In the first case, a



SCHEMATIC OF FABRY-PEROT MODULATOR

FIGURE IV-5

quarter-wave plate is inserted between the Nicols, with the latter either parallel or crossed; the introduction of the plate provides a bias which allows linear modulation.

A simpler and more efficient technique of modulation of light has been proposed by Johnson and Kahng (Reference 7). In this case, a transparent piezoelectric medium is utilized; the interference patterns that arise from multiple internal reflections in transmission through or reflection from the medium produce the desired amplitude modulation of a monochromatic coherent light beam.

With reference to Figure IV-6 where a narrow beam of coherent light is incident at an angle $\emptyset$ on a transparent plane parallel piezoelectric plate, the relative intensity of the transmitted beam (T) is found to be affected by the multiple internal reflections and is expressed as follows

$$T = \frac{I_T}{I_o} = \frac{(1 - R)^2}{(1 - 2R\cos\beta + R^2)} \qquad \text{(IV-16)}$$

where I_T is intensity of transmitted beam, $\beta = \frac{2\pi}{\lambda}(2nt\cos\emptyset')$ is the phase difference between two consecutive partial rays, n is the index of refraction of the crystal, $\emptyset'$ is the angle of refraction, t is the thickness of the plate, and $R = (n - 1)^2/(n + 1)^2$ is the reflecting power coefficient. When β is varied from $2m\pi$ to $(2m + 1)\pi$, the value of T correspondingly changes from $T = T_{max} = 1$ to $T = T_{min} = (1-R)^2/(1 + R)^2$. The general plot of T versus β is shown in Figure IV-7 for various values of R.

On the other hand, if the relative reflected light intensity is calculated, then

$$1 - T = \frac{2R(1 - \cos\beta)}{1 - 2R\cos\beta + R^2} \qquad \text{(IV-17)}$$

The intensity of the reflected beam varies between the limits 0 for $\beta = 2m\pi$ and $\frac{4R}{(1 + R)^2}$ for $\beta = (2m + 1)\pi$. Hence, it is possible to modulate the reflected light beam by 100%; the phase change necessary to produce a specified amount of modulation decreases with increasing R. The variation of thickness t, which brings a change of β from $2m\pi$ to $(2m + 1)\pi$, is

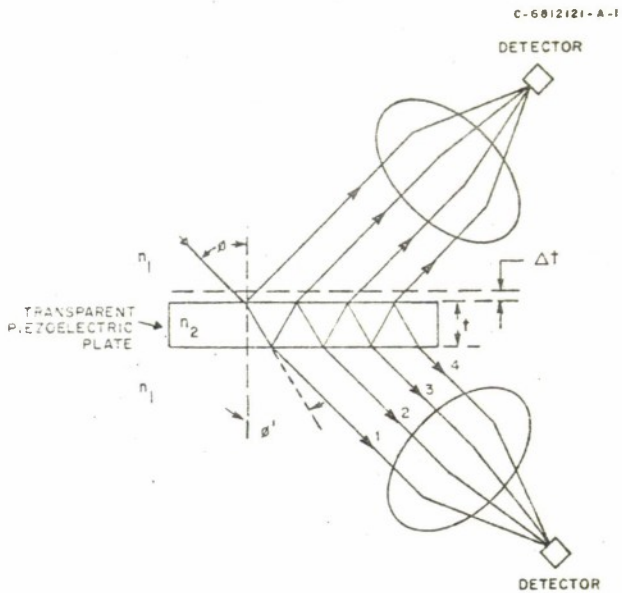
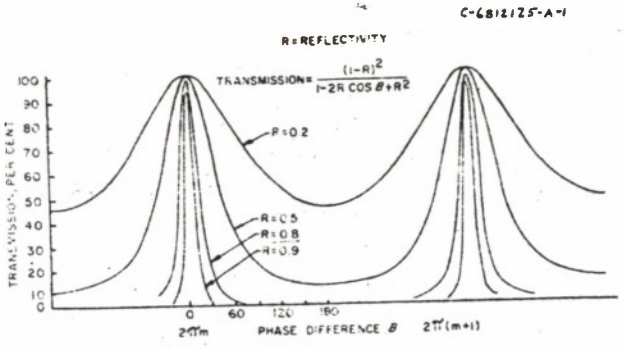


DIAGRAM OF LIGHT MODULATION BY A TRANSPARENT PIEZOELECTRIC MEDIUM

FIGURE IV-6



INTENSITY PATTERN FOR PIEZOELECTRIC OPTICAL-MASER MODULATOR

FIGURE IV-7

$$\Delta t = \frac{\Delta\beta}{2n\ (2\pi/\lambda)\cos\phi'} = \frac{\lambda}{4n\cos\phi'} \qquad \text{(IV-18)}$$

if the angle ϕ' remains constant. Since at maximum transmission

$$t = \frac{\beta\lambda}{4\pi n\cos\phi'} = \frac{m\lambda}{2n\cos\phi'} \qquad \text{(IV-19)}$$

the relative variation in thickness is

$$\frac{\Delta t}{t} = \frac{1}{2m} \qquad \text{(IV-20)}$$

In practice, if the reflectivity R is sufficiently large, a smaller change of phase (β) is required to produce a given relative change of the transmission intensity; for example, if R = 0.9, a modulation ratio of 5:1 is obtained with a phase change of $\pi/15$.

In a practical application, the piezoelectric plate is excited at its fundamental mechanical resonance frequency, f_R; if the electromechanical coupling factor is K, the bandwidth of modulation is:

$$\frac{\Delta f}{f_R} = \frac{2(K-1)}{(K+1)} \qquad \text{(IV-21)}$$

where $K^2 = (1+k)/(1-k)$ and k is the electromagnetic coupling coefficient. Hence, the bandwidth is larger than the values of f_R and of K. Johnson and Kahng have obtained 80% modulation of a 0.6328μ beam with a plane parallel plate of Barium Titanate of thickness t = 73μ; the reflection coefficient was R = 0.9, the fundamental resonance frequency was f_R = 34 mc; the fractional change of thickness was $\Delta t/t = 10^{-3}$, the bandwidth was 17 mc, the electromechancial coupling coefficient was k = 0.5. A dc bias of 10 kv/cm was used, to obtain operation in the region of polarization saturation, where the hysteresis loss is minimum.

1.2 MAGNETO-OPTIC EFFECT

Another class of phenomena of considerable interest for modulation of light applications is that based on the so-called magneto-optic effect. A brief description of the Faraday effect and the Cotton-Mouton effect follows.

The Faraday effect consists of rotating the plane of polarization of a linearly polarized light beam proportional to the path length (L) and to the H component of the magnetic field in the direction of propagation. The angle of rotation is expressed as

$$\theta = VHL \text{ minutes} \qquad \text{(IV-22)}$$

where V is the Verdet constant; at 0.5000μ for water, $V = 13.11 \times 10^{-3}$ min/gauss-cm; for CS_2, $V = 43.41 \times 10^{-3}$; for ZnS, $V = 225 \times 10^{-3}$; for lead glass ($PbO \cdot S_iO_2$), $V = 77.9 \times 10^{-3}$, etc. The Verdet constant varies with light frequency, medium temperature, etc.

The Faraday phenomenon is explained as a double refraction where normal modes of polarization are right and left circularly polarized waves, which propagate with different velocities, and, therefore, acquire a phase difference proportional to the path length within the medium. Quantitatively, in a medium where electrons move in an axially symmetric force field an external axial magnetic field causes precession of all motions around its axis with angular velocity $\omega_1 = eH/2mc$ (where e and m are the charge and mass of the electron, respectively); electrons oscillating in circular orbits at right angles to H have their frequency changed by $\pm\omega_1$ depending on their initial sense of rotation. Consequently, any term of type $A/[\omega_0^2 - \omega^2]$ in the expression of the dispersion formula is modified to

$$\frac{A}{(\omega_0 \pm \omega_1)^2 - \omega^2} \qquad \text{(IV-23)}$$

giving rise to a difference of phase propagation constants for right and for left circularly polarized light. Approximate expressions for the Verdet constant are

$$V = \frac{-e}{2mc^2} \lambda_0 \frac{\delta n}{\delta \lambda} \quad \frac{\text{min}}{\text{gauss-cm}} \qquad \text{(IV-24)}$$

$$V = \frac{\pi(n_r - n_e)}{\lambda_0(\bar{H} \cdot \bar{n})} \qquad \text{(IV-25)}$$

where λ_0 is the wavelength in vacuum, n_r and n_e are the indices of refraction for right and for left circular polarized light, $\bar{n}$ is the unit vector in the direction of propagation of light.

The Cotton-Mouton effect consists of a double refraction phenomenon of light propagated in a direction perpendicular to the magnetic field. More specifically, as a result of the same precession phenomena previously indicated, the index of refraction for light polarized perpendicularly to the magnetic field $H(n_p)$ is larger than that of light polarized parallel to $H(n_s)$; the difference $n_p - n_s$ is proportional to H^2; that is the spatial angle of rotation of the plane polarized light beam is

$$\theta = CH^2L = \frac{(n_p - n_s)\,L}{\lambda} \text{ minutes} \qquad \text{(IV-26)}$$

The Cotton-Mouton constant (C) is of the order of 37.6×10^{-3} min/cm gauss^2 for aceton, -65.8×10^{-13} for chloroform at room temperature and at 0.5000μ. In general the Cotton-Mouton effect is much smaller than the Faraday effect.

Crystals of large Faraday effect, such as neodymium ettrylsulphate display a rotation of 0.0014°/mm of crystal length for a magnetic field of 1 gauss at 4°K (Reference 8). InSb and Ge may also be employed (Reference 2).

Under suitable conditions, modulation of light up to a few gigacycles could be expected; however, compromises of bandwidth and percent modulation for crystal thickness and heating seem to make this technique quite unattractive.

2.0 DESCRIPTION OF INTERNAL MODULATION TECHNIQUES

In this case one modifies directly an operational parameter involved in the generation of the coherent radiation, such as the level of pumping power, the tuning of the cavity, the population level of the laser transition levels, the position of the laser transition levels, etc. Obviously, the modulation process takes place inside the laser resonator.

The principles suggested for external modulation can be used for internal modulation. The methods employed can be classified as follows:

(a) Regeneration-control modulation
(b) Pump-power modulation
(c) Zeeman and Stark modulation
(d) Geometry-variation modulation

A brief outline of these techniques is provided in the following paragraphs.

2.1 REGENERATION-CONTROL MODULATION

Modulation by varying the laser regeneration has proved most useful for obtaining controlled high power pulses and it is equally applicable for continuous amplitude modulation. A typical setup is shown in Figure IV-8.

In applying this method to the modulation of a ruby laser, modification of the conventional system is achieved by simply removing one of the reflectors from the end of the ruby and spacing it far enough away to permit the insertion of a Pockels or Kerr Cell shutter between the ruby and the reflector.

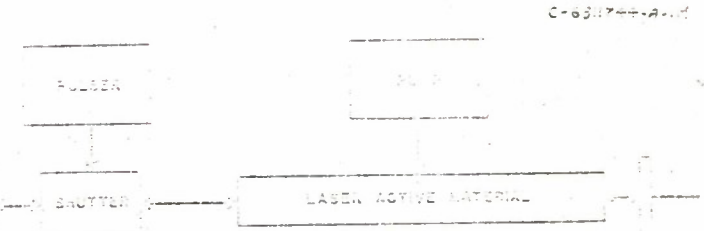
The time constants involved can be extremely short if the Q of the system is high. It is also quite possible to use this method for efficient continuous modulation of a laser although the output beam intensity will not be proportional to the modulator voltage. Because a relatively small change in transmission of the shutter can carry the laser across the threshold from zero output to a final output, it is clear that this method is more efficient than external modulation with the same Pockels or Kerr Cell.

Note that, taking advantage of the phase shift in a Pockels crystal, one can obtain internal frequency modulation or mode selection by applying a configuration similar to that of Figure IV-8.

2.2 PUMP-POWER MODULATION

The novel feature of hair-trigger mode of pumping, due to M. L. Stitch (Reference 9), is especially well adapted to the generation of a long series of controlled pulses. The method is based on the fact that in three-level devices such as ruby, a sizable fraction of the pumping energy is required just to transport half of the ground state population to the excited state to bring the laser to the point of oscillation. The additional amount required to provide stimulated emission is relatively small. Thus, it is advantageous to have two pumping sources: first, one serves to bring the ruby almost, but not quite, to threshold, and then another source provides a short intense flash to produce a pulsing laser output upon demand.

Since a relatively small amount of energy is required from the second flash lamp, the peak power can be made high and the pulse duration



MODULATION BY REGENERATION CONTROL
FIGURE IV-8

short so that the laser output will be more intense than the normal pulses and it will also occur at a specified time. It is also evident that the average power requirements can be met by the continuously pumped lamp, while the speed and peak power requirements can be met by the pulsed lamp. Hence, controlled pulses of considerably enhanced amplitude have been obtained.

Pump-power modulation has also been applied successfully to the He-Ne gas laser, which lends itself very easily to a direct amplitude modulation (Reference 10). When the discharge in the He-Ne gas mixture is excited by an rf field and the amplitude of the field modulated, the stimulated emission of the laser will also be modulated. However, the modulation bandwidth of such a method is inherently very limited (video or less) by the relaxation time of the discharge tube (Reference 11).

In the case of semiconductor lasers, pump power modulation is expected to allow much wider bandwidths. GaAs lasers have already been used to transmit both audio and video signals.

Direct modulation of the lasing levels have been suggested (Reference 11). One way to do this would be to use a subsidiary rf resonance that takes laser ions or atoms out of the lasing levels to some nearby level not directly involved in the laser transition. Nearly all laser materials have levels which would be appropriate for such "double resonance" techniques.

2.3 ZEEMAN AND STARK MODULATION

Laser frequency modulation can be achieved by employing Zeeman or Stark Effect. Where Zeeman effect is applicable, magnetic field is used to produce shifting in energy levels and, in turn, in frequencies.

Zeeman splitting in ruby has been thoroughly studied by Sugano (Reference 12) and Nedderman (Reference 13); the latter has been able to control the pulse times of a ruby laser by applying an inhomogeneous magnetic field to it. Beams have been switched on and off at rates up to 10^5 times per second. Magnetic fields of about 60 gausses were used.

If a first order Stark effect exists in the upper or lower laser level, the application of an electric field (E) to the material may be expected to shift the laser frequency by an amount of the order of 0.5×10^6 E cps (E in volts/cm). Such an effect is known to exist for

the ruby laser transition, and apparently not exist for other presently used laser materials. An upper limit to the modulation bandwidth is created by the requirement that the modulation wavelength be large compared with the ruby dimensions; this sets the limit to centimeter wavelengths (S-band). The power required turns out to be a function of the bandwidth raised to the third power. For a bandwidth of 1 mc only a few watts would be necessary, but the power increases very rapidly with frequency.

In the Zeeman effect case, the frequency shift per gauss needs a million times as much power as would be required for similar results using the Stark effect. One method suggested to enhance the Stark or Zeeman effect for modulation purposes consists in employing a second laser which would be pumped by the output of the frequency modulated laser. Small deviations in pump frequency may then amplitude modulate the second laser.

2.4 GEOMETRY VARIATION

With laser configurations that use detached end reflectors, the positions or angles of these reflectors could be physically changed to vary the effective regenerative power of the optical mode configuration so as to amplitude or frequency modulate the laser output. Interposing a Fabry-Perot Interferometer in the laser beam path has been used as a mode selector with considerable success (Reference 14). The modulation bandwidth is limited even using ultrasonic techniques to obtain mechanical motion.

An interesting method of control of the resonator properties is obtained by interposing an ultrasonic cell in the optical cavity. The theory of the phenomena of interaction of light and ultrasonic waves follows.

In 1921, Brillouin speculated that a transparent (nonabsorbing) medium traversed by compression waves of short wavelength would act as a diffraction grating when traversed by a light beam in a direction perpendicular to the gradient of the elastic waves. This prediction was verified by Debye and Sears, and by Lucas and Biquard in 1932.

If a gradient of pressure is set up in a medium in the vertical direction, the index of refraction varies according to the Lorentz law

$$\Delta n = \frac{K (n_0^2 - 1) (n_0^2 + 2) \Delta P}{6 n_0} \qquad \text{(IV-27)}$$

where n_0 and Δn are the index of refraction and its variation from equilibrium, ΔP is the pressure variation from equilibrium, and K is the compressibility of the medium. A monochromatic beam of light horizontally traversing the medium is refracted along a path of curvature $(r) = n_0 / \frac{dn}{dz}$ where z is the direction of the gradient. In practice, a pressure gradient can be established in an ultrasonic cell by setting up a standing wave; in this case the gradient is maximum at the nodal points of the pressure. If a light beam of diameter smaller than the wavelength of the ultrasonic wave is applied at the nodal point, it will be deviated periodically upward and downward with the period of the ultrasonic wave. If the light path within the cell is d, the maximum angular deviation within the medium is approximately the ratio d/r and is therefore proportional to d and to the pressure gradient. The quantity d is limited by the condition that it must be less than a quarter of the ultrasonic wavelength, and the resultant deviation is usually very small.

If the light beam has a diameter larger than the ultrasonic wavelength, the interaction results in a diffraction phenomenon. A diffraction pattern whose intensity varies at a frequency twice that of the ultrasonic wave is obtained.

These described effects have been applied extensively in the analysis of ultrasonic waves and, more recently, in the operation of lasers. For instance, an ultrasonic cell of the above type can be inserted within the optical cavity of a laser with the result that a periodic modulation of the laser output is obtained; if the laser beam is very narrow, the cell acts as a "Q-switch" and, if it is large, the cell modulates the light output.

When the ultrasonic wave is of traveling type, the fluctuation of the diffraction pattern disappears, and the light beam maintains a constant amplitude in time; on the other hand its frequency is modulated by the ultrasonic wave. Finally, if the traveling wave is amplitude modulated, an amplitude modulation of the light beam also results. It is

desirable to examine the above results in quantitative detail. Refer first to an ultrasonic cell (Figure IV-9) in which a traveling wave is set up such that the gradient of pressure is

$$\frac{dp}{dz} = \left(\frac{2\pi P}{\lambda_s}\right) \left[\cos\left(\omega_s t - \frac{2\pi z}{\lambda_s}\right)\right] \qquad \text{(IV-28)}$$

In the above relation ω_s and λ_s are respectively angular frequency and wavelength of the ultrasonic wave. If the light beam is assumed to have a very small diameter and its deviation is small with respect to λ_s, the coordinate z can be considered constant at the incidence point and also throughout the lightpath inside the cell. Hence, from Figure IV-9:

$$\sin \theta_s = x/r \cong \theta_s \qquad \text{(IV-29)}$$

$$\theta_s = \left(\frac{d}{n_0}\right)\left(\frac{dn}{dz}\right) = \left(\frac{dK (n_0^2 - 1) (n_0^2 + 2) 2\pi P}{6 n_0^2 \lambda_s}\right) \left(\cos \omega_s t\right) \qquad \text{(IV-30)}$$

where $n = n_0 + \Delta n \sin\left(\omega_s t - \frac{2\pi z}{\lambda_s}\right)$ ($z = 0$ for convenience) (IV-31)

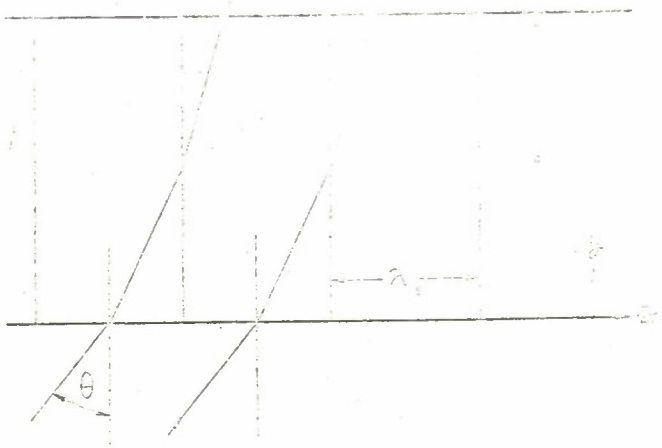
Taking into account the refraction from the cell medium to air, and indicating with θ_t the angular deviation of the emerging beam

$$\frac{\sin \theta_s}{\sin \theta_t} = \frac{1}{n} \qquad \text{(IV-32)}$$

$$\theta_t \cong \theta_s n_0 = \left(\frac{dK (n_0^2 - 1)(n_0^2 + 2) 2\pi P}{6 n_0 \lambda_s}\right) \left(\cos \omega_s t\right) \qquad \text{(IV-33)}$$

Hence, the emerging beam is deviated periodically upward and downward by

$$\theta_{max} = \frac{dK (n_0^2 - 1) (n_0^2 + 2) 2\pi P}{6 n_0 \lambda_s} \qquad \text{(IV-34)}$$



EQUIVALENT DIFFRACTION GRATING EFFECT OF ULTRASONIC CELL

FIGURE IV-9

Note that a similar result is obtained if the ultrasonic wave is a standing wave. In this case, the gradient of pressure is expressed as follows

$$\frac{dp}{dz} = \left(\frac{2\pi P}{\lambda_s}\right)\left(\cos \omega_s t\right)\left(\cos \frac{2\pi Z}{\lambda_s}\right) \qquad \text{(IV-35)}$$

If the light beam is incident at $z = 0, \pm \lambda_s, \pm 2\lambda_s$, etc, the analytical treatment is identical to that given previously. Clearly the maximum deviation permissible is, from the geometry of Figure IV-9:

$$\theta_s \max \leq \frac{\lambda_s}{4\, d} \qquad \text{(IV-36)}$$

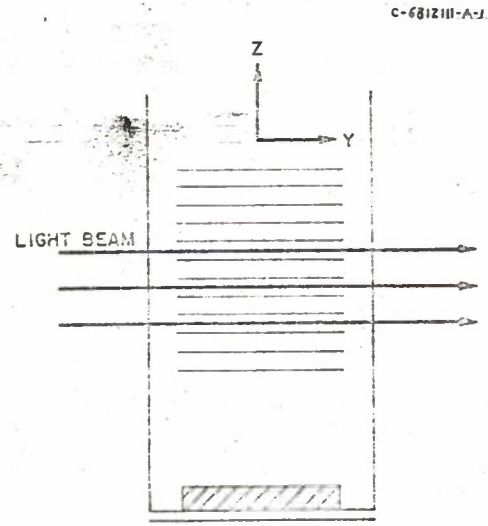
If the ultrasonic cell is placed inside a laser cavity, the light beam is switched off and on periodically with a frequency twice that of the ultrasonic wave; on the other hand, if one of the mirrors of the laser cavity is offset from the parallel condition, the periodicity of the switch is the same as that of the ultrasonic wave.

Assume that the light beam has a diameter larger than λ_s, Figure IV-10. Now to be solved is the difficult problem of the propagation of an electromagnetic wave through a medium with variable characteristics In general, the influence of matter on the propagation of an electromagnetic wave is equivalent to the effect of electric dipoles embedded in vacuum, where the induced dipole moment for an infinitesimal volume element $d\tau$ is proportional to the field E and to the number of molecules associated with $d\tau$. Hence, the Hertz vector associated with these dipoles is:

$$\overline{\Pi} = \alpha N\,(r, t - \tfrac{R}{c})\,\frac{\overline{E}\,(r, t - \frac{R}{c})}{R}\,d\tau \qquad \text{(IV-37)}$$

where retarded potential expressions are used; N is the number density of molecules. The field follows from solution of the integral equation

$$\overline{E}\,(r,t) = E_i\,(r,t) + \int_\tau \left[\frac{-1}{c^2}\cdot\frac{\partial^2}{\partial t^2} + \text{grad div}\right]\overline{\Pi}\,d\tau \qquad \text{(IV-38)}$$



DIFFRACTION THROUGH ULTRASONIC CELL

FIGURE IV-10

where E_i is the incident field (α is the polarizability of the molecules). Consider a light polarized normal to the plane incidence, that is $\overline{E}_i(r,t) = E_{iX}(r,t)$, and also assume $E_Z = E_y = 0$ throughout so that the above integral reduces to scalar form. Furthermore, if N is the molecular number density of the medium

$$N(r,t) = N_0 + N_1 \cos(\beta_s Z - \omega_s t) \tag{IV-39}$$

$$E_X(r,t) = Ae^{j(\beta Z \sin\theta + \beta y \cos\theta - \omega t)} + \frac{To}{4\pi} \iiint \left[\frac{-1}{c^2} \cdot \frac{\partial^2}{\partial t^2} + \frac{\partial^2}{\partial Z^2}\right] \left[\frac{1}{R} + \frac{N_1}{RN_0} \cos\left(\beta_s Z - \omega_s\left(t - \frac{R}{c}\right)\right)\right] E\left(r, t - \frac{R}{c}\right) dr \tag{IV-40}$$

where θ is the angle of incidence of the light beam, Figure IV-11, and

$$\tau_0 = 4\pi N_0 \alpha = \frac{3(n^2 - 1)}{n^2 + 2} \tag{IV-41}$$

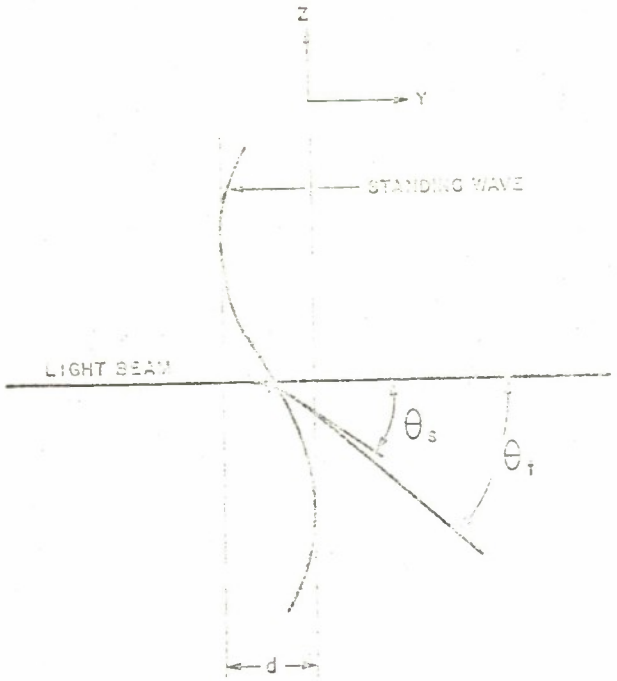
The above integral equation can be solved by approximation assuming a solution of the following type:

$$E_X = \sum E_{Xl} e^{j(P_l Z + Q_m y - \omega_l t)} \tag{IV-42}$$

Hence, the transmitted wave may be considered as consisting of the superposition of many plane waves, each with a different frequency and a different velocity of propagation; in particular one finds

$$\omega_l = \omega,\ \omega + l\omega_s,\ l = \pm 1, \pm 2, \text{ etc.}$$

$$P_l = \beta \sin\theta + l\beta_s$$



REFRACTION THROUGH ULTRASONIC CELL

FIGURE IV-11

$$Q_m = \left(\omega_\ell^2 c^{-2} - P_\ell^2\right)^{1/2}$$

$$E_{X\ell} = \frac{\mu^2 \alpha}{b} \; A e^{j\ell\pi} J_\ell \qquad \text{(IV-43)}$$

where

$$b^2 = \beta^2 (n_0^2 - \sin^2 \theta) \qquad \text{(IV-44)}$$

$$\mu^2 = \beta^2 n_0 \Delta n \qquad \text{(IV-45)}$$

$$n = n_0 + \Delta n \cos (\omega_s t - \beta_s Z) \qquad \text{(IV-46)}$$

The spatial distribution of the electromagnetic field thus appears as a diffraction pattern, with intensities proportional to Bessel functions of constant argument. The angles of the various orders are given by, Figure IV-12, $\sin \Phi_\ell = \left(2\lambda/\lambda_s\right) + \sin \theta$. While the above result applies for a traveling wave, the analysis is readily extended to the case of an ultrasonic standing wave. It is found that the spatial distribution of $E_{X\ell}$ is still represented by Bessel functions, where Δn is replaced with $\Delta n \cos \omega_s t$.

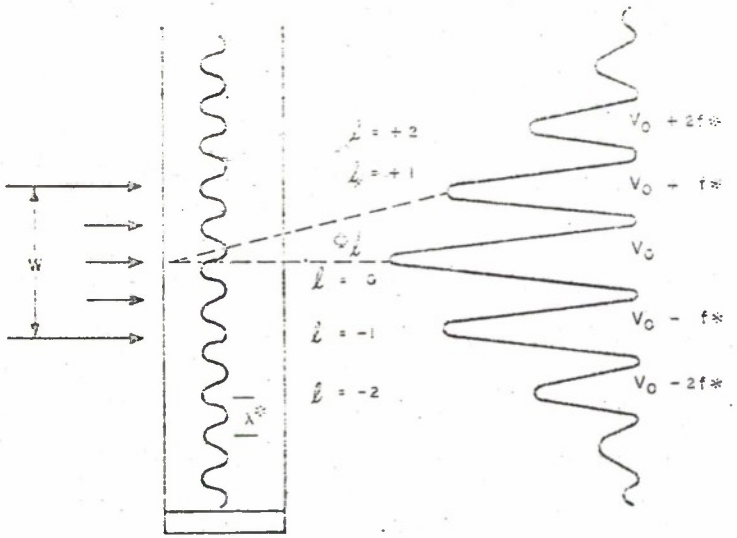
In conclusion, with a traveling wave the diffraction pattern is of constant intensity and with a standing wave a diffraction pattern varies in intensity at a rate twice that of the ultrasonic wave. A more general case can be considered, in which an ultrasonic traveling wave of frequency ω_{s1} is amplitude modulated with a standing wave of frequency ω_{s2}, where $\omega_{s2} < \omega_{s1}$. As a result, the diffraction pattern is now modulated at a rate equal to that of the ultrasonic wave.

Some numerical values of the characteristics of typical liquid media useful in connection with ultrasonic cells are given in Table IV-2.

3.0 MODULATION SYSTEM

For amplitude modulation systems some interesting theoretical analyses have been performed.

J. P. Gordon (Reference 15) has derived the information capacity of various communicationa systems taking into account the effects of quantum



DIFFRACTION OF LIGHT BEAM THROUGH A TRAVELING ULTRASONIC WAVE

FIGURE IV-12

TABLE IV-2

INDEX OF REFRACTION AND COMPRESSIBILITY OF VARIOUS LIQUIDS

Liquid	n_0	K per atmosphere
Water	1.33	5.2×10^{-5}
CS_2	1.62	6.6×10^{-5}
HNO_3	1.397	33.8×10^{-5}
Ethyl Alcohol	1.36	9.6×10^{-5}

noise. The capacity resulting is theoretical in that the number of signaling waveforms required to obtain the capacity approach infinity. The results show that at low S/N ratios (≤ 1) a binary quantum counter has approximately the same capacity as a homodyne receiver. This counter is assumed to ideally detect the number of photons arriving in an interval and decides whether a pulse was sent or not based on the number detected. At lower S/N ratios the quantum detector has a higher information capacity than any other modulation technique.

Reiffen and Sherman (Reference 16) have considered the general case of photon detectors where the receiver has a priori knowledge that one of a finite set of signaling waveforms was transmitted. The signaling waveform set $[\lambda(t)]$ is a sequence of length N of photon counts. The time duration of the sequence is divided into N-time segments of length Δt. In Δt it is assumed that Poisson statistics, which are non-time varying, hold. However, for longer intervals, time varying Poisson statistics hold. A condition is that for the time interval Δt,

$$\Delta t \gg \frac{1}{W} \qquad \text{(IV-47)}$$

where W is the spectral width of the source.

The ideal receiver calculates the conditional probability of receiving a given sequence n provided $\lambda^{(K)}$ was transmitted, and where K can take on every value in the signal set, and provides a basis for selection of the largest probability. For such a receiver, for only two signaling waveforms, and for high background level, S/N ratio at the receiver output becomes

$$\frac{S}{N} = \frac{\eta \Delta t}{\lambda_0} \sum_i \left[\lambda_i^{(1)} - \lambda_i^{(2)} \right]^2 \qquad \text{(IV-48)}$$

The S/N ratio is maximized if one of the signaling waveforms is made equal to zero and if the other signaling waveform is made a pulse of duration Δt with λ photons. In this case the output S/N ratio is

$$\frac{S}{N} = \frac{\eta \Delta t \lambda^2}{\lambda_0} \quad \text{for} \quad \frac{\lambda}{\lambda_0} \ll 1 \qquad \text{(IV-49)}$$

where η is the photon efficiency of the photon detector. A high S/N ratio and high background can result if

$$1 \ll \eta \lambda \Delta t \ll \lambda_0 \Delta t$$

The receiver may consist of a photon counter, reset every Δt seconds, which records a 0 for zero counts and a 1 for λ counts.

In these results the following are assumptions:

(a) $\lambda/\lambda_0 \ll 1$. Narrowing the pulse under a fixed energy constraint may violate this assumption.

(b) λ_0 is assumed constant independent of Δt. Therefore the optical filter preceding the pulse counter must have a bandwidth wide enough to pass the pulse Δt.

(c) The photon counter is assumed capable of resolving individual photons.

These results are interesting immediately for digital communications for even in high background conditions which may be the case due to atmospheric scintillation the output S/N ratio may be high. However they are also of interest in a form of pulse analog communication, pulse position modulation (PPM). In this case an analog signal may be transmitted by sampling the message and encoding the sample into the time position of the pulse. The receiver would consist of a photon counter reset every Δt seconds and when a 1 output was recorded the time portion of the received pulse would be delineated.

This form of modulation may be ideally suited for junction diode lasers. Goldstein and Welch (Reference 17) have reported modulating a

junction diode laser at a 2-gc rate which indicates that pulse durations of 10^{-9} seconds or less may be achieved. As discussed in Appendix II it appears that the average power capability of a junction diode laser may be maintained during pulse modulation with pulse duration shorter than the thermal time constant of the diode laser. That is, the peak power during pulse modulation times the duty factor of the pulse is the same order as the average power capability during CW modulation. PPM also conserves average transmitter power while maintaining good output S/N ratio. This is because PPM exchanges output S/N ratio for bandwidth on a fairly efficient basis (Reference 18). Thus average power can be reduced in exchange for bandwidth which is an important trade off when it is considered that as yet junction diode lasers must be cryogenically cooled which is an inefficient process.

4.0 REFERENCES

1. Methods of Modulating Infrared Beams; T. S. Moss; Infrared Physics; 1962; Vol. 2.

2. Modulation and Scanning With a CW Laser; L. M. Vallese; Technical Proposal No. 64939, ITT Federal Laboratories; Nov. 1963.

3. S. Namba; Journal of Optical Society of America; Jan. 1961; Vol. 51.

4. N. Bloembergen and P. S. Pershan; Proceedings of 2nd Quantum Electronics Conference; 1962.

5. C. J. Peters; Proceedings of the IEEE; Jan. 1963; Vol. 51.

6. The Fabry-Perot Electro-Optic Modulator; E. I. Gordon and J. D. Rigden; Nerem Record; 1962; Vol. 4.

7. L. F. Johnson and D. Kahng; Journal of Applied Physics; Dec. 1962; Vol. 33.

8. Microwave Modulation of Light; P. S. Pershan and N. Bloembergen; Advances In Quantum Electronics, Columbia University Press; 1961.

9. Repetitive Hair-Trigger Mode of Optical Maser Operation; M. L. Stitch, E. J. Woodbury, and J. H. Morse; Proceedings of the IRE; Oct. 1961; Vol. 49.

10. Direct Modulation of a He-Ne Gas Laser; E. J. Schiel and J. J. Bolmarcich; Proceedings of the IRE; June 1963.

11. Microwave Modulation of Light In Paramagnetic Crystals; N. Bloembergen, P. S. Pershan, and L. R. Wilcux; Cuft Laboratory, Harvard University, Astia AD No. 243873.

12. Absorption Spectra of Cr^{3+} in $Al_2 O_3$; S. Sugano, Y. Tanabe, and C. Tsuji Kawa; Journal of Physics Society of Japan; Aug. 1958; Vol. 13.

13. Control of Ruby Laser Oscillation by an Inhomogeneous Magnetic Field; H. C. Nedderman, Y. C. Kiany, and F. C. Unterleitner; Proceedings of the IRE; July 1962; Vol. 50.

14. Lasers and Applications; W. S. C. Chany; Published by Ohio State University; 1963.

15. Quantum Effects In Communication Systems; J. P. Gordon; Proceediogs of The IRE; Sept. 1962.

16. An Optimum Demodulator for Poisson Processes: Photon Source Detectors; B. Reiffen and H. Sherman; Proceeding of the IEEE; Oct. 1963.

17. Microwave Modulation of a GaAs Injection Laser; B. S. Goldstein and J. D. Welch; Proceedings of the IEEE.

18. Radio Telemetry; M. H. Nichols and L. L. Rsuch; John Wiley and Sons Inc; 1956.

APPENDIX V

HEURISTIC DISCUSSION OF RECIPROCITY EFFECTS IN THE TRANSMISSION AND RETURN OF A LASER BEAM

It has frequently been argued that reciprocity controls the transmission and return of a laser beam. By this is meant that since atmospheric effects are almost completely below a hundred cycles, or a time constant of 10^{-2} seconds, and a nanosecond (10^{-9} sec) is a light foot, if a distance of less than 10^7 feet is traveled, the atmosphere would not have changed, and the refraction in two opposite directions would be reciprocal. Figure V-1 illustrates an outgoing beam of light, with an angle of divergence α. Consider the top and bottom pencils of this beam. Their motion, or refraction, is the same until their separation is greater than the dimensions of the smallest turbulent element (that is, until $\alpha x_0 > \lambda_0$) after which they will be refracted independently. Thus, if the cross section of the beam at some distance $x \gg x_0 = \frac{\lambda_0}{\alpha}$ is examined an overall dancing, which is due to the nearer turbulent elements in the region $0 \rightarrow x_0$ would be apparent. Also the overall beam will not be uniform, but broken up into a large number of patches that move about, appear and disapear, in a random manner as the various portions of the beam are refracted independently in the region from x_0 to x. The turbulent elements near x will not affect this pattern very much, but will cause large phase shifts in the wavefront, that is, if dancing of an image in the focal plane is observed this dancing would be caused by elements near the telescope, as large angular deviations will not enter the telescope aperture if they are caused very far away. Referring to Figure V-2, note that at the receiving aperture it is possible to trade space and time averages, as increasing the aperture will give approximately the same effect as taking a time average.

A complicating factor has been avoided in assuming a single element size for the turbulence. This is of course not valid, and will be considered in due course. The entire model here is, of course, grossly oversimplified, but in dealing with the atmosphere this is unavoidable.

GEOMETRY OF α AND ℓ_0

FIGURE V-1

IMAGE CROSS SECTION AS A FUNCTION OF DISTANCE FROM TRANSMITTER

FIGURE V-2

Several devices that might be employed to return the beam are a diffuse reflector, a flat mirror, a corner cube, and a transmitted beam. A discussion of each device follows.

First, consider a diffuse reflector. Postulate an experiment in which a well collimated laser besm is projected a distance less than x_0, and observed on a white screen. For comparison a point source of light is placed nearby. One would then note that the laser beam is dancing, with peaks of 10 to 20 seconds of arc. Using a small telescope near the trsnsmitter one can observe the dancing of the besm, but would note that the point source is not dancing. Now, using a beam splitter, line up the receiving telescope with the transmitted beam. Here again, note that the laser beam appears to be dancing, until the aperture is reduced to the point smaller than the smallest turbulent element. At this point, the laser dsncing stops, but the point source will now be dancing. A critical question is what the dimension is under which reciprocity is obtained; this characteristic dimension may then be assigned to the turbulence as its inner scale. Observationally, at a meter height with moderate winds this is of the order of a centimeter.

Now consider transmitting two laser beams separated by several centimeters. If the telescope aperture is marked so that it has only two openings coincident with the outgoing beam one might expect to avoid dancing. But because each aperture is collecting light from both spots dancing still occurs. It is then apparent that both the transmitter and receiver must be smaller than the smallest turbulent element. This is then a critical point.

Now consider the use of a plane mirror. If the separation of the two beams is great enough and their divergence small enough, one may now make the two beams independent. Thus if the divergence is reduced to zero one may go to a limiting case of an open aperture. However, the returning light is reflected at a different angle than that st which it is received. Thus at a distance $x = \frac{\ell_0}{2\beta}$, where β is the angle st which the light strikes the mirror, reciprocity is lost again since independent elements are traversed knowing that $\ell_0 \simeq 1$ cm, and $\beta \simeq 5 \times 10^{-5}$, we have x (meters) $= \frac{10^{-2}}{10^{-4}} = 10^2$; a rather short distance.

A corner cube does not have this short distance defect, but neither does it return the light to the same point at which it entered. Thus the corner cube must be well under a centimeter in size, or reciprocity is immediately lost.

Instead of considering a corner cube further, consider a system that returna the light from a small element in the same direction from which that element receives it. Such a system might be some type of image tracker with a means of deflecting a beam from a laser. It is apparent that the system is now changed, and the previous criticism and limitation to roughly a hundred meters does not hold. However, assume that we are at some range $x > x_0$. At a distance x_0 from the transmitter the transmitted beam begins to break up. If the ray that enters the receiver is followed and then its path back again is traced one sees that at a distance x_0 from the receiver the return beam begins to break up. Thus only one ray will return, while the rest of the return beam will be refracted in a random manner with relation to the outgoing beam. Thus, even if the beam with a large number of individual elements is returned, the extension to the continuous case would not hold.

The result then is that at some distance $x_0 = \frac{\ell_0}{\alpha}$ one encounters a form of reciprocity failure. To determine the greatest distance x_0 assume that ℓ_0 is of the order of a centimeter as has been measured, then, assuming diffraction limiting, $x_0 \approx \frac{10^{-2}}{5 \times 10^{-5}} \approx 200$ meters. Even if the frequently quoted 10-cm correlation distance were used, $x_0 \simeq \frac{10^{-1}}{5 \times 10^{-6}} \simeq 2 \times 10^4 = 20$ kilometers. The smaller distance of one centimeter is fairly well authenticated, even though not explicitly found in much of the literature.

The resulting conclusions must be somewhat modified. Thus far only the inner scale of the turbulence has been discussed although larger turbulent elements also have their effects. It has just been shown that a significant increase of range, x_0, results when the element size increases from 1 cm to 10 cm. Elements as large as 1 meter are known to occur. These would result in an extremely large diffraction limited range. Thus, although a system might not be able to compensate for the smaller elements, it might be argued that it could compensate for the larger ones. Unfortunately, the larger elements do not usually refract

a beam as much as the smaller ones. Measured angles of 10 to 20 seconds are common for 1 cm elements, while 2 seconds is common for 10 cm elements. The exception to this results from the anomalies occasionally observed with frequencies in the order of a cycle per minute which have a deviation of 5 to 10 seconds of arc and dimensions of the order of a meter or more. These are apparently due to rising bubbles of warm air, and are encountered only under certain conditions.

The conclusion is then that the use of systems based on reciprocity is fruitless because of the nature of the turbulence. A much better approach would be to make the source as large as possible to aversge over the atmospheric turbulence, and thus to decrease the effects of scintillation and of the small elements. These small elements also give rise to a scattering attenuation which is frequently not noted but can be of large system importance.

APPENDIX VI

DIFFRACTIVE SCANNING[1]

1.0 INTRODUCTION

In 1921 Brillouin (Reference 1) predicted that a liquid traversed by compression waves of short wavelengths, when irradiated with visible light, would give rise to a diffraction phenomenon similar to that due to a grating. It is well known that the angular position of the diffraction images is dependent on the spacing of the rulings on conventional grating. A change in this spacing produces a change in the angular position of the diffraction image. Thus, a light beam could be made to scan by continuously changing the grating spacing. Such an experiment is not feasible with ruled grating.

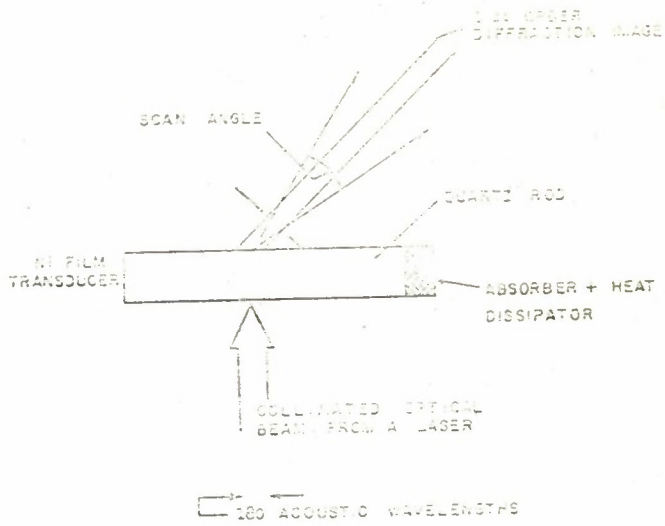
The diffraction phenomenon in an acoustic cell is related to the periodicity of the acoustic waves. Since this can be easily changed, by frequency modulation, it immediately follows that the angular position of the diffraction image would follow these wavelength changes. By employing this technique a device that will scan in one dimension, Figure VI-1, can be made.

The diffraction patterns produced by an acoustic cell were first observed by Debye and Sears (Reference 2). Since then many investigators have experimentally observed the diffraction phenomenon under a variety of experimental conditions. The parameters include, angle of incidence (θ), wavelength of the ultrasonic wave (λ_u), the wavelength of the incident light (λ_L), the amplitude of the ultrasonic beam. Naturally the position of the various orders, their number and relative intensities depend on one or more of these factors.

2.0 THEORY

The purpose of this paragraph is not to present the complete complex mathematical formalism of the solution to this problem but rather to show

1. The analysis presented in this appendix is similar to thet presented in Appendix IV of this report where this effect is analyzed as a technique for internal modulation of lasers. However, the analysis as presented here is slanted toward obtaining scanning of the laser beam and parameters are developed for that application.



DIFFRACTION OF LIGHT BY AN ULTRASONIC WAVE PROPAGATED IN QUARTZ

FIGURE VI-1

clearly the nature of the approximations involved to obtain the results that will be quoted.

The change in the properties of the medium are the result of the time and spatial variation in the density of the particles or equivalently (by the Lorentz - Lorenz law) of the permittivity. Let the number density of the atoms be denoted by $N(r,t)$. For an isotropic homogeneous medium traversed by a plane compression wave propagated in the positive x direction, $N(r,t)$ may be written in the form

$$N(r,t) = N_0 [1 + \Delta \cos (Kx - \Omega t)] \qquad \text{(VI-1)}$$

where N_0 is the average number density of the medium, $N_0\Delta$ the amplitude of the compression wave, $K = 2\pi/\lambda_a$ its wave number, and $\Omega = Kv$ the angular velocity of the ultrasonic disturbance. This describes a traveling wave; the generalization of the theory to include stationary waves requires that

$$N(r,t)_1 = N_0 (1 + \cos Kx \cos \Omega t)$$

and is straight forward.

The permittivity (Σ) shows a similar dependence

$$\Sigma = \Sigma_0 + \Sigma_1 \cos (Kx - \Omega t) \qquad \text{(VI-2)}$$

Σ_1 and Δ are related and by use of the Lorentz-Lorenz law it can be shown that

$$\Sigma_1 = \gamma\Delta \qquad \text{(VI-3)}$$

where $\gamma = 1/3 (\Sigma_0 - 1) (\Sigma_0 + 2)$ and is of the order of unity for most materials. If the incident light is a plane wave monochromatic beam of wavelength λ_l, polarized perpendicular to the plane of propagation of the acoustic wave, Maxwell's equation for the system can be written. (For definiteness assume that the light source is the visible output at 0.6328μ from a HeNe gas maser.) Further, if the material is nonmagnetic, then the integral form of the Maxwell equations may be employed. The most complete solution to the diffraction phenomenon can then be obtained. The main content of the integral equation method is that the influence of matter on the propagation of an electromagnetic wave is equivalent to the effect of electric dipoles embedded in a vacuum, the dipole moment induced in any physically infinitesimal volume element dr' of linear

dimenaions much smaller than λ_l (such volume elements, namely much larger than the volume of the individual atoms but of linear dimensions small compared with λ_l can always be chosen for optical wavelengths) being proportional to the field $E'(r't)$ acting on it and to the number of molecules (atoms) in that volume. Associated with such a dipole at r' is the Hertzian vector.

$$Z_e = \alpha N(r', t - R/c) \frac{E'(t - R/c, r')}{R} dr' \qquad \text{(VI-4)}$$

from which, the field at the point r and at time t may be derived by operating on it with

$$-\frac{\partial^2}{c^2 \partial t^2} + \text{grad div}$$

where $R = |r - r'|$ and the operator grad div acts on the variables r(xyz). The integro differential equation for the electric vector is obtained in the usual way and is

$$E'(r,t) = E^{(i)}(r,t) + \alpha \iiint \left(\frac{\partial^2}{c^2 \partial t^2} + \text{grad div}\right) \left[N(r', t - R/c) \frac{E(r', t - R/c)}{R}\right] dr' \qquad \text{(VI-5)}$$

where the integration extends throughout the whole medium, except for the small domain occupied by the atoms at the point of observation r(x,y,z). When this equation is solved for E' at all points inside the medium the field outside the medium is calculated by adding together the incident field $E^{(i)}(r,t)$ and the dipole field $E^{(d)}(r,t)$ given by the integral in equation (VI-1) but extending the integration now throughout the whole volume. Equation (VI-1) is valid only under certain restrictive conditions. First, the polarizability per molecule in general depends on the frequency of E', so that E' should be strictly monochromatic. However, unless one is too near the dispersion frequencies the variation of α with frequency of the internal field is small. Hence, provided that all component frequencies of E' lie close to each other, equation (VI-1) may be employed. Even when the incident field is strictly monochromatic, the field acting on a molecule and producing a dipole will not necessarily be monochromatic when N(r,t) depends on time, on account of the acoustic wave. Tha spread of frequencies now depends on the time variations of N (r,t). Hence, only when the variation in time of N is slow

in comparison with that of $E^{(i)}$ may equation (VI-1) be used with confidence. Because the proposed variations in N occur at microwave frequencies and the electromagnetic signal is the visible coherent output of a HeNe gas maser, these restrictions are well satisfied.

Further, α has been assumed to be a scalar, an assumption fully justified for atoms and molecules having special symmetries, but holding more generally whenever the molecules are oriented at random. (Hence, it applies to liquids.) Finally, absorption of light by the medium has been assumed negligible; it could be taken into account by choosing α complex. Since the incident light is linearly polarized with its electric vector perpendicular to the plane of incidence; the components of the electric vector $E^{(i)}(r,t)$ of the incident light wave (the real part representing the physical quantity) may be written

$$E_x^{(i)} = E_y^{(i)} = 0 \qquad \text{(VI-6)}$$

$$E_z^{(i)} = Be^{i(kx \sin\theta + ky \cos\theta - \omega t)} \qquad \text{(VI-7)}$$

The system has the same properties in all planes at right angles to the z axis, the vector E(txyz) inside the medium will also be parallel to the z axis, therefore $E_x = E_y = 0$, and the vector integral equation (VI-1) for E' reduces to a single integral equation of the form

$$E'_z(r,t) = Be^{i(kx \sin\theta + ky \cos\theta - \omega t)} + \frac{\tau_0}{4\pi} \iiint \left(-\frac{\partial^2}{c^2 \partial t^2} + \frac{\partial^2}{\partial z^2}\right) \left[\frac{1}{R} E'_z(r', t - R/c)\right] \left(1 + \frac{1}{2}\Delta e^{i[kx' - \Omega(t - R/c)]} + e^{i[kx' - \Omega(t - R/c)]}\right) \qquad \text{(VI-8)}$$

where

$$4\pi N_0 \alpha = \tau_0 = \frac{3(n^2 - 1)}{n^2 + 2}$$

Since all planes perpendicular to the z axis are physically equivalent, we take as the trial solution of the integral equation (VI-3) an expression of the form,

$$E'_z = \sum_{\ell,m} N_{\ell,m} e^{-i(\omega_{\ell,m} t - p_\ell x - q_m y)}$$

The solution to these equations has been found by A. B. Bhatia and W. J. Noble (Reference 3).

The transmitted wave complex is found to consist of many plane waves, each with a different frequency and a different direction of propagation. The directions of propagation of the various orders are given by

$$\sin\beta = c(k \sin\theta + \ell K)/\omega + \ell\Omega \qquad \text{(VI-9)}$$

where β denotes the angle between the direction of propagation of the ℓ'th order and the y axis. If we neglect terms of order v/c this becomes

$$\sin\beta - \sin\theta = \ell \frac{\lambda_\ell}{\lambda_u} \qquad \text{(VI-10)}$$

In contrast to a ruled grating the light in the diffracted images are frequency modulated at multiples of the acoustic frequency; each order consisting of the upper and lower sidebands. Thus, the frequency of the light in the ℓ'th order is

$$\omega_\ell = \omega_0 \pm \ell\Omega \qquad \text{(VI-11)}$$

These relationships for the frequencies and directions of the various order lines are the same as those obtained from the Raman-Nath (Reference 4) type of analysis. (Based on the approximation $\lambda_\ell \ll \lambda_u \Delta$.) However, the expressions describing the intensities of the various orders are much more complicated. A list of results for certain special conditions follows. Letting B equal the amplitude of the incident wave, n the refractive index, δ, ξ and β are defined by

$$\delta = \frac{\Delta\lambda_u^2}{\lambda_\ell^2}, \quad \xi = \frac{\lambda_\ell}{\lambda_u} \sin\theta, \quad \beta = \frac{\pi\lambda_\ell}{n\lambda_u^2}$$

For normal incidence (and for $\delta \ll 1$) we get the results that

$$I_1 = I_{-1} = B^2 \delta^2 \gamma^2 \sin^2 \tfrac{1}{2}\beta d$$

$$I_2 = I_{-2} = \frac{1}{48} B^2 \delta^4 \gamma^4 \left(-\frac{1}{4}\sin^2 [illegible] + \sin^2 \tfrac{1}{2}\beta d + \frac{1}{3}\sin^2 \tfrac{3}{2}\beta d\right) \qquad \text{(VI-12)}$$

and for angles of incidence such that $\xi = \frac{1}{2}$,

we get the results

$$I_0 = B^2 \cos^2 \tfrac{1}{2} \beta d \, \delta\gamma \qquad \text{(VI-13)}$$

$$I_{-1} = B^2 \sin^2 \tfrac{1}{2} \beta d \, \delta\gamma \qquad \text{(VI-14)}$$

$$I_1 = \frac{1}{16} B^2 \delta^2 \gamma^2 \left[- \sin^2 \tfrac{1}{2} \beta d \, \delta\gamma + 2 \sum_{+-} \sin^2 \beta d \left(1 \pm \tfrac{1}{4} \delta\gamma \right) \right] \qquad \text{(VI-15)}$$

$$I_{-2} = \frac{1}{16} B^2 \delta^2 \gamma^2 \sin^2 \tfrac{1}{2} \beta d \, \delta\gamma \qquad \text{(VI-16)}$$

The intensities of the reflected light orders are significantly lower than the transmitted orders and can therefore be entirely disregarded. With these results one can now ask the question as to what characteristics does an acoustic cell have when it is used as a means for optical scanning.

3.0 SCAN ANGLE

All experimental work on the diffraction of light by acoustic waves has been carried out at fairly low ultrasonic frequencies (tens of kilocycles). In these cases the angular position of the diffraction orders lie very close to the normal and are very closely spaced. To increase the angular separation of orders, therefore, it is necessary to decrease the acoustic wavelength to be of order of the optical wavelength (refer to equation (VI-10). Hence hypersonic waves must be considered.

Working at large angles has the advantage that the modulation depth can be significantly reduced. For, when θ is of order of 90 degrees, it requires only a small change in the acoustic wavelength λ_u, and hence sin θ to give a large change in the θ. Thus, a larger scan angle can be obtained with less bandwidth in the acoustic wave when θ is large.

However, since we wish to observe the light beyond the medium carrying the acoustic wave, the angular position of the image must not exceed the critical angle for the medium. For common materials this imposes an upper limit to the deflection angle of about 45 degrees. Since in this region the wavelength is nearly proportional to the angular deflection, the choice of the central position is governed by other considerations. It is advantageous not to use too high high-frequency acoustic waves because the acoustic attenuation increases as the square of the

frequency and is impossibly large above 100 mc in most liquids. Thus, it is advantageous to work with higher order images. Since the angular separation of orders decreases with increasing order number, one is limited by possible overlapping of orders giving rise to ambiguous signals. The velocity of sound waves in most optically transparent liquids is of the order of 1.5×10^5 cm/sec. Since frequencies above about 100 mc cannot be propagated in liquids the shortest ultrasonic wavelength which will propagate is 1.5×10^{-3} cm. This gives rise, by equation (VI-10), to a first order image at $\theta = 2$ degrees, 24 minutes. Thus the maximum scan angle obtainable without overlapping of orders is approximately 1 degree. Liquids do not, therefore, present themselves as a suitable medium when large scan angles are required. Solids do not have such a low high-frequency cut off and, hence will be the object of the rest of this discussion.

Suppose it is desired to have a beam which will scan over 10 degrees. Let the incident light be normal and let the central position of the first (for reasons to be seen later) order image occur at 10 degrees to the normal. Then for $\lambda_l = 0.6328\mu$, from equation (VI-10) we have that

$$\sin \theta = \frac{\lambda_l}{\lambda_u}$$

or

$$\lambda_u = \frac{6.328 \times 10^{-5}}{\sin 10} = 3.643 \times 10^{-4} \text{ cm}$$

The velocity of an acoustic shear wave in most solids is of the order of 6×10^5 cm/sec. Thus the required acoustic frequency is 1.65 gc. Waves of this frequency can certainly be propagated in crystalline quartz.

From equation (VI-10) one can also calculate that a change in frequency of ±0.80 gc is necessary to change the angular position of the first order diffraction image by 5 degrees to either side of the center.

Such an approach seems feasible and an examination of the relative efficiency of the process and the degree of resolution and scanning rates obtainable must be made.

4.0 TRANSDUCERS AND ACOUSTIC POWER LEVELS

Many workers have observed the diffraction pattern set up by both standing and progressive sinusoidal waves. However, no attempt has been made to modulate the acoustic wave and, hence, to scan the optical beam.

The reason seems to stem from the type of transducer used; all have been of the resonant structure type and not, therefore applicable to the requirements of high-frequency generation or scanning.

Recently a technique has been developed for depositing thin films of materials whose dimensions will very with an applied magnetic field; for example, nickel. These films of magnetostrictive alloys are very successful as transducers and have an electromechanical coupling coefficient reported as high as 45% compared to about 10% for natural quartz.

With these transducers and with quartz as the propagation medium, ultrasonic propagation has been observed over better than 800 mc bandwidth at 1.5 gc at room temperature. The film can be suitably magnetized so that only the longitudinal mode propagates. The power flow per unit area for an infintely wide ($\omega \gg \lambda_u$) istropic media or along any one of the crystal axis for crystalline media is given by (see Reference 5)

$$J = \frac{1}{2} \rho v^3 \left(\frac{\delta\rho}{\rho}\right)^2 \times 10^{-7} \frac{\text{watts}}{\text{cm}^2} \qquad \text{(VI-17)}$$

where $\delta\rho$ is the maximum deviation from the average density ρ. The upper limit for the acoustic power level in a crystal which has been achieved to date is approximately 3 watts per cm^2. For a specimen 5 mm high by 2 mm wide, the power required is 0.3 watts and the change produced in the number density

$$\Delta = \frac{\delta\rho}{\rho} = 1.1 \times 10^{-5} \qquad \text{(VI-18)}$$

5.0 INTENSITY OF DIFFRACTED BEAM

The intensity of the diffraction images is a function of both the acoustic amplitude and wavelength. The dependence on wavelength occurs in the argument of a sine term which is a very rapidly varying function and the average value will be assumed. Thus the relative intensity of the first order image is

$$\frac{I_1}{I_0} = \left(\frac{\gamma \Delta \lambda_u^2}{\lambda_\ell^2}\right)^2 = 3.31 \times 10^{-7} \qquad \text{(VI-19)}$$

If the incident beam is the output from a HeNe gas maser then the maximum incident power is approximately 30 milliwatts. Hence the intensity of the first order diffraction image would be 10^{-8} watts. Such a signal is detectable, however, obviously the second and higher order images are not. Equation (VI-19) can be rewritten as

$$\frac{I_1}{I_0} = \left(\frac{\gamma\lambda}{\sin^2\theta}\right)^2 \qquad \text{(VI-20)}$$

Thus it is seen that there is a fundamental relationship between intensity and angle of deflection which shows that one can only gain in one at the expense of the other.

6.0 BRAGG ANGLES

It is noticed, equation (VI-13), that when $\xi = \frac{1}{2}$, the intensities of the various orders on one side of the transmitted beam I_0 are one power lower in δ^2 than the intensities of the corresponding orders on the other side. It has been observed experimentally by Bhagavantum and Rao (Reference 6) that although at lower frequencies of the ultrasonic wave both I_{+1} and I_{-1} appear, at higher frequencies only I_{-1} appears. At exact Bragg incidence equation (VI-7) predicts I_{-1} should vanish whenever $d\Delta\alpha/2\lambda_\ell n$ takes integral values. This aspect of the theory has not had experimental verification.

Since $\xi = \frac{1}{2}$ the intensity of the first order is of the same magnitude as the zero order, this seems ideal for scanning. However, if we examine the conditions more closely we find $\xi = \frac{1}{2}$ implies that

$$\sin\theta = \frac{2}{\lambda_u} \qquad \text{(VI-21)}$$

This is the condition for Bragg reflection and thus we might expect an enhancement of the intensity (Reference 7). However, to continuously satisfy equation (VI-21), the incidence angle must change as the wavelength is changed. Thus, a means of scanning is required to change the incident angle to produce a beam which will scan.

7.0 SCAN RATE AND RESOLUTION

Even if the power does not place impossible limitations on the technique and it is possible that at some later time, further research will

increase the acoustic power which can be propagated in a solid, another more basic limitation exists. The scan rate is not just restricted by the rate at which the acoustic wave can be frequency modulated, but also by the resolution required. In order to achieve an angular resolution of 10^{-3} radians, the number of diffraction elements required is

$$N = \frac{}{\lambda_0 \cos \theta \, d\theta} \sim 180$$

Thus the acoustic wave must remain unchanged for 180 wavelengths, that is, 6.7×10^{-2} cm. The light beam must also have this width.

For a 10 degree (0.1745 radians) beam scan angle and a one milliradian beam divergence the number of resolution elements is of the order 175. It will be a function of the signal to noise ratio. Assume that the latter is such that the maximum number of resolution elements is 350, and that the beam does not sweep continuously but moves in 350 discrete steps. Each step corresponding to a different frequency of the acoustic wave. To achieve the one milliradian resolution we have seen that it is necessary for each acoustic wave train to remain unchanged in frequency for 6.7×10^{-2} cm, that is, for a time 1.1×10^{-7} sec. Thus the total time for a single scan is $350 \times 1.1 \times 10^{-7} = 4.82 \times 10^{-5}$ sec. Hence the maximum scan rate possible is 21 kc. Thus although it may be electronically possible to sweep from 2.45 to 0.85 gc at rates of several hundreds of megacycles, if a reasonable degree of fidelity is required, the maximum scan rates are inherently limited to some tens of kilocycles.

8.0 REFERENCES

1. L. Brillouin; Ann de Physic; 1921; Vol. 17.
2. P. Debye and F. W. Sears; Proc. Nat. Acad. Sci., Wash.; 1932; Vol. 18.
3. A. B. Bhatia and W. J. Noble; Proc. Roy. Soc.; 1953.
4. C. V. Raman and N. S. N. Nath; Proc. Ind. Acad. Sci.; 1936.
5. G. W. Willard, J. Acoustic; Soc. Am.; 1949.
6. S. Bhagavantum and B. R. Rao; Proc. Indian Acad. Sci.; 1945.
7. H. Z. Cummings and N. Knable; IEEE; 1963; Vol. 51.

DOCUMENT CONTROL DATA - R&D

(Security classification of title, body of abstract and indexing annotation must be entered when the overall report is classified)

1. ORIGINATING ACTIVITY (Corporate author) ITT Communication Systems, Inc., Paramus, New Jersey	2a. REPORT SECURITY CLASSIFICATION Unclassified 2b. GROUP
3. REPORT TITLE Applicability of Laser Techniques	
4. DESCRIPTIVE NOTES (Type of report and inclusive dates)	
5. AUTHOR(S) (Last name, first name, initial)	
6. REPORT DATE August 1964	7a. TOTAL NO. OF PAGES / 7b. NO. OF REFS
8a. CONTRACT OR GRANT NO. AF19(628)-3414 ✓ b. PROJECT NO. c. Task A-1 d.	9a. ORIGINATOR'S REPORT NUMBER(S) ICS-64-TR-480 ICS-64-TR-481 Appendices 9b. OTHER REPORT NO(S) (Any other numbers that may be assigned this report) ESD-TR-66-480
10. AVAILABILITY/LIMITATION NOTICES Special export control applies. Each transmittal of this document outside the Department of Defense must have prior approval of Hq ESD (ESTI).	
11. SUPPLEMENTARY NOTES	12. SPONSORING MILITARY ACTIVITY DEPUTY FOR COMMUNICATION SYSTEMS ELECTRONIC SYSTEMS DIVISION L.G. Hanscom Field, Bedford, Mass.
13. ABSTRACT	

DD FORM 1 JAN 64 1473

Security Classification

Unclassified

UNCLASSIFIED

When this document is no longer required by your activity, DESTROY IT in accordance with applicable security regulations.

DO NOT RETURN IT TO DDC

UNCLASSIFIED

Unclassified